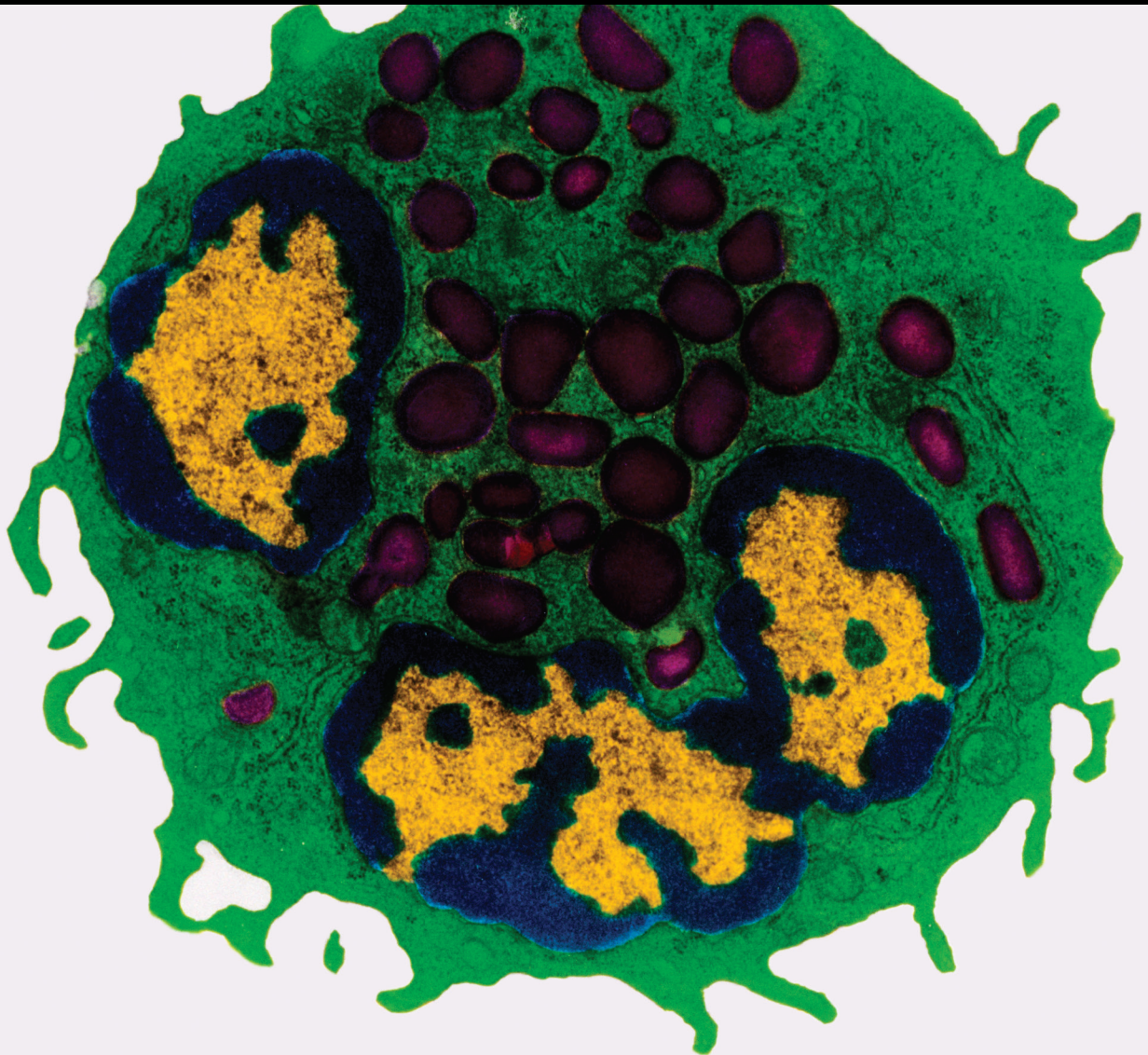# Pharmacological and Non-Pharmacological Therapies Applied to Inflammatory Disorders

Lead Guest Editor: Rômulo Dias Novaes
Guest Editors: Reggiani Vilela Gonçalves, Vinicio Granado-Soto, Eliziária Cardoso Santos, and Débora Esposito

Pharmacological and Non-Pharmacological Therapies Applied to Inflammatory Disorders

Pharmacological and Non-Pharmacological Therapies Applied to Inflammatory Disorders

Lead Guest Editor: Rômulo Dias Novaes
Guest Editors: Reggiani Vilela Gonçalves, Vinicio Granado-Soto, Eliziária Cardoso Santos, and Débora Esposito
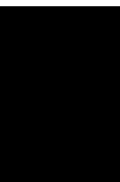
Contents

Research Article

Enhanced H3K4 Trimethylation in TNF-α Promoter Gene Locus with Cell Apoptosis in the Ventral-Medial Striatum following Opioid Withdrawal of Neonatal Rat Offspring from Morphine-Addicted Mothers

Pei-Ling Wu [ID],[1,2,3] **Jau-Ling Suen,**[3] **Chun-Hwa Yang** [ID],[2] **Kuang-Che Kuo** [ID],[4] **Yu-Chen S. H. Yang** [ID],[5] **and San-Nan Yang** [ID][1,2]

[1]*School of Medicine, College of Medicine, I-Shou University, Kaohsiung, Taiwan*
[2]*Department of Pediatrics, E-Da Hospital, Kaohsiung, Taiwan*
[3]*Graduate Institute of Medicine, College of Medicine, Kaohsiung Medical University, Kaohsiung, Taiwan*
[4]*Department of Pediatrics, Kaohsiung Chang Gung Memorial Hospital and Chang Gung University College of Medicine, Kaohsiung, Taiwan*
[5]*Joint Biobank, Office of Human Research, Taipei Medical University, Taipei, Taiwan*

Correspondence should be addressed to Yu-Chen S. H. Yang; can_0131@tmu.edu.tw and San-Nan Yang; y520729@gmail.com

Prenatal opioid exposure might disturb epigenetic programming in the brain of neonatal offspring with various consequences for gene expressions and behaviors. This study determined whether altered trimethylation of histone 3 at lysine 4 (H3K4me3) in the promoter of the tumor necrosis factor-α (*tnf-α*) gene with neural cell apoptosis was involved in the ventral-medial striatum, an important brain region for withdrawal symptoms, of neonatal rat offspring from morphine-addicted mothers. Female adult rats were injected with morphine before gestation and until 14 days after giving birth. On postnatal day 14 (P14), rat offspring from morphine-addicted mothers were subjected to an opioid-withdrawal protocol and were analyzed 2 or 8 h after administration of that protocol. Expressions of the TNF-α protein, H3K4me3 in the *tnf-α* promoter gene, and neural cell apoptosis within the ventral-medial striatum of neonatal rat offspring were evaluated. In the absence of significant opioid withdrawal (2 h after initiation of the opioid-withdrawal protocol on P14), prenatal morphine exposure led to increased levels of H3K4me3 in the *tnf-α* promoter gene, of the TNF-α protein, and of neural cell apoptosis within the ventral-medial striatum of neonatal rat offspring. Following opioid withdrawal (8 h after initiation of the opioid-withdrawal protocol on P14), differential expression of H3K4me3 in the *tnf-α* promoter gene locus and upregulation of the level of TNF-α protein expression were further enhanced in these offspring. In addition, increased levels of caspase-3 and neural cell apoptosis were also observed. Taken together, this study revealed that prenatal opioid exposure can activate an epigenetic histone mechanism which regulates proinflammatory factor generation, which hence, led to cell apoptotic damage within the ventral-medial striatum of neonatal rat offspring from morphine-addicted mothers. More importantly, the opioid-withdrawal episode may provide augmented effects for the abovementioned alterations and could lead to deleterious effects in the neonatal brain of such offspring.

1. Introduction

Early life adversity is related to increased risks for developing many behavioral and psychiatric disorders [1]. A spectrum of prenatal, intrapartum, and postnatal episodes is likely to contribute to neurodevelopment via interactions with the individual's genotype to disrupt specific neural and psychophysiological system-related cognitive functions, thereby enhancing the risk for psychopathologies later in life [2, 3]. Indeed, children exposed to perinatal opioid drugs appear

to have a higher mortality rate after birth and suffer from neurodevelopmental consequences and behavioral problems [4, 5].

During the fetal and neonatal periods, the central nervous system (CNS) displays highly significant plasticity and is vulnerable to changes by prenatal influences such as prenatal opioid exposure [6–8]. The mechanisms through which early life exposures play important roles for later-life psychopathologies remain undetermined, but an epigenetic mechanism represents a reasonable candidate [9, 10]. The ventral-medial striatum of the mammalian brain serves as an integration center to mediate goal-directed behaviors (i.e., rewards of drug craving and drug addiction) [11]. Previous studies demonstrated that morphine exposure can trigger the production of proinflammatory cytokines, including tumor necrosis factor- (TNF-) α, interleukin- (IL-) 1, and IL-6 [12–14]. Chronic opioid administration leads to increased messenger (m)RNA levels of IL-1 and IL-6 in the ventral-medial striatum of rats $in\ vivo$ [15]. In addition, morphine withdrawal neuro-behaviors can induce TNF-α release from neural cells [13]. Recently, TNF-α expression levels were found to increase in the amygdala during morphine-withdrawal episodes [14]. Indeed, inflammation in the brain not merely occurs with direct opioid exposure and withdrawal but has transplacental effects on newborn offspring as well; for instance, offspring suffering from prenatal opioid exposure exhibited increased TNF-α production in the hippocampus [16]. Prenatal stresses, such as chronic illicit drug abuse, can dysregulate the maternal immune function and cause elevated proinflammatory cytokine levels in the brain of neonatal offspring [17]. Taken together, those studies revealed that prenatal opioid exposure can generate transplacental inflammation cascades during early life.

The epigenetic histone regulation in a target promoter gene locus might play a role in the molecular basis of mammalian drug-craving and addiction [18, 19]. Recently, tri-methylation of histone H3 at lysine 4 (H3K4me3), one type of histone regulation, was suggested to act as a transcription booster for the $tnf\text{-}\alpha$ gene expression within the promoter region [18, 20]. In addition, early life stress or drug exposure can also induce histone modifications within the ventral tegmental area resulting in dysregulated signal conduction [21]. However, little is known about histone methylation as a result of perinatal opioid exposure with apoptosis in the offspring brain. Thus, the aim of this study was to examine the hypothesis that prenatal opioid exposure activates the tri-methylation of H3K4me3 in the $tnf\text{-}\alpha$ promoter gene and is associated with neural cell apoptosis in the ventral-medial striatum of neonatal rat offspring (on postnatal day 14; P14).

2. Materials and Methods

2.1. Experimental Animal Protocol. Female adult Sprague-Dawley (SD) rats which underwent the opioid-withdrawal protocol were housed under a 12 h light/dark cycle with humidity maintained around 60%~70% and were initially injected with morphine hydrochloride (2 mg/kg body weight (BW), subcutaneously twice daily with the dosage progressively increased at a rate of 1 mg/kg BW every 7 days with a maximum dose of 7 mg/kg BW) [6–8, 22]. These female rats were mated on about day 7 or 8. During pregnancy and after the rat offspring were born, morphine was still routinely administered as scheduled until the offspring were 14 days old. The last opioid injection was on postnatal day 13 (P13). Throughout the experimental course, there were no significant opioid withdrawal symptoms between the maternal opioid injections. The vehicle-control group consisted of maternal SD rats injected with NaCl at the same dose and interval as the experimental group.

We evaluated the growth of BW of rat offspring on postnatal day 7 (P7) and P14 (an age regarded as a neonate in the human lifespan) [23]. On P14, rat offspring from maternal rats were transferred to an observational chamber maintained at around 33°C with warm light and were observed for 2 h for cumulative episodes of and latency in exhibiting opioid-withdrawal behaviors, such as rearing, teeth chattering, backward locomotion, tremors, and wet-dog shaking. Rat offspring from morphine-addicted mothers were divided into two groups: an early group represented rat offspring observed for opioid withdrawal behaviors for 2 h immediately after transfer, after which they were sacrificed for biochemical experiments (the early group, $n = 48$ rats); and the late group represented rat offspring for observation of opioid-withdrawal behaviors for 2 h starting from the 6th hour after transfer. These rat offspring were then sacrificed for biochemical experiments (the late group, $n = 48$ rats). Rat offspring from the vehicle-control group were transferred to an observational chamber on P14 and were observed for opioid-withdrawal behaviors for 2 h starting from the 6th hour after transfer. These rat offspring were then sacrificed for biochemical experiments (the control group, $n = 48$ rats). There were no differences in sex among the three groups.

All experimental protocols were approved by the Animal Care and Use Committee at the National Defense Medical Center, Taiwan (NDMC-04-088 and IACUC-04-085) with all actions undertaken being designed to lessen suffering and decrease the number of animals used.

2.2. Preparation of Slices of the Ventral-Medial Striatum Brain Region. After the opioid-withdrawal protocol was completed on P14, the pups were sacrificed, and brain slices (400 μm) containing the ventral-medial striatum brain region were immediately harvested with a vibro-slicer (Campden Instruments, Sileby, Loughborough, UK). Brain slices were selectively transferred to an incubation chamber perfused with oxygenated artificial cerebrospinal fluid (95% O_2/5% CO_2 gas, at 30.0 ± 0.5°C) for 1 h. Artificial cerebrospinal fluid consisted of (in mM) NaCl (124), $MgCl_2$ (1), $CaCl_2$ (2), KCl (3.5), NaH_2PO_4 (1.25), $NaHCO_3$ (26), and D-glucose (10) at pH 7.4 and with an osmolarity of 305 ± 5 mOsm.

2.3. Immunoblotting. Cells of the ventral-medial striatum were lysed in buffer (10 mM Tris at pH 7.4, 150 mM NaCl, 1 mM PMSF, 0.2% Triton X-100, 2 mM EDTA, and 1× protease inhibitor mixture). The protein concentration was clarified with a BCA assay (Thermo Scientific, Rockford, IL, USA). Cell lysates were sorted on sodium dodecylsulfate polyacrylamide gel electrophoresis (SDS-PAGE), later

transferred to nitrocellulose membranes, and then probed with antibodies against TNF-α (SC-1351; Santa Cruz) and cleaved caspase-3 (no. 9662; Cell Signaling). Depending on the different types of primary antibody, either rabbit anti-mouse immunoglobulin G (IgG) or goat anti-rabbit IgG (1: 3000) was chosen as the secondary antibody. Immunoreactive proteins were detected using the BioSpectrum 810 Imaging System (UVP).

2.4. Real-Time Polymerase Chain Reaction (PCR). Isolation of RNA, including synthesis of complementary (c)DNA, and DNase treatment was accomplished using the Transcriptor First Strand cDNA Synthesis Kit RT-PCR System™ (Roche, Indianapolis, IN, USA) following the manufacturer's instructions. The two-step real-time PCR with the LightCycler™ System (Roche) and Sybr Green I dye was used for monitoring the PCR. FastStart DNA Master SYBR Green I (Roche) was performed according to the producer's instructions and used for the real-time PCR. This study utilized the following set of primers: TNF-α: forward (5′-CCCTACGGGTCATT GAGAGA-3′) and reverse (5′-GGTTGTGGACTGCCTT TTGT-3′); and 18s ribosomal (r)RNA: forward (5′-CCAG TAAGTGCGGGTCATAA-3′) and reverse (5′-TAGTCA AGTTCGACCGTCTTC-3′). The thermal protocol of the PCR was set to 95°C (for 4 min), followed by 30 amplification cycles of 94°C (for 30 s), 62°C (for 1 min), and 72°C (for 1 min), with a final melting curve analysis. Amplicons were analyzed by the melting curve (Light Cycler software) and agarose gel electrophoresis; the LightCycler analytical system was applied to decide cycle threshold (CT) values, and the relative messenger (m)RNA level of each experiment was assessed by a real-time PCR followed by measurement by the relative CT method ($\Delta\Delta$CT) (the expression of the objective was normalized to an endogenous standard (18S rRNA) and compared to a calibrator (cDNA from a pooled sample)).

2.5. Chromatin Immunoprecipitation (ChIP) Assay. A ChIP assay was performed as previously described [24, 25]. Briefly, 5×10^5 cells were treated with 1% formaldehyde at room temperature (for 10 min) accompanied by sonication of DNA and immunoprecipitation of chromatin overnight with antibodies of trimethylated H3K4 (2 μg for 25 μg of chromatin; antihistone H3K4me3 antibody, ChIP Grade; ab8580; Abcam) and later purification with a ChIP kit (no. 17-295; Upstate Biotechnology, Lake Placid, NY, USA). Probes and primers were planned by exploring the proximal promoter and intronic enhancer areas of the *tnf-α* gene [24, 25], including the following subregions as described below relative to the transcription start site: *tnf-α* 1 (-2686 to -2667); forward, 5′-CCCTAGTCCTCCTGGGATGT-3′ and reverse, 5′-GCC TGCTGCAACAGAGAGA-3′; *tnf-α* 2 (-2202 to -2183); forward, 5′-CGTCTCACTATGCCTGGGTCT-3′ and reverse, 5′-AAGCAAAGCACTTCTACCAAAT-3′; *tnf-α* 3 (-1672 to -1653); forward, 5′-AAACTCAGACCAGGCTGCAT-3′ and reverse, 5′-CAGGTCATCTCTTGACGTGGT-3′; *tnf-α* 4 (-502 to -480); forward, 5′-GAGTTCTGCATGTATT
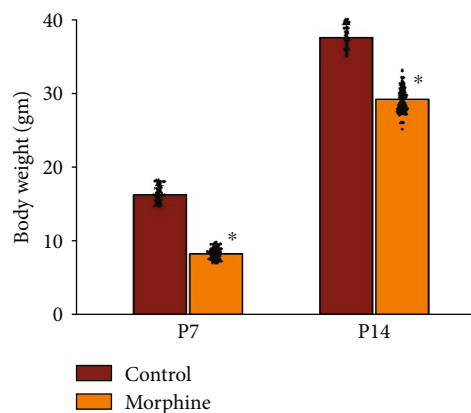
FIGURE 1: The BW of rat offspring of the prenatally opioid-exposure group was statistically significantly lower. The BW of rat offspring on P7 was as follows: the control group: 16.3 ± 1.3 g ($n = 48$ rats) vs. the prenatally opioid-exposure group: 8.3 ± 0.7 g ($n = 96$ rats). And the BW of rat offspring on P14 was as follows: the control group: 37.6 ± 1.7 ($n = 48$ rats) vs. the prenatally opioid-exposure group: 29.2 ± 1.6 g ($n = 96$ rats). Scatted dots represent the data points in each group. $^*p < 0.05$, compared to the control group.

GGATAGG-3′ and reverse, 5′-TGCTACCAAGCCTAAA GACC-3′; and *tnf-α* 5 (-230 to -213); forward, 5′-GGTT CAGTTCCCAGCACCTA-3′ and reverse, 5′-ATGGGC ATATCTGCACAGCA-3′. PCRs were conducted on the ABI Gene Amp ⓐ PCR System (Applied Biosystems). The quantity of immunoprecipitated DNA was calculated and compared to the quantity of total input DNA.

2.6. Apoptosis Evaluation. A double immunofluorescence investigation by laser-scanning confocal microscopy was applied to examine apoptosis in neurons of brain sections of the ventral-medial striatum, which were cut at a coronal plane and measured 30 μm and then stained with an anti-neuronal nuclei (NeuN) antibody (clone A60, MAB377; Chemicon, Temecula, CA, USA) to identify neuronal cells in the presence or absence of terminal uridine nick-end labeling (TUNEL; 11684795910, Sigma-Aldrich, St. Louis, MO, USA), and immunostaining was used to detect DNA breakdown. A Cy3-conjugated anti-mouse antibody for staining NeuN and a fluorescein-conjugated antibody for staining TUNEL were used for a secondary amplification that was visualized with a Zeiss LSM510 laser microscope (Thornwood, NY, USA). Quantitative analyses of the NeuN-sensitive cell density, TUNEL-sensitive cell density, and NeuN/TUNEL-sensitive cell density were performed in the ventral-medial striatum according to the brain atlas [26]. Average results for each group were taken from six slices per animal.

2.7. Statistical Analysis. Data are shown as mean ± standard error of the mean (SEM). Data were analyzed using Sigma-Plot 10.0 and Sigmastat 3.5. A one-way analysis of variance (ANOVA) with Bonferroni's test for post hoc comparisons was applied with the level of significance set to $p < 0.05$.

(a)

(b)
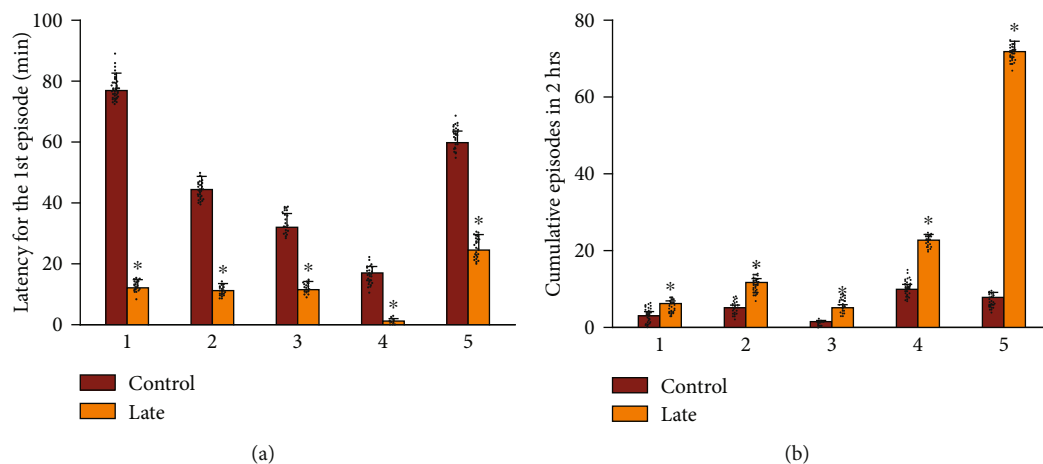
FIGURE 2: Observations of opioid-withdrawal behaviors in rat offspring on P14. (a) The rat offspring which were observed for 2 h starting from the 6th hour after transfer (the late group) exhibited shorter latency in exhibiting opioid-withdrawal behaviors. (b) There were more opioid-withdrawal behaviors in a 2 h period in the late group. 1: rearing; 2: teeth chattering; 3: backward locomotion; 4: tremor; 5: wet-dog shaking. Each group was derived from independent 48 rats, respectively. $^*p < 0.05$, compared to the control group.

(a)

(b)
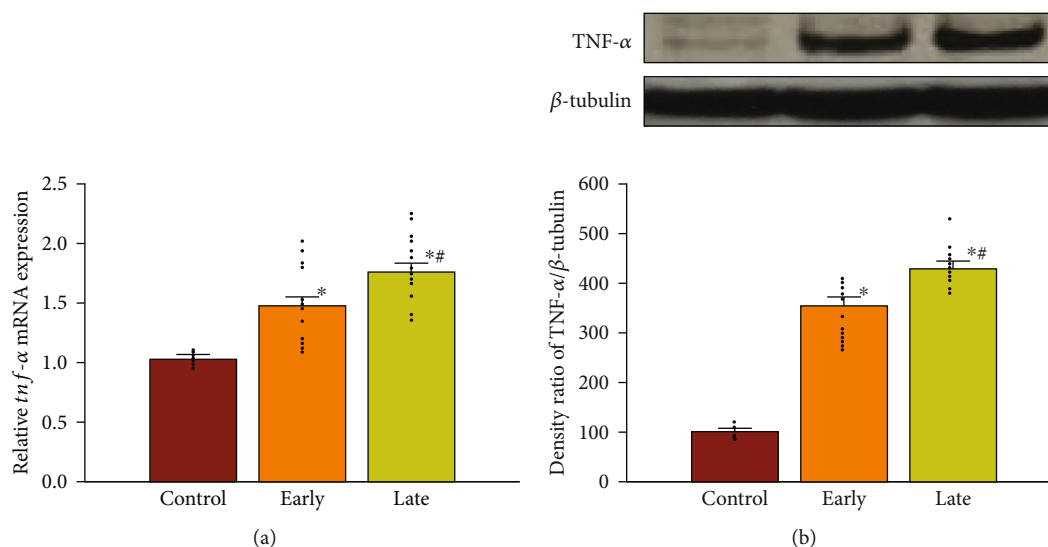
FIGURE 3: Prenatal opioid exposure enhanced the TNF-α expression in the ventral-medial striatum of neonatal rat offspring on P14. (a) The expression of TNF-α at mRNA level in the ventral-medial striatum of neonatal rat offspring from morphine-addicted mothers. (b) The expression of TNF-α at protein level in the ventral-medial striatum of neonatal rat offspring from morphine-addicted mothers. The groups were as follows: the control group ($n = 12$ rats), the early group ($n = 12$ rats), and the late group ($n = 12$ rats). The upper panel indicates representative immunoblots. β-Tubulin served as an internal standard control and was not significantly changed across lanes. Scatted dots represent the data points in each group. $^*p < 0.05$, compared to the control group. $^\#p < 0.05$, compared to the early group.

3. Results

3.1. Opioid-Withdrawal Behaviors.
We observed whether prenatal opioid exposure disrupted the growth in BW after birth. In Figure 1, the BW of rat offspring of the prenatally opioid-exposure group was statistically significantly lower (P7: the prenatally opioid-exposure group: 8.3 ± 0.7 g, $p < 0.05$, $n = 96$ rats vs. the vehicle-control group: 16.3 ± 1.3 g, $n = 48$ rats; P14: the prenatally opioid-exposure group: 29.2 ± 1.6 g, $p < 0.05$, $n = 96$ rats vs. the vehicle-control group: 37.6 ± 1.7, $n = 48$ rats).

Rat offspring in the early group did not express significant opioid-withdrawal behaviors, compared to the control group ($p > 0.05$, $n = 48$ rats in each group, data not shown). In contrast, as shown in Figure 2, the late group exhibited shorter latency in exhibiting opioid-withdrawal behaviors (e.g., rearing, teeth chattering, backward locomotion, tremors, or wet-dog shaking) and had more opioid-withdrawal behaviors in a 2 h period, compared to rat offspring born from the control group at the 6th hour after transfer ($p < 0.05$, $n = 48$ rats in each group).

3.2. Prenatal Opioid Exposure and TNF-α Expression.
Figure 3 shows levels of TNF-α mRNA and protein in the ventral-medial striatum of neonatal rat offspring (P14) from morphine-addicted mothers. There were significant increases

(a)

(b)

(c)
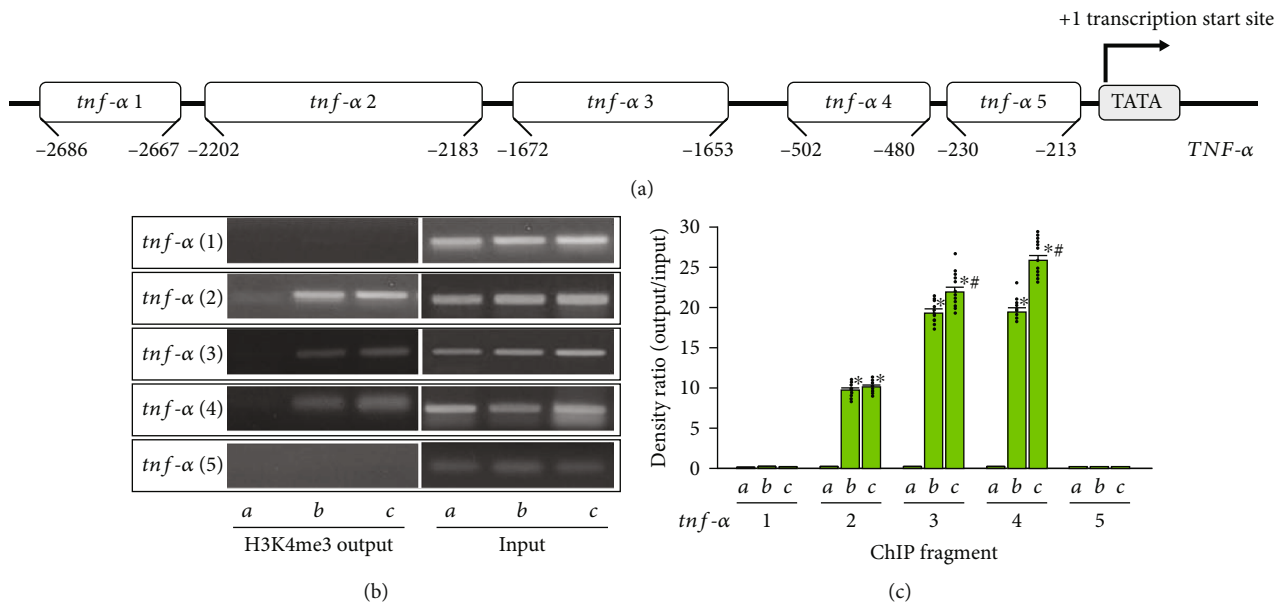
FIGURE 4: Prenatal opioid exposure activated differential enhancement of H3K4me3 in the *tnf-α* promoter gene locus in the ventral-medial striatum. (a) The figure demonstrated the subregions relative to the transcription start site of *tnf-α* promoter gene locus as follows: *tnf-α* 1 (−2667 to −2686), *tnf-α* 2 (−2183 to −2202), *tnf-α* 3 (−1653 to −1672), *tnf-α* 4 (−174 to −496), and *tnf-α* 5 (−205 to −224). (b) The panel illustrations indicate representative ChIP assay of the levels of trimethylated H3K4 in the *tnf-α* promoter gene locus at the subregions. The insets *a*, *b*, and *c* are as follows: the control group ($n = 12$ rats), the early group ($n = 12$ rats), and the late group ($n = 12$ rats). (c) The effects of prenatal opioid exposure in trimethylated H3K4 levels in the *tnf-α* promoter gene is summarized in three groups as described above. The DNA input signal served as the internal loading control and was not significantly different across lanes. Scatted dots represent the data points in each group. *$p < 0.05$, compared to the control group. #$p < 0.05$, compared to the early group.

at the mRNA and protein levels of the TNF-α expression in the early group compared to the control group ($p < 0.05$, $n = 12$ rats in each group). In addition, mRNA and protein levels of the TNF-α expression were further enhanced in the late group compared to the early group ($p < 0.05$, $n = 12$ rats in each group).

3.3. Prenatal Opioid Exposure and H3K4me3 Modifications in the tnf-α Promoter.

To determine whether activation of H3K4me3 in the *tnf-α* promoter gene was associated with increased levels of TNF-α as seen in Figure 3, ChIP analyses using PCR primers matching five subregions of the *tnf-α* promoter gene were performed in the ventral-medial striatum of neonatal rat offspring. As shown in Figure 4, prenatal opioid exposure increased levels of H3K4me3 in subregions 2, 3, and 4 of the *tnf-α* promoter gene ($p < 0.05$, $n = 12$ rats in each group). Furthermore, in the late group, there were further increased levels of H3K4me3 activity in subregions 3 and 4 of the *tnf-α* promoter gene locus compared to the early group ($p < 0.05$, $n = 12$ rats in each group).

3.4. Prenatal Opioid Exposure and Apoptotic Caspase-3 Activity.

To observe whether prenatal opioid exposure caused the abovementioned TNF-α enhancement combined with cell apoptosis, cleaved caspase-3 activity was evaluated in the ventral-medial striatum of neonatal rat offspring (P14) from morphine-addicted mothers. As shown in Figure 5, there was an increased level of the cleaved caspase-3 expression in the early group compared to the control group ($p < 0.05$). In addition, the level of cleaved caspase-3
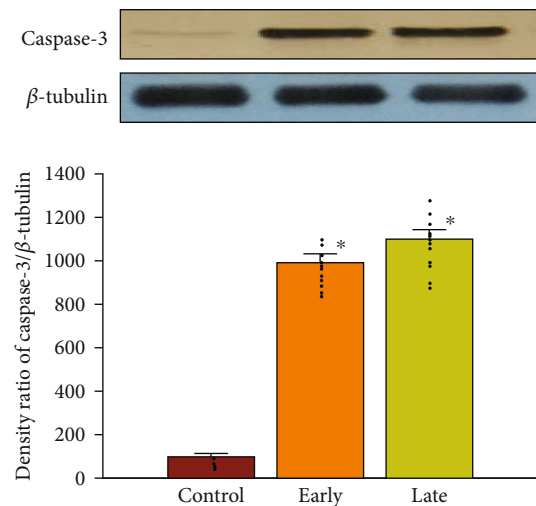
FIGURE 5: Prenatal opioid exposure enhanced the level of the caspase-3 expression in the ventral-medial striatum of neonatal rat offspring on P14. The level of cleaved caspase-3 in the ventral-medial striatum of neonatal rat offspring from morphine-addicted mothers is summarized in three groups as follows: the control group ($n = 12$ rats), the early group ($n = 12$ rats), and the late group ($n = 12$ rats), respectively. The upper panel reveals illustrative immunoblots. $β$-Tubulin was used as an internal standard control and was not significantly different across lanes. Scatted dots represent the data points in each group. *$p < 0.05$, compared to the control group. #$p < 0.05$, compared to the early group.

Control

(a1) (a2)

Early

(b1) (b2)

Late

(c1) (c2)

(a3) (b3) (c3)

(a) (b) (c)
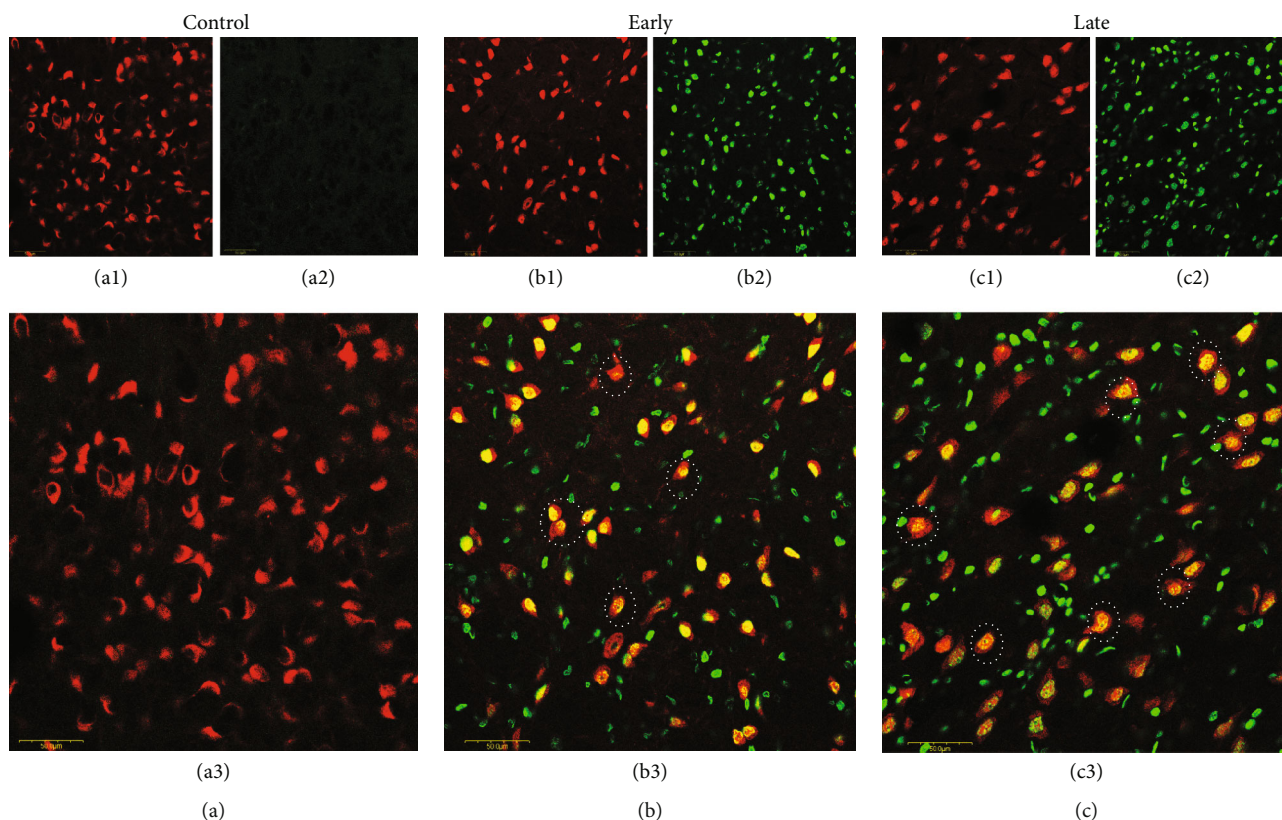
FIGURE 6: Prenatal opioid exposure induced cell apoptosis in the ventral-medial striatum of neonatal rat offspring (P14). Colocalization of NeuN- (red for neuron identification) and TUNEL- (green for apoptotic cells) sensitive cells was recognized by double immunofluorescence staining with laser-scanning confocal microscopy. The NeuN-sensitive cells (panel 1), TUNEL-sensitive cells (panel 2), and the combined pictures of the NeuN- and TUNEL-sensitive cells (panel 3) are as follows: the control (a1–a3), the early group (b1–b3), and the late group (c1–c3), respectively. The dotted circles reveal representative apoptotic neurons. Bar = 50 μm.

expression in the late group did not statistically differ compared to the early group ($p > 0.05$, $n = 12$ rats in each group).

3.5. Prenatal Opioid Exposure and Neural Cell Apoptosis. To confirm the increased levels of the above-described caspase-3 activity, confocal laser-scanning microscopy was applied to study neonatal rat offspring (P14) from morphine-addicted mothers. Figures 6(a)–6(c) are representative morphological illustrations, and Figures 7(a)–7(c) demonstrate summarized data. As indicated in Figure 7(a), there was an increased number of TUNEL-sensitive cells within the ventral-medial striatum in the early group compared to the control group ($p < 0.05$, $n = 12$ rats in each group). In addition, a further increase in TUNEL-sensitive cells was observed in the late group compared to the early group ($p < 0.05$, $n = 12$ rats in each group) (Figure 7(a)). Figure 7(b) shows that prenatal opioid exposure led to fewer NeuN-sensitive cells in the early group compared to the control group ($p < 0.05$). The number of NeuN-sensitive cells in the late group did not statistically differ compared to the early group ($p > 0.05$, $n = 12$ rats in each group) (Figure 7(b)). In Figure 7(c), the number of cells displaying colocalization of NeuN and TUNEL responses within the ventral-medial striatum was significantly higher in neonatal rat offspring (P14) from morphine-addicted mothers compared to the control group ($p > 0.05$, $n = 12$ rats in each group). These results

reveal that prenatal opioid exposure can induce neural cell apoptosis in the ventral-medial striatum of neonatal rat offspring from morphine-addicted mothers.

4. Discussion

The major findings of this study revealed that prenatal opioid exposure activated differential trimethylation of H3K4 modifications in the promoter locus of the *tnf-α* gene and was associated with cell apoptosis in the ventral-medial striatum of neonatal rat offspring from morphine-addicted mothers, suggesting possible early life adversity within the ventral-medial striatum of the mammalian brain.

Previous studies suggested that epigenetic histone modifications regulate gene expressions through a specific site over a promoter in response to various stimuli [27]. However, most studies evaluated global changes of epigenetic modifications rather than adopting an approach to investigate a specific gene. Previous studies indicated a higher possibility of DNA methylation located in specific loci of the *tnf-α* promoter gene as detected from human gingiva with periodontitis [28, 29]; additionally, exposure to lipopolysaccharide induced different but focused regions of histone modifications including methylation in the promoter region of the *tnf-α* gene [27]. This study further disclosed the differential enhancement of H3K4me3 modifications in the *tnf-α*
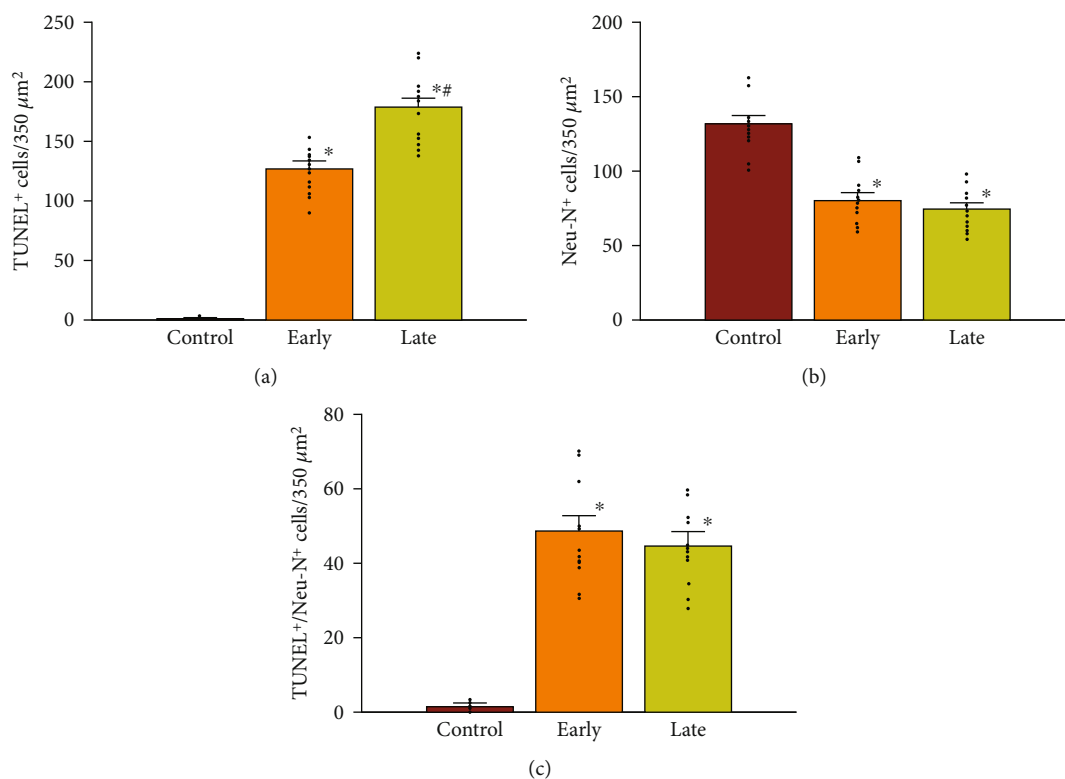
FIGURE 7: Prenatal opioid exposure induced cell apoptosis in the ventral-medial striatum of neonatal rat offspring (P14). The summarized data of TUNEL-sensitive cells (a), NeuN-sensitive cells (b), and colocalizations of TUNEL/NeuN-sensitive cells (c), for counted ventral-medial striatum are as follows: the control group, the early group, and the late group, respectively. Average results for each group were taken from six slices per animal ($n = 12$ rats in each group). Scatted dots represent the data points in each group. $^*p < 0.05$, compared to the control group. $^\#p < 0.05$, compared to the early group.

promoter gene locus of the ventral-medial striatum of neonatal rat offspring from morphine-addicted mothers, and this enhancement over a different promoter locus of the tnf-α gene implies that respective transcriptional factors can be recruited into transcription and become affected by prenatal opioid exposure. For example, signal transducer and activator of transcription 6 (STAT6) (located in the tnf-α 2 subregion) were reported to mediate neuroinflammation caused by ethanol in mice with a traumatic brain injury [30]. Engrailed homeobox 1 (En1) (located in the tnf-α 3 subregion) and pituitary homeobox 3 (Pitx3) (located in the tnf-α 4 subregion) are involved in dopaminergic neuronal development, which is related to drug addiction and reward behaviors [31]. In this study, we demonstrated increased levels of H3K4me3 in subregions 2, 3, and 4 of the tnf-α promoter gene in the ventral-medial striatum of neonatal rat offspring from morphine-addicted mothers (Figure 4), accompanied by increased levels of TNF-α mRNA and protein (Figure 3). These results hint at possible alterations in activation of transcription factors responsible for proinflammatory factor generation (e.g., TNF-α). However, which transcription factors are involved and are affected by epigenetic histone modifications in offspring due to prenatal opioid exposure are still unclear.

Epigenetic histone modifications persistently appear not only during acute or chronic exposure but are long-lasting as well, even after withdrawal episodes [32, 33]. Metham-

phetamine increased the expression of H3K4me3 during addiction in the dorsal striatum of animals, and it was globally expressed even after termination of methamphetamine exposure [34]. Similar, prenatal opioid exposure increased levels of H3K4me3 in the tnf-α promoter gene in this study. And as the late group presented opioid-withdrawal behaviors, there was a further enhancement of H3K4me3 activity in specific subregions. Taken together, epigenetic histone modifications seem to be related to mediation of priming or desensitization of specific genes in illicit drug exposure, and such epigenetic histone modifications can be latent, while persistently altering the chromatin structure after withdrawal episodes [35]. However, we mainly evaluated the H3K4me3 expression in the ventral-medial striatum from neonatal rat offspring in the acute stage of prenatal morphine exposure and/or withdrawal in this study, which might mimic the clinical state of neonatal abstinence syndrome. Future studies should also investigate histone modifications at additional time points in order to evaluate the long-term effects of prenatal opioid exposure.

Enhancement of TNF-α production was associated with cell apoptosis within the ventral-medial striatum by prenatal opioid exposure which increases the neurobiological basis of risks for neuropsychiatric disorders in later life. Such enhanced TNF-α release indicates an early proinflammatory response leading to activation of apoptotic pathways such as caspase-3 signaling [36–38]. However, in this study, there

was no significant decrease in apoptotic neurons in the late group (Figure 7). Indeed, morphine can directly induce apoptosis of microglia and neurons *in vitro*, but it seemed that chronic morphine exposure might not affect glial cells at an early age *in vivo* from animal models [36, 37]. Therefore, apoptosis did play a role in prenatal opioid exposure, but the detailed involvement of specific cell types remains to be investigated. In this study, prenatal opioid exposure and withdrawal induced TNF-α production might lead to neural cell apoptosis in the ventral-medial striatum. In addition, opioid exposure might also enhance apoptosis in selected, specific brain areas, such as the amygdala, ventral-medial striatum, or prefrontal cortex *in vivo* [36, 38]. Prenatal heroin exposure enhances apoptosis in the hippocampus and results in impairments to learning and memory [39]. Those results indicate that prenatal opioid exposure and withdrawal might induce apoptosis in other specific brain areas and result in neurological impairments.

Recently, a closely interactive and related relationship between inflammation and neuropsychiatric disorders was proposed in the mammalian brain [40]. For instance, proinflammatory cytokines can affect cognition and mood behaviors by promoting neuroexcitatory reactions and impairing neuron plasticity [41]. Furthermore, as shown in this study, the epigenetic H3K4me3 mechanism for the upregulation of the TNF-α expression was associated with increased neural cell apoptosis in the ventral-medial striatum, which might contribute to neurological impairments. Such neural cell apoptotic damage within the ventral-medial striatum during early life might lead to increased dose requirements for opioid drugs to satisfy the need to increase the dosage and to fulfill drug-craving and addictive behaviors later in life. In addition, prenatal opioid exposure may initiate long-lasting alterations in the gene expressions of the synapse structure in the ventral-medial striatum in rat offspring [8, 22]. Such effects of prenatal opioid exposure seem to exist longer than expected. Our current results showed that prenatal opioid exposure induced neural cell apoptosis within the ventral-medial striatum in early life. However, whether neural cell apoptosis persistently appears in later life or the next generation is still unknown, and this has motivated us to conduct further experiments on the long-term effect of prenatal opioid exposure and withdrawal.

5. Conclusions

In summary, this study revealed that prenatal opioid exposure can activate an epigenetic histone mechanism for regulating proinflammatory factor generation and hence lead to cell apoptotic damage within the ventral-medial striatum of neonatal rat offspring from morphine-addicted mothers. More importantly, the opioid-withdrawal episode may provide augmented effects for such abovementioned alterations and may lead to adverse effects in the neonatal brain of these offspring.

Data Availability

The data used to support the findings of this study are available from the corresponding author upon request.

Conflicts of Interest

The authors declare that there is no conflict of interest regarding the publication of this paper.

Authors' Contributions

PLW contributed to the data curation, writing—original draft, and funding acquisition. JLS contributed to the resources, writing—review and editing, and visualization. CHY contributed to the investigation and data curation. KCK contributed to the methodology and visualization. YCY and SNY contributed to the conceptualization, methodology, writing—review and editing, supervision, and funding acquisition. All authors contributed to the manuscript revision and read and approved the submitted version.

References

[1] A. Agorastos, P. Pervanidou, G. P. Chrousos, and D. G. Baker, "Developmental trajectories of early life stress and trauma: a narrative review on neurobiological aspects beyond stress system dysregulation," *Frontiers in Psychiatry*, vol. 10, p. 118, 2019.

[2] S. Lisonkova, L. L. Richter, J. Ting et al., "Neonatal abstinence syndrome and associated neonatal and maternal mortality and morbidity," *Pediatrics*, vol. 144, no. 2, p. e20183664, 2019.

[3] K. Ramphul, S. G. Mejias, and J. Joynauth, "An update on the burden of neonatal abstinence syndrome in the United States," *Hospital Pediatrcs*, vol. 10, no. 2, pp. 181–184, 2020.

[4] R. W. S. Coulter, J. E. Egan, S. Kinsky et al., "Mental health, drug, and violence interventions for sexual/gender minorities: a systematic review," *Pediatrics*, vol. 144, no. 3, p. e20183367, 2019.

[5] A. J. Czynski, J. M. Davis, L. M. Dansereau et al., "Neurodevelopmental outcomes of neonates randomized to morphine or methadone for treatment of neonatal abstinence syndrome," *The Journal of pediatrics*, vol. 219, 2020.

[6] S. N. Yang, L. T. Huang, C. L. Wang et al., "Prenatal administration of morphine decreases CREBSerine-133 phosphorylation and synaptic plasticity range mediated by glutamatergic transmission in the hippocampal CA1 area of cognitive-deficient rat offspring," *Hippocampus*, vol. 13, no. 8, pp. 915–921, 2003.

[7] S. N. Yang, C. A. Liu, M. Y. Chung et al., "Alterations of postsynaptic density proteins in the hippocampus of rat offspring from the morphine-addicted mother: beneficial effect of dextromethorphan," *Hippocampus*, vol. 16, no. 6, pp. 521–530, 2006.

[8] C. S. Lin, P. L. Tao, Y. J. Jong et al., "Prenatal morphine alters the synaptic complex of postsynaptic density 95 with N-methyl-D-aspartate receptor subunit in hippocampal CA1 subregion of rat offspring leading to long-term cognitive deficits," *Neuroscience*, vol. 158, no. 4, pp. 1326–1337, 2009.

[9] H. J. Harder and A. Z. Murphy, "Early life opioid exposure and potential long-term effects," *Neurobiology of Stress*, vol. 10, p. 100156, 2019.

[10] E. J. Ross, D. L. Graham, K. M. Money, and G. D. Stanwood, "Developmental consequences of fetal exposure to drugs: what we know and what we still must learn," *Neuropsychopharmacology*, vol. 40, no. 1, pp. 61–87, 2015.

[11] M. D. Scofield, J. A. Heinsbroek, C. D. Gipson et al., "The nucleus accumbens: mechanisms of addiction across drug classes reflect the importance of glutamate homeostasis," *Pharmacological Reviews*, vol. 68, no. 3, pp. 816–871, 2016.

[12] L. C. Loram, P. M. Grace, K. A. Strand et al., "Prior exposure to repeated morphine potentiates mechanical allodynia induced by peripheral inflammation and neuropathy," *Brain Behavior, and Immunity*, vol. 26, no. 8, pp. 1256–1264, 2012.

[13] S. Hao, S. Liu, X. Zheng et al., "The role of TNFα in the periaqueductal gray during naloxone-precipitated morphine withdrawal in rats," *Neuropsychopharmacology*, vol. 36, no. 3, pp. 664–676, 2011.

[14] S. J. O'Sullivan, E. Malahias, J. Park et al., "Single-cell glia and neuron gene expression in the central amygdala in opioid withdrawal suggests inflammation with correlated gut dysbiosis," *Frontiers in Neuroscience*, vol. 13, p. 665, 2019.

[15] S. L. Chen, P. L. Tao, C. H. Chu et al., "Low-dose memantine attenuated morphine addictive behavior through its anti-inflammation and neurotrophic effects in rats," *Journal of Neuroimmune Pharmacology*, vol. 7, no. 2, pp. 444–453, 2012.

[16] J. Amri, M. Sadegh, N. Moulaei, and M. R. Palizvan, "Transgenerational modification of hippocampus TNF-α and S100B levels in the offspring of rats chronically exposed to morphine during adolescence," *The American Journal of Drug and Alcohol Abuse*, vol. 44, no. 1, pp. 95–102, 2018.

[17] L. Hantsoo, S. Kornfield, M. C. Anguera, and C. N. Epperson, "Inflammation: a proposed intermediary between maternal stress and offspring neuropsychiatric risk," *Biological Psychiatry*, vol. 85, no. 2, pp. 97–106, 2019.

[18] K. Hyun, J. Jeon, K. Park, and J. Kim, "Writing, erasing and reading histone lysine methylations," *Experimental & molecular medicine*, vol. 49, no. 4, p. e324, 2017.

[19] E. J. Nestler, "Epigenetic mechanisms of drug addiction," *Neuropharmacology*, vol. 76, pp. 259–268, 2014.

[20] T. Kusch, "Histone H3 lysine 4 methylation revisited," *Transcription*, vol. 3, no. 6, pp. 310–314, 2012.

[21] R. D. Shepard and F. S. Nugent, "Early life stress- and drug-induced histone modifications within the ventral tegmental area," *Frontiers in cell and developmental biology*, vol. 8, p. 588476, 2020.

[22] P. L. Wu, Y. N. Yang, J. L. Suen, Y. C. S. Yang, C. H. Yang, and S. N. Yang, "Long-lasting alterations in gene expression of postsynaptic density 95 and inotropic glutamatergic receptor subunit in the mesocorticolimbic system of rat offspring born to morphine-addicted mothers," *BioMed Research International*, vol. 2018, Article ID 5437092, 9 pages, 2018.

[23] P. Sengupta, "The laboratory rat relating its age with human's," *International Journal of Preventive Medicine*, vol. 4, no. 6, pp. 624–630, 2013.

[24] Y. N. Yang, Y. T. Su, P. L. Wu et al., "Granulocyte colony-stimulating factor alleviates bacterial-induced neuronal apoptotic damage in the neonatal rat brain through epigenetic histone modification," *Oxidative Medicine and Cellular Longevity*, vol. 2018, Article ID 9797146, 10 pages, 2018.

[25] Y. N. Yang, Y. C. S. H. Yang, P. L. Wu, C. H. Yang, K. C. Kuo, and S. N. Yang, "Dextromethorphan suppresses lipopolysaccharide-induced epigenetic histone regulation in the tumor necrosis factor-α expression in primary rat microglia," *Mediators of Inflammation*, vol. 2020, Article ID 9694012, 8 pages, 2020.

[26] S. R. Jones, S. J. O'Dell, J. F. Marshall, and R. M. Wightman, "Functional and anatomical evidence for different dopamine dynamics in the core and shell of the nucleus accumbens in slices of rat brain," *Synapse*, vol. 23, no. 3, pp. 224–231, 1996.

[27] K. E. Sullivan, A. B. M. Reddy, K. Dietzmann et al., "Epigenetic regulation of tumor necrosis factor alpha," *Molecular and Cellular Biology*, vol. 27, no. 14, pp. 5147–5160, 2007.

[28] S. Zhang, S. P. Barros, A. J. Moretti et al., "Epigenetic regulation of TNFA expression in periodontal disease," *Journal of Periodontology*, vol. 84, no. 11, pp. 1606–1616, 2013.

[29] A. Kojima, T. Kobayashi, S. Ito, A. Murasawa, K. Nakazono, and H. Yoshie, "Tumor necrosis factor-alpha gene promoter methylation in Japanese adults with chronic periodontitis and rheumatoid arthritis," *Journal of Periodontal Research*, vol. 51, no. 3, pp. 350–358, 2016.

[30] F. O. Heuvel, S. Holl, A. Chandrasekar et al., "STAT6 mediates the effect of ethanol on neuroinflammatory response in TBI," *Brain, Behavior, and Immunity*, vol. 81, pp. 228–246, 2019.

[31] M. T. Alves dos Santos and M. P. Smidt, "En1 and Wnt signaling in midbrain dopaminergic neuronal development," *Neural Development*, vol. 6, no. 1, p. 23, 2011.

[32] Y. D. Black, F. R. Maclaren, A. V. Naydenov, Carlezon WA Jr, M. G. Baxter, and C. Konradi, "Altered attention and prefrontal cortex gene expression in rats after binge-like exposure to cocaine during adolescence," *The Journal of Neuroscience: The Official Journal of the Society for Neuroscience*, vol. 26, no. 38, pp. 9656–9665, 2006.

[33] A. Kumar, K. H. Choi, W. Renthal et al., "Chromatin remodeling is a key mechanism underlying cocaine-induced plasticity in striatum," *Neuron*, vol. 48, no. 2, pp. 303–314, 2005.

[34] I. N. Krasnova, M. Chiflikyan, Z. Justinova et al., "CREB phosphorylation regulates striatal transcriptional responses in the self- administration model of methamphetamine addiction in the rat," *Neurobiology of Disease*, vol. 58, pp. 132–143, 2013.

[35] A. J. Robison and E. J. Nestler, "Transcriptional and epigenetic mechanisms of addiction," *Nature Reviews Neuroscience*, vol. 12, no. 11, pp. 623–637, 2011.

[36] D. Bajic, K. G. Commons, and S. G. Soriano, "Morphine-enhanced apoptosis in selective brain regions of neonatal rats," *International journal of developmental neuroscience: the official journal of the International Society for Developmental Neuroscience*, vol. 31, no. 4, pp. 258–266, 2013.

[37] S. Hu, W. S. Sheng, J. R. Lokensgard, and P. K. Peterson, "Morphine induces apoptosis of human microglia and neurons," *Neuropharmacology*, vol. 42, no. 6, pp. 829–836, 2002.

[38] S. N. Katebi, Y. Razavi, S. Z. Alamdary, F. Khodagholi, and A. Haghparast, "Morphine could increase apoptotic factors in the nucleus accumbens and prefrontal cortex of rat brain's reward circuitry," *Brain Research*, vol. 1540, pp. 1–8, 2013.

[39] Y. Wang and T. Z. Han, "Prenatal exposure to heroin in mice elicits memory deficits that can be attributed to neuronal apoptosis," *Neuroscience*, vol. 160, no. 2, pp. 330–338, 2009.

[40] G. Z. Réus, G. R. Fries, L. Stertz et al., "The role of inflammation and microglial activation in the pathophysiology of psychiatric disorders," *Neuroscience*, vol. 300, pp. 141–154, 2015.

[41] M. E. Bauer and A. L. Teixeira, "Inflammation in psychiatric disorders: what comes first?," *Annals of the New York Academy of Sciences*, vol. 1437, no. 1, pp. 57–67, 2019.

Research Article

Vagal Nerve Stimulation-Modulation of the Anti-Inflammatory Response and Clinical Outcome in Psoriatic Arthritis or Ankylosing Spondylitis

C. Brock [ID],[1] **S. E. Rasmussen** [ID],[2] **A. M. Drewes** [ID],[2] **H. J. Møller** [ID],[3] **B. Brock** [ID],[4] **B. Deleuran** [ID],[2] **A. D. Farmer** [ID],[5,6] **and M. Pfeiffer-Jensen** [ID][2,7]

[1]*Mech-Sense, Department of Gastroenterology and Hepatology, Clinical Institute, Aalborg University Hospital, Aalborg, Denmark*
[2]*Department of Rheumatology, Aarhus University Hospital, Aarhus, Denmark*
[3]*Department of Clinical Biochemistry, Aarhus University Hospital, Denmark*
[4]*Steno Diabetes Center Copenhagen, Region Hovedstaden, Gentofte, Denmark*
[5]*Centre for Trauma and Neuroscience, Blizard Institute, Wingate Institute of Neurogastroenterology, Barts and the London School of Medicine & Dentistry, Queen Mary University of London, London, UK*
[6]*Institute of Applied Clinical Sciences, University of Keele, Stoke on Trent, UK*
[7]*Copenhagen Center for Arthritis Research (COPECARE), Center for Rheumatology and Spine Diseases, Rigshospitalet, Glostrup, Copenhagen, and Department of Clinical Medicine, University of Copenhagen, Denmark*

Correspondence should be addressed to C. Brock; christina.brock@rn.dk

Objectives. The vagal nerve exerts an essential pathway in controlling the cholinergic anti-inflammatory reflex. Thus, the study is aimed at investigating the acute effect of a noninvasive transcutaneous vagus nerve stimulation on clinical disease activity and systemic levels of inflammation in patients with psoriatic arthritis or ankylosing spondylitis. *Methods*. Twenty patients with psoriatic arthritis (PsA) and 20 patients with ankylosing spondylitis (AS) were included and stimulated bilaterally with a handheld vagal nerve stimulator for 120 seconds 3 times a day for 5 consecutive days. All patients were in remission. Cardiac vagal tone, clinical scores, CRP, and cytokine levels were assessed. *Results*. In PsA and AS, decreased heart rate was observed, confirming compliance. Furthermore, in PsA, a clear reduction of clinical disease activity associated with a 20% reduction in CRP was shown. In AS, a reduction in interferon-γ, interleukin- (IL-) 8, and 10 was shown. No side effects were described. *Conclusion*. This open-label study provides support for an anti-inflammatory effect of transcutaneous vagus nerve stimulation in patients with psoriatic arthritis and ankylosing spondylitis. The modulated immune response and reduced disease activity and CRP-levels raise the fascinating possibility of using neuromodulation as an add-on to existing pharmacological treatments.

1. Introduction

Psoriatic arthritis (PsA) and ankylosing spondylitis (AS) are chronic autoimmune diseases characterized by peripheral and spinal joint inflammation. The global prevalence of PsA and AS is approximately 0.5% [1–3], and the chronic inflammation of peripheral and spinal joints in PsA and AS leads to various degrees of impaired functionality associated with increased risks of cardiovascular comorbidities and mortality [4–6] and substantial socioeconomic expenses

[7]. Currently, PsA and AS are typically treated with nonsteroidal anti-inflammatory drugs (NSAIDs) and/or disease-modifying antirheumatic drugs (DMARDs) such as methotrexate (MTX) [8] and targeted biological therapies, i.e., tumour necrosis factor-alpha (TNF-α) inhibitors, interleukin- (IL-) 17, and IL-12/23 inhibitors [9–12]. Frequent blood monitoring of the disease activity and presence of opportunistic infections is needed, and whilst most patients respond to these expensive treatments, a proportion of patients do not [13–15].

Circulating proinflammatory cytokines, such as TNF-α, has an important role in the pathophysiology of these disorders [16]. In a seminal animal study, Borovikova et al. showed the existence of the cholinergic anti-inflammatory pathway (CAP). Serum levels of TNF-α were decreased in endotoxin-treated animals that received electrical stimulation of the vagus nerve (VN) in comparison to vagotomised animals [17]. The anti-inflammatory effect is exerted through multiple neuroimmune interactions primarily via vago-vagal and vago-splenic pathways [18, 19], often referred to as the cholinergic anti-inflammatory pathway/reflex [20]. Many immune-mediated inflammatory disorders are characterized by a relative paucity of vagal tone, and therefore, vagal nerve stimulation (VNS) has been proposed as a potential anti-inflammatory intervention [18]. Clinical reduction of serum levels of TNF-α and clinical disease activity scores in rheumatoid arthritis [21] and C-reactive protein (CRP) in Crohn's disease have been reported [22], in response to invasive VNS-devices, which necessitates operative implantation with potential postoperative complications [23]. Consequently, novel noninvasive transcutaneous VNS (t-VNS) devices are emerging in the field of bioelectronics [24]. In healthy participants, bilateral t-VNS of the cervical part of the VN for 90 seconds caused a significant increase in cardiac vagal tone (CVT), a validated biomarker of efferent vagal tone, and a reduction in TNF-α lasting for up to 24 hours [25]. In rheumatoid arthritis, t-VNS resulted in reductions in disease activity, CRP, interferon-γ, and interleukin-10 [26], but hitherto, such transcutaneous devices have not been explored in the treatment of PsA or AS. We hypothesized that t-VNS would increase resting CVT and reduce the level of systemic inflammation and disease activity in such patients. Hence, this study is aimed at investigating the acute and short-term effect of t-VNS on CVT and the short-term effect of t-VNS on the disease activity and systemic level of inflammation.

2. Materials and Methods

2.1. Ethical Considerations.
All participants provided written informed consent. The study was approved by the Ethical Committee in "Region Midt," Denmark (1-10-72-199-16), the Danish Data Protection Agency (1-16-02-442-16), and the European Databank for Medical Devices (CIV-16-03-015125). The study was conducted in accordance to Good Clinical Practice (CPMP/ICH/135/95) and in compliance with the Declaration of Helsinki and its revised editions.

2.2. Study Design.
This single-center, open-label, proof-of-concept study was designed to investigate the potential anti-inflammatory effects of t-VNS in two parallel cohorts diagnosed with PsA and AS. Participants were recruited from the Department of Rheumatology, Aarhus University Hospital, Denmark. Eligible participants, according to the inclusion and exclusion criteria, had their clinical disease activity measured using the DAS28-CRP and ASDAS scores, underwent noninvasive evaluation of autonomic parameters, and had venous blood drawn for the analysis of cytokines. Participants were then thoroughly instructed on how to deliver t-

VNS, using the noninvasive, handheld stimulator (gamma-Core; electroCore Inc. Basking Ridge, NJ, USA) to both the left and right cervical vagus nerves. In order to personalize stimulation to a therapeutic level, the t-VNS intensity was slowly increased until participants experienced a nonpainful mild pulling of the ipsilateral oral commissure. Participants then self-stimulated the left and right cervical vagus nerves using the gammaCore device three times daily (morning, afternoon, and evening) during the four-day intervention period (24 stimulations in total). Each stimulation lasted for 120 seconds. On the second study day, participants were asked to demonstrate the t-VNS to the study personnel in order to enhance patient safety, correct application, and study compliance. The study protocol is summarized in Figure 1. In addition to the baseline visit, study site visits took place at day 2 and day 5 including autonomic measures and venous blood sampling.

2.3. Study Participants.
Eligible study participants included females and males with an established diagnosis of PsA or AS according to ACR criteria. Adult participants (>18 years) were included if they had no known contradictions to t-VNS such as known cardiovascular diseases including uncontrolled hyper/hypotension. Exclusion criteria included treatment with oral or intra-articular corticosteroids within the preceding five weeks or pregnancy (positive urine-HCG or lactating). None of the included patients had underwent previous vagotomy and/or had a currently implanted electrical or neurostimulating device.

2.4. Vagus Nerve Stimulation.
Noninvasive t-VNS was performed using the handheld, portable gammaCore stimulator. The device contains two stainless steel electrodes, which deliver electrical stimulation to the cervical part of the vagus nerve. The electrical signal is comprised of small electrical bursts with a 1-millisecond duration (five 5 kHz sine waves, each lasting 200 milliseconds) repeated at 25 Hz. The low-voltage signal produced by the gammaCore can be varied according to tolerability but is limited to a peak voltage of 24 volts and a maximum output current of 60 mA when placed on the skin.

2.5. Cardiac-Derived Parameters.
Autonomic measures were assessed by a portable ECG recording device (Faros 180°; Bittium, Oulu, Finland) connected to three ECG electrodes (Ambu BlueSensor P; Ambu, Copenhagen, DK). The electrodes were placed on clean and dry skin with the left and right arm electrodes positioned in the infraclavicular fossae and the left leg electrode near apex cordis. Five-minute resting recordings were performed on days 1, 2, and 5. The recordings were subsequently analysed using the bespoke software (ProCVT; ProBiometrics, London, UK) from which R-R intervals, HR, and cardiac vagal tone (CVT) were derived. CVT is a validated cardiometrically derived beat-to-beat measure of efferent vagal influence on the heart, and parasympathetic tone can be derived in recordings in epochs as short as 5 minutes, and details are described elsewhere [27]. CVT is measured on a linear vagal scale where 0 refers to full atropinisation. Any changes in heart rate
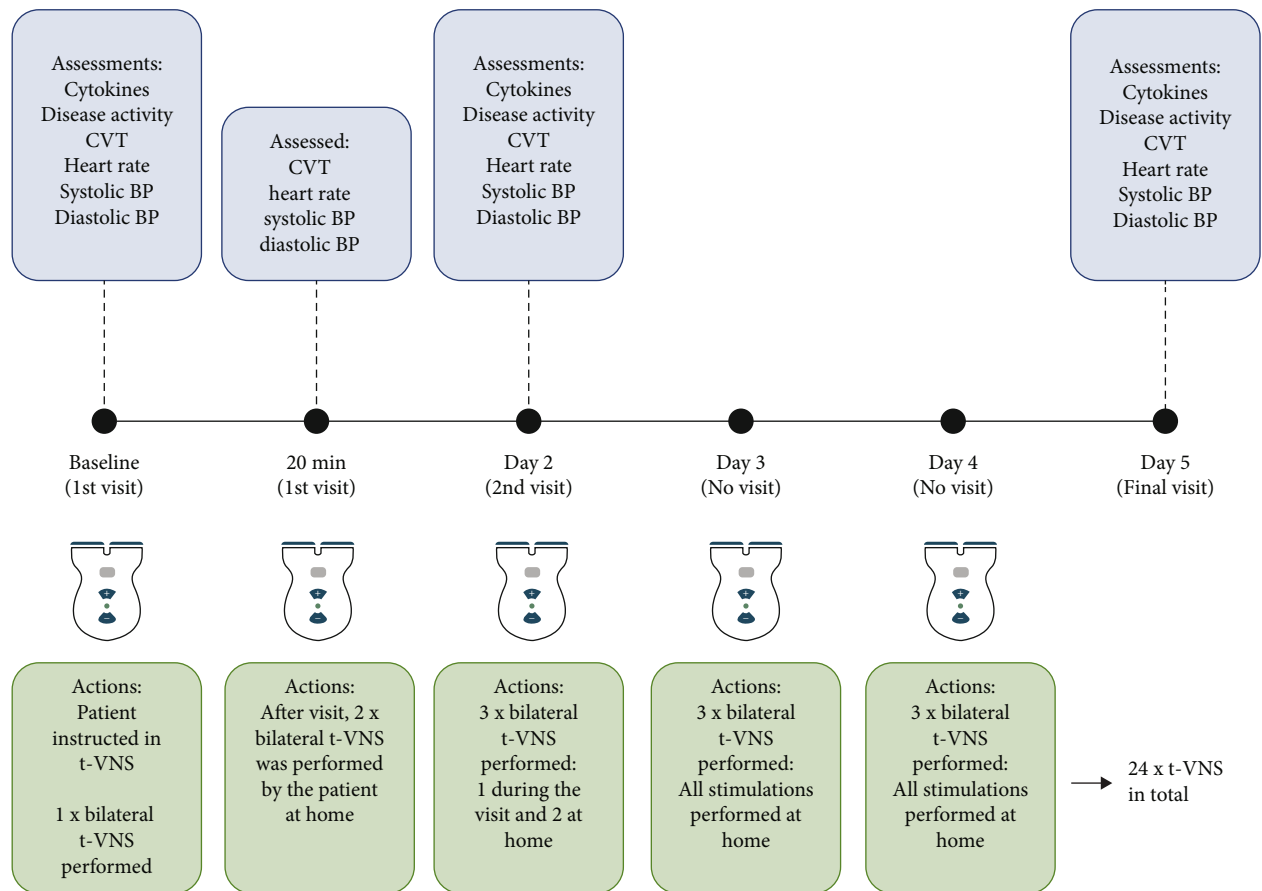
FIGURE 1: Schematic presentation of the study protocol.

(HR) of two consecutive heart beats at rest larger than 15 beats per minute (bpm) were removed from the recording as they were considered as artefacts due to sudden moves by the patient (e.g., coughing, sneezing, and change of position). Blood pressure (BP) was measured on the upper right arm using an electronic sphygmomanometer (UA-852; A&D Company Ltd., Tokyo, Japan).

2.6. Disease Activity.

Disease activity was assessed on days 1, 2, and 5 via a physical examination and a combination of self-reported indices electronically entered in the Danish DAN-BIO database. Physical examinations included a count of tender and swollen joint(s) and an assessment of axial inflammation using the Bath Ankylosing Spondylitis Metric Index (BASMI) [28]. Calculated values of DAS28-CRP, BASMI, and Ankylosing Spondylitis Disease Activity Score (ASDAS) were then extracted from the DANBIO database. DAS28-CRP was originally developed to assess disease activity in rheumatoid arthritis, but performs well in clinical studies with patients with PsA [29–31]. Similarly, ASDAS was originally developed for patients with AS, but has shown to be valid in patients with peripheral spondyloarthropathies [32].

2.7. Cytokine Analysis.

Venous blood was collected by experienced personnel at BY-lab, Aarhus University Hospital. Levels of C-reactive protein (CRP) were measured as part of a standard biochemical analysis, in addition to a variety of different biomarkers, at the hospitals' biochemical laboratory. Once collected, samples were centrifuged at $800 \times g$ for 10 minutes, and the plasma was collected and frozen at -80°C. An electrochemiluminescence (ECL) immunoassay was then performed using two multiplex cytokine assays (V-PLEX Proinflammatory Panel 1 Human Kit and V-PLEX Custom Human Cytokine; Meso Scale Diagnostics, Rockville, Maryland, USA) and a plate reader (MESO QuickPlex SQ 120; Meso Scale Diagnostics, Rockville, Maryland, USA). The following cytokines were analysed: IFN-γ, IL-1β, IL-2, IL-4, IL-6, IL-8, IL-10, IL-12p70, IL-13, IL-17, IL-23, and TNF-α. Only measurements of IFN-γ, IL-8, IL-10, and TNF-α demonstrated data sets where <5% of the observations were below detection range.

2.8. Statistical Analyses.

Data are presented as mean ± standard deviation (SD) or median and interquartile range (IQR) depending on data distribution as assessed by visual inspection of histograms and Q-Q plots. Group differences in demographics, clinical characteristics, and t-VNS aspects were assessed with Student's t-test, Mann-Whitney test, chi-squared, or Fisher's exact test. A mixed effect model and post hoc analyses were conducted on CVT, HR, BP, DAS28-CRP, and ASDAS and cytokines to test differences between pre- and posttreatment. CRP measurements below detection rates (<0.6) were assigned the value 0.60 for further

analyses. Cytokine measurements below detection rate were assigned a value corresponding to "Limit of detection/$\sqrt{2}$" [33]. If >5% of data were missing due to too low values, the cytokines were not analysed and included in the study. Linear associations were assessed using Pearson's correlation. As this was a preliminary exploratory proof of principle study, a sample size calculation was not performed. P values <0.05 were considered statistically significant. All statistical analyses were performed using a standard software package (Stata Statistical Software, Release 14; StataCorp LLC, College Station, TX, USA).

3. Results

3.1. Participant Disposition, Demographics, and General Characteristics.
A total of 118 possible participants were prescreened, and a total of 20 patients diagnosed with PsA and 20 patients diagnosed with AS were included in the study. For further details, see Figure 2. Due to concomitant infection (pneumonia and UTI) during the study, 3 patients diagnosed with AS were withdrawn by the study personnel, leaving 17 for final analyses.

The two cohorts differed in numbers treated with MTX usage, body mass index, and median stimulation amplitude. In other aspects, the groups displayed similar demographics; details are provided in Table 1.

3.2. Participants with Psoriatic Arthritis.
Cardiac-derived parameters ($n = 19$): CVT recordings from one patient in the PsA group were uninterpretable due to significant movement artefact. The acute response to t-VNS was a significant decrease in HR 20 minutes after stimulation (71 bpm vs. 68, $P = 0.019$). Furthermore, t-VNS caused a significant reduction in median CVT from baseline to day 5 (5.73 LVS vs. 4.69, $P = 0.017$).

Disease activity data ($n = 20$): t-VNS reduced median ASDAS from baseline to day 5 (2.22 vs. 2.03, $P = 0.012$). The clinical composite score DAS28-CRP was unchanged, but in comparison to baseline t-VNS caused a reduction in median CRP on day 2 (3.23 vs. 2.72, $P = 0.043$) and day 5 (3.23 vs. 2.59, $P = 0.001$).

Cytokine data ($n = 20$): t-VNS induced an increase in TNF-α on the 5th day (1.65 vs. 1.81, $P = 0.005$). Please see Figure 2 and Table 2 for details.

3.3. Participants with Ankylosing Spondylitis.
Cardiac-derived parameters ($n = 17$): the acute response to t-VNS was a significant decrease in HR (69 bpm vs. 65, $P = 0.028$) and an increase in median CVT (5.38 LVS vs. 6.03, $P = 0.027$).

Disease activity data ($n = 17$): t-VNS did not change DAS28-CRP, ASDAS, or CRP.

Cytokine data ($n = 17$): t-VNS induced a decrease in IFN-γ (4.36 vs. 3.76, $P = 0.02$), IL-8 (3.83 vs. 3.03, $P = 0.02$), and IL-10 (0.46 vs. 0.42, $P = 0.008$) on the 2nd day.

Please see Table 3 for details.

4. Discussion

This preliminary proof-of-concept report is the first to examine the potential anti-inflammatory effects of short-term t-VNS in patients with PsA and AS. t-VNS lowered HR in patients with PsA and reduced the objective biomarker CRP and clinical disease activity, despite slightly increased levels of the proinflammatory cytokine TNF-α. Taken together, we consider t-VNS as a promising add-on therapy to existing pharmaceutical intervention in PsA. In patients with AS, t-VNS lowered HR, increased the cardiac vagal tone, and reduced the proinflammatory cytokines IFN-γ, IL-8, and the anti-inflammatory cytokine IL-10, indicating modulation of the overall immune response in patients with AS.

4.1. The Link between Inflammation and Parasympathetic Tone.
It has become increasingly accepted that the ANS—and the VN in particular—is involved in control and regulation of the immune system, the so-called neuroimmune interaction [34]. Tracey has described an inflammatory reflex in which biochemical signals of systemic inflammation are transmitted to the brain by afferent vagal nerve fibres [20]. In response to these, the vagal nerve exerts a combined anti-inflammatory effect by activation of the hypothalamic-pituitary-adrenal (HPA) axis, the cholinergic anti-inflammatory pathway/reflex, and the spleen. Taken together, although considerable uncertainty exists, the clinical effect that we observed has been suggested to be mediated by vagal modulation of nociplastic pain including the inhibition of inflammation, the sympathetic tone, and the pain neuromatrix—all of which are factors that contribute to development of central sensitization and chronic pain [35].

In addition, a growing body of evidence supports the notion that inflammation is associated with a sympathovagal imbalance. For example, in a murine model, Huang et al. demonstrated that lipopolysaccharide-induced endotoxemia caused a sympathetic-vagal disequilibrium with an overexcitation of the sympathetic nervous system [36]. These findings suggest that systemic inflammation may lead to the observed imbalance in the ANS, supporting the afferent mechanism. Moreover, long-term VN stimulation using an implanted VNS-device reduced disease activity and inhibited production of TNF-α in patients with rheumatoid arthritis [21], suggesting treatment efficacy of t-VNS in similar autoimmune and inflammatory diseases.

In healthy participants, there is a wide range of normal CVT, ranging from 2 to 18 LVS [37]. In the two patient cohorts with PsA and AS, we demonstrated that median CVT at baseline was in the lower end, but not outside the normal range. This contrasts the findings in patients with chronic pancreatitis, Crohn's disease, and type 1 diabetes, where chronic inflammation and neuropathy are considered to influence the autonomic dysfunction [38–40]. In AS patients, we demonstrated that in response to bilateral t-VNS, the CVT was increased and HR reduced, implicating increase parasympathetic tone. We did not assess CVT between the two stimulations, and thus, this data does not contain information on the t-VNS modulatory effect of stimulating right versus left cervical vagal nerve. Nevertheless, the findings resemble those observed in healthy participants [25] and support that t-VNS has a modulatory effect on the parasympathetic branch in these patients. This modulation did however not cause any alterations in clinical disease activity.
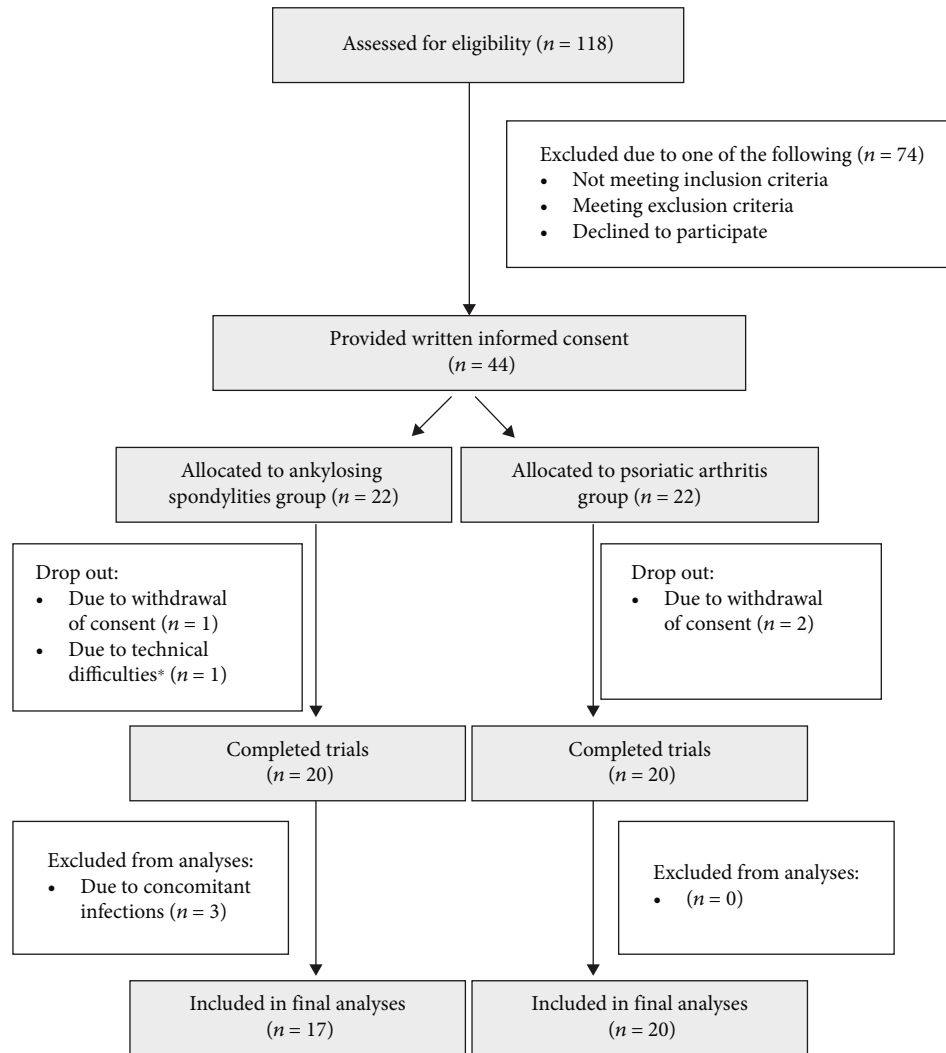
FIGURE 2: Flowchart illustrating screening process. *Temporary failure in the ECG-recording device.

In contrast, the PsA group failed to show acute increase in CVT but on the contrary demonstrated a decrease in CVT following stimulation. The different response in CVT, which is believed to reflect the efferent vagal tone accounting for 20% of the vagal nerve fibres, between the two cohorts may therefore be due to the differences in the pathogeneses of the diseases. For example, the promising effects of interleukin- (IL-) 17 and IL-23 inhibitors in patients with PsA (and not AS) suggest that there are differences in the nature of the inflammation between these patient groups [41]. Another explanation is that the response to t-VNS assessed with CVT seems to be influenced of systemic inflammation. For example, we have previously showed that CVT was raised in response to t-VNS in patients with rheumatoid arthritis in remission but not with flare [26], which may indicate that CVT is less robust in chronic inflammation; however, to clarify this, further investigations in other cohorts of inflammatory diseases are needed.

4.2. Vagal Nerve Stimulation and Anti-Inflammation. The basic scientific basis of the anti-inflammatory effect of t-

VNS is widely accepted. Physiological modulation of the parasympathetic tone has also been demonstrated to have analgesic effects in healthy subjects. Using a validated acid-induced oesophageal pain model of central sensitization, it was shown that deep breathing, which increased parasympathetic tone, exerted an analgesic effect. This effect that was abolished by the coadministration of atropine suggests the cholinergic mediated signalling [42]. Moreover, t-VNS prevented the development of, and reversed established, acid-induced oesophageal hypersensitivity, by increasing parasympathetic tone [35]. Moreover, synergistically applied deep breathing and electrical stimulation of the auricular branch of the VN in healthy increased experimental thresholds of bone pain, indicating analgesic properties [43]. Furthermore, a single bilateral t-VNS caused a significant increase in CVT and a serum reduction in TNF-α lasting for up to 24 hours [25]. Taken together, these results suggest therapeutic implications for the management of pain. In addition, VNS has demonstrated anti-inflammatory effect in patients with Crohn's disease [22] and Koopman et al. demonstrated that long-term (84 days) invasive VNS

TABLE 1: Patient characteristics.

	Psoriatic arthritis ($n = 20$)	Ankylosing spondylitis ($n = 17$)	P value
General characteristics*			
Age, (years, median (IQR))	45 (34-54)	45 (38-51)	0.77
Female, no. (%)	11 (55%)	6 (35%)	0.33
Disease duration, (years, median (IQR))	7 (3-8.5)	4.5 (2.5-15.5)	0.78
Caucasian ethnicity, no. (%)	20 (100%)	17 (100%)	N/A
Current smoker, no. (%)	1 (5%)	1 (6%)	1.00
Daily caffeine use, no. (%)	18 (90%)	16 (94%)	1.00
Methotrexate, no. (%)	15 (75%)	1 (6%)	<0.0001
Methotrexate dose amongst users, (mg per week)	16.5 ± 1.4	25 ± 0	0.15
Prescription NSAID, no. (%)	13 (65%)	11 (65%)	0.99
NSAID prescription dose (mg per day, median (IQR))	1200 (1000-1800)	1000 (800-1200)	0.11
Height (cm)	176.0 ± 10.6	177.4 ± 8.3	0.66
Weight (kilogram)	86.3 ± 17.6	79.3 ± 16.3	0.22
Body mass index (BMI)	27.7 ± 3.9	25.1 ± 4.4	0.02[†]
Vagnus nerve stimulation*			
Stimulations used (no./patient, median (IQR))	24 (24-25)	24 (22-24)	0.3
Stimulation amplitude (intensity) (intensity, median (IQR))	30 (29-35)	27 (25-30)	0.04[†]

*Data are presented as mean ± SD unless otherwise indicated. [†]Significant difference, $P < 0.05$.

TABLE 2: Result—psoriatic arthritis.

	Baseline	20 min	P value	Day 2	P value	Day 5	P value	Overall P value
Cardiometric data								
Cardiac vagal tone (LVS)*	5.73 (0.72)	5.68 (0.72)	0.892	5.49 (0.72)	0.531	4.69 (0.71)	0.007	0.023
Heart rate (bpm)	71 ± 3	68 ± 3	0.017	69 ± 3	0.077	73 ± 3	0.307	0.002
Systolic BP (mmHg)	130 ± 4	130 ± 4	0.872	126 ± 4	0.150	133 ± 4	0.141	0.031
Diastolic BP (mmHg)	83 ± 3	85 ± 3	0.310	82 ± 3	0.710	85 ± 3	0.173	0.255
Disease activity								
DAS28-CRP*	2.54 (0.16)	-	-	2.53(0.16)	0.876	2.45 (0.16)	0.162	0.309
ASDAS*	2.22 (0.20)	-	-	2.07 (0.20)	0.063	2.03 (0.20)	0.012	0.033
CRP (mg/L)*	3.23 (0.84)	-	-	2.72 (0.84)	0.043	2.59 (0.84)	0.001	0.004
Cytokines								
IFN-γ (pg/L)*	4.96 (0.92)	-	-	5.19 (0.12)	0.735	6.27 (0.89)	0.101	0.089
IL-8 (pg/mL)	3.41 (0.30)	-	-	3.72 (0.30)	0.324	3.99 (0.30)	0.061	0.172
IL-10 (pg/mL)	0.29 (0.05)	-	-	0.26 (0.04)	0.281	0.30 (0.05)	0.482	0.193
TNF-α (pg/mL)	1.65 (0.17)	-	-	1.69 (0.17)	0.476	1.81 (0.17)	0.005	0.014

*Data are presented as estimated mean and standard error.

significantly reduced disease activity and serum levels of TNF-α in patients with rheumatoid arthritis [21]. These intriguing results are in line with a novel study using t-VNS in 5 days, showing reduced disease activity (DAS28-CRP), CRP, and interferon-γ in patients with rheumatoid arthritis and flare [26].

In contrast to these studies, PsA patients in the current study were only stimulated during a 5-day protocol, and in response to that, we saw a clear reduction of clinical disease activity measured by the ASDAS score, associated with a 20% reduction in CRP, and such disease attenuation would not otherwise be expected in the normal natural history of this disorder. We saw that t-VNS modulated the immune response in both diseases.

The immune response is complex and can be considered as a dynamic balance between pro- and anti-inflammatory cytokines, as it requires and responds to continuous feedback mechanisms at the molecular, organ, and whole-host level.

TABLE 3: Results—ankylosing spondylitis.

	Baseline	20 min	P value	Day 2	P value	Day 5	P value	Overall P value
Cardiometric data								
Cardiac vagal tone (LVS)	5.59 (0.77)	6.56 (0.77)	0.014	5.75 (0.77)	0.692	5.22 (0.77)	0.361	0.008
Heart rate (bpm)	69 ± 3	65 ± 3	0.009	67 ± 3	0.401	68 ± 3	0.796	0.041
Systolic BP (mmHg)	131 ± 4	131 ± 4	0.822	129 ± 4	0.565	131 ± 4	0.920	0.861
Diastolic BP (mmHg)	83 ± 3	83 ± 3	0.900	83 ± 3	0.616	83 ± 3	0.900	0.911
Disease activity								
DAS28-CRP	1.78 (0.17)	-	-	1.76 (0.17)	0.598	1.77 (0.17)	0.845	0.868
ASDAS	1.75 (0.21)	-	-	1.66 (0.21)	0.128	1.67 (0.21)	0.139	0.220
CRP (mg/L)	3.02 (0.88)	-	-	3.08 (0.88)	0.784	3.09 (0.88)	0.211	0.408
Cytokines								
IFN-γ (pg/L)	4.36 (0.95)	-	-	3.76 (0.95)	0.017	4.44 (0.95)	0.440	0.055
IL-8 (pg/mL)	3.83 (0.33)	-	-	3.03 (0.35)	0.024	3.90 (0.33)	0.840	0.026
IL-10 (pg/mL)	0.46 (0.05)	-	-	0.42 (0.05)	0.008	0.44 (0.05)	0.090	0.024
TNF-α (pg/mL)	1.43 (0.19)	-	-	1.44 (0.19)	0.861	1.51 (0.19)	0.167	0.331

*Data are presented as estimated mean and standard error.

Interpretation of the observed decreased anti-inflammatory and increased proinflammatory cytokines should be done with caution because patients were investigated at relatively low levels of inflammation due to concomitant immunomodulatory treatment and disease remission *ab initio*; other studies have used lipopolysaccharide-stimulated blood samples, and the focus on the dynamic balance which may not necessarily be quantitative (e.g., equal concentrations of pro- and anti-inflammatory cytokines) but rather should be considered as a qualitative harmonization in downstream activation and inhibition [44].

5. Limitations

This study has some intrinsic limitations. Firstly, as this was an open-label study, it was conducted without blinding and thus the lack of a placebo-arm/sham stimulation limits any firm conclusion on the anti-inflammatory efficacy of t-VNS in PsA and AS. Secondly, the small sample size, although comparable to similar studies, limits the generalisability of these findings. Nevertheless, further work is now warranted in larger patient groups with higher disease activity, with a potential possibility of categorizing participants according to their current treatment regimens, e.g., biological and/or conventional DMARDs. Thirdly, the assessment of clinical disease activity may have been vulnerable to bias as the reduction in the clinical scores such as DAS28-CRP and ASDAS yields a subjective part, which involves an assessment of tender and swollen joints. However, the natural history of PsA and AS and the clear objective reduction in CRP levels in PsA support that an anti-inflammatory effect was achieved through t-VNS in the short five-day treatment period. Finally, in spite of our efforts in terms of education and training in t-VNS stimulation, we cannot guarantee that participants positioned the gammaCore correctly at every stimulation, and thus, insufficient stimulation may have

occurred; however, the decreased HR supports that the t-VNS modulated the ANS in patients with PsA and AS.

In conclusion, this open-label preliminary report provides support for an anti-inflammatory effect of t-VNS in patients with PsA and AS, evident as convincing reduction in HR, disease activity, and CRP-levels. This raises the fascinating possibility of using neuromodulation as an add-on to existing pharmacological treatments; however, these initial findings warrant further investigation in larger randomized sham-controlled trials.

Data Availability

Data is available upon request to the corresponding author.

Disclosure

The company had no influence on study design, data collection, or data analysis.

Conflicts of Interest

None of the authors have conflicts of interest to declare.

Authors' Contributions

All authors contributed to the authoring of this paper and approved the final manuscript.

Acknowledgments

analysing blood samples. Additionally, the authors would like to thank the participating patients.

References

[1] Y. Alamanos, P. Voulgari, and A. A. Drosos, "Incidence and prevalence of psoriatic arthritis: a systematic review," *The Journal of Rheumatology*, vol. 35, pp. 1353–1358, 2008.

[2] J.-T. Liu, H.-M. Yeh, S.-Y. Liu, K.-T. Chen Jung-Tai Liu, and K.-T. Chen, "Psoriatic arthritis: epidemiology, diagnosis, and treatment," *World Journal of Orthopedics*, vol. 18, pp. 537–543, 2014.

[3] L. E. Dean, G. T. Jones, A. G. Macdonald, C. Downham, R. D. Sturrock, and G. J. Macfarlane, "Global prevalence of ankylosing spondylitis," *Rheumatology (Oxford)*, vol. 53, no. 4, pp. 650–657, 2014.

[4] C. Han, D. W. Robinson Jr., M. V. Hackett, L. C. Paramore, K. H. Fraeman, and M. V. Bala, "Cardiovascular disease and risk factors in patients with rheumatoid arthritis, psoriatic arthritis, and ankylosing spondylitis," *The Journal of Rheumatology*, vol. 33, no. 11, pp. 2167–2172, 2006.

[5] A. Ogdie, K. Haynes, A. B. Troxel et al., "risk of mortality in patients with psoriatic arthritis, rheumatoid arthritis and psoriasis: a longitudinal cohort study," *Annals of the Rheumatic Diseases*, vol. 73, no. 1, pp. 149–153, 2014.

[6] G. Bakland, J. T. Gran, and J. C. Nossent, "Increased mortality in ankylosing spondylitis is related to disease activity," *Annals of the Rheumatic Diseases*, vol. 70, no. 11, pp. 1921–1925, 2011.

[7] W. Tillett, G. Shaddick, A. Askari et al., "Factors influencing work disability in psoriatic arthritis: first results from a large UK multicentre study," *Rheumatology*, vol. 54, no. 1, pp. 157–162, 2015.

[8] D. Van Der Heijde, S. Ramiro, R. Landewé et al., "2016 update of the ASAS-EULAR management recommendations for axial spondyloarthritis," *Annals of the Rheumatic Diseases*, vol. 76, no. 6, pp. 978–991, 2017.

[9] L. Gossec, J. S. Smolen, S. Ramiro et al., "European League Against Rheumatism (EULAR) recommendations for the management of psoriatic arthritis with pharmacological therapies: 2015 update," *Annals of the Rheumatic Diseases*, vol. 75, no. 3, pp. 499–510, 2016.

[10] A. Kavanaugh, P. J. Mease, A. M. Reimold et al., "Secukinumab for long-term treatment of psoriatic arthritis: a two-year followup from a phase III, randomized, double-blind placebo-controlled study," *Arthritis Care & Research*, vol. 69, no. 3, pp. 347–355, 2017.

[11] C. Ritchlin, P. Rahman, A. Kavanaugh et al., "Efficacy and safety of the anti-IL-12/23 p40 monoclonal antibody, ustekinumab, in patients with active psoriatic arthritis despite conventional non-biological and biological anti-tumour necrosis factor therapy: 6-month and 1-year results of the phase 3, multicentre, double-blind, placebo-controlled, randomised PSUMMIT 2 trial," *Annals of the Rheumatic Diseases*, vol. 73, no. 6, pp. 990–999, 2014.

[12] A. Kavanaugh, L. Puig, A. B. Gottlieb et al., "Maintenance of clinical efficacy and radiographic benefit through two years of stekinumab therapy in patients with active psoriatic arthritis: results from a randomized, placebo-controlled phase III trial," *Arthritis Care & Research*, vol. 67, no. 12, pp. 1739–1749, 2015.

[13] R. Conway and J. J. Carey, "Risk of liver disease in methotrexate treated patients," *World Journal of Hepatology*, vol. 9, no. 26, pp. 1092–1100, 2017.

[14] P. A. Bryant and J. W. Baddley, "Opportunistic infections in biological therapy, risk and prevention," *Rheumatic Disease Clinics of North America*, vol. 43, no. 1, pp. 27–41, 2017.

[15] D. M. Saunte, U. Mrowietz, L. Puig, and C. Zachariae, "Candida infections in patients with psoriasis and psoriatic arthritis treated with interleukin-17 inhibitors and their practical management," *British Journal of Dermatology*, vol. 177, no. 1, pp. 47–62, 2017.

[16] C. Ambarus, N. Yeremenko, P. P. Tak, and D. Baeten, "Pathogenesis of spondyloarthritis: autoimmune or autoinflammatory?," *Current Opinion in Rheumatology*, vol. 24, no. 4, pp. 351–358, 2012.

[17] L. V. Borovikova, S. Ivanova, M. Zhang et al., "Vagus nerve stimulation attenuates the systemic inflammatory response to endotoxin," *Nature*, vol. 405, no. 6785, pp. 458–462, 2000.

[18] B. Bonaz, V. Sinniger, and S. Pellissier, "Vagus nerve stimulation: a new promising therapeutic tool in inflammatory bowel disease," *Journal of Internal Medicine*, vol. 282, no. 1, pp. 46–63, 2017.

[19] M. Rosas-Ballina, M. Ochani, W. R. Parrish et al., "Splenic nerve is required for cholinergic antiinflammatory pathway control of TNF in endotoxemia," *Proceedings of the National Academy of Sciences of the United States of America*, vol. 105, no. 31, pp. 11008–11013, 2008.

[20] K. J. Tracey, "The inflammatory reflex," *Nature*, vol. 420, no. 6917, pp. 853–859, 2002.

[21] F. A. Koopman, S. S. Chavan, S. Miljko et al., "Vagus nerve stimulation inhibits cytokine production and attenuates disease severity in rheumatoid arthritis," *Proceedings of the National Academy of Sciences*, vol. 113, no. 29, pp. 8284–8289, 2016.

[22] B. Bonaz, V. Sinniger, D. Hoffmann et al., "Chronic vagus nerve stimulation in Crohn's disease: a 6-month follow-up pilot study," *Neurogastroenterology & Motility*, vol. 28, no. 6, pp. 948–953, 2016.

[23] E. L. Air, Y. M. Ghomri, R. Tyagi, A. W. Grande, K. Crone, and F. T. Mangano, "Management of vagal nerve stimulator infections: do they need to be removed?," *Journal of Neurosurgery: Pediatrics*, vol. 3, no. 1, pp. 73–78, 2009.

[24] E. Ben-Menachem, D. Revesz, B. J. Simon, and S. Silberstein, "Surgically implanted and non-invasive vagus nerve stimulation: a review of efficacy, safety and tolerability," *European Journal of Neurology*, vol. 22, no. 9, pp. 1260–1268, 2015.

[25] C. Brock, B. Brock, Q. Aziz et al., "Transcutaneous cervical vagal nerve stimulation modulates cardiac vagal tone and tumor necrosis factor-alpha," *Neurogastroenterology & Motility*, vol. 29, no. 5, 2017.

[26] A. Drewes, C. Brock, S. Rasmussen et al., "Short-term transcutaneous non-invasive vagus nerve stimulation may reduce disease activity and pro-inflammatory cytokines in rheumatoid arthritis: results of a pilot study," *Scandinavian Journal of Rheumatology*, vol. 50, no. 1, pp. 20–27, 2021.

[27] C. J. L. Little, P. O. O. Julu, S. Hansen, and S. W. J. Reid, "Real-time measurement of cardiac vagal tone in conscious dogs," *American Journal of Physiology - Heart and Circulatory Physiology*, vol. 276, no. 2, pp. H758–H765, 1999.

[28] T. R. Jenkinson, P. A. Mallorie, H. C. Whitelock, L. G. Kennedy, S. L. Garrett, and A. Calin, "Defining spinal mobility in

ankylosing spondylitis (AS). The Bath AS Metrology Index," *The Journal of Rheumatology*, vol. 21, no. 9, pp. 1694–1698, 1994.

[29] M. Schoels, "Psoriatic arthritis indices," *Clinical and Experimental Rheumatology*, vol. 35, pp. 109–112, 2014.

[30] B. Michelsen, R. Fiane, A. P. Diamantopoulos et al., "A comparison of disease burden in rheumatoid arthritis, psoriatic arthritis and axial spondyloarthritis," *PloS One*, vol. 10, no. 4, p. e0123582, 2015.

[31] G. Wells, J.-C. Becker, J. Teng et al., "Validation of the 28-joint Disease Activity Score (DAS28) and European League Against rheumatism response criteria based on C-reactive protein against disease progression in patients with rheumatoid arthritis, and comparison with the DAS28 based on erythrocyte sedimentation rate," *Annals of the Rheumatic Diseases*, vol. 68, no. 6, pp. 954–960, 2009.

[32] P. M. Machado and S. P. Raychaudhuri, "Disease activity measurements and monitoring in psoriatic arthritis and axial spondyloarthritis," *Best Practice & Research Clinical Rheumatology*, vol. 28, no. 5, pp. 711–728, 2014.

[33] C. Croghan and P. P. Egeghy, "Methods of dealing with values below the limit of detection using SAS," *Southern SAS User Group*, vol. 22, p. 24, 2003.

[34] S. Rasmussen, M. Pfeiffer-Jensen, A. Drewes et al., "Vagal influences in rheumatoid arthritis," *Scandinavian Journal of Rheumatology*, vol. 47, no. 1, pp. 1–11, 2018.

[35] A. D. Farmer, A. Albusoda, G. Amarasinghe et al., "Transcutaneous vagus nerve stimulation prevents the development of, and reverses, established oesophageal pain hypersensitivity," *Alimentary Pharmacology and Therapeutics*, vol. 52, no. 6, pp. 988–996, 2020.

[36] J. Huang, Y. Wang, D. Jiang, J. Zhou, and X. Huang, "The sympathetic-vagal balance against endotoxemia," *Journal of Neural Transmission*, vol. 117, no. 6, pp. 729–735, 2010.

[37] A. D. Farmer, S. J. Coen, M. Kano et al., "Normal values and reproducibility of the real-time index of vagal tone in healthy humans: a multi-center study," *Annals of Gastroenterology*, vol. 27, no. 4, pp. 362–368, 2014.

[38] J. Juel, C. Brock, S. S. Olesen et al., "Acute physiological and electrical accentuation of vagal tone has no effect on pain or gastrointestinal motility in chronic pancreatitis," *Journal of Pain Research*, vol. Volume 10, pp. 1347–1355, 2017.

[39] C. Brock, N. Jessen, B. Brock et al., "Cardiac vagal tone, a non-invasive measure of parasympathetic tone, is a clinically relevant tool in type 1 diabetes mellitus," *Diabetic Medicine*, vol. 34, no. 10, pp. 1428–1434, 2017.

[40] T. Engel, S. Ben-Horin, and M. Beer-Gabel, "Autonomic dysfunction correlates with clinical and inflammatory activity in patients with Crohn's disease," *Inflammatory Bowel Diseases*, vol. 21, no. 10, pp. 2320–2326, 2015.

[41] P. J. Mease, "Inhibition of interleukin-17, interleukin-23 and the TH17 cell pathway in the treatment of psoriatic arthritis and psoriasis," *Current Opinion in Rheumatology*, vol. 27, no. 2, pp. 127–133, 2015.

[42] C. Botha, A. D. Farmer, M. Nilsson et al., "Preliminary report: modulation of parasympathetic nervous system tone influences oesophageal pain hypersensitivity," *Gut*, vol. 64, no. 4, pp. 611–617, 2015.

[43] J. B. Frøkjær, S. Bergmann, C. Brock et al., "Modulation of vagal tone enhances gastroduodenal motility and reduces somatic pain sensitivity," *Neurogastroenterology and Motility*, vol. 28, no. 4, pp. 592–598, 2016.

[44] J. M. Cicchese, S. Evans, C. Hult et al., "Dynamic balance of pro- and anti-inflammatory signals controls disease and limits pathology," *Immunological Reviews*, vol. 285, no. 1, pp. 147–167, 2018.

Research Article

Basil Polysaccharide Reverses Development of Experimental Model of Sepsis-Induced Secondary Staphylococcus aureus Pneumonia

Xi Chen,[1] Yue He,[2] Qiang Wei,[1] and Chuanjiang Wang [iD] [3]

[1]*Department of Laboratory Medicine, The First Affiliated Hospital of Chongqing Medical University, Chongqing, China*
[2]*Department of Urology, North Kuanren General Hospital, Chongqing, China*
[3]*Department of Critical Care Medicine, The First Affiliated Hospital of Chongqing Medical University, Chongqing, China*

Correspondence should be addressed to Chuanjiang Wang; wangchuanjiang@cqmu.edu.cn

Background. Basil polysaccharide (BPS) represents a main active ingredient extracted from basil (Ocimum basilicum L.), which can regulate secondary bacterial pneumonia development in the process of sepsis-mediated immunosuppression. *Methods.* In this study, a dual model of sepsis-induced secondary pneumonia with cecal ligation and puncture and intratracheal instillation of *Staphylococcus aureus* or *Pseudomonas aeruginosa* was constructed. *Results.* The results indicated that BPS-treated mice undergoing CLP showed resistance to secondary *S. aureus* pneumonia. Compared with the IgG-treated group, BPS-treated mice exhibited better survival rate along with a higher bacterial clearance rate. Additionally, BPS treatment attenuated cell apoptosis, enhanced lymphocyte and macrophage recruitment to the lung, promoted pulmonary cytokine production, and significantly enhanced CC receptor ligand 4 (CCL4). Notably, recombinant CCL4 protein could enhance the protective effect on *S. aureus*-induced secondary pulmonary infection of septic mice, which indicated that BPS-induced CCL4 partially mediated resistance to secondary bacterial pneumonia. In addition, BPS priming markedly promoted the phagocytosis of alveolar macrophages while killing *S. aureus in vitro*, which was related to the enhanced p38MAPK signal transduction pathway activation. Moreover, BPS also played a protective role in sepsis-induced secondary *S. aureus* pneumonia by inducing Treg cell differentiation. *Conclusions.* Collectively, these results shed novel lights on the BPS treatment mechanism in sepsis-induced secondary *S. aureus* pneumonia in mice.

1. Introduction

Sepsis is a complex immunopathological syndrome characterized by life-threatening organ dysfunction caused by a deregulated host response to systemic infection [1]. It is attributed to a persistent and complicated interaction of the proinflammatory process with the anti-inflammatory one in the body, leading to high inflammatory response and subsequent immune dysfunction [2, 3]. Globally, sepsis continues to be a major reason for deaths at intensive care unit (ICU) [4]. Recently, a global study reported approximately 49 million diagnosed patients along with 11 million deaths due to sepsis in the world in 2017, which accounted for around 20% total death cases globally. Furthermore, a study reported

that the pooled incidence of hospital-treated sepsis patients was 189/100,000 person-years, whereas the estimated mortality rate was 26.7%. The study also reported that the prevalence of ICU-treated sepsis was 58/100,000 person-years, including 41.9% dying before hospital discharge. Notably, the incidence of hospital-treated sepsis considerably increased after 2008 [5]. Great inflammatory response is previously reported to induce sepsis-related deaths early, whereas compensatory anti-inflammatory response is suggested to cause deaths following organ failure via the dominant congenital immunity, affecting endothelial function, blood flow, and parenchymal cell metabolism [6]. However, recent studies have revealed that the persistent counterregulatory anti-inflammatory and proinflammatory state

triggered by the imbalanced innate along with restrained adaptive immune responses leads to prolonged organ damage and dysfunction, leading to patient death [7]. Primary infections in patients with severe sepsis may not be the leading cause of death; however, persistent inflammation and immunosuppression represent the predominant cause of secondary infections and mortality [8]. In recent years, the increased prevalence of infection with antibiotic-resistant bacteria represents a significant challenge to the effective treatment of sepsis-induced secondary bacterial pneumonia in the hospital [9]. Pulmonary immunity exerts an important part in resisting the pulmonary respiratory pathogens, while different inflammatory mediators (such as chemokines, cytokines, or growth factors) modulate responses to various kinds of infection or injury [10]. Thus, further understanding pulmonary immunity together with the molecular and cellular immune responses upon microbial infection would significantly enhance our understanding of secondary lung infections' pathogenesis during the immunosuppressive phase of sepsis. Several studies have identified the association between suppression-mediated immunosuppression and secondary bacteria-induced pulmonary infection. Moreover, macrophage dysfunction [11], neutrophil paralysis [12], and lymphopenia [13] are related to secondary bacteria-induced pulmonary infection post-sepsis. Therefore, the immunosuppression induced by sepsis may markedly alter the modulation of pulmonary immunity in the host, resulting in the enhanced sensitivity among septic cases complicated by nosocomial pneumonia [14].

Basil or *Ocimum basilicum* L., belongs to the family Lamiaceae, is known as the "king of herbs" due to its extensive traditional use in medicine and for culinary and perfumery purposes worldwide. It is native to Southeast Asia, America, and parts of Africa and frequently planted within the gardens and pots across Southwest Asia, the USA, and Europe [15]. Basil has been shown to exhibit potential pharmacological effects, including anticancer, antistress, antidiabetic, antipyretic, antioxidant, immunomodulatory, hypolipidemic antiatherosclerotic effect, and antibacterial activities [16–19]. Among the essential active compounds of basil, basil polysaccharide has been shown to exhibit a variety of pharmacological activities [20]. Studies have demonstrated that basil polysaccharide (BPS) is adopted to be the immunopotentiator for stimulating macrophages, protecting immune organs, while building the complement system for exerting immune enhancement effects. Moreover, basil polysaccharide exhibits good antibacterial activity [21]. BPS can also inhibit various bacteria infected in clinic [22, 23]. Currently, BPS has been extensively utilized to lower blood lipids, prevent atherosclerosis, and treat cancer and diabetes [24, 25]. However, there is a paucity of literature on the effects of basil polysaccharide on sepsis-induced secondary bacterial infection in the lungs.

Hospital-acquired secondary pneumonia, a frequent nosocomial bacterial infection, accounts for a major reason leading to deaths among severe sepsis cases [26]. Organisms causing hospital-acquired secondary pneumonia leading to severe sepsis are dominated by *Staphylococcus aureus* (20.5%), followed by *Pseudomonas* species (19.9%), fungi (19%), and Enterobacter (mostly *Escherichia coli*, 16.0%) [27]. Herein, a dual model of sepsis-induced secondary pneumonia with cecal ligation and puncture (CLP) along with intranasal instillation of *Pseudomonas aeruginosa* or *Staphylococcus aureus* was established to elucidate the effects of basil polysaccharide in sepsis-induced secondary lung bacterial infection.

2. Materials and Methods

2.1. Animals. The 8-12-week-old C57BL/6 male mice (weight, 20-24 g) were provided by Laboratory Animal Center of Chongqing Medical University (Chongqing, China). The license number is SYXK (Chongqing, China) 2018-0003. Thereafter, all animals were raised in the specific pathogen-free (SPF) environment under 24°C, 50%-60% relative humidity (RH), and 12 h/12 h light/dark cycle conditions. Each mouse was allowed to drink water and eat standard food. Each animal was healthy and infection-free throughout the experiment.

All mice were treated following the Guidelines for the Care and Use of Laboratory Animals in China. The Institutional Animal Care and Use Committee of Chongqing Medical University approved our study protocol.

2.2. "Double-Hit" Mice Model. CLP and intratracheal injection of *S. aureus* or *P. aeruginosa* were carried out as the first and second hits, respectively. Briefly, each mouse was given intraperitoneal injection of ketamine (1 mg/ml) and 100 μl xylazine (20 mg/ml) contained within PBS for anesthesia, followed by cecal ligation and puncture using the 26G needle (nonsevere CLP, resulting in the mortality rate of 5%–10% in WT mice). Later, we put back the cecum into peritoneal cavity, followed by incision closure using the surgical staples. All mice were given subcutaneous administration of 0.9% sterile normal saline at the dose of 5 ml/100 g body weight (BW) preheated at 37°C for replacing the 3rd space loss; thereafter, the warm pad was prepared for resuscitation [28].

At 3 days after CLP, the xylazine/ketamine mixture was administered into the surviving mice for anesthesia. Then, each mouse was placed in the "head-up" position, and the trachea was exposed, followed by intratracheal injection (i.t.) with *P. aeruginosa* (5×10^7 colony-forming units (CFUs) within 50 μl PBS) or *S. aureus* (5×10^7 CFUs within 50 μl PBS) [29].

2.3. In Vivo Administration of Basil Polysaccharides. For *in vivo* basil polysaccharide treatment, each mouse was administered i.p. with 75 mg/kg of basil polysaccharides [30] (Shanxi kingreg Biotech. Ltd., China) or IgG 2 h after the second hit. With regard to CCL4 exposure *in vivo*, all animals were given 500 ng IgG or recombinant mouse CCL4 (R&D Systems, USA) i.p. at the time of the second hit of *S. aureus*.

2.4. Lung Tissue and Bronchoalveolar Lavage Fluid Collection. At 24 h following S. aureus or P. aeruginosa i.t., the animals were killed under anesthesia. Lungs were extracted, and tissues were harvested, followed by the immediate collection of bronchoalveolar lavage fluid (BALF). After

chest clapping, right bronchial bundling and left lung lavage were carried out. In addition, after resecting the right lung, we obtained the right upper lobe to count the bacterial numbers, whereas the rest right lung tissues were preserved under −70°C at once for further analysis.

2.5. Determination of Lung and Plasma Bacterial Burdens.

Plasma samples were obtained at specific time periods. Meanwhile, we also resected the right upper lung lobe under aseptic condition, followed by homogenization within 1 ml sterile saline using the tissue homogenizer by the use of a vented hood. Later, we diluted plasma and lung homogenate at serial concentrations. For every dilution, 10 ml sample was added on the predried tryptic soy-base blood agar plates, followed by overnight incubation under 37°C. Afterwards, CFUs were counted and expressed as total CFU per lung or per milliliter of plasma.

2.6. Measurement of Inflammatory Mediators.

Blood samples were collected in heparinized tubes *via* the ophthalmic vein. Inflammatory mediators, such as CCL4, IL-10, CXCL-1, TNF-α, IL-1β, IL-6, and IL-17A, were assessed by the Mice Cytokine Magnetic Bead Panel Kit (eBioscience, USA) following the manufacturer's protocol.

2.7. Determination of Chemokine CCL4 Produced by Neutrophils.

The neutrophils were sorted from the bronchoalveolar lavage using magnetic separation (Miltenyi Biotec) and were suspended in 10% FBS (Sigma, USA) and RPMI1640 (Sigma, USA) and then inoculated on the culture plate. To determine whether basil polysaccharides promote the secretion of CCL4 by neutrophils, we supplemented basil polysaccharide [31] (100 μg/ml, kingreg Biotech, China) or PBS to the culture. After incubation for 48 h, the chemokine CCL4 in the supernatant was quantified by ELISA using kits (R&D, USA) following specific protocols. The absorbance of each sample was read at 450 nm.

2.8. Lung Injury Index Assessment.

Lung injury index assessment is as follows: (1) Morphological evaluation: as for the right upper lung lobe, it was subjected to 10% formalin fixation, paraffin embedding, and sectioning into 4 μm sections. Then, the sections were deparaffinized, dehydrated, and stained by hematoxylin and eosin (H&E) to carry out histological examinations. Mikawa's method was adopted to estimate lung injury score by adopting the 4 indicators below: (1) alveolar hyperemia, (2) hemorrhage, (3) neutrophil or interstitial aggregation or infiltration, (4) hyaline membrane formation or alveolar septal thickening, where 0-4 marks indicated no/very mild, mild, moderate, severe, and very severe damage, respectively. All scores were added up as the final score, and the ARDS pathological score was indicative of increases in lesion number. Lung injury was rated according to the 0-4 scale based on lesion severity of every indicator, where 0-4 points indicated normal results, mild (<25%), moderate (25-50%), severe (50-75%), and very severe (>75%) lung involvements, separately. A greater score was indicative of the more severe lesion. The light microscope (Olympus, Japan) was utilized to evaluate the abnormal histological results. (2) Albumin assessment: albumin for lung permeability assessment was performed using a Albumin Quantification Kit (Bethyl Laboratories, Montgomery, TX) following specific protocols. (3) Myeloperoxidase (MPO) measurement: the MPO activity in the tissue was measured to quantify lung neutrophil infiltration. In brief, we homogenized lung tissues with the 20 mmol/l PBS (pH 7.4), followed by 10 min of centrifugation at 4°C and 10,000 g. Later, pellets were resuspended with 50 mmol/l PBS (pH 6.0) contained within 0.5% hexadecyltrimethylammonium bromide (Sigma), and then, the homogenate was treated with 4 freeze-thawing cycles, followed by 40 s of sonication for disruption. Afterwards, the samples were subjected to 5 min of centrifugation for 40 s at 10,000 g and 40,000 ion. The sample was assayed for the myeloperoxidase activity according to previous description, with tetramethylbenzidine (Sigma) being the substrate. Later, we detected the absorbance (OD) values at 460 nm and adjusted them based on tissue weights (fold change (FC) relative to control). (4) Wet/dry weight: after dissecting left lung, we weighed the wet weight. The lung was incubated, then dried in an oven at 60°C for 3–4 days and reweighed as dry weight. Then, the wet weight was divided by dry weight to calculate the wet-to-dry (W/D) weight ratio [32]

2.9. TUNEL Assay.

The In situ Cell Apoptosis Detection Kit I, POD (Roche, Switzerland) was utilized to measure cell apoptosis rate by TUNEL assay following specific instructions. In brief, after xylene deparaffinage, the 4 μm sections were subjected to gradient ethanol rehydration. Thereafter, 3% hydrogen peroxide (H_2O_2) was used to block endogenous peroxidase activity for a period of 10 min; afterwards, 10–20 μg/ml proteinase K solution was utilized to digest sections under 37°C for 15 min. After PBS washing, terminal deoxynucleotidyl transferase diluted at 1 : 20 supplemented within the reaction buffer (digoxigenin-labeled nucleotides) was used to react with sections for 2 h under 37°C. Thereafter, the stop/wash buffer was used to rinse slides for 2 min thrice. Subsequently, antidigoxin antibody previously diluted at 1 : 100 was used to incubate sections under 37°C for 30 min, and later, ABC was employed to further incubate sections for 30 min under 37°C. Apoptosis was measured through incubating sections using 3,3′-diaminobenzidine chromogen for about 20 min, followed by hematoxylin counterstaining. Later, 5 fields of view (FOVs) were selected randomly from every section (×400 magnification). Then, TUNEL-positive cell proportion per field was recorded at ×400 magnification in 5 random fields.

2.10. Western Blot Analysis.

The protein extraction kit (Beyotime, China) was utilized to extract total macrophage proteins in accordance with specific protocols. Bicinchoninic acid (BCA) protein assay kit (Pierce, USA) was employed for detecting protein contents. Thereafter, proteins were separated through 10%SDS-PAGE, followed by transfer to the nitrocellulose membranes. After transfer, the membranes were incubated in blocking buffer containing 5% (w/v) skimmed milk supplemented within the Tris-buffered saline that contained 0.05% Tween-20, followed by overnight incubation with primary antibody under 4° C and then secondary

antibody incubation. At last, the ECL detection system was used to visualize protein blots.

2.11. Flow Cytometry. After PBS washing, cells were prepared into pellets and analyzed by the flow cytometer. The following monoclonal antibodies including CD4, CD25, Foxp3, CD11b, Ly6G, F4/80. To stain CD4, CD25, Foxp3, CD11b, Ly6G, F4/80, the Fixation/Permeabilization kit (eBioscience, USA), anti-CD4-FITC, anti-CD11b-APC, anti-Ly6G-FITC, anti-F4/80-FITC, anti-CD25-PE, and anti-Foxp3-APC (eBioscience, USA) were utilized following specific protocols. The FACScan flow cytometer (Becton Dickinson) was used to collect cells (10^5), whereas FlowJo software 7.6 was adopted for analysis.

2.12. Cell Purification and Culture. We adopted the Lymphocyte Separation Medium (GE healthcare, USA) to isolate splenic peripheral blood mononuclear cells (PBMCs) from mice. Thereafter, magnetic activated cell sorting (Miltenyi Biotec) was carried out to isolate naïve CD4+ T cells from PBMCs using the Naïve CD4+ T Cell Isolation Kit II (Stem-Cell, Canada) following specific protocols. Then, flow cytometric analysis was performed to measure the naïve CD4+ T cell purity (> 90%). Then, we cultivated cells within the RPMI 1640 complete medium (Gibco, Grand Island, NY, USA) that contained 10% fetal bovine serum (FBS) and incubated them under 37°C and 5% CO_2 conditions.

2.13. Treg Cell Subset Generation. In this study, we produced Treg cell subsets through exposing to 50 mM β-mercaptoethanol, 2 mM L-glutamine, 2 μg/ml anti-CD28, 5 μg/ml anti-CD3, 2.5 ng/ml TGF-β, and 50 U/ml IL-2 for a period of 3 days. To determine whether basil polysaccharide was involved in the induction process, we supplemented basil polysaccharide (100 μg/ml, kingreg Biotech, China) to the culture. Flow cytometric analysis was performed to assess intracellular staining and surface marker expression.

2.14. Macrophage Phagocytosis Assays. BALFs were incubated using 0.5 mg/ml FITC (Sigma) under 37°C for 20 min, so that macrophages adhered to the plastic, FITC-labeled S. aureus for separation. Thereafter, FITC-labeled bacteria (MOI, 100) were used to incubate the separated macrophages under 37°C for 30 min. Then, cells were washed, and nuclei were subjected to DAPI (Invitrogen) staining and visualized under the confocal laser scanning microscope (LSM 510, Zeiss). One independent reviewer was responsible for quantifying engulfed bacterial proportion of the 300 cells counted/well. For certain experiments, 100 μg/ml BPS (kingreg Biotech, China) was used to pretreat bronchoalveolar macrophages before infection with FITC-labeled S. aureus.

2.15. Macrophage Killing Assays. Alive S. aureus (with the multiplicity of infection (MOI) of 10) was used to infect 1 $\times 10^5$ bronchoalveolar macrophages for 1 h under 37°C. Later, buffer that contained 100 μg/ml tobramycin was adopted to wash cells for removing extracellular bacteria, whereas lysis buffer (Promega) was used for lysis. Lysate culture was utilized to quantify alive intracellular bacteria so as to assess bacterial uptake as well as intracellular killing

($t = 0$ and 2, respectively). Killing was determined by colony proportion occurring at $t = 2$ h in comparison with that at $t = 0$ h, 100 − [CFU number at $t = 2$ h/CFU number $t = 0$ h]. In certain experiment, 100 μg/ml BPS (kingreg Biotech, China) was used to pretreat bronchoalveolar macrophages prior to alive S. aureus infection.

2.16. Statistical Analysis. SPSS19.0 (IBM, Armonk, New York, USA) was employed for statistical analysis. Values were presented in the manner of median (interquartile ranges) or mean ± SD. Differences of two groups were evaluated by Mann–Whitney U tests, whereas those among several groups were evaluated by one-way ANOVA. Log-rank (Mantel-Cox) test was used to analyze survival curves. $p < 0.05$ indicated statistical significance.

3. Results

3.1. Basil Polysaccharide Can Significantly Improve the Prognosis of the Sepsis-Induced Secondary S. aureus Pneumonia Mice Model, but Not in Secondary P. aeruginosa Pneumonia. For investigating the possible effect of BPS on the sepsis-mediated secondary bacterial pulmonary infection, we treated C57BL/6 mice with CLP, followed by intratracheal injection with bacteria (S. aureus or P. aeruginosa) and BPS or IgG treatment. The entire experimental design and procedures were presented in Figure 1(a). As shown in Figures 1(b)–1(g), in the CLP-induced nonsevere sepsis model, survival rate between BPS-exposed and IgG control groups showed no significant difference, and their survival rate was about 90%. Therefore, there was no significant difference in mouse lung injury indicators such as protein in BALF, MPO, and W/D ratio. However, in the bacterial pneumonia model, mice's mortality began to increase, and the mortality was the highest in the CLP-induced secondary bacterial pneumonia mouse model. Next, we found that basil polysaccharide administration can improve the survival rate of S. aureus pneumonia or CLP-induced secondary S. aureus pneumonia mouse model. Moreover, it can also reduce the bacterial load in mice's blood and lungs and improve lung injury indicators. However, these results were not observed in P. aeruginosa pneumonia or CLP-induced secondary P. aeruginosa pneumonia mice model (supplementary data (available here)).

3.2. CLP Resulted in Impaired Host Pulmonary Immunity in the Mice. For confirming the effect of CLP on attenuating pulmonary response based on the microbial sepsis model, firstly, we detected the mice of immune status after CLP. The results showed that 24 hours after CLP, lung injury and inflammatory mediators including MIP-1β/CCL4, IL-10, TNF-α, IL-1β, IL-6, and IL-17A in serum or BALF were increased significantly. However, 72 hours after CLP, the lung injury was gradually recovered. Proinflammatory cytokines including MIP-1β/CCL4, TNF-α, IL-1β, IL-6, and IL-17A in serum or BALF were decreased, while the anti-inflammatory cytokine IL-10 continued to increase (Figures 2(a)–2(d)). Next, we treated WT C57BL/6 mice with sham operation or CLP, followed by intratracheal infection
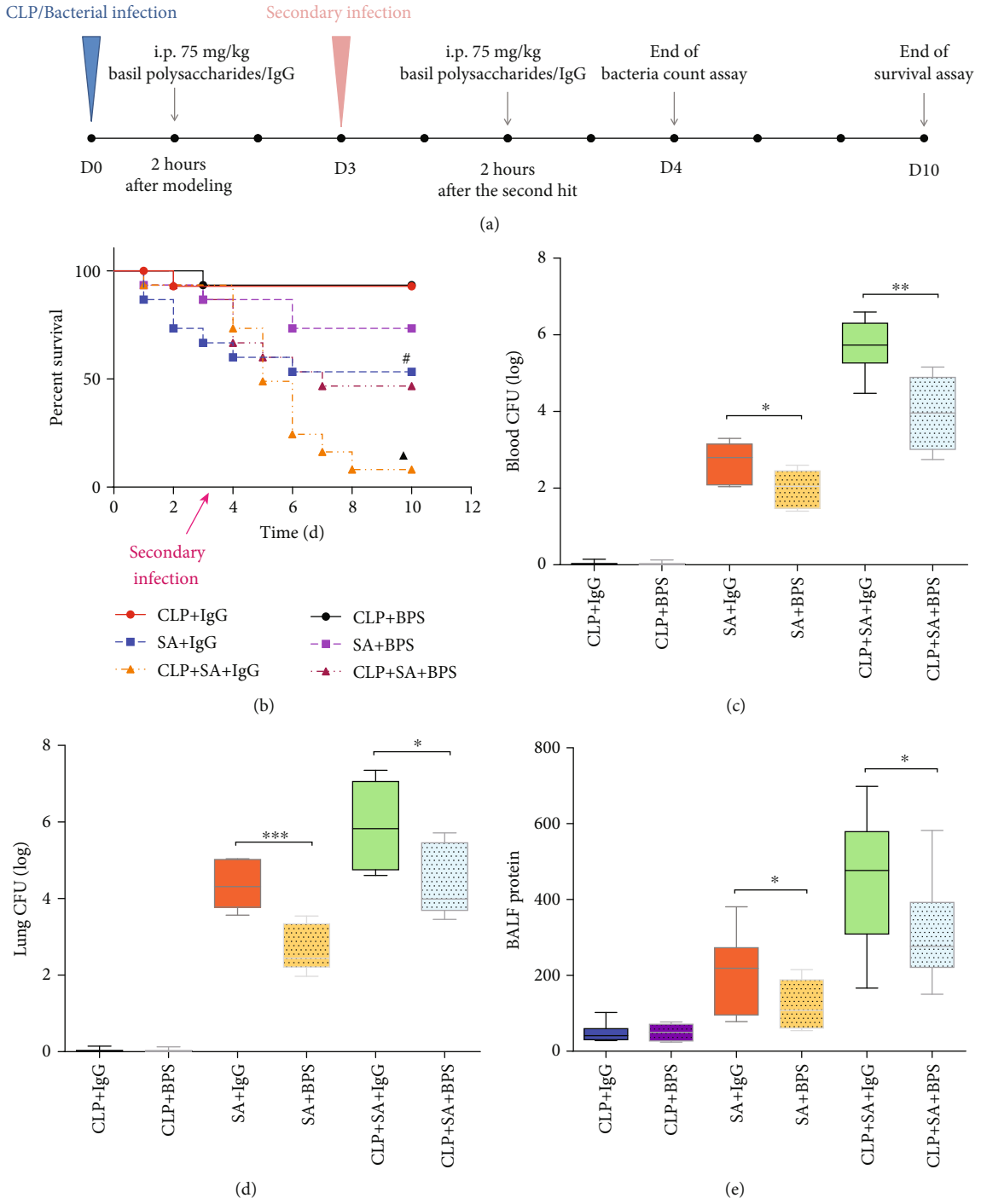
(a)

(b)
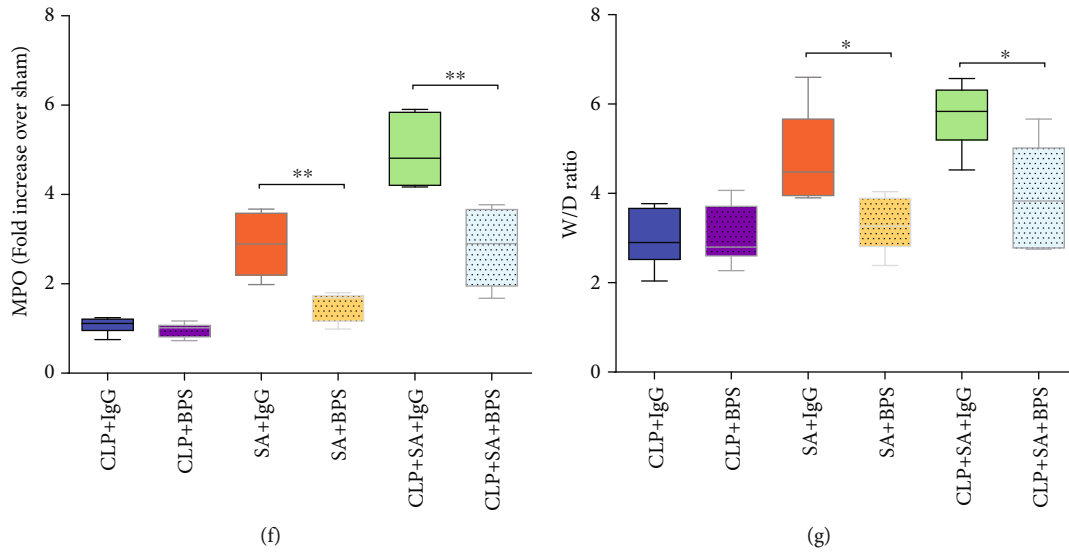
(c)

(d)

(e)

Figure 1: Continued.

(f)

(g)

FIGURE 1: (a) Experimental procedure. We randomized mice into 6 groups, including 4 receiving CLP at D0 and 2 receiving sham operation. At 3 days later (D3) or at D0 in the sham operation group, mice were given intratracheal injection with *P. aeruginosa* (PA, 5×10^7 CFU) or *S. aureus* (SA, 5×10^7 CFU). Two hours after the bacterial hit or the second bacterial hit, basil polysaccharide or IgG was injected intraperitoneally as an intervention. We collected lung tissues, blood, and BALF at 24 h after a bacterial infection or secondary bacterial infection for analysis. In the 10-day experimental period, we recorded the mortality rates of all groups to analyze the survival. (b) The mortality rates were monitored for 10 days after the challenge with *S. aureus* ($n = 15$ mice/group). (c, d) Lung or blood bacterial CFU in each group after administration with *S. aureus* ($n = 5$ mice/group). (e–g) Lung injury assessment indicators such as protein in BALF, myeloperoxidase, and wet/dry weight ratio in the lung were measured after challenge with *S. aureus* ($n = 5$ mice/group). Log-rank (Mantel-Cox) test was performed to analyze survival curves. Values were presented in the manner of mean ± SD, while one-way ANOVA as well as LSD multiple comparisons test was adopted for data analysis. $^{\#}p < 0.05$, compared with *S. aureus* infection treated with basil polysaccharide. $^{\blacktriangle}p < 0.05$, compared with CLP-surgery mice upon secondary *S. aureus* infection treated with basil polysaccharide. $^{*}p < 0.05$, $^{**}p < 0.01$, and $^{***}p < 0.001$, upon one-way ANOVA as well as LSD multiple comparisons. Compared with *S. aureus* infection treated with basil polysaccharide group or CLP-surgery mice upon secondary *S. aureus* infection treated with the basil polysaccharide group.

by *S. aureus* at 72 h after CLP. All mice undergoing sham operation survived, whereas over 90% mice receiving CLP with the 26G needle survived. Nonetheless, after *S. aureus* intrapulmonary administration at 5×10^7 CFU, 67% animals in the sham operation group survived. On the contrary, most animals exposed to sublethal CLP died upon subsequent intratracheal injection of *S. aureus* (Figure 2(e)). In addition, animals subjected to CLP that developed secondary *S. aureus* pneumonia showed markedly reduced BALF or serum inflammatory mediator production, such as IL-1β, IL-6, IL-17A, TNF-α, and MIP-1β/CCL4, whereas upregulated anti-inflammatory mediator (IL-10) production relative to the sham operation group, and pneumonia occurred at 24 h following infection (Figure 2(f)). Collectively, the above results conformed to previous results suggesting that CLP led to compromised pulmonary immune response upon secondary *S. aureus* infection.

3.3. Basil Polysaccharide Protected Mice from Lethality, Ablated Lung Pathology, and Regulated Inflammatory Responses in Sepsis-Induced Secondary S. aureus Pneumonia Mice Model.

To assess the involvement of basil polysaccharide in host defense against *S. aureus* in septic mice, IgG or basil polysaccharide was administered to intervene in mice. The results revealed that the basil polysaccharide-treated mice group receiving CLP had remarkably elevated survival rate after secondary *S. aureus* infection, relative to the IgG

group (Figure 3(a)). From the lung histopathological examination, in mice treated with basil polysaccharide, the lung injury scores were significantly reduced, indicated by improved hemorrhage, edema, and inflammatory cell infiltration in the CLP-induced secondary *S.aureus* pneumonia mouse model (Figures 3(b) and 3(c)). Additionally, pulmonary TUNEL-positive cell proportion declined following BPS exposure (Figures 3(d) and 3(e)). As presented in Figure 3(f), although there was no statistical significance, the basil polysaccharide-treated group exhibited comparatively increased chemokine or cytokine production (such as CXCL1, TNF-α, IL-6, IL-1β, and IL-17A) within alveolar lavage fluid and serum, compared with the IgG group, with statistically significant differences in CCL4 levels. Together, these findings indicated that the therapeutic effect of basil polysaccharide may be related to the recruitment of chemokines CCL4 in the lungs.

3.4. Effects of Basil Polysaccharide on Leukocyte Recruitment in Sepsis-Induced Secondary S. aureus Pneumonia Mice.

For identifying the possible mechanisms of BPS in changing the antibacterial defense in the host, this study measured the leukocyte influx into primary infection site following sepsis-mediated secondary *S. aureus* pulmonary infection. The overall cell number within mouse alveolar lavage fluid (BALF) increased significantly after treatment with basil polysaccharide (Figures 4(a) and 4(b)). Notably, treatment

(a)

(b)

(c)
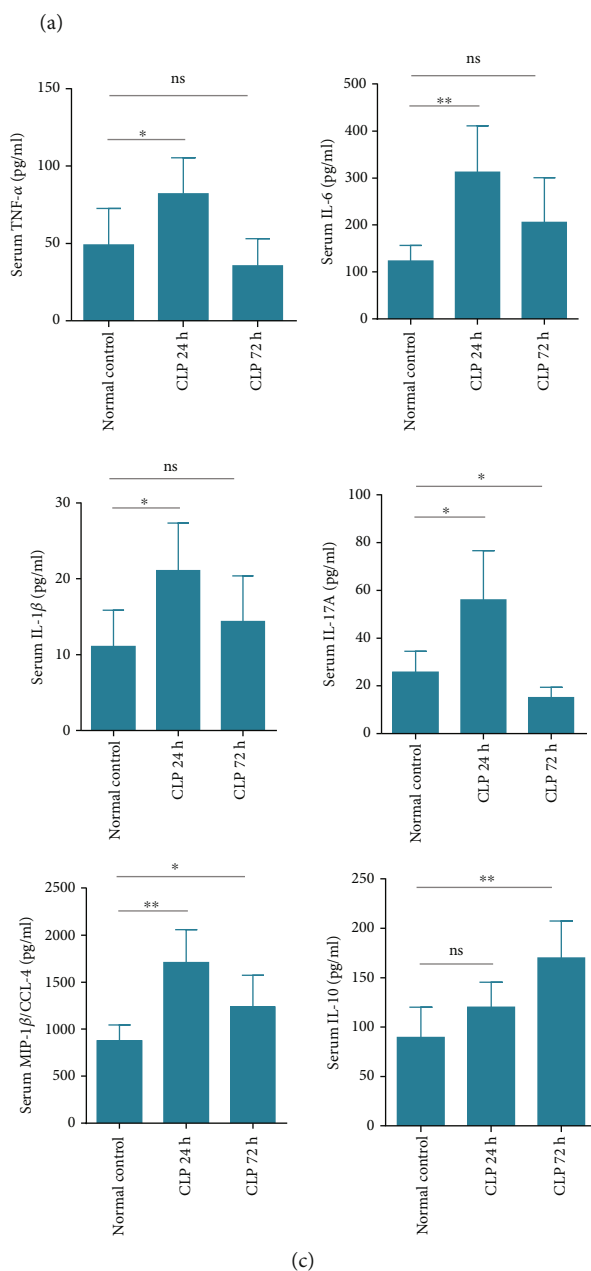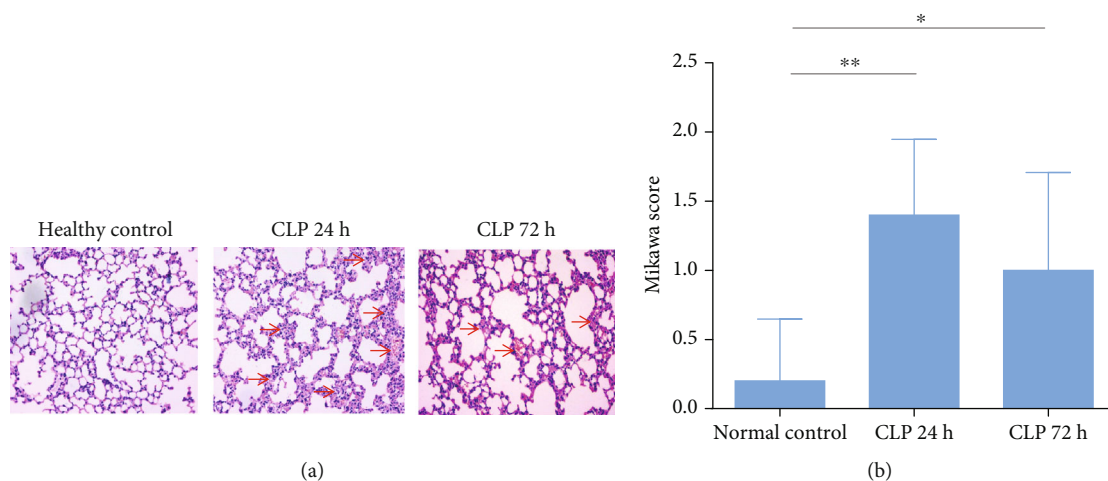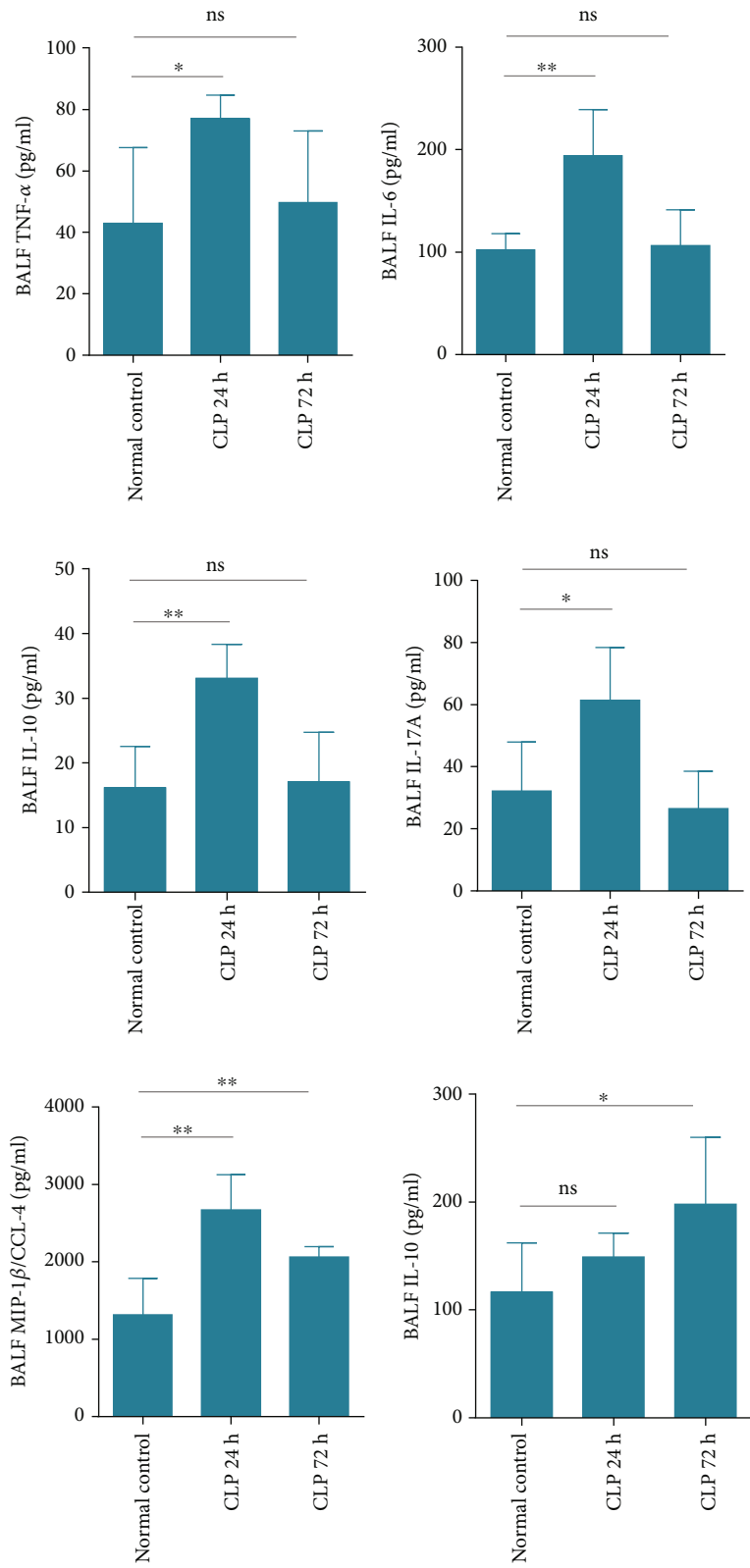
FIGURE 2: Continued.

(d)
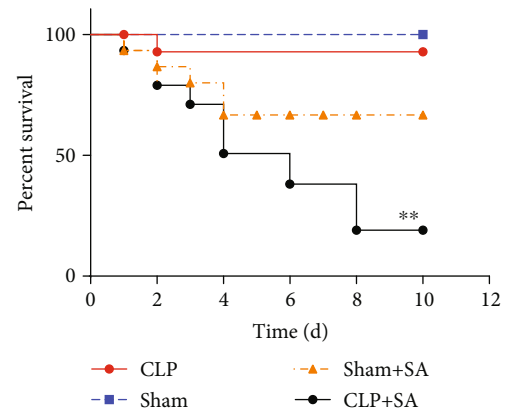
(e)

Figure 2: Continued.

(f)
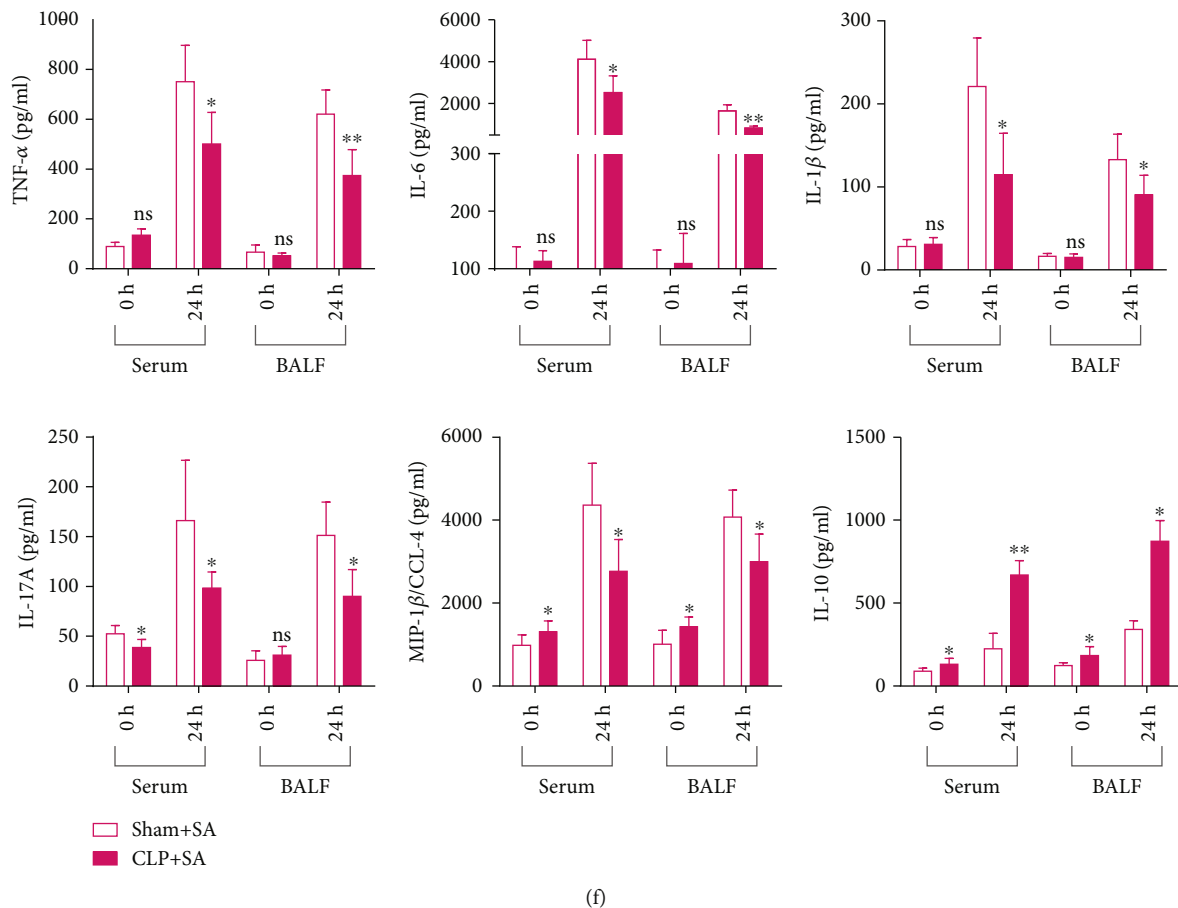
FIGURE 2: CLP led to damaged pulmonary immune responses in the host. Mice receiving CLP or sham operation. (a, b) Histological scores for CLP-induced nonsevere sepsis model ($n = 5$ mice/group). (c, d) At 24 h and 72 h after CLP, we detected contents of cytokines in serum and BALF. Mice Cytokine Magnetic Bead Panel Kit ($n = 5$ for every group) was performed to analyze the obtained specimens. (e) 72 h after CLP, mice were given intratracheal injection with *S. aureus* (5×10^7 CFU). Following challenge ($n = 15$ for every group), we observed mortality rates over the 10-day period. Log-rank (Mantel-Cox) test was performed to analyze survival curves. (f) At 24 h following secondary infection with *S. aureus*, we detected contents of chemokines and cytokines in serum and BALF. Mice Cytokine Magnetic Bead Panel Kit ($n = 5$ for every group) was performed to analyze the obtained specimens. Values were presented in the manner of mean ± SD, whereas nonparametric Mann–Whitney U test was adopted for data analysis. $^*p < 0.05$, $^{**}p < 0.01$, compared with normal control or sham-surgery mice upon secondary S. aureus infection.

with basil polysaccharide significantly enhanced lymphocyte and macrophage counts within BALF relative to the IgG treatment group (Figures 4(c)–4(f)). On the contrary, differences in overall neutrophil count were not significant (Figures 4(g) and 4(h)). These results collectively suggest that the protection of basil polysaccharide during infection is still crucial to recruit lymphocytes and macrophages in this model.

3.5. Basil Polysaccharides Improve the Survival Rate of Sepsis-Induced Secondary S. aureus Pneumonia Mice by Promoting CCL4 Secretion from Neutrophils. Previous studies have found that the chemokine CCL4 exerts a vital part in the pathogenic mechanism of pulmonary diseases like bacterial pneumonia and respiratory defense [33]. Our study revealed that basil polysaccharide can significantly increase the level of CCL4 in the lungs of sepsis-induced secondary *S. aureus* pneumonia mice (Figure 3(f)). This indicated that the therapeutic effect of basil polysaccharide may be related to the

recruitment of chemokine CCL4 in the lungs. Therefore, we investigated the role of CCL4 in sepsis-induced secondary *S. aureus* pneumonia mouse model. First, we observed that in secondary *S. aureus* pneumonia induced by sepsis, recombinant CCL4 could improve lung pathology and lung injury, increase the clearance rate of bacteria from the lung and blood, reduce lung injury and mortality, and effectively promote macrophage recruitment in the lungs (Figures 5(a)–5(i)). Neutrophils are immune cells that can secrete a variety of chemokines, such as IL-1β, IL-8, interferon-γ inducible protein 10 (IP-10), and CCL4 [32]. Although we did not identify the ability of basil polysaccharide in promoting neutrophil recruitment in the lungs, *in vitro* experimental results revealed that basil polysaccharide could effectively promote the secretion of CCL4 by neutrophils. These findings highlighted the molecular immune mechanism of basil polysaccharide in regulating sepsis-induced secondary *S. aureus* pneumonia in mice (Figure 5(j)).

(a)

(b)

(c)

(d)

(e)
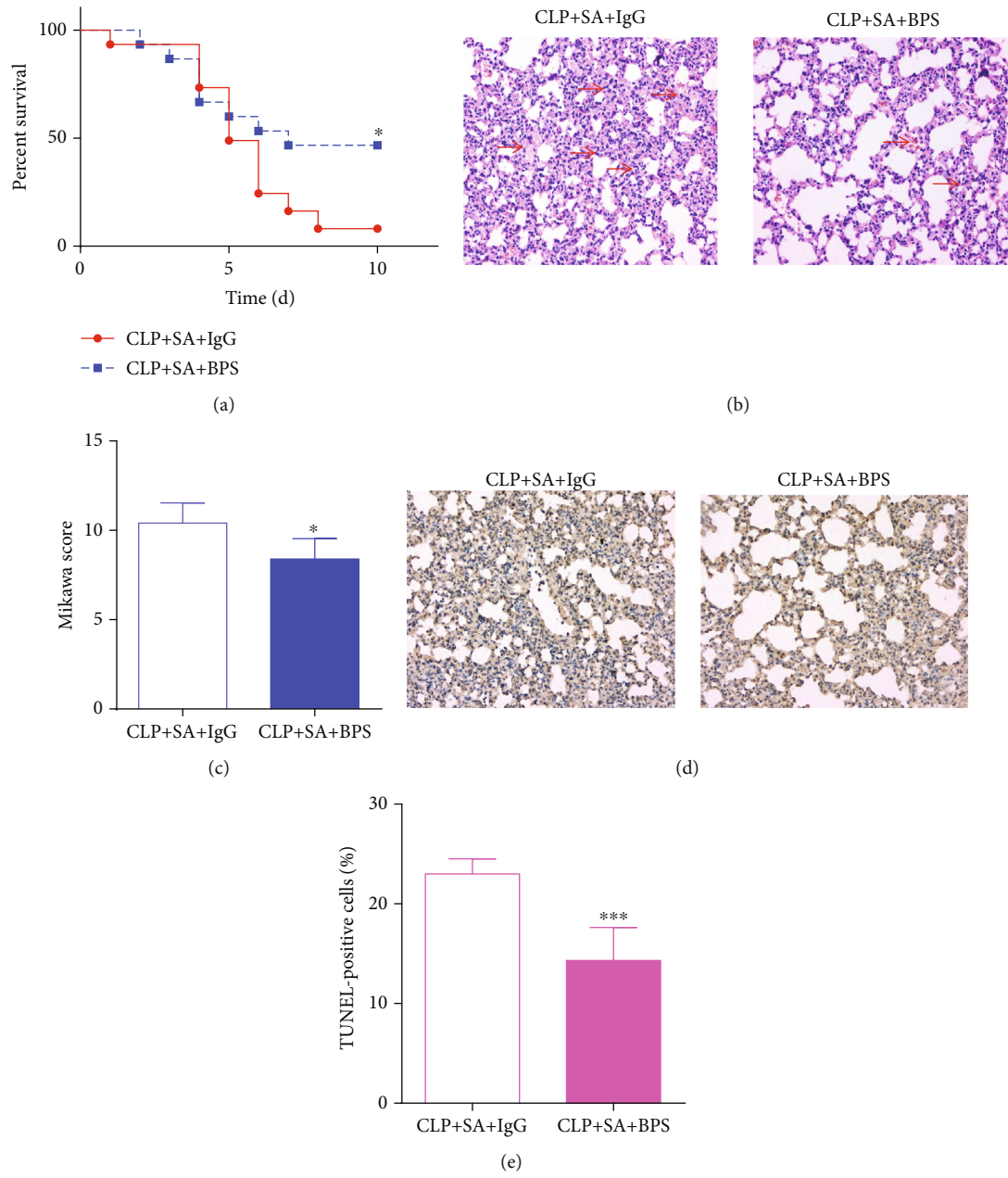
FIGURE 3: Continued.
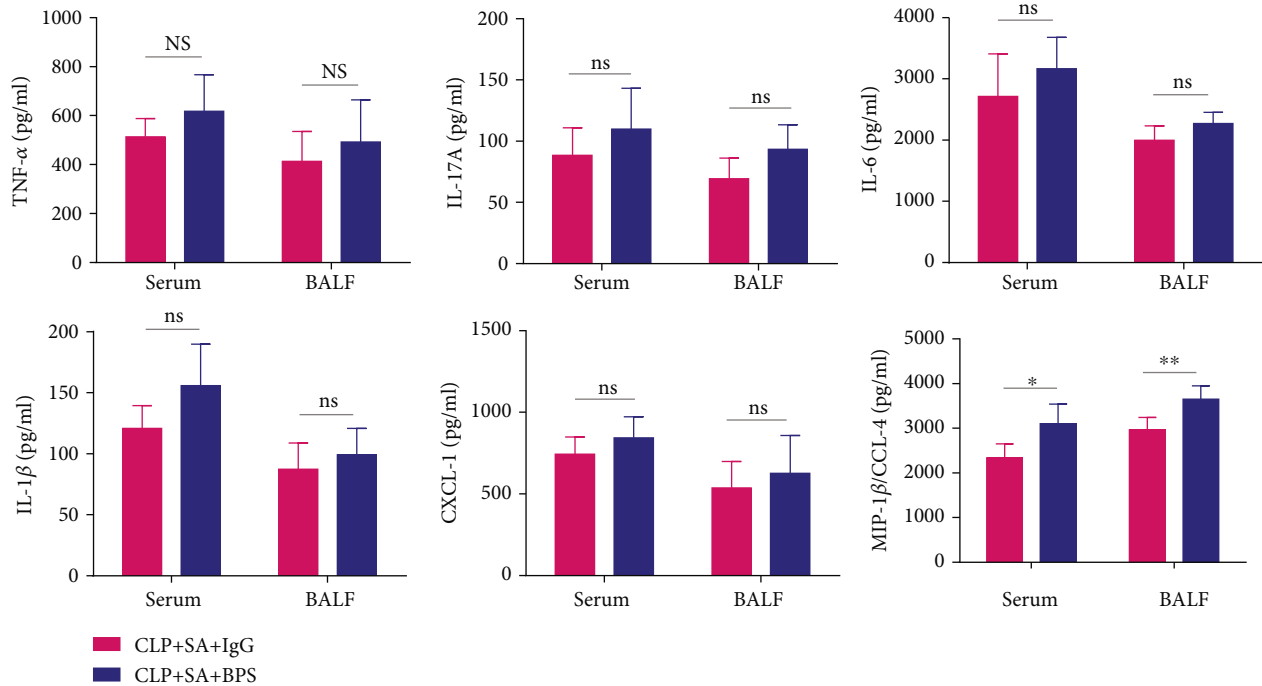
(f)

FIGURE 3: Postseptic basil polysaccharide is resistant to S. aureus pneumonia. (a) Survival of mice treated with basil polysaccharide upon S. aureus infection during sepsis ($n = 15$ mice/group). (b) Typical HE staining for lung tissue samples at 24 h postinfection with S. aureus during sepsis and following treatment with IgG or basil polysaccharide group. (c) Histological scores for secondary pulmonary infection with S. aureus within septic mice, as well as following treatment with IgG or basil polysaccharide ($n = 5$ mice/group). (d, e) TUNEL assay was performed to determine cell apoptosis, where the nuclei of TUNEL-positive cells were dark-brown. (f) BALF and serum cytokine or chemokine contents were detected at 24 h after treatment with IgG or basil polysaccharide during sepsis-induced secondary S. aureus pneumonia in mice. Specimens were collected for analysis by Mice Cytokine Magnetic Bead Panel Kit ($n = 5$ mice/group). Survival curves were analyzed using the log-rank (Mantel-Cox) test. Data were expressed as mean ± SD, whereas nonparametric Mann–Whitney U test was applied for data analysis. $^{*}p < 0.05$, $^{**}p < 0.01$, and $^{***}p < 0.001$, relative to secondary pulmonary infection with S. aureus of septic mice in the IgG group.

3.6. Basil Polysaccharide Induces Macrophage Phagocytosis and Killing S. aureus by p38 MAPK Signaling Pathway.

To determine whether basil polysaccharide induced the inherent bacteria defense ability of phagocytes, this study examined bacterial absorption and macrophage clearance in the bronchoalveolar lavage fluid. Pretreatment with basil polysaccharide promoted phagocytosis and intracellular killing of S. aureus by macrophages (Figures 6(a) and 6(b)). Moreover, this study explored the possible mechanism by which BPS affected the S. aureus killing and phagocytosis abilities. The p38 MAPK signaling pathways exert vital parts in the regulation of bacterial clearance and macrophage phagocytosis [32, 34]. As a result, this study conducted Western blotting assay for analyzing the expression of proteins related to such signal transduction pathways. Following BPS treatment, the p38 MAPK signal expression increased significantly (Figures 6(c) and 6(d)).

3.7. Basil Polysaccharides Promote the Differentiation of Regulatory T Lymphocytes in Sepsis-Induced Secondary S. aureus Pneumonia Mice.

The previous results found that CD4+ lymphocytes increased significantly in sepsis-induced secondary S. aureus pneumonia mice (Figures 4(e) and 4(f)). Next, we used flow cytometry to detect Treg lymphocytes in mouse BALF. The results revealed that after basil polysaccharide administration, the Treg cells in mice BALF increased significantly (Figures 7(a) and 7(b)). In order to further analyze the effect of basil polysaccharide on the differentiation of Treg lymphocytes, naïve CD4+ T lymphocytes were isolated from the mouse spleens and cultured in vitro. Afterwards, cells were intervened with BPS. At 3 days later, a trend of differentiation to Treg cells was observed among the naïve CD4+ T lymphocytes (Figures 7(c) and 7(d)). Taken together, these data demonstrated that basil polysaccharide could promote naïve CD4+ T lymphocytes to differentiate to Treg cells, thus exerting the immunomodulatory effect in sepsis-induced secondary S. aureus pneumonia mice.

4. Discussion

Following clinical cure, patients with microbiologic treatment failure experience significantly high rates of recurrent pneumonia and high susceptibility to sepsis-induced secondary lung infection [35]. These findings have been associated with the development of sepsis-induced immunosuppression

(a)

(b)

(c)

(d)
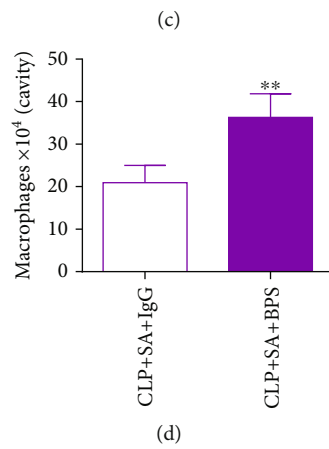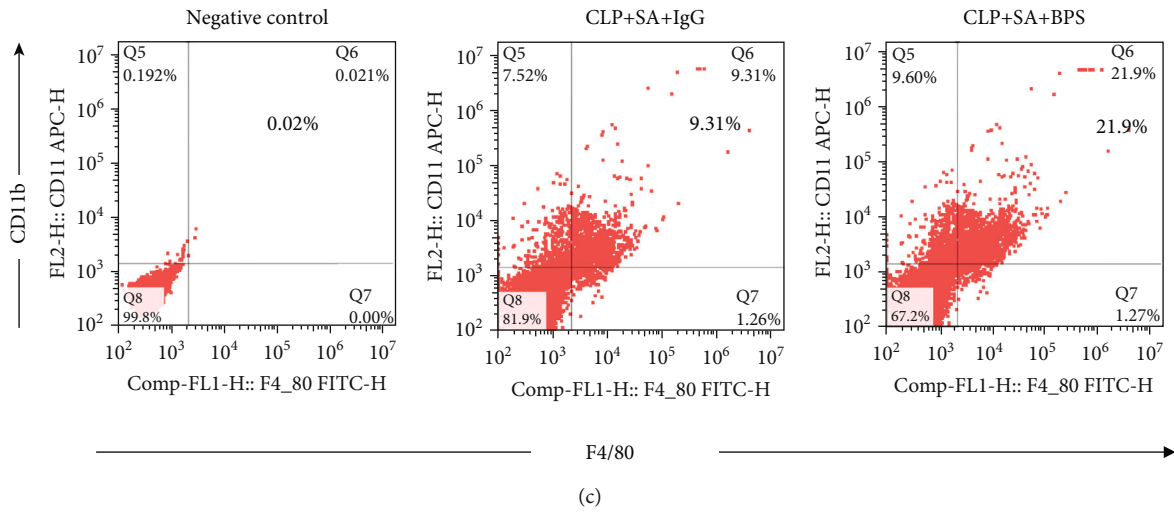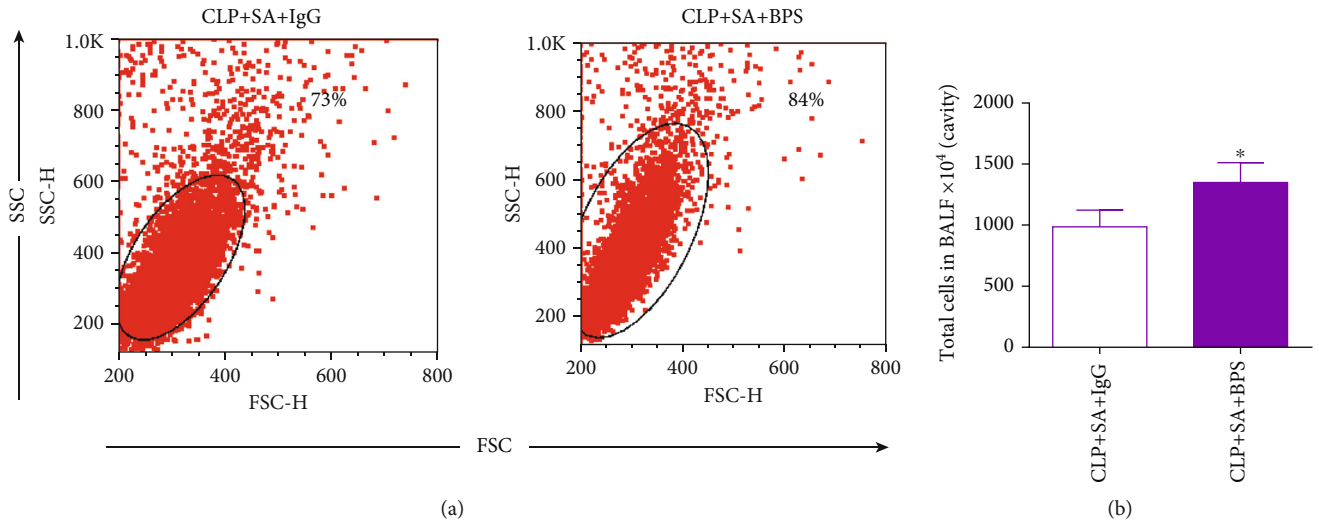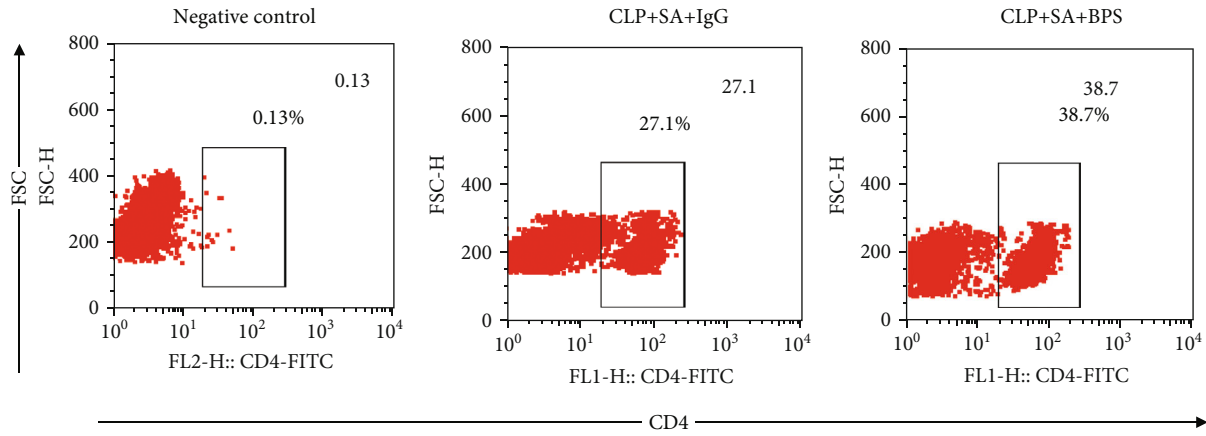
FIGURE 4: Continued.

(e)
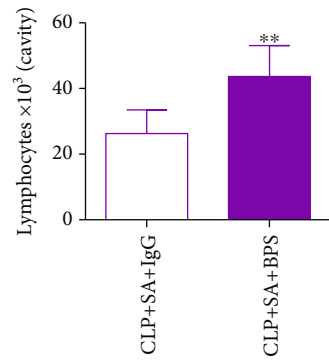
(f)
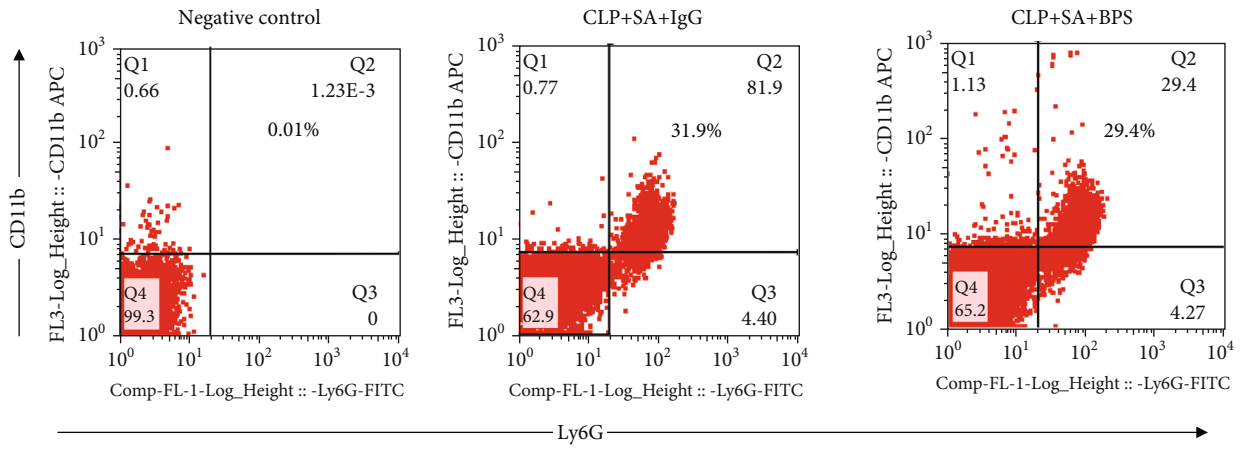
(g)

Figure 4: Continued.

(h)
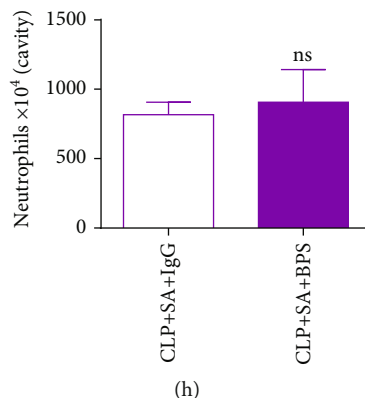
FIGURE 4: (a, b) Gating strategy to analyze total cells within BALF. (c, d) Gating of CD11b+F4/80+ cells was conducted to determine overall macrophage count within BALF. (e, f) Gating of CD4+ cells was conducted to determine overall T lymphocyte count within BALF. (g, h) Gating of CD11b+Ly6G+ cells was conducted to determine overall neutrophil count within BALF. Kaplan–Meier analysis and log-rank tests were conducted to compare two groups. $^{*}p < 0.05$, $^{**}p < 0.01$, compared with secondary *S. aureus* pneumonia in septic mice treated with the isotypical IgG control.

[36]. Several new therapies have been reported to reduce sepsis-induced immunosuppression rates and limit the susceptibility to secondary pneumonia in recent years. However, these new approaches' efficacy remains poor and represents a significant challenge for clinicians [37]. Great attempts have been tried to avoid antimicrobial resistance spread; the development of resistant bacteria remains inevitable over time [38]. A possible method is related to the immunity-specific targeted treatment [39]. Basil, with diverse medicinal applications, has been incorporated into the Pharmacopeia (2015 edition). Basil polysaccharide is considered the most important active compound of basil, whereas mannose (Man), rhamnose (Rha), glucose (Glc), fructose (Fru), and Arabian sugar (Ara) represent its main components [40–42]. Studies have revealed that polysaccharides may be adopted to be immunopotentiators for stimulating macrophages, protecting immune organs, in the meantime of building the complement system, thus exerting the role of immunoenhancers [43, 44]. Not only that, basil polysaccharide also exhibits a wide range of antibacterial activities. They also exhibit inhibitory effects on a variety of common bacterial infections [45]. In this study, we observed that in experimental sepsis-induced secondary *S. aureus* pneumonia model, basil polysaccharides could improve lung pathology and lung injury, increase the clearance rate of bacteria from the lungs and blood, and effectively reduce mortality(Figure 1); however, no such effects were observed in experimental sepsis-induced secondary *P. aeruginosa* pneumonia model (Supplementary data (available here)). These findings indicate that basil polysaccharide could serve as a new type of adjuvant treatment to sepsis-induced secondary *S. aureus* pneumonia.

The out-of-balance between proinflammatory cytokine levels and anti-inflammatory cytokine levels is a characteristic of sepsis-mediated immunosuppression, and this makes the host susceptible to secondary pneumonia, especially nosocomial pneumonia [46, 47]. In general, as presented in Figures 2(c) and 2(d), at 72 hours after CLP, proinflammatory cytokines including MIP-1β/CCL4, TNF-α, IL-1β, IL-

6, and IL-17A in serum or BALF were decreased and the anti-inflammatory cytokine IL-10 was significantly increased. Meanwhile as compared with the control group (sham+SA), the alveolar lavage fluid and serum samples of mice in the CLP+SA group revealed lower levels of proinflammatory cytokines or chemokines (including TNF-α, IL-1β, IL-17A, IL-6, and CCL-4) and higher levels of anti-inflammatory cytokines (IL-10), indicating that the sepsis-induced secondary S. aureus pneumonia mouse model presented an immunosuppressive state (Figure 2(f)).

Next, we intervened by administrating basil polysaccharide 2 hours after the second hit. As shown in Figure 3(f), although there is no statistical significance, the basil polysaccharide-treated group exhibited slightly increased chemokine and cytokine expressions (such as IL-1β, TNF-α, IL-6, IL-17A, and CXCL1) within the alveolar lavage fluid and serum samples, compared with the IgG group, with statistically significant differences in CCL4 levels. Together, these findings indicate that the therapeutic effect of basil polysaccharide may be related to the recruitment of chemokine CCL4 in the lungs. As for host defense, recruiting immune and inflammatory effector cells into tissue injury, neoplasia, and infection sites is still an important part. Such response can be partially modulated through the locally produced mediator network, such as lipids or chemotactic proteins [46]. Chemokines are critical proinflammatory cytokines related to the host defense regulating the activation and recruitment (chemotaxis) of leukocytes or additional cell types into the neoplasia, infection, or injury sites [47]. MIP-1β, also known as CCL4, belongs to the chemokine family and is essential in immune responses to infection and inflammation. CCL4 is a crucial chemotactic mediator for recruiting mononuclear macrophages, natural killer cells, T lymphocytes, and cytokine production regulation [33]. Furthermore, studies have shown that CCL4 (MIP-β) chemokines exert vital parts within cytokine networks modulating immune and inflammatory responses of the respiratory tracts, which possibly facilitate the pathogenic mechanism of pulmonary diseases [48–50]. According

(a)

(b)

(c)

(d)

(e)

(f)
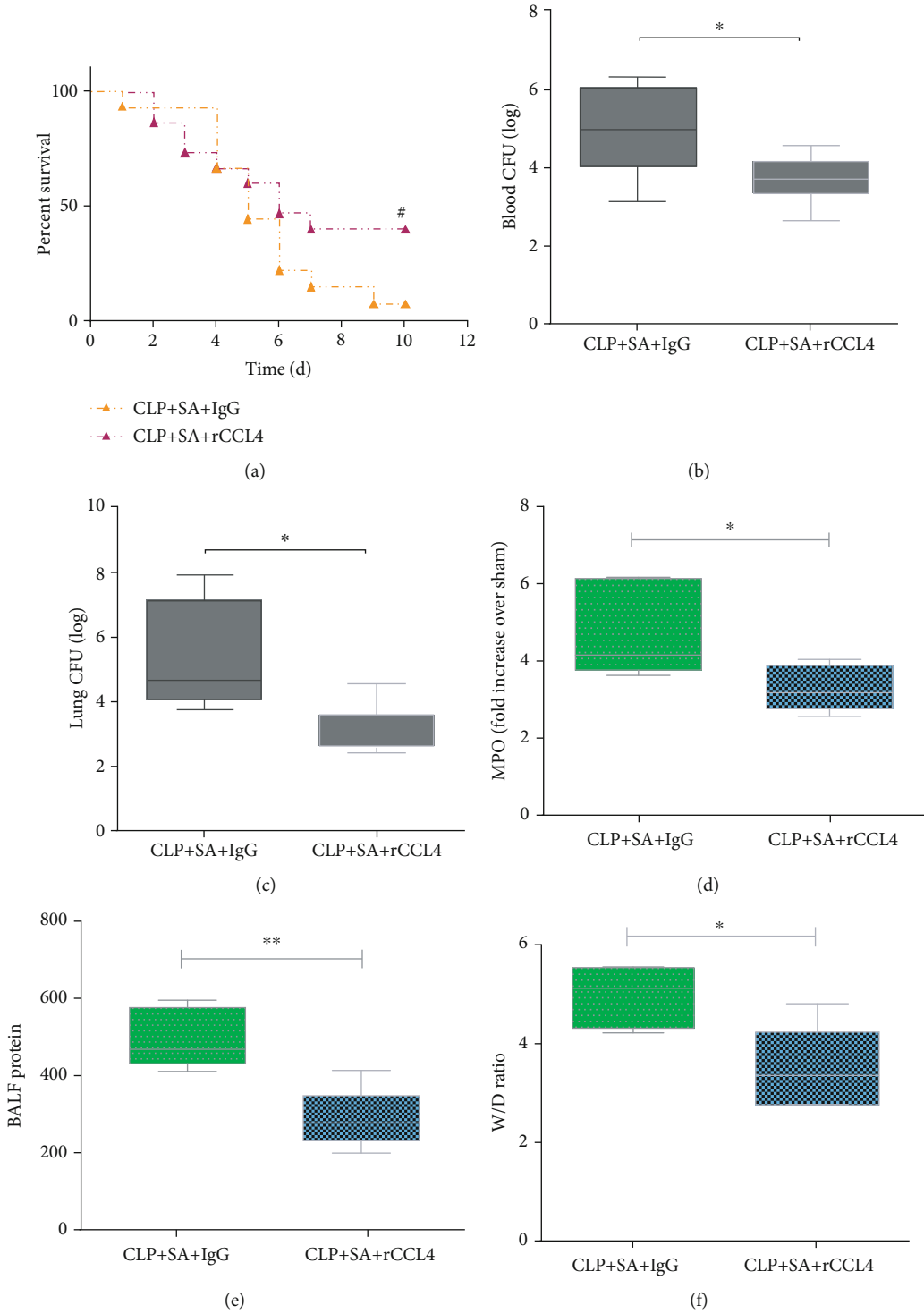
Figure 5: Continued.

(g)

(h)

(i)

(j)
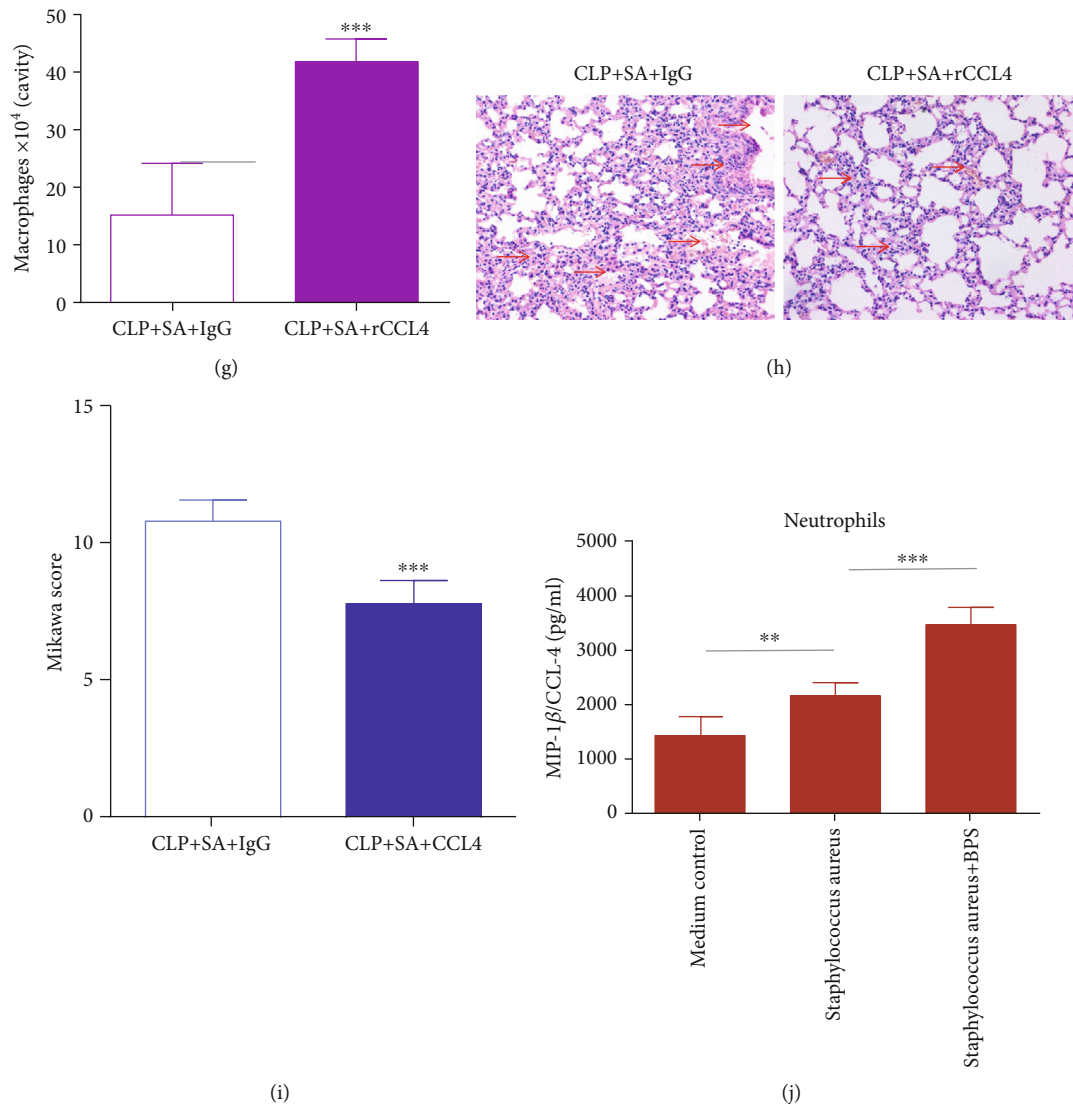
FIGURE 5: Effect of recombinant protein CCL4 (CC receptor ligand 4) on resistance in septic mice with *S. aureus* pneumonia. Recombinant protein CCL4 was administered (500 ng) 2 hours after *S. aureus* inoculation in septic mice. The control group was given equivalent IgG control. (a) Survival of septic mice with secondary *S. aureus* infection ($n = 15$ mice/group) following recombinant protein CCL4 administration. (b, c) Blood and lung CFU of septic mice with secondary *S. aureus* infection ($n = 5$ mice/group) following recombinant protein CCL4 administration. (d–f) Lung damage assessment indicators such as protein in BALF, myeloperoxidase (MPO), and wet/dry weight ratio in septic mice with secondary *S. aureus* infection ($n = 5$ mice/group) following recombinant protein CCL4 administration. (g) The total number of macrophages in BALF in septic mice with secondary *S. aureus* infection ($n = 5$ mice/group) following recombinant protein CCL4 administration. (h, i) Histological scores for secondary pulmonary infection with *S. aureus* of septic mice ($n = 5$ for every group). Log-rank (Mantel-Cox) test was performed to analyze survival curves. Values were presented in the manner of mean ± SD, whereas nonparametric Mann–Whitney U test was adopted for data analysis. $^{\#}p < 0.05$, $^{*}p < 0.05$, $^{**}p < 0.01$, and $^{***}p < 0.001$, relative to secondary pulmonary infection with *S. aureus* of septic mice receiving recombinant protein CCL4 treatment. (j) The concentration of CCL4 in the cell supernatant after *S. aureus* or basil polysaccharide stimulates neutrophils for 48 hours. $^{**}p < 0.01$, $^{***}p < 0.001$, upon one-way ANOVA and LSD multiple comparisons, relative to the *S. aureus* group.

to articles that assess the interstitial pulmonary disease [51], pulmonary sepsis [52], or oxidant lung damage [53] animal models, CCL4 (MIP-β) exerts an important part in the disease pathogenic mechanism and respiratory tract defenses. Therefore, we investigated the role of CCL4 in the sepsis-induced secondary *S. aureus* pneumonia mouse model. Firstly, we observed that in experimental sepsis-induced secondary *S. aureus* pneumonia, recombinant CCL4 could improve lung pathology and lung injury, increase the clear-

ance rate of bacteria from the lungs and blood, and effectively promote macrophage recruitment in the lungs and reduce mortality (Figures 5(a)–5(i)). Secondly, neutrophils were the first immune cells recruited at the site of inflammation [54]. They can secrete a variety of chemokines, including IL-1β, IL-8, interferon-γ inducible protein 10(IP-10), macrophage inflammatory protein 1α (MIP-1α), and MIP-1β(CCL4) [55]. According to previous reports, following the release of neutrophils, MIP-1β (CCL4), a critical

(a)

(b)

(c)

(d)
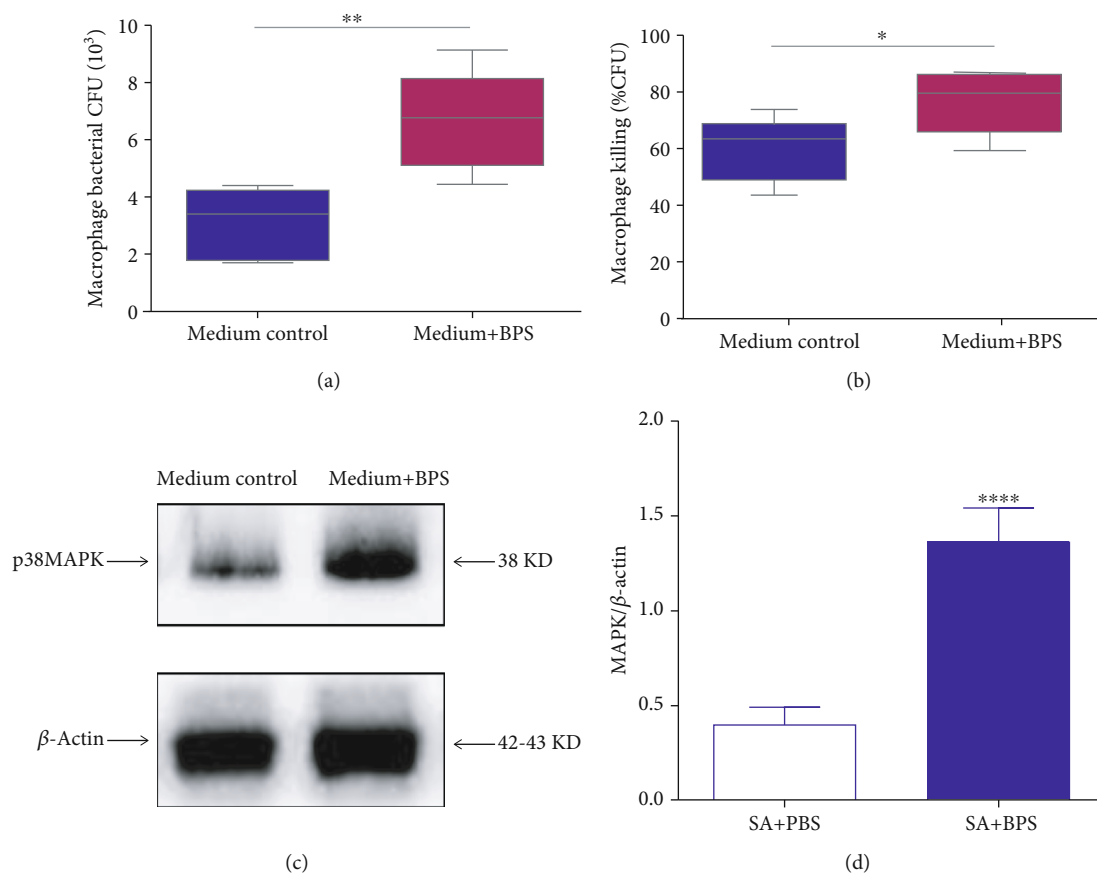
FIGURE 6: Effects of basil polysaccharide treatment on the ability of macrophages to eliminate and swallow bacteria. (a, b) 12 h BPS treatment was conducted on macrophages, followed by 30 min of S. aureus (MOI, 10) or FITC-labeled S. aureus infection under 37°C. We then determined the swallowed FITC-labeled S. aureus count and intracellular bacterial killing ($t = 2$ h) according to specific descriptions. (c, d) After 12 h of BPS treatment, Western blotting assay was conducted to determine p38MAPK signals within macrophages. $^*p < 0.05$, $^{**}p < 0.01$, and $^{****}p < 0.0001$, upon one-way ANOVA as well as LSD multiple comparisons, in comparison with the BPS group.

chemotactic mediator for the recruitment of monocytes/macrophages, promotes macrophages' endocytosis, leading to regression of inflammation [56]. Therefore, we further investigated whether basil polysaccharide can promote the secretion of CCL4 from neutrophils; we extracted mouse peritoneal centrioles for in vitro culture. The results indicated that BPS could effectively promote the secretion of CCL4 by neutrophils (Figure 5(j)). This may possibly be the molecular immune mechanism underlying the basil polysaccharide regulating the sepsis-induced secondary S. aureus pneumonia.

Phagocytes, especially resident macrophages and recruited neutrophils, exert an important part in immune responses at the infection sites, either in early or late stage; in addition, they express various 'scavenger' receptors, thus clearing the senescent host cells, proteins, and foreign bacteria [57]. Our in vitro experiments demonstrated that pretreatment with basil polysaccharide could effectively promote the phagocytosis and killing ability of macrophages to phagocytose S. aureus (Figures 6(a) and 6(b)). Activating the intracellular signal transduction pathways is necessary for the interaction of host cells with foreign pathogens [58]. This study also explored the effect of BPS treatment of macrophages on changing intracellular signal transduction upon

secondary infection with S. aureus. According to our findings, BPS remarkably promoted p38MAPK signal transduction pathway activation within macrophages after S. aureus challenge (Figures 6(c) and 6(d)) [34]. The abovementioned pathway participates in the ability for host cells to recognize and absorb bacteria, and the BPS-mediated enhanced abilities for macrophages to kill and swallow bacteria were partly regulated through the promoted p38MAPK signal transduction pathway activation.

Apoptosis is an essential part of normal physiological mechanisms and occurs as a homeostatic mechanism to balance cell proliferation and cell death. The initiation of apoptosis is genetically and biochemically regulated by intracellular stimuli and extracellular signals [59]. Under physiological conditions, apoptosis is necessary to eliminate pathogen-invaded cells and is involved in removing inflammatory cells; however, under pathological conditions, it is related to the development of multisystem diseases [60]. Some studies have found that the cytotoxic effect of S. aureus during epithelial and endothelial cell invasion is mediated through apoptosis [61, 62]. By coculturing human T lymphocytes with S. aureus exotoxin, Jonas et al. found that the nanomolecular concentration of toxin can cause irreversible
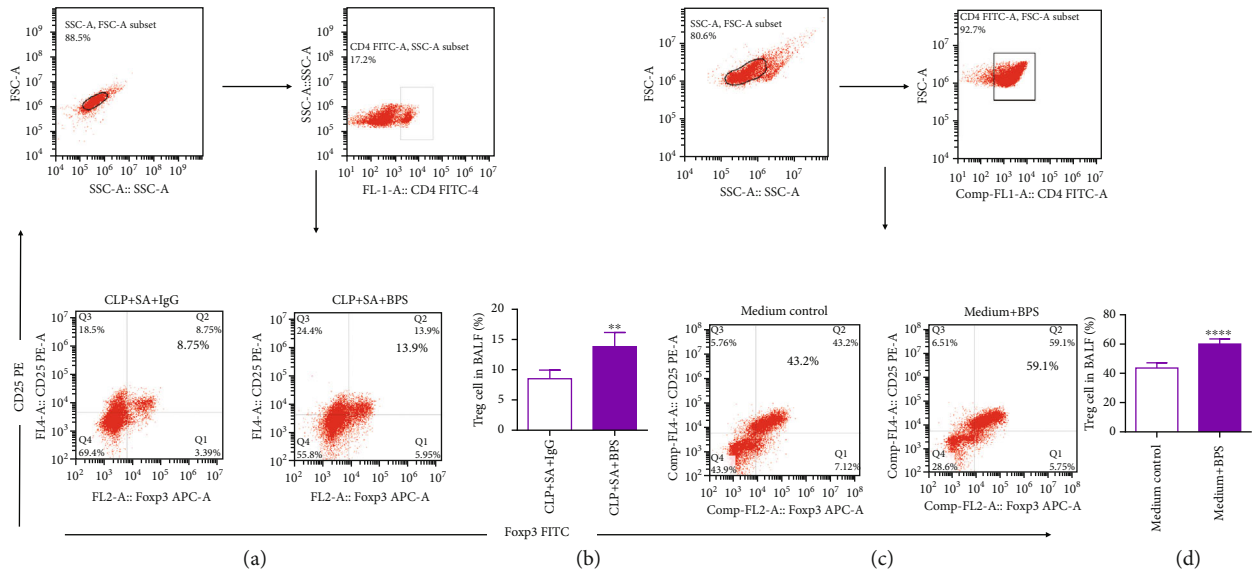
FIGURE 7: BPS promoted naive CD4 T lymphocytes to differentiate to Treg cells. (a, b) We separated T cells from BALF of mice. CD4+CD25+Foxp3 Treg cell proportion was then measured through flow cytometric analysis, where the findings indicated the means from 5 mice at each time point. (c, d) Treg proportion elevates relative to the nontreatment group following BPS challenge. $^{**}p < 0.01$, $^{****}p < 0.0001$, one-way ANOVA as well as LSD multiple comparisons test was conducted to compare two groups.

ATP depletion of activated or resting T lymphocytes. The T lymphocyte membrane is more permeable to monovalent ions, leading to nuclear DNA degradation and cell apoptosis [63]. These studies indicate that the pathogenesis of *S. aureus* is closely associated with cell apoptosis. In this study, we found that in the sepsis-induced secondary *S. aureus* pneumonia mouse model, the lung apoptosis was significantly increased. However, treatment with basil polysaccharide can significantly reduce cell apoptosis in the lungs of mice (Figures 3(d) and 3(e)). These findings highlight another important mechanism of regulation by basil polysaccharide in sepsis-induced secondary *S. aureus* pneumonia.

The body's immune system has several functions in resisting pathogenic bacteria, regulating inflammatory response and anti-inflammatory response [64, 65]. The human immune system includes humoral immunity and cellular immunity; among cellular components, T lymphocytes represent the primary cells involved in realizing the cell-mediated immune response [66]. Studies have previously revealed that CD4 T lymphocytes are essential for the lungs to resist specific pathogens [67]. Reports also indicate that in CD4 knockout (KO) mice, the clearance rate of *S. aureus* is significantly impaired. And in *S. aureus*-mediated experimental pleurisy, CD4 T lymphocytes play an important role [68]. Therefore, we analyzed the effect of basil polysaccharide on CD4+ lymphocytes in a mouse model of sepsis-induced secondary *S. aureus* pneumonia. First, we tested the number of CD4+ lymphocytes in mouse BALF and found that basil polysaccharide can significantly increase CD4+ lymphocytes in the lungs (Figures 4(e) and 4(f)). As previous studies have also shown that BPS enhances T cell activation and antigen presentation within dendritic cells (DCs), thus enhancing the immune response and surveillance [21]. Next, we tested the CD4+ T lymphocyte subsets (Treg cells) in the BALF of experimental mice, and the results indicated that basil poly-

saccharide could increase the proportion of Treg cells in BALF (Figures 7(a) and 7(b)). To further illustrate that BPS affected T lymphocyte differentiation, naive CD4+ T lymphocytes were isolated from the mouse spleen for *in vitro* culture, and the result revealed that basil polysaccharide could significantly promote naive CD4+ T lymphocytes to differentiate to Treg cells (Figures 7(c) and 7(d)).

5. Conclusion

Collectively, in this study, we found that BPS can effectively accelerate MIP-1β (CCL4) secretion by neutrophils for the recruitment of monocytes/macrophages (MΦ) in the lung, enhance macrophage endocytosis and killing of *S. aureus* through activation of the p38MAPK signal pathway, significantly reduce cell apoptosis in the lung, and promote naive CD4+ T lymphocytes to differentiate to Treg cells. Besides, this study highlights an essential mechanism of BPS in playing a protective role in sepsis-induced secondary *S. aureus* pneumonia.

Data Availability

The datasets used or analyzed during the current study are available from the corresponding author on reasonable request.

Ethical Approval

This study was carried out in accordance with the recommendations of The Institutional Animal Care and Use Committee at Chongqing Medical University. All experimental protocols were approved by the Institutional Animal Care and Use Committee at Chongqing Medical University.

Conflicts of Interest

All authors do not have any possible conflicts of interest.

Authors' Contributions

Conception hypothesis and design was performed by Chuanjiang Wang and Xi Chen. Data acquisition and analysis was performed by Yue He. Manuscript preparation was done Yue He and Xi Chen. Revision of the manuscript was performed by Chuanjiang Wang. Searching and collection of bibliography was performed by Qiang Wei. We confirm that the manuscript has been read and approved by all named authors and that there are no other persons who satisfied the criteria for authorship but are not listed. We further confirm that the order of authors listed in the manuscript has been approved by all of us. Xi Chen and Yue He contributed equally to this work.

Acknowledgments

Supplementary Materials

Supplementary Figure: (A) following *P. aeruginosa* infection ($n = 15$ for every group), we observed mortality rate over the 10-day period. (B, C) Lung or BALF bacterial CFU in each group after challenge with *P. aeruginosa* ($n = 5$ mice/group). (D, E) Lung injury assessment indicators such as protein in BALF, myeloperoxidase, and wet/dry weight ratio in the left lung were measured after challenge with *P. aeruginosa* ($n = 5$ mice/group). $^{*}p < 0.05$, $^{**}p < 0.01$, and $^{***}p < 0.001$, upon one-way ANOVA as well as LSD multiple comparisons. Compared with *S. aureus* infection treated with basil polysaccharide group or CLP-surgery mice upon secondary *S. aureus* infection treated with basil polysaccharide group. ns: no statistical significance between the groups challenged with *P. aeruginosa*. (Supplementary Materials)

References

[1] A. Rhodes, L. E. Evans, W. Alhazzani et al., "Surviving sepsis campaign: international guidelines for management of sepsis and septic shock: 2016," *Intensive Care Medicine*, vol. 43, no. 3, pp. 304–377, 2017.

[2] M. Singer, C. S. Deutschman, C. W. Seymour et al., "The Third International Consensus Definitions for Sepsis and Septic Shock (Sepsis-3)," *JAMA*, vol. 315, no. 8, pp. 801–810, 2016.

[3] M. J. Delano and P. A. Ward, "The immune system's role in sepsis progression, resolution, and long-term outcome," *Immunological Reviews*, vol. 274, no. 1, pp. 330–353, 2016.

[4] J. Stoller, L. Halpin, M. Weis et al., "Epidemiology of severe sepsis: 2008-2012," *Journal of Critical Care*, vol. 31, no. 1, pp. 58–62, 2016.

[5] C. Fleischmann-Struzek, L. Mellhammar, N. Rose et al., "Incidence and mortality of hospital- and ICU-treated sepsis: results from an updated and expanded systematic review and meta-analysis.," *Intensive Care Medicine*, vol. 46, no. 8, pp. 1552–1562, 2020.

[6] D. C. Angus and S. Opal, "Immunosuppression and secondary infection in sepsis: part, not all, of the story," *JAMA*, vol. 315, no. 14, pp. 1457–1459, 2016.

[7] R. P. Wenzel and M. B. Edmond, "Septic shock–evaluating another failed treatment," *The New England Journal of Medicine*, vol. 366, no. 22, pp. 2122–2124, 2012.

[8] R. S. Hotchkiss and S. Opal, "Immunotherapy for sepsis–a new approach against an ancient foe," *The New England Journal of Medicine*, vol. 363, no. 1, pp. 87–89, 2010.

[9] B. Morton, S. H. Pennington, and S. B. Gordon, "Immunomodulatory adjuvant therapy in severe community-acquired pneumonia," *Expert Review of Respiratory Medicine*, vol. 8, no. 5, pp. 587–596, 2014.

[10] J. P. Mizgerd, "Respiratory infection and the impact of pulmonary immunity on lung health and disease," *American Journal of Respiratory and Critical Care Medicine*, vol. 186, no. 9, pp. 824–829, 2012.

[11] J. C. Deng, G. Cheng, M. W. Newstead et al., "Sepsis-induced suppression of lung innate immunity is mediated by IRAK-M," *The Journal of Clinical Investigation*, vol. 116, no. 9, pp. 2532–2542, 2006.

[12] I. Tancevski, M. Nairz, K. Duwensee et al., "Fibrates ameliorate the course of bacterial sepsis by promoting neutrophil recruitment via CXCR2," *EMBO Molecular Medicine*, vol. 6, no. 6, pp. 810–820, 2014.

[13] J. Unsinger, M. McGlynn, K. R. Kasten et al., "IL-7 promotes T cell viability, trafficking, and functionality and improves survival in sepsis," *Journal of Immunology*, vol. 184, no. 7, pp. 3768–3779, 2010.

[14] Z. Song, J. Zhang, X. Zhang et al., "Interleukin 4 deficiency reverses development of secondary Pseudomonas aeruginosa pneumonia during sepsis-associated immunosuppression," *The Journal of Infectious Diseases*, vol. 211, no. 10, pp. 1616–1627, 2015.

[15] P. Sestili, T. Ismail, C. Calcabrini et al., "The potential effects of Ocimum basilicum on health: a review of pharmacological and toxicological studies," *Expert Opinion on Drug Metabolism & Toxicology*, vol. 14, no. 7, pp. 679–692, 2018.

[16] D. P. Uma, "Radioprotective, anticarcinogenic and antioxidant properties of the Indian holy basil, Ocimum sanctum (Tulasi)," *Indian Journal of Experimental Biology*, vol. 39, no. 3, pp. 185–190, 2001.

[17] V. Vats, J. K. Grover, and S. S. Rathi, "Evaluation of anti-hyperglycemic and hypoglycemic effect of _Trigonella foenum_ - _graecum_ Linn, _Ocimum sanctum_ Linn and _Pterocarpus marsupium_ Linn in normal and alloxanized diabetic rats," *Journal of Ethnopharmacology*, vol. 79, no. 1, pp. 95–100, 2002.

[18] C. Jayasinghe, N. Gotoh, T. Aoki, and S. Wada, "Phenolics composition and antioxidant activity of sweet basil (Ocimum basilicum L.)," *Journal of Agricultural and Food Chemistry*, vol. 51, no. 15, pp. 4442–4449, 2003.

[19] T. Koga, N. Hirota, and K. Takumi, "Bactericidal activities of essential oils of basil and sage against a range of bacteria and the effect of these essential oils on _Vibrio parahaemolyticus_," *Microbiological Research*, vol. 154, no. 3, pp. 267–273, 1999.

[20] B. Feng, Y. Zhu, S. M. He, G. J. Zheng, Y. LIu, and Y. Z. Zhu, "effect of basil polysaccharide on histone H3K9me2 methylation and expression of G9a and JMJD1A in hepatoma cells under hypoxic conditions," *Journal of Chinese medicinal materials*, vol. 38, no. 7, pp. 1460–1465, 2015.

[21] Y. Zhan, X. An, S. Wang, M. Sun, and H. Zhou, "Basil polysaccharides: a review on extraction, bioactivities and pharmacological applications," *Bioorganic & Medicinal Chemistry*, vol. 28, no. 1, article 115179, 2020.

[22] D. Benedec, A. E. Pârvu, I. Oniga, A. Toiu, and B. Tiperciuc, "Effects of Ocimum basilicum L. extract on experimental acute inflammation," *Revista Medico-Chirurgicala A Societatii de Medici si Naturalisti din Iasi*, vol. 111, no. 4, pp. 1065–1069, 2007.

[23] I. Kaya, N. Yigit, and M. Benli, "Antimicrobial activity of various extracts of Ocimum basilicum L. and observation of the inhibition effect on bacterial cells by use of scanning electron microscopy," *African journal of traditional, complementary, and alternative medicines : AJTCAM*, vol. 5, no. 4, pp. 363–369, 2008.

[24] H. El-Beshbishy and S. Bahashwan, "Hypoglycemic effect of basil (Ocimum basilicum) aqueous extract is mediated through inhibition of α-glucosidase and α-amylase activities," *Toxicology and Industrial Health*, vol. 28, no. 1, pp. 42–50, 2012.

[25] S. Amrani, H. Harnafi, D. Gadi et al., "Vasorelaxant and anti-platelet aggregation effects of aqueous _Ocimum basilicum_ extract," *Journal of Ethnopharmacology*, vol. 125, no. 1, pp. 157–162, 2009.

[26] F. B. Mayr, S. Yende, and D. C. Angus, "Epidemiology of severe sepsis," *Virulence*, vol. 5, no. 1, pp. 4–11, 2014.

[27] J. L. Vincent, J. Rello, J. Marshall et al., "International study of the prevalence and outcomes of infection in intensive care units," *JAMA*, vol. 302, no. 21, pp. 2323–2329, 2009.

[28] C. J. Wang, M. Zhang, H. Wu, S. H. Lin, and F. Xu, "IL-35 interferes with splenic T cells in a clinical and experimental model of acute respiratory distress syndrome," *International Immunopharmacology*, vol. 67, pp. 386–395, 2019.

[29] S. Zou, Q. Luo, Z. Song et al., "Contribution of progranulin to protective lung immunity during bacterial pneumonia," *The Journal of Infectious Diseases*, vol. 215, no. 11, pp. 1764–1773, 2017.

[30] B. Feng, Y. Zhu, Z. Su et al., "Basil polysaccharide attenuates hepatocellular carcinoma metastasis in rat by suppressing H3K9me2 histone methylation under hepatic artery ligation-induced hypoxia," *International Journal of Biological Macromolecules*, vol. 107, pp. 2171–2179, 2018.

[31] J. LV, Q. SHAO, H. WANG et al., "Effects and mechanisms of curcumin and basil polysaccharide on the invasion of SKOV3 cells and dendritic cells," *Molecular Medicine Reports*, vol. 8, no. 5, pp. 1580–1586, 2013.

[32] X. Chen, Q. Wei, Y. Hu, and C. Wang, "Role of Fractalkine in promoting inflammation in sepsis-induced multiple organ dysfunction," *Infection, genetics and evolution : journal of molecular epidemiology and evolutionary genetics in infectious diseases*, vol. 85, article 104569, 2020.

[33] K. E. Driscoll, "Macrophage inflammatory proteins: biology and role in pulmonary inflammation," *Experimental Lung Research*, vol. 20, no. 6, pp. 473–490, 1994.

[34] T. Yamamori, O. Inanami, H. Nagahata, Y. D. Cui, and M. Kuwabara, "Roles of p38 MAPK, PKC and PI3-K in the signaling pathways of NADPH oxidase activation and phagocytosis in bovine polymorphonuclear leukocytes," *FEBS Letters*, vol. 467, no. 2-3, pp. 253–258, 2000.

[35] M. Bouras, K. Asehnoune, and A. Roquilly, "Contribution of dendritic cell responses to sepsis-induced immunosuppression and to susceptibility to secondary pneumonia," *Frontiers in Immunology*, vol. 9, article 2590, 2018.

[36] L. A. van Vught, B. P. Scicluna, M. A. Wiewel et al., "Comparative analysis of the host response to community-acquired and hospital-acquired pneumonia in critically ill patients," *American Journal of Respiratory and Critical Care Medicine*, vol. 194, no. 11, pp. 1366–1374, 2016.

[37] K. M. Sundar and M. Sires, "Sepsis induced immunosuppression: implications for secondary infections and complications," *Indian journal of critical care medicine : peer-reviewed, official publication of Indian Society of Critical Care Medicine*, vol. 17, no. 3, pp. 162–169, 2013.

[38] J. S. Lee, D. L. Giesler, W. F. Gellad, and M. J. Fine, "Antibiotic therapy for adults hospitalized with community-acquired pneumonia: a systematic review," *JAMA*, vol. 315, no. 6, pp. 593–602, 2016.

[39] R. E. Hancock, A. Nijnik, and D. J. Philpott, "Modulating immunity as a therapy for bacterial infections," *Nature Reviews Microbiology*, vol. 10, no. 4, pp. 243–254, 2012.

[40] A. Pielesz, "Vibrational spectroscopy and electrophoresis as a "golden means" in monitoring of polysaccharides in medical plant and gels," *Spectrochimica acta Part A, Molecular and biomolecular spectroscopy*, vol. 93, pp. 63–69, 2012.

[41] Z. Yu, G. Ming, W. Kaiping et al., "Structure, chain conformation and antitumor activity of a novel polysaccharide from _Lentinus edodes_," *Fitoterapia*, vol. 81, no. 8, pp. 1163–1170, 2010.

[42] C. Li, X. Li, L. You, X. Fu, and R. H. Liu, "Fractionation, preliminary structural characterization and bioactivities of polysaccharides from _Sargassum pallidum_," *Carbohydrate Polymers*, vol. 155, pp. 261–270, 2017.

[43] X. Li, W. Xu, and J. Chen, "Polysaccharide purified from _Polyporus umbellatus_ (Per) Fr induces the activation and maturation of murine bone-derived dendritic cells via toll-like receptor 4," *Cellular Immunology*, vol. 265, no. 1, pp. 50–56, 2010.

[44] Z. Wang, J. Meng, Y. Xia et al., "Maturation of murine bone marrow dendritic cells induced by acidic Ginseng polysaccharides," *International Journal of Biological Macromolecules*, vol. 53, pp. 93–100, 2013.

[45] G. Opalchenova and D. Obreshkova, "Comparative studies on the activity of basil–an essential oil from _Ocimum basilicum_ L. –against multidrug resistant clinical isolates of the genera _Staphylococcus_ , _Enterococcus_ and _Pseudomonas_ by using different test methods," *Journal of Microbiological Methods*, vol. 54, no. 1, pp. 105–110, 2003.

[46] E. Cornejo, P. Schlaermann, and S. Mukherjee, "How to rewire the host cell: a home improvement guide for intracellular bacteria," *The Journal of Cell Biology*, vol. 216, no. 12, pp. 3931–3948, 2017.

[47] J. W. Griffith, C. L. Sokol, and A. D. Luster, "Chemokines and chemokine receptors: positioning cells for host defense and immunity," *Annual Review of Immunology*, vol. 32, no. 1, pp. 659–702, 2014.

[48] A. Barczyk, W. Pierzchala, and E. Sozanska, "Levels of CC-chemokine (MCP-1 alpha, MIP-1 beta) in induced sputum

of patients with chronic obstructive pulmonary disease and patients with chronic bronchitis," *Pneumonologia i Alergologia Polska*, vol. 69, no. 1-2, pp. 40–49, 2001.

[49] X. Sun, H. P. Jones, L. M. Hodge, and J. W. Simecka, "Cytokine and chemokine transcription profile during Mycoplasma pulmonis infection in susceptible and resistant strains of mice: macrophage inflammatory protein 1beta (CCL4) and monocyte chemoattractant protein 2 (CCL8) and accumulation of CCR5+ Th cells," *Infection and Immunity*, vol. 74, no. 10, pp. 5943–5954, 2006.

[50] Y. Kobayashi, Y. Konno, A. Kanda et al., "Critical role of CCL4 in eosinophil recruitment into the airway," *Clinical and experimental allergy : journal of the British Society for Allergy and Clinical Immunology*, vol. 49, no. 6, pp. 853–860, 2019.

[51] M. Vasakova, M. Sterclova, L. Kolesar et al., "Bronchoalveolar lavage fluid cellular characteristics, functional parameters and cytokine and chemokine levels in interstitial lung diseases," *Scandinavian Journal of Immunology*, vol. 69, no. 3, pp. 268–274, 2009.

[52] M. Aziz, Y. Ode, M. Zhou et al., "B-1a cells protect mice from sepsis-induced acute lung injury," *Molecular Medicine*, vol. 24, no. 1, p. 26, 2018.

[53] J. Wagner, K. M. Strosing, S. G. Spassov et al., "Sevoflurane posttreatment prevents oxidative and inflammatory injury in ventilator-induced lung injury," *PLoS One*, vol. 13, no. 2, article e0192896, 2018.

[54] H. R. Jones, C. T. Robb, M. Perretti, and A. G. Rossi, "The role of neutrophils in inflammation resolution," *Seminars in Immunology*, vol. 28, no. 2, pp. 137–145, 2016.

[55] P. Scapini, J. A. Lapinet-Vera, S. Gasperini, F. Calzetti, F. Bazzoni, and M. A. Cassatella, "The neutrophil as a cellular source of chemokines," *Immunological Reviews*, vol. 177, no. 1, pp. 195–203, 2000.

[56] E. von Stebut, M. Metz, G. Milon, J̈. Knop, and M. Maurer, "Early macrophage influx to sites of cutaneous granuloma formation is dependent on MIP-1alpha /beta released from neutrophils recruited by mast cell-derived TNFalpha," *Blood*, vol. 101, no. 1, pp. 210–215, 2003.

[57] T. Hussell and T. J. Bell, "Alveolar macrophages: plasticity in a tissue-specific context," *Nature Reviews Immunology*, vol. 14, no. 2, pp. 81–93, 2014.

[58] A. M. Krachler, A. R. Woolery, and K. Orth, "Manipulation of kinase signaling by bacterial pathogens," *The Journal of Cell Biology*, vol. 195, no. 7, pp. 1083–1092, 2011.

[59] T. A. Fleisher, "Apoptosis," *Annals of Allergy, Asthma & Immunology : Official Publication of the American College of Allergy, Asthma, & Immunology*, vol. 78, no. 3, pp. 245–250, 1997.

[60] S. Elmore, "Apoptosis: a review of programmed cell death," *Toxicologic Pathology*, vol. 35, no. 4, pp. 495–516, 2007.

[61] B. E. Menzies and I. Kourteva, "Internalization of Staphylococcus aureus by endothelial cells induces apoptosis," *Infection and Immunity*, vol. 66, no. 12, pp. 5994–5998, 1998.

[62] B. E. Menzies and I. Kourteva, "Staphylococcus aureus alphatoxin induces apoptosis in endothelial cells," *FEMS Immunology and Medical Microbiology*, vol. 29, no. 1, pp. 39–45, 2000.

[63] D. Jonas, I. Walev, T. Berger, M. Liebetrau, M. Palmer, and S. Bhakdi, "Novel path to apoptosis: small transmembrane pores created by staphylococcal alpha-toxin in T lymphocytes evoke internucleosomal DNA degradation," *Infection and Immunity*, vol. 62, no. 4, pp. 1304–1312, 1994.

[64] L. S. Miller, V. G. Fowler, S. K. Shukla, W. E. Rose, and R. A. Proctor, "Development of a vaccine against Staphylococcus aureus invasive infections: evidence based on human immunity, genetics and bacterial evasion mechanisms," *FEMS Microbiology Reviews*, vol. 44, no. 1, pp. 123–153, 2020.

[65] C. E. Zielinski, "Human T cell immune surveillance: phenotypic, functional and migratory heterogeneity for tailored immune responses," *Immunology Letters*, vol. 190, pp. 125–129, 2017.

[66] C. O. Sahlmann and P. Strobel, "Pathophysiologie der Entzündung," *Nuklearmedizin Nuclear medicine*, vol. 55, no. 1, pp. 1–6, 2016.

[67] D. R. Neill, V. E. Fernandes, L. Wisby et al., "T regulatory cells control susceptibility to invasive pneumococcal pneumonia in mice," *PLoS Pathogens*, vol. 8, no. 4, article e1002660, 2012.

[68] K. A. Mohammed, N. Nasreen, M. J. Ward, and V. B. Antony, "Induction of acute pleural inflammation by Staphylococcus aureus. I. CD4+ T cells play a critical role in experimental empyema," *The Journal of Infectious Diseases*, vol. 181, no. 5, pp. 1693–1699, 2000.

Research Article

Assessment of the Vanillin Anti-Inflammatory and Regenerative Potentials in Inflamed Primary Human Gingival Fibroblast

Erica Costantini [ID],[1] **Bruna Sinjari** [ID],[2] **Katia Falasca** [ID],[3] **Marcella Reale** [ID],[2] **Sergio Caputi** [ID],[1] **Srinivas Jagarlapodii** [ID],[1] and **Giovanna Murmura** [ID][2]

[1]*Department of Medical, Oral and Biotechnological Science, University G.d'Annunzio, Chieti-Pescara, Italy*
[2]*Department of Innovative Technologies in Medicine and Dentistry, University G.d'Annunzio, Chieti-Pescara, Italy*
[3]*Department of Medicine and Aging Science, University G.d'Annunzio, Chieti-Pescara, Italy*

Correspondence should be addressed to Erica Costantini; erica.costantini@unich.it and Marcella Reale; mreale@unich.it

Background. Inflammatory responses have been associated with delayed oral mucosal wound healing and the pathogenesis of the periodontal disease. The invasion of microbes into the tissues and the establishment of a chronic infection may be due to impaired healing. The protracted inflammatory phase may delay wound healing and probably support tissue fibrosis and reduce tissue regeneration. Vanillin is a well-known natural compound with potential anti-inflammatory capacity. Hence, we hypothesized that Vanillin could accelerate wound healing reducing inflammation and especially cytokine production making the oral tissue repair process easier. *Methods.* Our hypothesis was tested using primary human gingival fibroblast (HGF) cell pretreated with Vanillin and primed with IL-1β, as inductor of proinflammatory environment. After 24 hours of treatments, the gene expression and production of IL-6, TNF-α, IL-8, COX-2, iNOS, and nitric oxide (NO) generation and the wound healing rate were determined. *Results.* In IL-1β-primed cells, preincubation with Vanillin reduced IL-6, IL-8, COX-2, and iNOS expression and NO release, compared to IL-1β-primed cells. Moreover, Vanillin determines the increased gene expression of nAChRα7, leading us to hypothesize a role of Vanillin in the activation of the cholinergic anti-inflammatory pathway. Furthermore, in presence of mechanical injury, the Vanillin preincubation, wound closure may be reducing the expression and release of IL-6 and TNF-α and upregulation of COX-2 and IL-8. *Conclusion.* Together, the results of this study highlight the anti-inflammatory and tissue repair ability of Vanillin in IL-1β-primed HGF. Therefore, Vanillin shows a potential therapeutic interest as an inflammatory modulator molecule with novel application in periodontal regeneration and oral health.

1. Introduction

Inflammation is defined as an essential biological event occurring for the defence of the body. It involves immune cells and multiple mechanisms that operate at different levels, including alterations in immune cell types in tissues, changes in cellular reactivity to inflammatory stimuli, regulation of signaling pathways, and control of gene expression [1]. In fact, macrophages promote the innate host defence and inflammatory reaction, with the release of inflammatory mediators like interleukin- (IL-) 1β, IL-6, IL-8, tumour necrosis factor- (TNF-) α, reactive oxygen species (ROS), and nitric oxide (NO) [2]. These molecules mediate the inflammatory response and trigger adaptive immune activa-

tion, through the interaction with cellular specific receptors [3]. Periodontal diseases, inflammatory conditions with an infectious aetiology including gingivitis and periodontitis, are amongst the prevalent oral health illnesses that may ultimately lead to severe chronic conditions in the oral cavity [4]. Inflammation seems to be linked to microorganism growth associated with the destruction of oral tissues and release of harmful nutrients, such as degraded collagen, heme-containing compounds, sources of amino acids, and iron. These events can drive the establishment of a proinflammatory microenvironment and the production of oxidative stress mediators with the periodontal pocket formation and gingival tissue, alveolar bone, and periodontal ligament destruction. Therefore, the prominent

role of the inflammatory response in periodontal disease pathogenesis suggests that reduction of bacterial load and regulation of inflammation are the main goals for the treatment of periodontal disease. Recently, it has become clear that natural compounds are important regulators of immune responses [5]. To date, natural phenolic compounds have gained considerable attention for the improvement of human health. The increase in the use of herbal medicines has renewed interest in the effects of plant extracts for the control of plaque and other oral diseases [5–7]. In their review, Kouidhi et al. [8] documented the potential use of plant extracts, essential oils, and natural compounds as biofilm preventive agents in dentistry, and the search for natural anti-inflammatory agents with fewer side effects has made the leap from research laboratories to the pharmaceutical industry. Different natural common herb components such as the tea tree oil, aloe vera, vanillin, curcumin, and chamomile have been recently introduced as anti-inflammatory molecules for *dental* treatments [9].

Vanillin (4-hydroxy-3-methoxybenzaldehyde) is the major component of natural vanilla, which is one of the most widely used flavor components in food and personal products [10] with antimicrobial, antimutagenic, and antiangiogenic effects [11, 12]. Many studies have investigated the role of Vanillin in nervous systems, demonstrating the protection against rotenone-induced neurotoxicity in SH-SY5Y cells [13] or the antineuroinflammatory properties in microglial cells [14]. Keeping in mind the antimicrobial and anti-inflammatory capacity of Vanillin and since to date, there are no reports on the effects of Vanillin on the oral tissue cells, this study is aimed at investigating the ability of Vanillin to modulate the inflammatory response, oxidative stress, and oral tissue repair. Human gingival fibroblasts (HGFs) are the most abundant resident cells in the oral mucosa, and inflammatory cytokine produced by HGF may have a central role during gingival inflammation and periodontal tissue repair. Thus, to mimic in vitro the inflammatory microenvironment in periodontal disease, we used IL-1β as inductor and enhancer of the proinflammatory response on primary gingival fibroblasts [15]. With this in vitro model, we aim to evaluate the effects of Vanillin on inflammation, oxidative stress, and tissue repair, in order to open a way for its potential use in periodontal diseases.

2. Materials and Methods

2.1. HGF Sampling. Healthy patients, aged between 20 and 25 years, were recruited at the Dental Clinic of "G.d'Annunzio" of Chieti-Pescara University, Chieti, Italy, for wisdom tooth extraction. After written informed consent release, discarded gingival tissues were obtained and processed for primary human gingival fibroblast (HGF) isolation. The gingival tissues were placed in physiological solution, at room temperature, for transport to the cell culture laboratory. The study was approved with the committee report no. 14, on 23 July 2015 by the Inter-Institutional Ethic Committee of the University of Chieti-Pescara, Italy. Each sample was coded to guarantee the anonymity of the donors.

2.2. Cell Isolation and Culture. For each healthy donor, gingival fragments were washed with physiological sodium chloride solution and placed in a T25 culture flask (Merck KGaA, Darmstadt, Germany) filled with Dulbecco's Modified Eagle's Medium (DMEM) (pH 7.2; Merck KGaA, Darmstadt, Germany) supplemented with 10% heat-inactivated fetal bovine serum (FBS), 100 U/mL penicillin, 100 μg/mL streptomycin, and 2 mmol/L l-glutamine (Merck KGaA, Darmstadt, Germany) and left in a humidified CO_2 incubator set at 37°C till cell adhesion occurred. The culture media were replaced with fresh medium twice a week for 15 days to obtain primary HGF. Cells were collected after adding of 1X trypsin-EDTA solution (Merck KGaA, Darmstadt, Germany) and used for subsequential experiments. Primary HGFs were used for experiments between passages 4 and 5 after isolation.

2.3. Cell Viability Assay. HGFs were seeded into the wells of the 96-well plates at a density of 0.4×10^3 cells/well. The following day, IL-1β (Peprotech, Rocky Hill, USA) within a concentration range 0.1–10 ng/mL or Vanillin (Merck KGaA, Darmstadt, Germany) within a concentration range 100-300 μM or negative control (0.1% (v/v) DMSO) and positive control (100% (v/v) DMSO) were added to the attached cells, in presence of fresh culture medium, for 24 h. Cell viability was determined by the 3-(4,5-dimethylthiazol-2-yl)-2,5-diphenyltetrazolium bromide (MTT) assay, according to the recommendations of the manufacturer (Merck KGaA, Darmstadt, Germany). At the end of incubation, MTT reagent was added for 2 h and incubated at 37°C, the absorbance was measured at OD590 nm. Absorbance data were normalized to the untreated control group, considered as 100% of viability.

2.4. In Vitro Treatments. The inflammatory condition of periodontal disease was mimic *in vitro* priming HGFs with IL-1β (1 ng/ml). To evaluate the ability of Vanillin on inflammatory response modulation, we have designed two different experimental conditions. In the first experimental condition, 0.15×10^5 cells/cm^2 HGF were preincubated for 2 h with 200 μM of Vanillin and treated with IL-1β for the following 24 h of incubation at 37°C, 5% CO_2, and then, gene expression and production of inflammatory mediators were evaluated. In the second experimental condition, HGFs were seeded at a cell density of 0.15×10^5 cells/cm^2 in two sets of 6-well plates in a complete medium (10% FBS) and grown until the monolayer was confluent. Subsequently, to mimic the oral wound, a scratch was made mechanically with a 10 μl sterile pipette tip. Detached cells and debris were removed by washing with Dulbecco's Phosphate Buffered Saline (PBS), fresh medium containing IL-1β, or Vanillin was added to carry on the incubation at 37°C, 5% CO_2 for 24 h. Alternatively, Vanillin was added 2 h before the scratch, and the added fresh medium was supplemented with Vanillin+IL-1β. The effect of Vanillin on the rate of scratched monolayer closure was monitored by observing the cell repopulation of the area between the wound edges, using an inverted phase-contrast microscope (Leica,

TABLE 1: Primer sequences used for real-time PCR reactions.

Gene	Forward primer sequence (5′-3′)	Reverse primer sequence (5′-3′)	Amplicon length
18s	CTTTGCCATCACTGCCATTAAG	TCCATCCTTTACATCCTTCTGTC	199 bp
IL-6	GTACATCCTCGACGGCATC	ACCTCAAACTCCAAAAGACCAG	198 bp
TNF-α	CCTTCCTGATCGTGGCAG	GCTTGAGGGTTTGCTACAAC	184 bp
IL-8	GTGTAAACATGACTTCCAAGCTG	GTCCACTCTCAATCACTCTCAG	182 bp
iNOS	GGTATCCTGGAGCGAGTGGT	CTCTCAGGCTCTTCTGTGGC	212 bp
COX-2	GACAGTCCACCAACTTACAATG	GGCAATCATCAGGCACAGG	105 bp
nAChRα7	CTGCTCGTGGCTGAGATCAT	CTGGTCCACTTGGGCATCTT	167 bp

Germany) equipped with a CCD camera, and the remaining cell-free area was measured.

At the end of incubation, the cells were harvested for analysis of inflammatory mediators involved in wound healing.

2.5. Nitrite Determination. To measure the NO production, nitrite concentration in the culture supernatant was determined using Griess reagent (1% sulfanilamide and 0.1% N-(1-naphthyl)-ethylenediamine dihydrochloride in 5% H3PO4) (Cayman Chemical, Ann Arbor, Michigan, USA). 100 μl of cell culture supernatant and 100 μl Griess reagent were mixed and incubated for 10 min, to color development. The absorption was estimated at 540 nm, using a Glomax Multireader spectrophotometer (Promega, Madison, WI, USA). Nitrite standard (Cayman Chemical, Ann Arbor, Michigan, USA) was used to generate a standard curve for quantification. Results were obtained from three independent experiment measurements.

2.6. ELISA Analysis. The culture supernatants were quantitatively assayed for IL-6, TNF-α, and IL-8 (BOOSTER PicokineTM ELISA, Boster Biological Technology, Pleasanton, CA, USA), with concentrations following the manufacturer's instructions. Optical density was measured at 450 nm. The inflammatory cytokine levels were determined in all the different condition samples through duplicated measurements requiring 100 μL of culture supernatant. Results were standardized by using internal controls supplied with each kit, with a known concentration of the target protein. For IL-6, sensitivity < 0.3 pg/ml; for TNF-α and IL-8, sensitivity < 1 pg/ml.

2.7. RNA Isolation and Real-Time RT-PCR Analysis. Total RNA was isolated using the classic phenol-chloroform method. Total RNA was quantified at 260 nm using Nano-Drop 2000 ultraviolet-visible (UV-Vis) spectrophotometer (Thermo Fisher Scientific, Waltham, MA, USA). 1 μg of RNA was reverse transcribed to cDNA for 15 min at 42°C and 3 min at 90°C to inactivate Quantiscript Reverse Transcriptase, according to the protocol of QuantiTectReverse Transcription Kit (Qiagen, Hilden, DE). Real-time PCR was performed in a CFX Real-Time PCR Detection Systems (Bio-Rad, Hercules, California, USA), using GoTaq® qPCR Master Mix (Promega, Madison, WI, USA) to evaluate the gene expression of IL-6, nAChRα7, TNF-α, IL-8, iNOS, COX-2, and 18S housekeeping gene (Table 1). The amplifica-
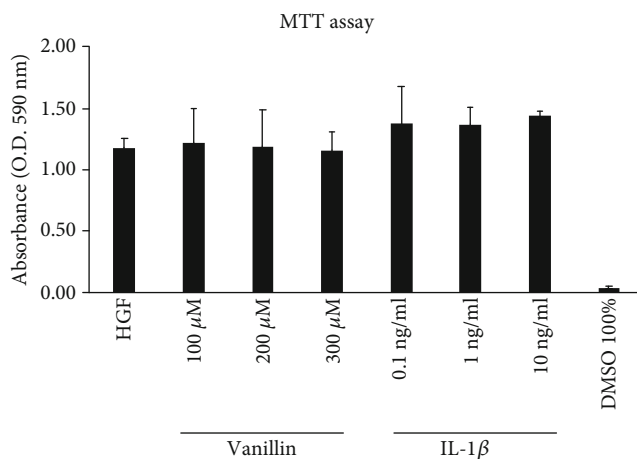
FIGURE 1: MTT viability assay in HGF cell treated for 24 h with Vanillin (100, 200, and 300 μM) or IL-1β (0.1, 1, and 10 ng/ml). Absorbance values are given as media ±SD of three independent experiments.

tion program consisted of a preincubation step for cDNA denaturation (2 min 95°C), followed by 40 cycles consisting of a denaturation step (30 s 95°C), an annealing step (60 s 60°C), and an extension step (30 s 68°C). At the end of each run, melting curve was performed in the temperature range of 60 to 95°C. Expression levels for each gene were performed according to the $2^{-\Delta\Delta Ct}$ method.

2.8. Statistical Analysis. Quantitative variables are summarized as the mean value and standard deviations (SD) in the figures. Precision of the fold change, calculated with $2^{-\Delta\Delta Ct}$ method, was determined using the 95% confidence interval (95% CI). Student t-test for unpaired sample was applied to evaluate statistical differences. Tests threshold of will be assumed equal to p value ≤0.05. Analyses were performed by the SPSS Inc. statistical software package (Version 23.0). One, two, and three symbols represent a significant difference between two groups with $p \leq 0.05$, $p < 0.01$, and $p < 0.001$, respectively.

3. Results

3.1. Effects of Vanillin and IL-1β on HGF Viability. Preliminarily, using 3-(4,5-dimethylthiazol-2-yl)-2,5-diphenyltetrazolium bromide (MTT) assay, we analyzed the effects of
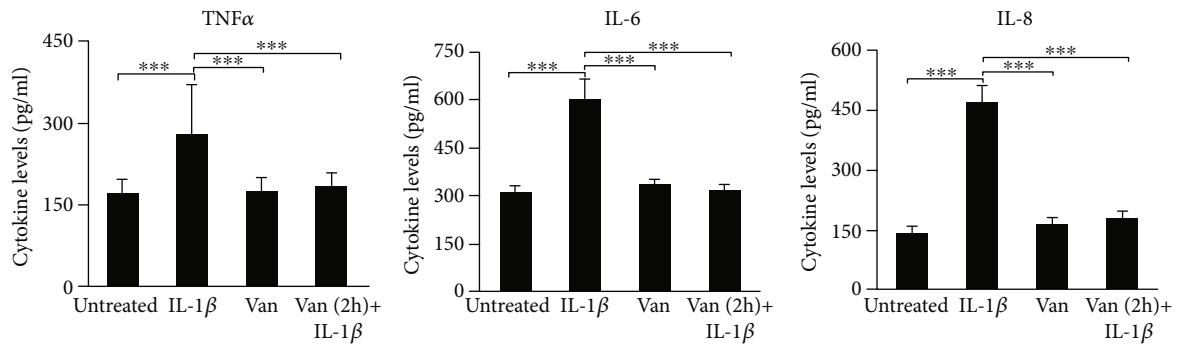
FIGURE 2: TNF-α, IL-6, and IL-8 levels in HGF cell culture supernatant. The mean values ± SD were reported, ***$p < 0.001$. All experiments were repeated in triplicate.

Vanillin (100, 200, and 300 μM) and IL-1β (0.1, 1, and 10 ng/ml), on HGF survival. The dose-response experiments suggested that cell viability after 24 h of incubation with Vanillin or IL-1β was not affected at any of the tested concentrations (Figure 1). Thus, the concentration of 1 ng/mL of IL-1β and 200 μM of Vanillin were selected for all the following experiments.

3.2. Production of Inflammatory Mediators.

To investigate the effects of Vanillin, on inflammation, we have used IL-1β to promote the proinflammatory response in HGF cells. After 24 h incubation of HGF with IL-1β, Vanillin alone or Vanillin (2 h pretreatment) plus IL-1β, IL-6, IL-8, and TNF-α levels were evaluated in cell culture supernatant, by ELISA assay. TNF-α, IL-6 ($p < 0.001$), and IL-8 ($p < 0.001$) were upregulated by the treatment with IL-1β. Meanwhile, in presence of Vanillin, alone or as pretreatment of inflamed HGF, a significant reduction of TNF-α, IL-6, and IL-8 was observed compared to IL-1β primed cells ($p < 0.001$) (Figure 2).

3.3. Gene Expression of Inflammatory Mediators.

In order to investigate if differences in supernatant levels of cytokine mirror a different gene expression profile of proinflammatory cytokine, we have evaluated the cytokine expression in treated and untreated HGF, using real-time PCR. TNF-α gene expression levels were significantly ($p = 0.047$) induced in IL-1β-primed HGF, such as levels of IL-8 ($p = 0.037$) compared to the untreated cells. Treatment with Vanillin does not significantly affect gene expression levels, compared to the other conditions. Unlike the pretreatment with Vanillin, for 2 h, reduces the expression of IL-6 ($p = 0.049$) and IL-8 ($p = 0.042$) with respect to IL-1β-primed HGF. Moreover, due to the nAChRα7 can represent an important marker for the stabilization of tissue homeostasis in the presence of persistent chronic inflammation, we have evaluated Vanillin effects on nAChRα7 gene expression. As shown in Figure 3, IL-1β-primed HGF showed no statistically significant variation in nAChRα7 expression levels ($p > 0.05$) with respect to untreated cells. Meanwhile, the Vanillin alone led to a slight increase of nAChRα7 gene expression, and in Vanillin-pretreated HGF cells, the nAChRα7 mRNA expres-

sion was significantly increased, compared to untreated cells ($p = 0.049$) and to the IL-1β-primed HGF ($p = 0.42$).

3.4. COX-2 and iNOS Gene Expression and NO Production.

Inflammatory stimuli induce the COX-2 and iNOS expression in the sites of inflammation and damaged tissue; thus, we have evaluated the effect of Vanillin on IL-1β-primed HGF. Both HGFs treated with Vanillin alone or with Vanillin (2 h pretreatment) plus IL-1β showed a significant downregulation of COX-2 gene expression ($p = 0.42$) with respect to IL-1β-primed HGF. The iNOS gene expression, responsible also for NO production, was significantly upregulated in all the treatment conditions, with higher increase in Vanillin pretreatment of inflamed HGF (Figure 4).

In addition, as shown in Figure 5, the production of NO was significantly increased in HGF IL-1β primed, compared to untreated cells. Vanillin pretreatment of IL-1β-primed HGF cells downregulates NO production levels, compared to IL-1β-primed HGF cells. These results underline the ability of Vanillin to regulate NO production acting by iNOS inhibition. In addition, as shown in Figure 5, the production of NO was significantly increased in HGF IL-1β primed, compared to untreated cells. Vanillin pretreatment, in IL-1β-primed HGF cells, showed a downregulation of NO production levels, compared to IL-1β-primed HGF cells. These results underline the ability of Vanillin to regulate NO production acting by iNOS inhibition.

3.5. Effect of Vanillin Pretreatment on Inflamed HGF Scratched Cells

3.5.1. Wound Healing.

Infections are the primary factors underlying inflammation, but also, injury or trauma can trigger inflammatory responses. The wound-healing assay was used to study the molecular mechanisms of tissue repair, as well as to study potential application of Vanillin as treatment to improve soft tissue healing. As showed in Figure 6(a), an increased HGF migration was observed in Vanillin-pretreated cells after 24 h scratching, reaching the 100% of wound closure. In IL-1β-primed cells, an impaired coverage of cell-free area (25% reduction of wound size compared to T0) was detected (Figures 6(a) and 6(b)).
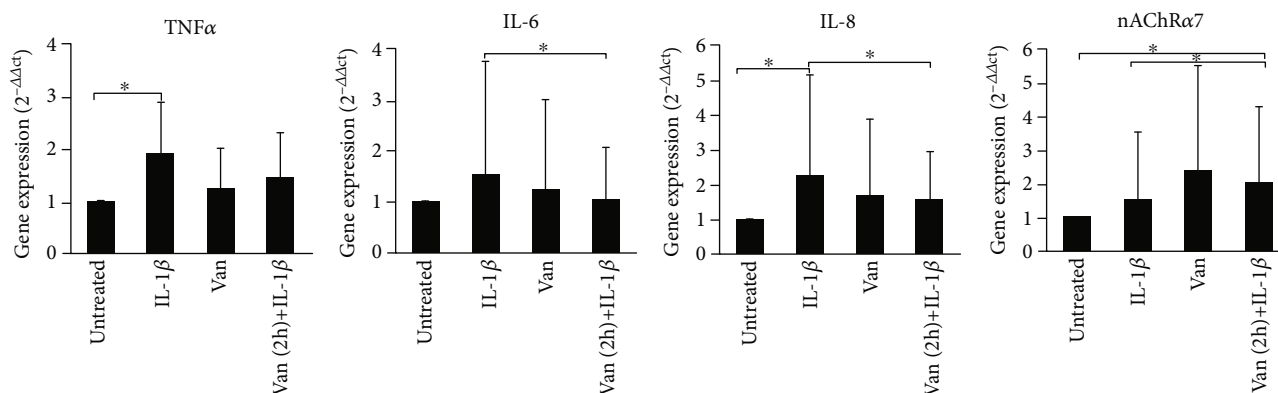
FIGURE 3: Gene expression of TNF-α, IL-6, IL-8, and nAChRα7 in HGF cells. Data are reported as mean and 95% CI, of three independent experiments. $^*p < 0.05$. IL-1β: IL-1β-primed cells; Van: Vanillin; Van (2 h)+IL-1β: Vanillin (2 h pretreatment) plus IL-1β.
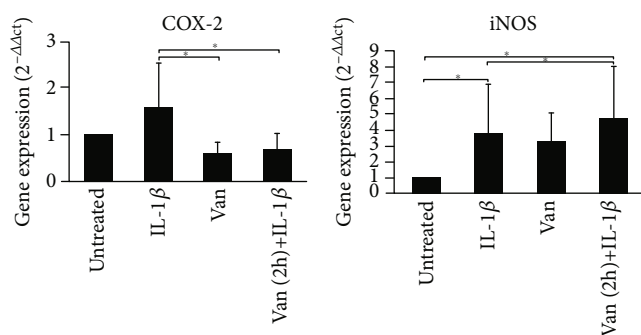
FIGURE 4: Gene expression of COX-2 and iNOS in HGF cells. Data are reported as mean and 95% CI, of three independent experiments, $^*p < 0.05$. IL-1β: IL-1β-primed cells; Van: Vanillin; Van (2 h)+IL-1β: Vanillin (2 h pre-treatment) plus IL-1β.

FIGURE 5: Levels of NO in HGF cells were determined based on Griess reagent reaction. Experiments were conducted in duplicate, and changes were reported as mean ± SD; $^{***}p < 0.001$. IL-1β: IL-1β-primed cells; Van: Vanillin; Van (2 h)+IL-1β: Vanillin (2 h pretreatment) plus IL-1β.

3.5.2. Inflammatory Mediator Expression and Production during Wound Healing. The repair process is mediated by the interaction of molecular signals, which orchestrate the cellular activities underling inflammation and healing. Thus, we have determined the effect of Vanillin on production and

gene expression of proinflammatory mediators. The preincubation with Vanillin in the scratched HGF monolayer reduced the production of IL-6 compared to IL-1β-primed cells ($p = 0.037$) and with respect to the untreated cells ($p = 0.004$), whereas the production of TNF-α and IL-8 was not significantly modified (Figure 7).

On the other hand, the gene expression of TNF-α and IL-8 was significantly affected by the treatments. In particular, a reduction of TNF-α in HGF scratched cells was induced by Vanillin ($p = 0.010$) and even more with Vanillin (2 h pretreatment) plus 1β cells ($p = 0.002$) (Figure 8). The IL-6 gene expression was reduced in cells treated with Vanillin ($p = 0.043$) and downregulated by Vanillin (2 h pretreatment) plus 1β ($p = 0.049$), compared to 1β-primed cells. In the scratched HGF monolayer, we observed higher levels of IL-8 gene expression in Vanillin (2 h pretreatment) plus 1β, with respect to both untreated ($p < 0.001$) and IL-1β-primed cells ($p < 0.001$).

3.5.3. Vanillin Effect on iNOS and COX-2 Gene Expression and NO Production in Inflamed HGF Scratched Cells. A cross-talk between NOS and COX enzymes, key inflammatory mediators, has been suggested [16]. Thus, we have evaluated the mRNA expression levels of COX-2 and iNOS in scratched HGF cell monolayer preincubated with Vanillin and primed with IL-1β. After 24 h of incubation in presence of mechanical damage and treatments, a significant increase of COX-2 gene expression ($p < 0.01$) was detected in Vanillin (2 h pretreatment) plus 1β, compared to other conditions (Figure 9). Meanwhile, Vanillin ($p = 0.022$) alone or as pretreatment ($p = 0.024$) of inflamed HGF showed a significant upregulation of iNOS, with respect to 1β-primed cells.

The weak induction of NO production observed in inflamed HGF scratched cells ($p < 0.001$) was reverted by Vanillin (2 h pretreatment) plus 1β ($p = 0.028$). Reduction is $p = 0.028$, as shown in Figure 10.

4. Discussion

The interest in the therapeutic potential of phenolic compounds, present in food and medicinal plants, had an

(a)

(b)
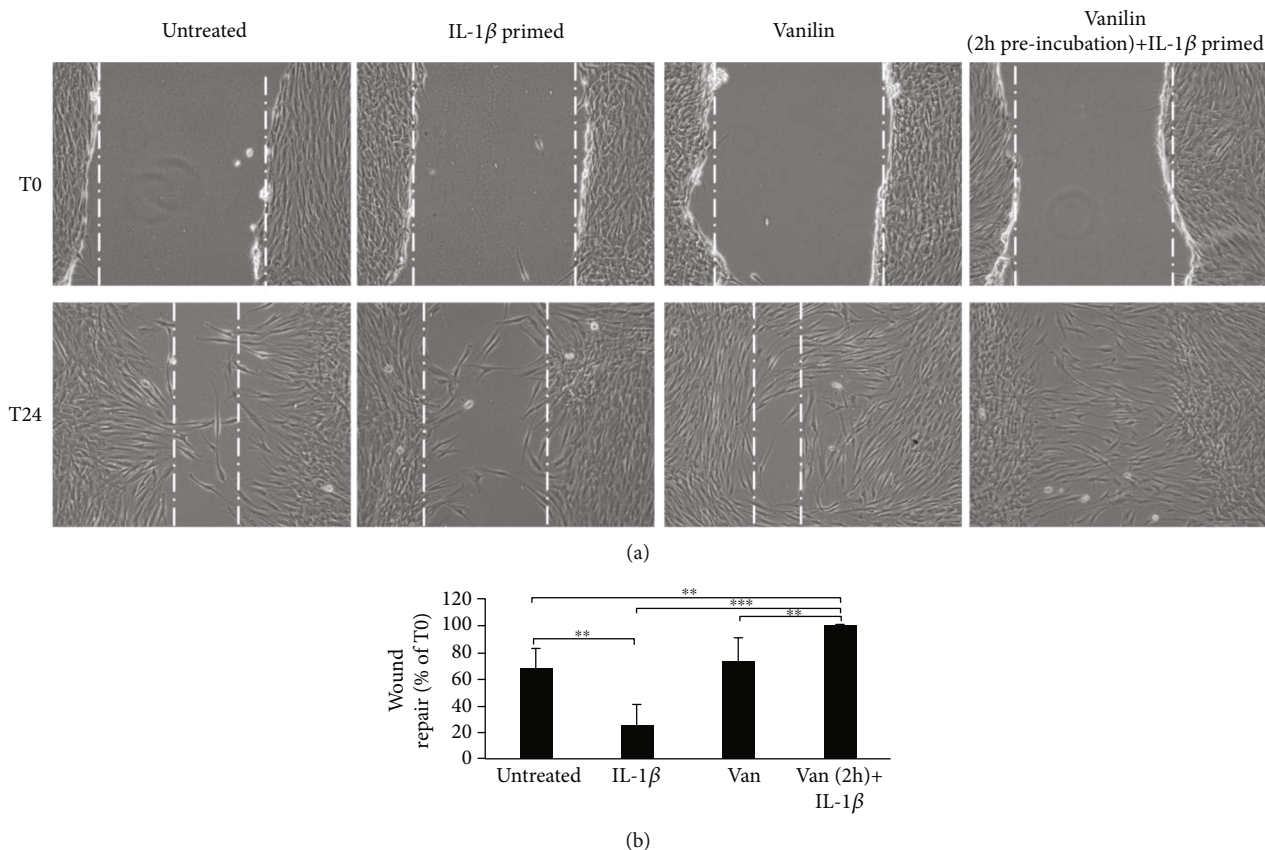
FIGURE 6: Wound healing of scratched oral fibroblast monolayer photographs and measurement of wound area were made immediately after the scratch (T0) and after 24 h (T24). (a) Representative images of wound-healing assay. (b) Wound repair was evaluated measuring the remaining cell-free area after 24 h and expressed as a percentage of the initial wound size (T0) assumed as 100%. $**p < 0.01$; $***p < 0.001$. IL-1β: IL-1β-primed cells; Van: Vanillin; Van (2 h)+IL-1β: Vanillin (2 h pretreatment) plus IL-1β.
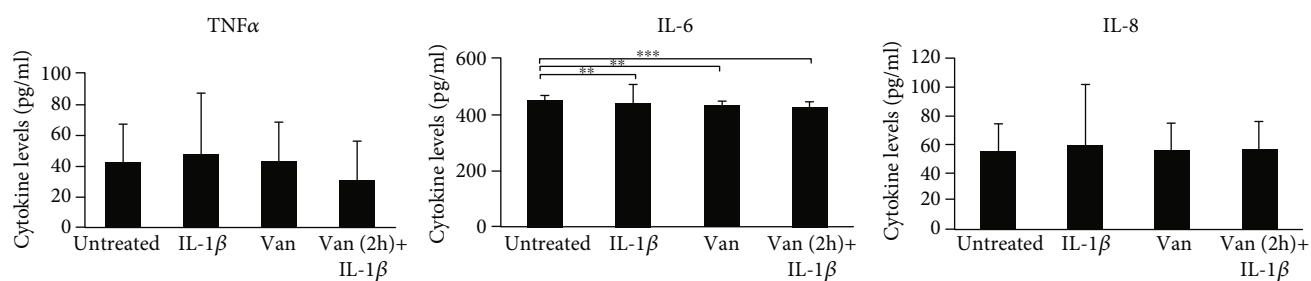
FIGURE 7: Levels of TNF-α, IL-6, and IL-8 in supernatant of HGF scratched cells. Data are reported as mean and 95% CI, of three independent experiments. $**p < 0.01$; $***p < 0.001$. IL-1β: IL-1β-primed cells; Van: Vanillin; Van (2 h)+IL-1β: Vanillin (2 h pretreatment) plus IL-1β.

increased relevance in the last decade [15, 17]. In many diseases, local inflammation could determine systemic inflammation, characterized by systemic oxidative stress, activation of circulating inflammatory cells, and increased circulating levels of inflammatory cytokines. The influence of inflammatory response by phenolic compounds has become the focus of several new treatment strategies with promising results [18, 19]. The use of Vanillin in oral inflammatory diseases has not yet been evaluated, although its interesting effects on oxidative stress and inflammation may represent a new strategy for the treatment of inflammatory

diseases. Oral fibroblasts, other than by macrophages, dendritic cells, epithelial, and keratinocytes cells, have a central role in the inhibition of bacterial products and proinflammatory cytokine production [20–22]. In periodontitis, proinflammatory cytokines, such as IL-1β, IL-6, IL-8, and TNF-α, seem to be the major mediators, involved in the destruction of periodontal tissue. Individuals with periodontal infections show high concentrations of circulating inflammatory markers that directly correlated with the severity of tissue destruction and inflammatory serum markers [20–23]. High levels of IL-6 and TNF-α, important mediators in
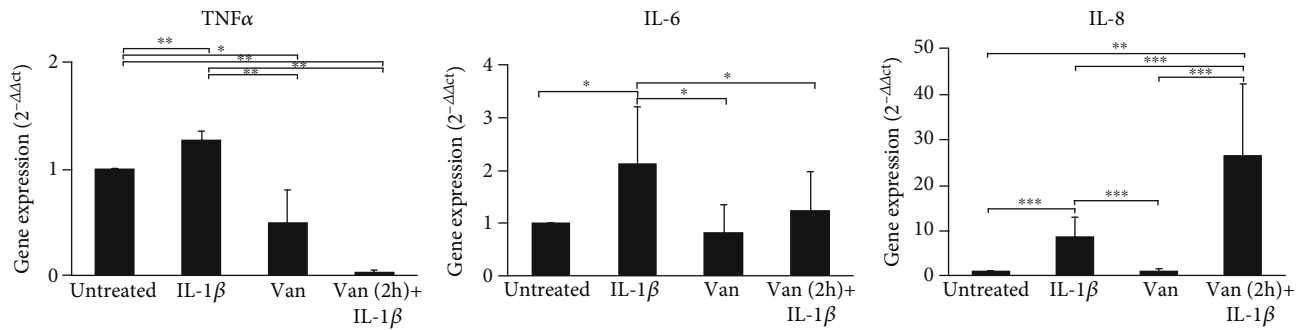
FIGURE 8: Gene expression of TNF-α, IL-6, and IL-8 in HGF scratched cells. Data are reported as mean and 95% CI, of three independent experiments. $^{*}p < 0.05$; $^{**}p < 0.01$; $^{***}p < 0.001$. IL-1β: IL-1β-primed cells; Van: Vanillin; Van (2 h)+IL-1β: Vanillin (2 h pretreatment) plus IL-1β.
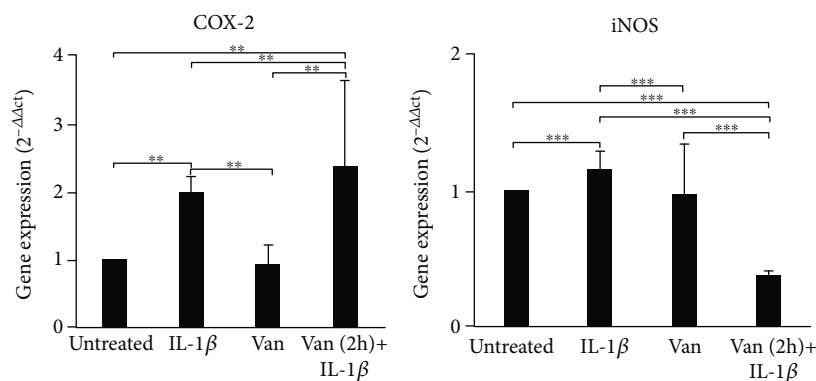
FIGURE 9: Gene expression of COX-2 and iNOS in HGF cells. Data are reported as mean and 95% CI, of three independent experiments. $^{**}p < 0.01$; $^{***}p < 0.001$. IL-1β: IL-1β-primed cells; Van: Vanillin; Van (2 h)+IL-1β: Vanillin (2 h pretreatment) plus IL-1β.
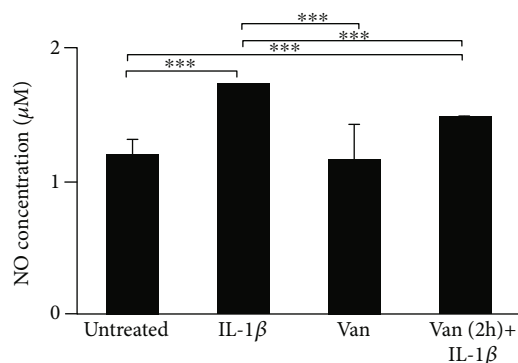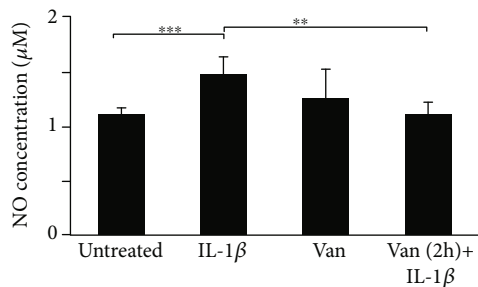

FIGURE 10: Levels of NO in HGF cells were determined based on Griess reagent reaction. Experiments were conducted in duplicate, and changes were reported as mean ± SD. $^{**}p < 0.01$; $^{***}p < 0.001$. IL-1β: IL-1β-primed cells; Van: Vanillin; Van (2 h)+IL-1β: Vanillin (2 h pretreatment) plus IL-1β.

the switch from acute to chronic inflammation, are present in periodontal gingival crevicular fluid and gingival tissues, and after nonsurgical periodontal therapy, reduced levels of TNF-α, IL-1β, and IL-6 were observed, confirming their role in periodontal disease [24, 25]. In this study, we have simulated the proinflammatory microenvironment by IL-1β priming of HGF and we have evaluated the effect of Vanillin on inflammatory mediator gene expression and production. Our results showed that in IL-1β-primed HGF cells, Vanillin pretreatment decreases expression and production of proin-

flammatory mediators, such as IL-8, IL-6, and TNF-α. Progression of periodontal disease may be derived by NO and COX-2 signaling pathways [26, 27]. In Vanillin pretreated cells, we detected a reduction of iNOS and COX-2 gene expression and NO production. Together, these results underline the ability of Vanillin to modulate inflammatory response in HGF-inflamed cells. nAChα7 receptor is a critical regulator of the "cholinergic anti-inflammatory pathway" [28, 29] and is expressed in HGF cells. Thus, we investigate if the anti-inflammatory ability of Vanillin may be linked to nAChRα7 expression. Our results showed the Vanillin-induced increase of nAChRα7 expression in accord with the reduction of proinflammatory cytokine gene expression. Taking into account that inflammatory mediators drive the onset and progression of connective tissue degradation, our second goal was to analyze the effect of Vanillin on wound healing [30–32]. Vanillin, in our in vitro model of wound healing, quickens wound closure. Moreover, the gene expression of IL-1β-induced mediators (IL-6 and TNF-α) in scratched HGF monolayer was reduced in Vanillin-pretreated cells, while no significant difference on IL-6, TNF-α, and IL-8 production was observed. Interestingly, in mechanical damaged IL-1β-priming HGF, IL-8 gene expression was increased in presence of Vanillin pretreatment, as a response to a double mechanical and inflammatory stimulation. In fact, in vivo and in vitro studies have been reported

that IL-8 induces neutrophil recruitment in the damaged area, stops the bacterial invasion, and promotes local neoangiogenic, cell proliferation, and tissue reepithelization in the hell of human wounds [33, 34].

IL-1β is known to increase COX-2 expression and prostaglandin (PG) production in HGF [35–37]. In the present study, we observed that the IL-1β upregulation of COX-2 expression was increased by Vanillin (pretreatment) plus 1β treatment, in accord with the role of COX-2 in early and late regulation of the outcome of wound repair [35–37]. iNOS expression occurs very early after tissue injury, suggesting that this enzyme is necessary in the early inflammatory phase; in fact, our results showed a reduction of iNOS and NO at 24 h, when the complete wound healing was detected.

5. Conclusions

Overall, our results suggest that Vanillin may be useful in the management of the inflammatory periodontal disease by decreasing the excessive production of proinflammatory mediators and free radicals, as well as stimulating tissue regeneration and the management of soft tissue restoration. It is known that anti-inflammatory and antioxidant molecules added to oral hygiene products improve the indexes of periodontal disease [38, 39], with a reduction of the risk of associated systemic diseases. Thus, Vanillin could be potentially used in formulations suitable for oral application as a nonpharmacological agent for periodontal health and also as integral care of several disease managements, such as people with diabetes or HIV-infection, with tissue healing delayed rate.

Data Availability

The authors confirm that the data supporting the results of this study are available within the article and can be requested from the correspondent in case of further clarification.

Conflicts of Interest

The authors declare no conflict of interest.

Authors' Contributions

Conceptualization was performed by C.E. and R.M.; methodology was done by C.E. and J.S.; investigation was done by C.E and S.B; R.M. and M.G. contributed to the resources of the study; writing original draft preparation was carried out by C.E., S.B., and R.M.; writing-review and editing was done by K.F., C.S., and M.G.; supervision was done by R.M. All authors have read and agreed to the published version of the manuscript.

References

[1] L. Chen, H. Deng, H. Cui et al., "Inflammatory responses and inflammation-associated diseases in organs," *Oncotarget*, vol. 9, no. 6, article 23208, pp. 7204–7218, 2018.

[2] S. Kany, J. T. Vollrath, and B. Relja, "Cytokines in inflammatory disease," *International Journal of Molecular Sciences*, vol. 20, no. 23, p. 6008, 2019.

[3] M. Reale, L. Velluto, M. di Nicola et al., "Cholinergic markers and cytokines in OSA patients," *International Journal of Molecular Sciences*, vol. 21, no. 9, p. 3264, 2020.

[4] B. L. Pihlstrom, B. S. Michalowicz, and N. W. Johnson, "Periodontal diseases," *Lancet*, vol. 366, no. 9499, pp. 1809–1820, 2005.

[5] E. A. Palombo, "Traditional medicinal plant extracts and natural products with activity against oral bacteria: potential application in the prevention and treatment of oral diseases," *Evidence-based complementary and Alternative Medicine*, vol. 2011, Article ID 680354, 15 pages, 2011.

[6] B. Sinjari, J. Pizzicannella, M. D'Aurora et al., "Curcumin/liposome nanotechnology as delivery platform for anti-inflammatory activities via NFkB/ERK/pERK pathway in human dental pulp treated with 2-hydroxyethyl methAcrylate (HEMA)," *Frontiers in Physiology*, vol. 10, p. 633, 2019.

[7] M. Mizan and M. A. Kamrunnahar, "Antibacterial activity of Bohera (Terminaliabellirica) extract against dental carries causing bacteria Streptococcus mutans," *Journal of Environmental Science and Natural Resources*, vol. 10, no. 2, pp. 117–120, 2017.

[8] B. Kouidhi, Y. M. A. al Qurashi, and K. Chaieb, "Drug resistance of bacterial dental biofilm and the potential use of natural compounds as alternative for prevention and treatment," *Microbial Pathogenesis*, vol. 80, pp. 39–49, 2015.

[9] M. Seal, R. Rishi, G. Satish, K. T. Divya, P. Talukdar, and R. Maniyar, "Herbal panacea: the need for today in dentistry," *Journal of International Society of Preventive & Community Dentistry*, vol. 6, no. 2, article 178744, pp. 105–109, 2016.

[10] N. J. Walton, M. J. Mayer, and A. Narbad, "Vanillin," *Phytochemistry*, vol. 63, no. 5, pp. 505–515, 2003.

[11] A. Tai, T. Sawano, F. Yazama, and H. Ito, "Evaluation of antioxidant activity of vanillin by using multiple antioxidant assays," *Biochimica et Biophysica Acta (BBA)-General Subjects*, vol. 1810, no. 2, pp. 170–177, 2011.

[12] K. Ho, N. I. Yazan, N. Ismail, and M. Ismail, "Apoptosis and cell cycle arrest of human colorectal cancer cell line HT-29 induced by vanillin," *Cancer epidemiology*, vol. 33, no. 2, pp. 155–160, 2009.

[13] X. Yan, D. F. Liu, X. Y. Zhang et al., "Vanillin protects dopaminergic neurons against inflammation-mediated cell death by inhibiting ERK1/2, P 38 and the NF-κB signaling pathway," *International Journal of Molecular Sciences*, vol. 18, no. 2, p. 389, 2017.

[14] M. E. Kim, J. Y. Na, Y. Park, and J. S. Lee, "Anti-neuroinflammatory effects of vanillin through the regulation of inflammatory factors and NF-κB signaling in LPS-stimulated microglia," *Applied Biochemistry and Biotechnology*, vol. 187, no. 3, article 2857, pp. 884–893, 2019.

[15] M. Gómez-Florit, M. Monjo, and J. Ramis, "Quercitrin for periodontal regeneration: effects on human gingival fibroblasts and mesenchymal stem cells," *Scientific Reports*, vol. 5, no. 1, article 16593, 2015.

[16] R. Clancy, B. Varenika, W. Huang et al., "Nitric oxide synthase/COX cross-talk: nitric oxide activates COX-1 but inhibits COX-2-derived prostaglandin production," *Journal of Immunology*, vol. 165, no. 3, pp. 1582–1587, 2000.

[17] M. Nokhbehsaim, J. Winter, B. Rath, A. Jäger, S. Jepsen, and J. Deschner, "Effects of enamel matrix derivative on periodontal wound healing in an inflammatory environment in vitro," *Journal of Clinical Periodontology*, vol. 38, no. 5, pp. 479–490, 2011.

[18] H. Khan, M. Reale, H. Ullah et al., "Anti-cancer effects of polyphenols via targeting p53 signaling pathway: updates and future directions," *Biotechnology Advances*, vol. 38, article 107385, 2020.

[19] M. Reale, E. Costantini, S. Jagarlapoodi, H. Khan, T. Belwal, and A. Cichelli, "Relationship of wine consumption with Alzheimer's disease," *Nutrients*, vol. 12, no. 1, p. 206, 2020.

[20] T. Ramich, A. Asendorf, K. Nickles et al., "Inflammatory serum markers up to 5 years after comprehensive periodontal therapy of aggressive and chronic periodontitis," *Clinical oral investigations*, vol. 22, no. 9, article 2398, pp. 3079–3089, 2018.

[21] M. Chiquet, C. Katsaros, and D. Kletsas, "Multiple functions of gingival and mucoperiosteal fibroblasts in oral wound healing and repair," *Periodontology 2000*, vol. 68, no. 1, pp. 21–40, 2015.

[22] N. Tawfig, "Proinflammatory cytokines and periodontal disease," *Journal of Dental Problems and Solutions*, vol. 3, no. 1, pp. 12–17, 2016.

[23] S. Offenbacher, S. Barros, L. Mendoza et al., "Changes in gingival crevicular fluid inflammatory mediator levels during the induction and resolution of experimental gingivitis in humans," *Journal of Clinical Periodontology*, vol. 37, no. 4, pp. 324–333, 2010.

[24] P. Palmqvist, P. Lundberg, I. Lundgren, L. Hänström, and U. H. Lerner, "IL-1beta and TNF-alpha regulate IL-6-type cytokines in gingival fibroblasts," *Journal of Dental Research*, vol. 87, no. 6, pp. 558–563, 2008.

[25] T. Yucel-Lindberg and T. Båge, "Inflammatory mediators in the pathogenesis of periodontitis," *Expert Reviews in Molecular Medicine*, vol. 15, pp. e15–e27, 2013.

[26] Y. Wang, X. Huang, and F. He, "Mechanism and role of nitric oxide signaling in periodontitis," *Experimental and Therapeutic Medicine*, vol. 18, pp. 3929–3935, 2019.

[27] K. Noguchi and I. Ishikawa, "The roles of cyclooxygenase-2 and prostaglandin E2 in periodontal disease," *Periodontology 2000*, vol. 43, no. 1, pp. 85–101, 2007.

[28] X. J. Wang, Y. F. Liu, Q. Y. Wang et al., "Functional expression of alpha 7 nicotinic acetylcholine receptors in human periodontal ligament fibroblasts and rat periodontal tissues," *Cell and Tissue Research*, vol. 340, no. 2, pp. 347–355, 2010.

[29] K. R. Rajeswari and M. Satyanarayana, "Cholinergic components in human gingiva in healthy and inflamed states," *Indian Journal of Dental Research*, vol. 2, no. 2-3, pp. 166–169, 1990.

[30] E. Costantini, B. Sinjari, C. D'Angelo, G. Murmura, M. Reale, and S. Caputi, "Human gingival fibroblasts exposed to extremely low-frequency electromagnetic fields: in vitro model of wound-healing improvement," *International Journal of Molecular Sciences*, vol. 20, no. 9, p. 2108, 2019.

[31] P. C. Smith, C. Martínez, J. Martínez, and C. A. McCulloch, "Role of fibroblast populations in periodontal wound healing and tissue remodeling," *Frontiers in Physiology*, vol. 10, p. 270, 2019.

[32] A. Ridiandries, J. T. M. Tan, and C. A. Bursill, "The role of chemokines in wound healing," *International Journal of Molecular Sciences*, vol. 19, no. 10, p. 3217, 2018.

[33] R. M. Devalaraja, L. B. Nanney, Q. Qian et al., "Delayed wound healing in CXCR2 knockout mice," *The Journal of Investigative Dermatology*, vol. 115, no. 2, pp. 234–244, 2000.

[34] L. S. Finoti, R. Nepomuceno, S. C. Pigossi, S. C. T. Corbi, R. Secolin, and R. M. Scarel-Caminaga, "Association between interleukin-8 levels and chronic periodontal disease: a PRISMA-compliant systematic review and meta-analysis," *Medicine*, vol. 96, no. 22, article e6932, 2017.

[35] A. Futagami, M. Ishizaki, Y. Fukuda, S. Kawana, and N. Yamanaka, "Wound healing involves induction of cyclooxygenase-2 expression in rat skin," *Laboratory Investigation*, vol. 82, no. 11, pp. 1503–1513, 2002.

[36] T. A. Wilgus, V. K. Bergdall, K. L. Tober et al., "The impact of cyclooxygenase-2 mediated inflammation on scarless fetal wound healing," *The American Journal of Pathology*, vol. 165, no. 3, pp. 753–761, 2004.

[37] S. Seutter, J. Winfield, A. Esbitt et al., "Interleukin 1β and Prostaglandin E2 affect expression of DNA methylating and demethylating enzymes in human gingival fibroblasts," *Journal of Dental Problems and Solutions*, vol. 78, article 105920, p. 78, 2020.

[38] E. F. Andrade, D. R. Orlando, A. Araújo et al., "Can resveratrol treatment control the progression of induced periodontal disease? A systematic review and meta-analysis of preclinical studies," *Nutrients*, vol. 11, no. 5, p. 953, 2019.

[39] I. Palaska, E. Papathanasiou, and T. C. Theoharides, "Use of polyphenols in periodontal inflammation," *European Journal of Pharmacology*, vol. 720, no. 1-3, pp. 77–83, 2013.

Research Article

Zataria multiflora and Pioglitazone Affect Systemic Inflammation and Oxidative Stress Induced by Inhaled Paraquat in Rats

Fatemeh Amin [ID],[1,2] **Arghavan Memarzia,**[3,4] **Ali Roohbakhsh** [ID],[5] **Farzaneh Shakeri** [ID],[6,7] **and Mohammad Hossein Boskabady** [ID][3,4]

[1]*Physiology-Pharmacology Research Center, Research Institute of Basic Medical Sciences, Rafsanjan University of Medical Sciences, Rafsanjan, Iran*

[2]*Department of Physiology and Pharmacology, School of Medicine, Rafsanjan University of Medical Sciences, Rafsanjan, Iran*

[3]*Applied Biomedical Research Center, Mashhad University of Medical Sciences, Mashhad, Iran 9177948564*

[4]*Department of Physiology, School of Medicine, Mashhad University of Medical Sciences, Mashhad, Iran 9177948564*

[5]*Pharmaceutical Research Center, Pharmaceutical Technology Institute, Mashhad University of Medical Sciences, Mashhad, Iran 9177948564*

[6]*Natural Products and Medicinal Plants Research Center, North Khorasan University of Medical Sciences, Bojnurd, Iran*

[7]*Department of Physiology and Pharmacology, School of Medicine, North Khorasan University of Medical Sciences, Bojnurd, Iran 7487794149*

Correspondence should be addressed to Mohammad Hossein Boskabady; boskabadymh@mums.ac.ir

The effects of *Zataria multiflora* (*Z. multiflora*) and pioglitazone (a PPAR-γ agonist) alone and in combination, on systemic inflammation and oxidative stress induced by inhaled paraquat (PQ) as a herbicide, which induced inflammation in rats, were examined. Rats were exposed to (1) saline (control) and (2) 54 mg/m^3 PQ aerosols (8 times, every other day, each time for 30 min) without treatment or treated with (3 and 4) two doses of *Z. multiflora* (200 and 800 mg/kg/day), (5 and 6) two doses of pioglitazone (5 and 10 mg/kg/day), (7) low doses of *Z.multiflora* + pioglitazone, (Pio-5+Z-200 mg/kg/day) or (8) dexamethasone (0.03 mg/kg/day) for 16 days, after the last PQ exposure. Different variables were measured at the end of the treatment period. Exposure to PQ significantly increased total and differential white blood cells (WBC) counts, serum levels of nitrite (NO$_2$), malondialdehyde (MDA), interleukin- (IL) 17, and tumor necrosis factor alpha (TNF-α), but reduced thiol, superoxide dismutase (SOD), catalase (CAT), IL-10, and interferon-gamma (INF-γ) ($p < 0.05$ to $p < 0.001$). Most measured parameters were significantly improved in groups treated with either doses of the extract, pioglitazone, Pio-5+Z-200 mg/kg/day, or dexamethasone compared to the PQ group ($p < 0.05$ to $p < 0.001$). The combination of low doses of Pio-5+Z-200 mg/kg/day showed significantly higher effects compared to each one alone ($p < 0.05$ to $p < 0.001$). Systemic oxidative stress and inflammation due to inhaled PQ were improved by *Z. multiflora* and pioglitazone. Higher effects of Pio-5+Z-200 mg/kg/day compared to each one alone suggest modulation of PPAR-γ receptors by the plant extract, but further studies using PPAR-γ antagonists need to be done in this regard.

1. Introduction

Paraquat (PQ) (C12 H14 N2), a bipyridinium and nonselective quaternary nitrogen herbicide, is commonly used worldwide [1]. In 1985, only in Japan, approximately 2000 deaths occurred/year due to PQ digestion which were mostly intentional, and in 2020, more than 150,000 people died due to pesticide poisoning [2, 3]. PQ intoxication is characterized by swelling, bleeding, inflammation, and proliferation of bronchial epithelial cells [4]. Exposure to PQ is accidental
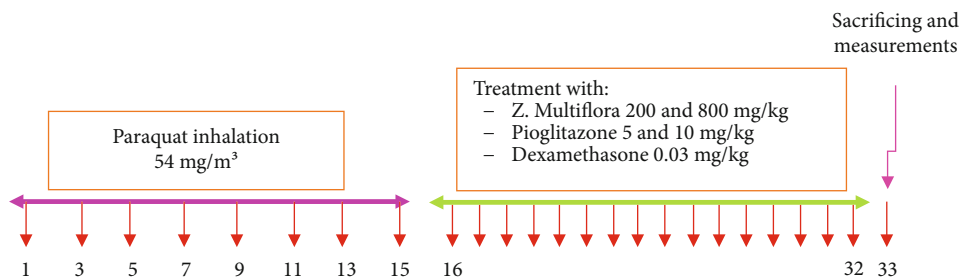
FIGURE 1: Protocol of exposing animals to t inhaled PQ (54 mg/m^3) and treatment of animals with the extract, pioglitazone and dexamethasone.

or intentional in humans and animals, and the most common routes of exposure are inhalation and dermal [5]. Following oral administration, PQ causes burning and swelling of the mouth and throat, followed by gastrointestinal symptoms such as abdominal pain, loss of appetite, nausea, vomiting, diarrhea, and systemic inflammation [6]. It has also been reported that administration of PQ can lead to an increase in inflammatory factors such as TNF-α [7].

Zataria multiflora Boiss (*Z. multiflora*) from Lamiaceae family grows in southern Iran, Afghanistan, and Pakistan [8]. The constituents of *Z. multiflora* are terpenes, phenols, aliphatic alcohols, flavonoids, saponins, tannins, thymol, carvacrol, apigenin, luteolin, and 6-hydroxyluteolin glycosides, as well as di-, tri-, and tetramethoxylated. Oral administration of *Z. multiflora* aqueous extract (boiled) is used in traditional medicine for its analgesic, antiseptic, antioxidant, anti-inflammatory, anthelmintic, and antidiarrheal properties [8]. *Z. multiflora* extract has been used in inflammatory and immune deficiency diseases or against conditions associated with increased oxidative stress [8].

Peroxisome proliferator-activated receptors (PPARs) are a group of ligand-dependent nuclear receptors that act as transcription factors and have three known α, β/δ, and γ isoforms in humans [9]. PPAR-γ agonists were shown to affect the cardiovascular system [10]. PPAR-γ agonists are insulin-sensitive drugs used to treat insulin resistance [11]. The activation of PPAR-γ receptors showed anti-inflammatory and anticancer effects as well as the regulations of cellular metabolism, cell differentiation, and apoptosis [9, 12].

Therefore, in the present study, the effects of *Z. multiflora* hydroalcoholic extract and a PPAR-γ agonist and their combination, on systemic inflammation and oxidative stress induced by inhaled PQ in rats, were investigated. The effect of combination of low dose of the extract and pioglitazone was studied to evaluate their synergistic effect.

2. Materials and Methods

2.1. Animals and Groups. The study was performed in forty-eight male Wistar rats (weighing approximately 200–250 g) kept in the animal house, School of Medicine, Mashhad University of Medical Sciences, Iran. The animals were kept at $22 \pm 2°C$ with a 12 h light/dark cycle and fed a standard diet and tap drinking water *ad libitum*. The ethics committee of Mashhad University of Medical Sciences approved the Ani-

mal Experiments of the present study with allowance Code 961202.

Eight groups of rats ($n = 6$ in each group) were studied: (1) control group, which was exposed to normal saline aerosol; (2) animals exposed to PQ (Sigma-Aldrich Co., China) aerosol at dose of 54 mg/m^3 [13–15]; (3 and 4) two groups exposed to PQ 54 mg/m^3 and treated with two doses of the extract of *Z. multiflora* (200 and 800 mg/kg/day); (5 and 6) two groups exposed to PQ 54 mg/m^3 and treated with two doses (5 and 10 mg/kg/day) of the pioglitazone (Samisaz Pharmaceutical Company, Iran); (7) one group exposed to PQ 54 mg/m^3 and treated with Pio-5+Z-200 mg/kg/day; and (8) one group exposed to PQ 54 mg/m^3 and treated with dexamethasone (Sigma-Aldrich Co., St. Louis, MO, Germany; 0.03 mg/kg/day). The control group was exposed to saline and other groups to PQ (Sigma-Aldrich Co., China) aerosols 8 times on days 1, 3, 5, 7, 9, 11, 13, and 15, each time for 30 min during a 16-day period. In treated groups, the extract, pioglitazone, or dexamethasone was administered by gavage for 16 days after the end of PQ exposure [15, 16] (Figure 1).

2.2. Exposure to PQ. For production of PQ aerosol, a nebulizer (Omron CX3, Japan, particle size 3–5 μm) with an air flow of 8 L/min was used. A volume of 4.5 mL of 1.33 mg/mL PQ solution was added to the nebulizer chamber each time. The solution output of the nebulizer was 0.15 L/min and its air output was 3.7 L/min. The aerosol was delivered to exposure box, with dimensions $15 \times 18 \times 30$ cm as previously described [15]. Therefore, the PQ dose in the exposure box was 54 mg/m^3 [13].

2.3. Plant Extract Preparation. Plant collection and extract preparation were fully described in our previous study [15]. The plant was identified by Mr. Joharchi, Herbarium of the School of Agriculture, Ferdowsi University, and a voucher specimen was preserved (Herbarium No. 35314, FUMH). Briefly, the hydro-ethanolic extract was prepared by mixing 100 g of dried shoots and powdered *Z. multiflora* with 875 mL of 50% ethanol and shacked for 72 h at room temperature. The solvent was removed under reduced pressure, and the yield extract was 33.2 g. The studied doses of the extract were freshly prepared for gavage by adding water to dried extract [15].
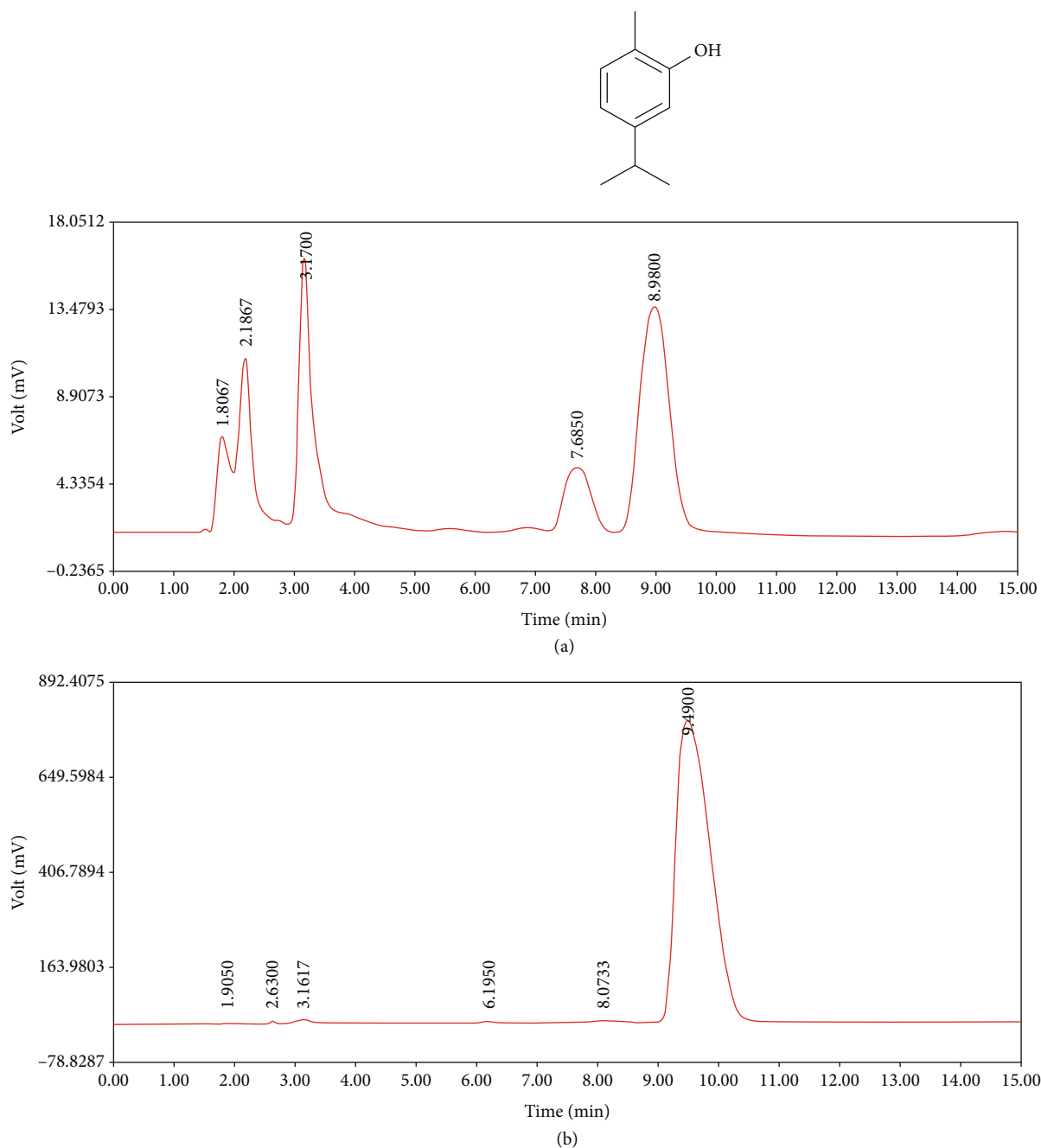
FIGURE 2: Fingerprint of (a) the extract of *Z. multiflora* (50 mg/mL) and the (b) pure carvacrol (C10H14O, 5/1000) (Boskabady et al., 2011). The extract showed a peak appears on 8.98 min which was as the same as retention time (RT) of pure carvacrol (9.49 min).

2.4. Characterization of the Extract of Z. multiflora by HPLC.

The extract of the plant was characterized in our previous study by a HPLC-UV (multiwavelengths) (Waters 474, Waters Corporation, Milford, MA, USA) finger print. Figure 2 illustrates chromatographic profile of pure carvacrol (5/1000) with retention time at about 9 min.

2.5. Total and Differential WBC Counts.

After the end of the treatment period (day 33), the rats were anesthetized by intraperitoneal injections of ketamine (50 mg/kg) and xylazine (5 mg/kg). Peripheral blood (2.5 mL) was prepared from the heart immediately after animal sacrificing. Then, 0.5 mL of blood was mixed with Turk solution, and total WBC number was determined in a hemocytometer (Burker chamber). For differential WBC count, the smear of blood was prepared and stained with Wright-Giemsa. Differential cell analysis was carried as previously described [17].

2.6. Oxidant and Antioxidant Biomarker Measurement.

The blood samples (2 mL) were centrifuged at 2000 revolution per minute (rpm) for 10 minutes. Concentrations of oxidants biomarkers including malondialdehyde (MDA) and nitrite (NO_2), as well as status of antioxidants including total thiol content, superoxide dismutase (SOD), and catalase (CAT)

activities in the serum, were evaluated as previously described.

2.7. Cytokine Measurement. Serum levels of cytokines IL-10, IFN-γ, IL-17, and TNF-α were measured using specific enzyme-linked immunosorbent assay (ELISA) kits (Hangzhou Eastbiopharm, Iran) according to the manufacturer's protocol as previously reported.

2.8. Statistical Analysis. The normal distribution of the data was checked using the Kolmogorov-Smirnov test. Data were analyzed by one-way analysis of variance (ANOVA) followed by Tukey's multiple comparison test, and results are presented as the mean ± SEM. Values of $p < 0.05$ were considered statistically significant.

3. Results

3.1. Total and Differential WBC Counts. Total and differential WBC were increased in the blood of animals exposed to inhaled PQ compared to the control group ($p < 0.05$ for lymphocytes and $p < 0.001$ for other cases). Total WBC and neutrophil were reduced in all treated groups except for the group treated with low dose of the extract; eosinophil was reduced in groups treated with the two doses of pioglitazone, Pio-5+Z-200 mg/kg/day, and dexamethasone; lymphocyte was decreased in groups treated with high-dose pioglitazone, Pio-5+Z-200 mg/kg/day, and dexamethasone; and monocyte was reduced in groups treated with high-dose extract, Pio-5+Z-200 mg/kg/day, and dexamethasone ($p < 0.05$ to $p < 0.001$) (Table 1).

The effect of dexamethasone treatment on neutrophil was significantly higher than that of both doses of the extract, low-dose pioglitazone, and Pio-5+Z-200 mg/kg/day. Dexamethasone effect on monocyte was higher than both doses of the extract and pioglitazone, and its effect on eosinophil count was higher than both doses of the extract and low-dose pioglitazone; however, dexamethasone effect on lymphocyte was lower than the Pio-5+Z-200 mg/kg/day group ($p < 0.05$ to $p < 0.001$) (Table 1).

The effects of high-dose extract and pioglitazone treatment on total WBC and eosinophil and the effect of high-dose pioglitazone on neutrophil and lymphocyte were significantly higher than their low doses ($p < 0.05$ to $p < 0.001$) (Table 1).

In addition, treatment with low-dose pioglitazone + extract had significantly higher effects on total WBC and lymphocyte counts compared to low-dose extract and on monocyte than low-dose extract and pioglitazone alone ($p < 0.001$ for lymphocyte and $p < 0.05$ for other cases) (Table 1).

3.2. Oxidant and Antioxidant Biomarkers. Significant increases in MDA and NO$_2$ concentrations and significant decreases in total thiol content, and SOD and CAT activities were seen in the group exposed to inhaled PQ compared to the control group ($p < 0.001$ for all cases) (Figures 3 and 4).

The levels of NO$_2$ in all treated groups, MDA level in all groups except low-dose extract, SOD activity except low-dose pioglitazone, and CAT and thiol levels in all treated groups except groups treated with low-dose extract and pioglitazone were significantly improved compared to the PQ group ($p < 0.05$ to $p < 0.001$) (Figures 3 and 4).

The effects of dexamethasone treatment on MDA and thiol levels were significantly higher than all other treated groups. Dexamethasone effect was significantly higher on CAT activity than all treated groups except for high-dose pioglitazone, on SOD activity than only treated groups with low-dose extract and pioglitazone and on NO$_2$ level than only treated group with low-dose extract ($p < 0.05$ to $p < 0.001$) (Figures 3 and 4).

The effects of high-dose extract and pioglitazone treatment on MDA and CAT levels, the effect of high-dose extract on NO$_2$ level, and the effect of high-dose pioglitazone on SOD activity were significantly higher than their low doses ($p < 0.05$ to $p < 0.001$) (Figures 3 and 4).

Treatment with Pio-5+Z-200 mg/kg/day had significantly higher effects on MDA, SOD, and CAT levels than low doses of the extract and pioglitazone and on NO$_2$ level than low-dose extract alone ($p < 0.01$ for CAT and SOD and $p < 0.001$ for MDA and NO$_2$) (Figures 3 and 4).

3.3. Serum Cytokine Level. Serum levels of IL-17 and TNF-α were significantly increased, but IL-10 and INF-γ were decreased in PQ-exposed animals compared to the control group ($p < 0.001$ for all cases). Serum levels of IL-10 in all treated groups and INF-γ, TNF-α, and IL-17 in all treated groups except groups treated with low-dose extract and pioglitazone were significantly improved compared to the PQ group ($p < 0.05$ to $p < 0.001$) (Figures 5 and 6).

The effects of dexamethasone treatment were significantly higher on the IL-10 level compared to low-dose extract, on IL-17 and TNF-α than low-dose extract and pioglitazone, and on INF-γ than both doses of the extract and low-dose pioglitazone-treated groups ($p < 0.01$ and $p < 0.001$) (Figures 5 and 6). However, the effect of treatment with combination of Pio-5+Z-200 mg/kg/day was significantly higher on TNF-α than dexamethasone ($p < 0.01$) (Figure 6).

The effects of high-dose extract and pioglitazone treatment on IL-10 and TNF-α and the effect of high-dose pioglitazone on IL-17 and INF-γ levels were significantly higher than their low dose ($p < 0.05$ to $p < 0.001$) (Figures 5 and 6).

Treatment with Pio-5+Z-200 mg/kg/day was significantly higher effects on IL-10, IL-17, TNF-α, and INF-γ levels compared to low doses of the extract and pioglitazone alone ($p < 0.05$ to $p < 0.001$) (Figures 5 and 6).

4. Discussion

Total and all differential WBC were significantly increased due to inhaled PQ in the current study which are supported by the previous animal and human studies [18–21].

Treatment with *Z. multiflora* extract and pioglitazone decreased total and differential WBC counts in rats exposed to inhaled PQ in a concentration-dependent manner which was higher in the treated group with Pio-5+Z-200 mg/kg/day than low-dose pioglitazone or extract alone which showed a

TABLE 1: Total and differential WBC counts in the blood of control group (Ctrl), group exposed to paraquat aerosol at doses of 54 mg/m^3 (PQ-54), groups exposed to PQ-54 mg/m^3 and treated with 5 and 10 mg/kg/day pioglitazone, 200 and 800 mg/kg/day *Zataria multiflora*, 0.03 mg/kg/day dexamethasone, and 5 mg/kg/day pioglitazone + 200 mg/kg/day *Zataria multiflora* (Pio-5, Pio-1, Z-200, Z-800, Dexa 0.03, and Pio-5 + Z-200, respectively).

White blood cells (WBC)	Total WBC	Neutrophil	Lymphocyte	Monocyte	Eosinophil
Ctrl	4300 ± 620.48	1114.2 ± 138.6	3069.4 ± 410.17	50.4 ± 16.027	20.6 ± 3.9
PQ-54	12440 ± 679.4***	7665.8 ± 585.22***	4315.4 ± 595.14***	388.6 ± 57.8***	241.2 ± 57.06***
Z-200	11438.3 ± 784.28¥	6533.91 ± 656.46###	3873.18 ± 192.06¥¥¥	235.71 ± 59##,¥	212.18 ± 23.49###,¥¥¥
Z-800	8303.3 ± 650++,$	5239.08 ± 679.16++,###	3055.66 ± 309.11	144.91 ± 19.96++,#	149.08 ± 17.96++,$,###,¥¥
Pio-5	9080 ± 492.3++	5430.4 ± 357.6++,###	3321.2 ± 243.2	265.4 ± 38.64##,¥	114.8 ± 14.82++,##,¥¥
Pio-10	7110 ± 1131.2+++,$	3219.5 ± 672.5+++,$$$	2580 ± 400.03+,$	201.6 ± 40.56+,##	25.6 ± 5.6+++,$$$
Pio-5 + Z-200	7946.66 ± 1415.4+	4614.76 ± 873.2++,#	2367.2 ± 464.4++	201.86 ± 35.66++,#	20.55 ± 9.43+++
Dexa 0.03	8860 ± 1449.3+	2323.4 ± 264.47+++	3826.2 ± 597.15	82.8 ± 38.88+++	33.2 ± 15.53+++

The results are expressed as the mean ± SEM ($n = 6$ in each group). ***$p < 0.01$ compared to the control group. +$p < 0.05$, ++$p < 0.01$, and +++$p < 0.001$ compared to the PQ group; #$p < 0.05$ and ###$p < 0.001$ compared to dexamethasone. $$p < 0.05$ and $$$$p < 0.001$ compared to low dose of *Zataria multiflora* and pioglitazone groups. ¥$p < 0.05$ compared to Pio-5 mg/kg + Z-200 mg/kg group. Comparisons between different groups were made using one-way ANOVA followed by Tukey's multiple comparison test.

(a)

(b)

FIGURE 3: Serum levels of malondialdehyde (MDA) (a) and nitrite (NO$_2$) (b) of control group (Ctrl), group exposed to paraquat aerosol at doses of 54 mg/m^3 (PQ-54), and groups exposed to PQ-54 mg/m^3 and treated with 5 and 10 mg/kg/day pioglitazone, 200 and 800 mg/kg/day *Zataria multiflora*, 0.03 mg/kg/day dexamethasone, and 5 mg/kg/day pioglitazone + 200 mg/kg/day *Zataria multiflora* (Pio-5, Pio-10, Z-200, Z-800, Dexa 0.03, and Pio-5 + Z-200, respectively). The results are expressed as the mean ± SEM ($n = 6$ in each group). ***$p < 0.001$ compared to the control group. +$p < 0.05$, ++$p < 0.01$, and +++$p < 0.001$ compared to the PQ group; #$p < 0.05$, ##$p < 0.01$, and ###$p < 0.001$ compared to treatment with other treated groups; $$p < 0.05$ and $$$$p < 0.01$ compared to low dose of *Zataria multiflora* and pioglitazone groups; ¥¥¥$p < 0.001$ compared to the Pio-5 mg/kg + Z-200 mg/kg group. Comparisons between different groups were made using one-way ANOVA followed by Tukey's multiple comparison test.

(a)

(b)

(c)
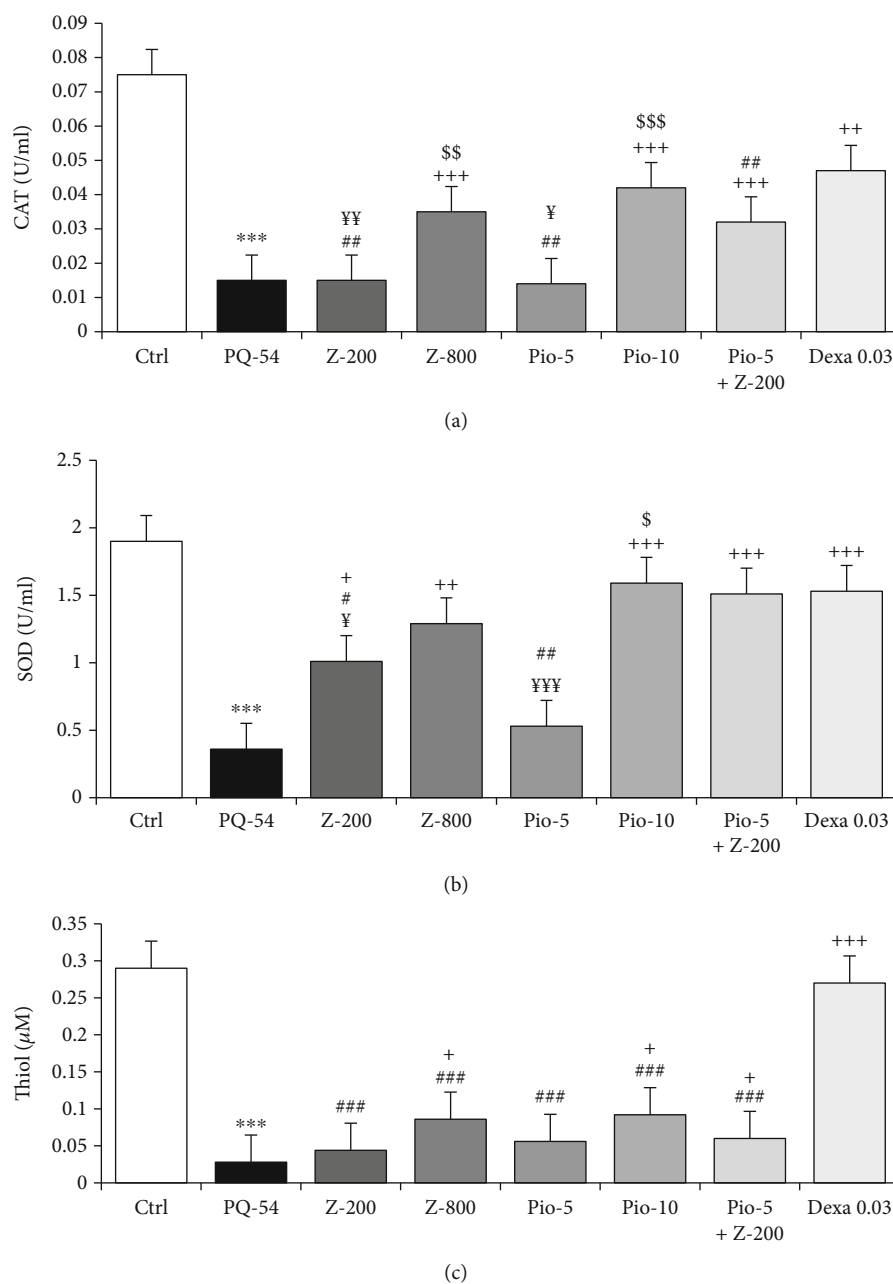
Figure 4: Serum levels of catalase (CAT) (a), superoxide dismutase (SOD) (b) activities, and thiol concentration (c) of the control group (Ctrl), group exposed to paraquat aerosol at doses of 54 mg/m^3 (PQ-54), and groups exposed to PQ-54 mg/m^3 and treated with 5 and 10 mg/kg/day pioglitazone, 200 and 800 mg/kg/day *Zataria multiflora*, 0.03 mg/kg/day dexamethasone, and 5 mg/kg/day pioglitazone + 200 mg/kg/day *Zataria multiflora* (Pio-5, Pio-10, Z-200, Z-800, Dexa 0.03, and Pio-5 + Z-200, respectively). The results are expressed as the mean ± SEM ($n = 6$ in each group). ***$p < 0.001$ compared to the control group. +$p < 0.05$, ++$p < 0.01$, and +++$p < 0.001$ compared to the PQ group. #$p < 0.05$, ##$p < 0.01$, and ###$p < 0.001$ compared treatment with other dexamethasone-treated groups. $\$ $p < 0.05$, $\$\$ $p < 0.01$, and $\$\$\$ $p < 0.001$ compared to low dose of *Zataria multiflora* and pioglitazone groups. ¥$p < 0.05$, ¥¥$p < 0.01$, and ¥¥¥$p < 0.001$ compared to the Pio-5 mg/kg + Z-200 mg/kg group. Comparisons between different groups were made using one-way ANOVA followed by Tukey's multiple comparison test.

synergistic effect for these two agents. This synergistic effect may indicate the effect of *Z. multiflora* extract on PPAR-γ receptors. The activated PPAR-γ receptors and inhibited COX-2, by carvacrol, the main constituent of *Z. multiflora*, support the potential effect of *Z. multiflora* on PPAR-γ receptors [22].

Reductions of total and differential WBC in both the blood and the BALF in animal models of asthma and COPD [23] and in subjects exposed to sulfur mustard [8] were shown by the extract of *Z. multiflora* as well as by pioglitazone treatment in patients with metabolic syndrome [24, 25] which support the results of the current study.

(a)

(b)
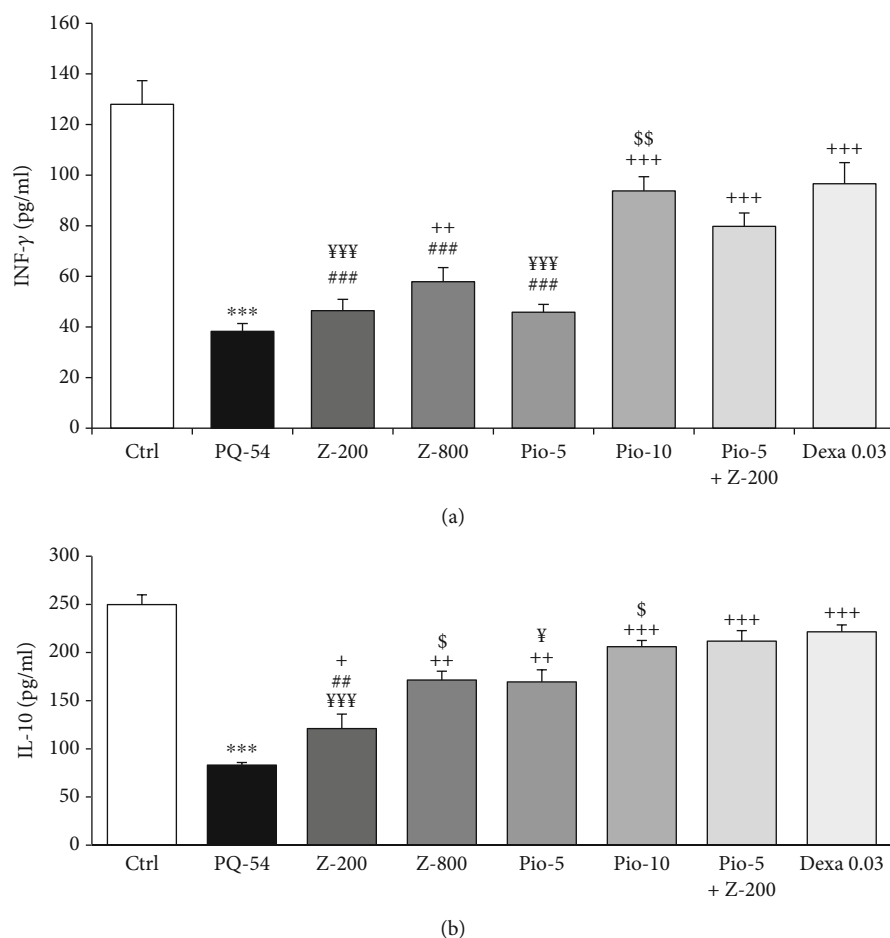
Figure 5: Values of interferon gama (INF-γ) (a) and interleukin-10 (IL-10) (b) in the serum of control group (Ctrl), group exposed to paraquat aerosol at doses of 54 mg/m^3 (PQ-54), and groups exposed to PQ-54 mg/m^3 and treated with 5 and 10 mg/kg/day pioglitazone, 200 and 800 mg/kg/day *Zataria multiflora*, 0.03 mg/kg/day dexamethasone, and 5 mg/kg/day pioglitazone + 200 mg/kg/day *Zataria multiflora* (Pio-5, Pio-10, Z-200, Z-800, Dexa 0.03, and Pio-5 + Z-200, respectively). The results are expressed as the mean ± SEM ($n = 6$ in each group). ***$p < 0.001$ compared to the control group. $^+p < 0.05$, $^{++}p < 0.01$, and $^{+++}p < 0.001$ compared to the PQ group. $^{\#\#}p < 0.01$ and $^{\#\#\#}p < 0.001$ compared dexamethasone treatment with other treated groups. $^\$p < 0.05$ and $^{\$\$}p < 0.01$ compared to low dose of *Zataria multiflora* and pioglitazone groups. $^{¥¥¥}p < 0.001$ comparison between Pio-5 mg/kg + Z-200 mg/kg with low dose of *Zataria multiflora* and pioglitazone groups. $^¥p < 0.05$ and $^{¥¥¥}p < 0.001$ compared to Pio-5 mg/kg + Z-200 mg/kg group. Comparisons between different groups were made using one-way ANOVA followed by Tukey's multiple comparison test.
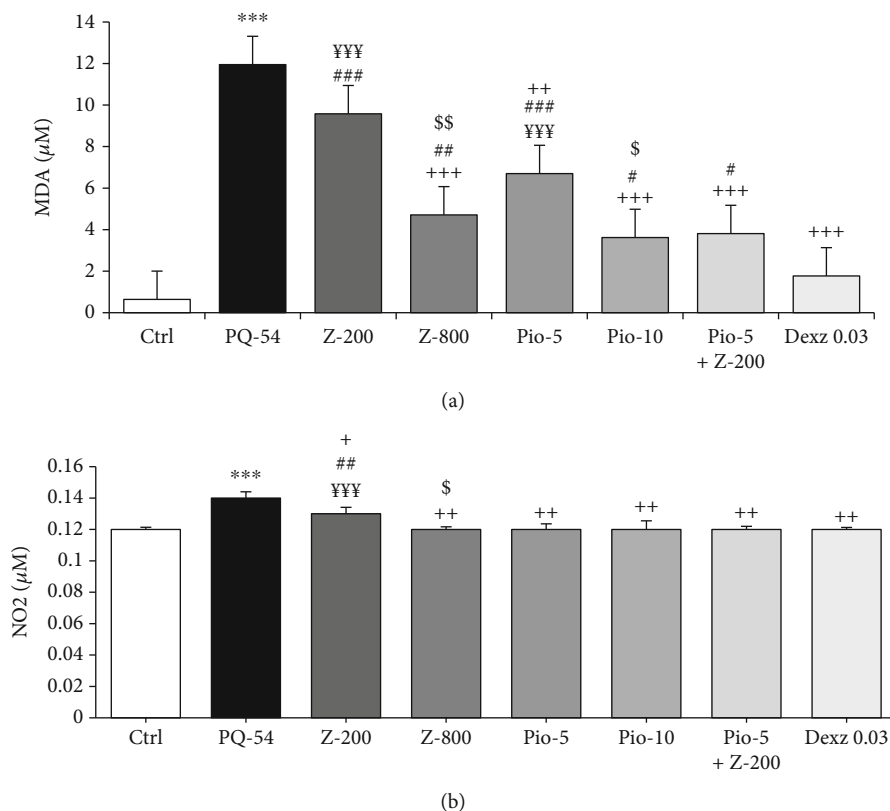
The serum levels of NO$_2$ and MDA were significantly increased, but SOD, CAT, and thiol were decreased in t PQ-exposed rats. Previous studies also showed reduction of SOD and CAT activity in animal models of PQ poisoning [26, 27], the role of free radical generation in PQ-induced injuries [28], and decreased SOD and CAT activities in animal lung tissues due to PQ administration [29]. A positive correlation between enhanced levels of oxidants and inflammatory mediators with administered PQ doses [30], increased oxidant, and decreased antioxidant markers in the hippocampus due to PQ poisoning were shown [6, 31], which support the findings of the present study.

Treatment with *Z. multiflora* extract and pioglitazone improved oxidative stress markers in an animal exposed to PQ which was supported by the previous studies indicating the effects of *Z. multiflora* extract on oxidative stress markers [8, 23, 32, 33]. Treatment with pioglitazone also reduced oxi-

dant markers and increased antioxidants in animal exposed to inhaled PQ. Previous studies showed reduction of inflammation and oxidative stress by pioglitazone and rosiglitazone [34–36] which was consistent with the results of the present study. However, treatment of PQ-exposed animals by the combination of low-dose pioglitazone + *Z.multiflora* extract showed higher improvement effects on oxidant and antioxidant biomarkers compared to low-dose pioglitazone or *Z. multiflora* extract alone.

Increased serum levels of IL-17 and TNF-α and decreased levels of IL-10 and INF-γ were observed in PQ-exposed rats. Increased serum level of TNF-α in patients with acute PQ poisoning [37], increased IL-1 β and TNF-α nuclear factor kappa (NF-κB) activity nuclear factor kappa (NF-κB) activity, reduced IL-10 in the lung due to PQ administration in rats [35], increased inflammatory cytokines in PQ-poisoned individuals [37], decreased serum levels of anti-inflammatory cytokines

(a)

(b)
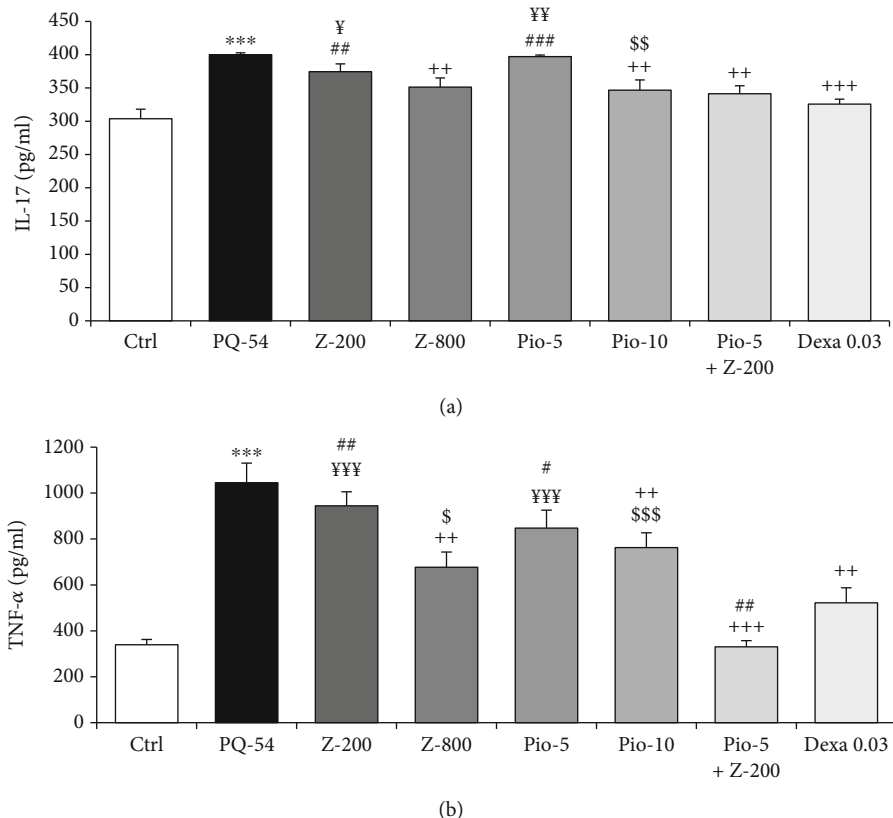
Figure 6: Values of IL-17 (a), INF-α (b) in serum of control group (Ctrl), group exposed to paraquat aerosol at doses of 54 mg/m^3 (PQ-54), groups exposed to PQ-54 mg/m^3 and treated with 5 and 10 mg/kg/day pioglitazone, 200 and 800 mg/kg/day *Zataria multiflora*, 0.03 mg/kg/day dexamethasone, and 5 mg/kg/day pioglitazone + 200 mg/kg/day *Zataria multiflora* (Pio-5, Pio-10, Z-200, Z-800, Dexa 0.03, and Pio-5 + Z-200, respectively). The results are expressed as the mean ± SEM ($n = 6$ in each group). $^{***}p < 0.001$ compared to the control group. $^{++}p < 0.01$ and $^{+++}p < 0.001$ compared to the PQ group. $^{#}p < 0.05$, $^{##}p < 0.01$, and $^{###}p < 0.001$ compared dexamethasone treatment with other treated groups. $^{\$}p < 0.05$, $^{\$\$}p < 0.01$, and $^{\$\$\$}p < 0.001$ compared to low dose of *Zataria multiflora* and pioglitazone groups. $^{¥}p < 0.05$ and $^{¥¥¥}p < 0.001$ compared to Pio-5 mg/kg + Z-200 mg/kg group. Comparisons between different groups were made using one-way ANOVA followed by Tukey's multiple comparison test.

[31], and enhanced gene expression for IL-4, TGF-β, IL-17, and TNF-α after PQ challenge were reported [38], supporting the results of this study.

Treatment of PQ-exposed animals with *Z. multiflora* extract and pioglitazone decreased serum levels of IL-17 and TNF-α but increased IL-10 and INF-γ. The immunomodulatory effects of *Z. multiflora* extract were comprehensively reviewed previously [31], and the effects of the plant on various cytokine levels in animal models of asthma and COPD [23], on gene expression of various cytokine in a mouse model of asthma [39], and on different cytokines in patients with lung disorders due to sulfur mustard exposure also [8] were shown supporting the results of the present study. Two doses of the extract were chosen according to our previous studies [12, 20, 21, 36] which showed its minimum and maximum effects. Pioglitazone treatment also affects intestinal TNF-α [40]; increased IL-4 but decreased IFN-γ, TNF-α, and IL-6 [41]; decreased lung adenoma [42]; decreased NO, TNF-α, IL-1β, IL-6, and IL-8; increased IL-4 and IL-10 levels in LPS-stimulated astrocytes [43]; and decreased degranulation and adhesion of neutrophils in LPS-induced lung

injury [44]. The effects of *Z. multiflora* extract and pioglitazone on cytokine levels in PQ-exposed rats were supported by the above studies. The protective effect of carvacrol, one of the main constituents of this plant on lung inflammation induced by inhaled PQ, was also reported [45].

Higher effects of the combination of low-dose *Z. multiflora* extract + pioglitazone on serum cytokine levels compared to the effects of each one alone indicated a synergistic effect of the two agents suggesting the PPAR-γ receptor-mediated effect of *Z. multiflora* extract, which is supported by the effect of carvacrol on PPAR-γ receptors [22]. However, further studies examining the effect of *Z. multiflora* extract and PPAR-γ receptors antagonist are needed to confirm this suggestion.

Dexamethasone, a known anti-inflammatory used in this study as positive control drug, showed a similar effect as *Z. multiflora* extract and pioglitazone on measured variables in PQ-exposed rats. These results support the anti-inflammatory effects of *Z. multiflora* extract and pioglitazone and their combination on systemic inflammation induced by inhaled PQ.

In a previous preliminary study, the effects of the *Z. multiflora* and its constituents carvacrol on only MDA, NO2, IL-6, and IFN-γ and the ratio of the two cytokine [13] and, in another study, the effects of low dose of pioglitazone, the extract and combination of low dose pioglitazone and *Z multiflora*, and low dose of pioglitazone on CAT, NO2, and MDA as well as the serum levels of IL-6 and INF-γ and the ratio of the two cytokine on PQ-induced systemic inflammation were examined [46]. However, in the present study, the effect of two doses of *Z multiflora*, two doses of pioglitazone, and the combination of low dose of the extract and pioglitazone on systemic inflammation and oxidative stress induced by inhaled PQ was examined more precisely and in more variables in different animals. In fact, in the published paper, a definite conclusion regarding the synergistic effect of the extract and pioglitazone and the interaction of the extract on PPAR-γ receptors could not be suggested while in the present study this goal was achieved.

A preventive effect for *Z. multiflora* extract and pioglitazone, a PPAR-γ agonist on systemic inflammation and oxidative stress induced by inhaled PQ in rats similar to the effects of dexamethasone, was indicated. The synergistic effects of low-dose extract + pioglitazone also suggested that *Z. multiflora* effects could be mediated by PPAR-γ receptors, but this suggestion requires further investigations using PPAR-γ antagonists.

Data Availability

The data (excel format) used to support the findings of this study are available from the corresponding author upon request.

Conflicts of Interest

The authors declared no potential conflicts of interest with respect to the research, authorship, and/or publication of this article.

Authors' Contributions

FA, AM, and FSH carried out the experimental work, performed statistical analysis, and prepared the figures and draft first version of the manuscript. AR and MHB designed and supervised the study, helped in statistical analysis, and corrected the manuscript. All authors read and approved the final manuscript.

Acknowledgments

References

[1] M. J. Khodayar, M. Kiani, A. A. Hemmati et al., "The preventive effect of atorvastatin on paraquat-induced pulmonary fibrosis in the rats," *Advanced Pharmaceutical Bulletin*, vol. 4, no. 4, pp. 345–349, 2014.

[2] N. Castro-Gutiérrez, R. McConnell, K. Andersson, F. Pacheco-Antón, and C. Hogstedt, "Respiratory symptoms, spirometry and chronic occupational paraquat exposure," *Scandinavian Journal of Work, Environment & Health*, vol. 23, no. 6, pp. 421–427, 1997.

[3] M. Eddleston, "Poisoning by pesticides," *Medicine*, vol. 48, no. 3, pp. 214–217, 2020.

[4] N. Gupta, A. Chugh, B. S. Kanwar, and B. Lamba, "A case report of paraquat poisoning," *Journal, Indian Academy of Clinical Medicine*, vol. 19, no. 3, pp. 210-211, 2018.

[5] M. R. B. Baharuddin, I. B. Sahid, M. A. B. M. Noor, N. Sulaiman, and F. Othman, "Pesticide risk assessment: a study on inhalation and dermal exposure to 2, 4-D and paraquat among Malaysian paddy farmers," *Journal of Environmental Science and Health, Part B*, vol. 46, no. 7, pp. 600–607, 2011.

[6] Q. Chen, Y. Niu, R. Zhang et al., "The toxic influence of paraquat on hippocampus of mice: involvement of oxidative stress," *Neurotoxicology*, vol. 31, no. 3, pp. 310–316, 2010.

[7] G. Zhao, S. Li, G. Hong et al., "The effect of resveratrol on paraquat-induced acute lung injury in mice and its mechanism," *Zhonghua wei zhong bing ji jiu yi xue*, vol. 28, no. 1, pp. 33–37, 2016.

[8] M. R. Khazdair, O. Rajabi, M. Balali-Mood, F. Beheshti, and M. H. Boskabady, "The effect of Zataria multiflora on pulmonary function tests, hematological and oxidant/antioxidant parameters in sulfur mustard exposed veterans, a randomized doubled-blind clinical trial," *Environmental Toxicology and Pharmacology*, vol. 58, pp. 180–188, 2018.

[9] L. Wang, B. Waltenberger, E.-M. Pferschy-Wenzig et al., "Natural product agonists of peroxisome proliferator-activated receptor gamma (PPARγ): a review," *Biochemical Pharmacology*, vol. 92, no. 1, pp. 73–89, 2014.

[10] A. Oyekan, "PPARs and their effects on the cardiovascular system," *Clinical and Experimental Hypertension*, vol. 33, no. 5, pp. 287–293, 2011.

[11] F. Chiarelli and D. Di Marzio, "Peroxisome proliferator-activated receptor-gamma agonists and diabetes: current evidence and future perspectives," *Vascular Health and Risk Management*, vol. 4, no. 2, pp. 297–304, 2008.

[12] S. Tyagi, S. Sharma, P. Gupta, A. S. Saini, and C. Kaushal, "The peroxisome proliferator-activated receptor: a family of nuclear receptors role in various diseases," *Journal of Advanced Pharmaceutical Technology & Research*, vol. 2, no. 4, pp. 236–240, 2011.

[13] F. Amin, A. Roohbakhsh, A. Memarzia, H. R. Kazerani, and M. H. Boskabady, "Paraquat-induced systemic inflammation and increased oxidative markers in rats improved by <i>Zataria multiflora</i> extract and carvacrol," *Avicenna Journal of Phytomedicine*, vol. 10, no. 5, pp. 513–522, 2020.

[14] H. Burleigh-Flayer and Y. Alarie, "Concentration-dependent respiratory response of guinea pigs to paraquat aerosol," *Archives of Toxicology*, vol. 59, no. 6, pp. 391–396, 1987.

[15] M. Heydari, A. Mokhtari-Zaer, F. Amin et al., "The effect ofZataria multiflorahydroalcoholic extract on memory and lung changes induced by rats that inhaled paraquat," *Nutritional Neuroscience*, pp. 1–14, 2019.

[16] H. Malekinejad, M. Khoramjouy, R. Hobbenaghi, and A. Amniattalab, "Atorvastatin attenuates the paraquat-

induced pulmonary inflammation via PPARγ receptors: a new indication for atorvastatin," *Pesticide Biochemistry and Physiology*, vol. 114, pp. 79–89, 2014.

[17] S. Saadat, F. Beheshti, V. R. Askari, M. Hosseini, N. M. Roshan, and M. H. Boskabady, "Aminoguanidine affects systemic and lung inflammation induced by lipopolysaccharide in rats," *Respiratory Research*, vol. 20, no. 1, pp. 1–13, 2019.

[18] M. Delirrad, M. Majidi, and B. Boushehri, "Clinical features and prognosis of paraquat poisoning: a review of 41 cases," *International Journal of Clinical and Experimental Medicine*, vol. 8, no. 5, article 8122, 2015.

[19] R. Dinis-Oliveira, J. Duarte, A. Sanchez-Navarro, F. Remiao, M. Bastos, and F. Carvalho, "Paraquat poisonings: mechanisms of lung toxicity, clinical features, and treatment," *Critical Reviews in Toxicology*, vol. 38, no. 1, pp. 13–71, 2008.

[20] Z. Oghabian, J. Williams, M. Mohajeri et al., "Clinical features, treatment, prognosis, and mortality in paraquat poisonings: a hospital-based study in Iran," *Journal of Research in Pharmacy Practice*, vol. 8, no. 3, pp. 129–136, 2019.

[21] Y. Zhang, H. Sun, and L. Jiang, "Prognostic value of white blood cell count, C-reactive protein, and pentraxin-3 levels in patients with acute paraquat poisoning," *Journal of Clinical Laboratory Medicine*, vol. 2, no. 2, 2017.

[22] M. Hotta, R. Nakata, M. Katsukawa, K. Hori, S. Takahashi, and H. Inoue, "Carvacrol, a component of thyme oil, activates PPARα and γ and suppresses COX-2 expression," *Journal of Lipid Research*, vol. 51, no. 1, pp. 132–139, 2010.

[23] M. H. Boskabady and L. G. Mahtaj, "Lung inflammation changes and oxidative stress induced by cigarette smoke exposure in guinea pigs affected by Zataria multiflora and its constituent, carvacrol," *BMC Complementary and Alternative Medicine*, vol. 15, no. 1, pp. 1–10, 2015.

[24] P. O. Szapary, L. T. Bloedon, F. F. Samaha et al., "Effects of pioglitazone on lipoproteins, inflammatory markers, and adipokines in nondiabetic patients with metabolic syndrome," *Arteriosclerosis, Thrombosis, and Vascular Biology*, vol. 26, no. 1, pp. 182–188, 2006.

[25] R. Agarwal, "Anti-inflammatory effects of short-term pioglitazone therapy in men with advanced diabetic nephropathy," *American Journal of Physiology. Renal Physiology*, vol. 290, no. 3, pp. F600–F605, 2006.

[26] P. L. Keeling and L. L. Smith, "Relevance of NADPH depletion and mixed disulphide formation in rat lung to the mechanism of cell damage following paraquat administration," *Biochemical Pharmacology*, vol. 31, no. 20, pp. 3243–3249, 1982.

[27] F. Pourgholamhossein, F. Sharififar, R. Rasooli et al., "Thymoquinone effectively alleviates lung fibrosis induced by paraquat herbicide through down-regulation of pro-fibrotic genes and inhibition of oxidative stress," *Environmental Toxicology and Pharmacology*, vol. 45, pp. 340–345, 2016.

[28] K. Facecchia, L.-A. Fochesato, S. D. Ray, S. J. Stohs, and S. Pandey, "Oxidative toxicity in neurodegenerative diseases: role of mitochondrial dysfunction and therapeutic strategies," *Journal of Toxicology*, vol. 2011, Article ID 683728, 12 pages, 2011.

[29] P. Cheresh, S.-J. Kim, S. Tulasiram, and D. W. Kamp, "Oxidative stress and pulmonary fibrosis," *Biochimica et Biophysica Acta (BBA) - Molecular Basis of Disease*, vol. 1832, no. 7, pp. 1028–1040, 2013.

[30] Z. E. Suntres, "Exploring the potential benefit of natural product extracts in paraquat toxicity," *Fitoterapia*, vol. 131, pp. 160–167, 2018.

[31] Y.-H. Sun, Y. Li, Y.-J. Niu, Q. Chen, and R. Zhang, "Effects of paraquat on the learning and memory ability in developing mice," *Zhonghua lao dong wei sheng zhi ye bing za zhi*, vol. 29, no. 6, pp. 437–439, 2011.

[32] A. Ahmadipour, F. Sharififar, F. Nakhaipour, M. Samanian, and S. Karami-Mohajeri, "Hepatoprotective effect of Zataria multiflora Boisson cisplatin-induced oxidative stress in male rat," *Journal of Medicine and Life*, vol. 8, no. 4, p. 275, 2015.

[33] M. R. Khazdair, V. Ghorani, A. Alavinezhad, and M. H. Boskabady, "Pharmacological effects of Zataria multiflora Boiss L. and its constituents focus on their anti-inflammatory, antioxidant, and immunomodulatory effects," *Fundamental & Clinical Pharmacology*, vol. 32, no. 1, pp. 26–50, 2018.

[34] A. A. El-Sheikh and R. A. Rifaai, "Peroxisome proliferator activator receptor (PPAR)-γ ligand, but not PPAR-α, ameliorates cyclophosphamide-induced oxidative stress and inflammation in rat liver," *PPAR Research*, vol. 2014, Article ID 626319, 10 pages, 2014.

[35] J. Han, D. Ma, M. Zhang, X. Yang, and D. Tan, "Natural antioxidant betanin protects rats from paraquat-induced acute lung injury interstitial pneumonia," *BioMed Research International*, vol. 2015, Article ID 608174, 9 pages, 2015.

[36] C. Zou, H. Hu, X. Xi, Z. Shi, G. Wang, and X. Huang, "Pioglitazone protects against renal ischemia-reperfusion injury by enhancing antioxidant capacity," *Journal of Surgical Research*, vol. 184, no. 2, pp. 1092–1095, 2013.

[37] Z. Meng, Y. Dong, H. Gao et al., "The effects of ω-3 fish oil emulsion-based parenteral nutrition plus combination treatment for acute paraquat poisoning," *Journal of International Medical Research*, vol. 47, no. 2, pp. 600–614, 2019.

[38] P. F. Piguet, M. A. Collart, G. E. Grau, A.-P. Sappino, and P. Vassalli, "Requirement of tumour necrosis factor for development of silica-induced pulmonary fibrosis," *Nature*, vol. 344, no. 6263, pp. 245–247, 1990.

[39] M. Kianmehr, A. Rezaei, M. Hosseini et al., "Immunomodulatory effect of characterized extract of Zataria multiflora on Th1, Th2 and Th17 in normal and Th2 polarization state," *Food and Chemical Toxicology*, vol. 99, pp. 119–127, 2017.

[40] Y. Naito, T. Takagi, K. Matsuyama, N. Yoshida, and T. Yoshikawa, "Pioglitazone, a specific PPAR-γ ligand, inhibits aspirin-induced gastric mucosal injury in rats," *Alimentary Pharmacology & Therapeutics*, vol. 15, no. 6, pp. 865–873, 2001.

[41] T. Shigenobu, T. Ohtsuka, and M. Shimoda, "The prevention of tracheal graft occlusion using pioglitazone: a mouse tracheal transplant model study," *Transplant Immunology*, vol. 53, pp. 21–27, 2019.

[42] D. E. Seabloom, A. R. Galbraith, A. M. Haynes et al., "Fixed-dose combinations of pioglitazone and metformin for lung cancer prevention," *Cancer Prevention Research*, vol. 10, no. 2, pp. 116–123, 2017.

[43] D. Qiu and X.-N. Li, "Pioglitazone inhibits the secretion of proinflammatory cytokines and chemokines in astrocytes stimulated with lipopolysaccharide," *International Journal of Clinical Pharmacology and Therapeutics*, vol. 53, no. 9, pp. 746–752, 2015.

[44] J. Grommes, M. Mörgelin, and O. Soehnlein, "Pioglitazone attenuates endotoxin-induced acute lung injury by reducing neutrophil recruitment," *European Respiratory Journal*, vol. 40, no. 2, pp. 416–423, 2012.

[45] F. Amin, A. Memarzia, H. K. Rad, H. R. Kazerani, and M. H. Boskabady, "Carvacrol and PPARγ agonist, pioglitazone, affects inhaled paraquat-induced lung injury in rats," *Scientific Reports*, vol. 11, no. 1, p. 8129, 2021.

[46] F. Amin, A. Memarzia, H. R. Kazerani, and M. H. Boskabady, "Carvacrol and <i>Zataria multiflora</i> influenced the PPARγ agonist effects on systemic inflammation and oxidative stress induced by inhaled paraquat in rat," *Iranian Journal of Basic Medical Sciences*, vol. 23, no. 7, pp. 930–936, 2020.

Research Article

The Proresolving Lipid Mediator Maresin1 Alleviates Experimental Pancreatitis via Switching Macrophage Polarization

Yingying Lu [ID],[1] **Guotao Lu** [ID],[2] **Lin Gao,**[3] **Qingtian Zhu,**[2] **Jing Xue,**[4] **Jingzhu Zhang,**[3] **Xiaojie Ma,**[3] **Nan Ma,**[3] **Qi Yang,**[3] **Jie Dong,**[3] **Weijuan Gong,**[2] **Weiqin Li** [ID],[1,3] **and Zhihui Tong** [ID][1,3]

[1]*Department of Surgical Intensive Care Unit (SICU), Department of General Surgery, Jinling Hospital, Medical School of Southeast University, No. 305 Zhongshan East Road, Nanjing, 210002 Jiangsu, China*
[2]*Pancreatic Center, Department of Gastroenterology, Affiliated Hospital of Yangzhou University, No. 368 Hanjiang Media Road, Yangzhou, 225000 Jiangsu, China*
[3]*Surgical Intensive Care Unit (SICU), Department of General Surgery, Jinling Hospital, Medical School of Nanjing University, No. 305 Zhongshan East Road, Nanjing, 210002 Jiangsu, China*
[4]*State Key Laboratory of Oncogenes and Related Genes, Stem Cell Research Center, Ren Ji Hospital, School of Medicine, Shanghai Jiao Tong University, Shanghai 200127, China*

Correspondence should be addressed to Weiqin Li; njzy_pancrea@163.com and Zhihui Tong; njzyantol@hotmail.com

Background and Purpose. Previous studies showed that Maresin1 (MaR1), one of the metabolites from docosahexaenoic acid (DHA), could alleviate acute inflammation and prompt inflammation resolution. Also, it attenuated pancreatic injury in caerulein-induced acute pancreatitis (AP) in mice. However, the mechanisms underlying this suppression of inflammation and AP remain unknown. *Method.* Repeated caerulein injection was used to induce AP and chronic pancreatitis (CP) models in mice. The histopathological and serological changes were examined for evaluating the severity of the AP model, and flow cytometry was used for detecting macrophage phagocytosis and phenotype. Meanwhile, clodronate liposomes were used for macrophage depletion in mice. Finally, the CP model was adopted to further observe the protective effect of MaR1. *Result.* MaR1 administration manifested the improved histopathological changes and the lower serum levels of amylase and lipase. However, MaR1 played no protective role in the pancreatic acinar cell line *in vitro*. It obviously reduced the macrophage infiltration in the injured pancreas, especially M1-type macrophages. After macrophage clearance, MaR1 showed no further protection *in vivo*. This study also demonstrated that MaR1 could alleviate fibrosis to limit AP progression in the CP model. *Conclusion.* Our data suggests that MaR1 was a therapeutic and preventive target for AP in mice, likely operating through its effects on decreased macrophage infiltration and phenotype switch.

1. Introduction

Acute pancreatitis (AP) is one of the common acute abdominal fatal diseases. Severe AP (SAP) accounts for about 15%-20% of patients with AP and develops approximately 30% mortality [1, 2]. Activated innate immune cells increase the severity of AP. The prognosis of AP is related to an excessive inflammatory response. In this process, deregulated immune cells mediate the inflammatory cascade, leading to systemic inflammatory response syndrome and multiple organ failure [3]. However, no cure is available for AP, especially SAP patients with persistent organ failure.

Omega-3 polyunsaturated fatty acids (ω-3 FAs) mainly include docosahexaenoic acid (DHA) and eicosapentaenoic acid. ω-3 FA/DHA plays an indisputable role in hyperlipidemia and cardiovascular diseases [4, 5]. Studies involving humans as participants indicated that the use of enteral nutrition enriched with ω-3 FAs for treating AP might be

beneficial to the time of jejunal feeding and hospital stay [6]. A meta-analysis revealed that administering ω-3 FAs might be beneficial for decreasing mortality, infection-related complications, and length of hospital stay in AP, especially when used parenterally [7]. Previous clinical data indicated that ω-3 FA-supplemented parenteral nutrition could decrease hyperinflammatory response and improve immune function of patients with SAP [8, 9].

Inflammation can be divided into three phases: inflammation, resolution, and post-resolution [10]. Specialized pro-resolving mediators (SPMs), including resolvins, protectins, lipoxins, and maresins, play a key role in resolution and post-resolution [11, 12]. Inflammation is a protective response in maintaining homeostasis. However, excessive inflammation may lead to injury in normal tissues and finally develop into chronic diseases [2, 13]. SPMs provide a new avenue for inflammation; they prevent inflammation from spreading and halt the transition from acute to chronic [14, 15].

Maresins are newly described macrophage-derived mediators of inflammation resolution; they are one of the metabolites from ω-3 FAs and biosynthesized via 12-lipoxygenase [14, 16, 17]. Maresin1 (7,14-dihydroxydocosa-4Z, 8Z,10,12,16Z,19Z-hexaenoic acid, MaR1) has been shown to be a potent mediator to inhibit neutrophil infiltration, promote macrophage efferocytosis, and enhance tissue regeneration in acute inflammation [18–20]. MaR1 exerts protective effects in murine models of colitis and sepsis [21, 22]. Recently, it has been reported that MaR1 protected mice from nonalcoholic fatty liver disease in a RORα-dependent manner [23]. Several studies reported the protective effects of MaR1 on AP without clarifying its specific target cells [24, 25].

Compared with other SPMs, the effect of MaR1 on AP remains unknown. The purpose of this study was to verify the hypothesis of whether MaR1 could protect against AP, as well as exploring the possible underlying mechanism.

2. Materials and Methods

2.1. Animals and Reagents. ICR male mice (aged 8 weeks), weighing 28-30 g, were purchased from the Yangzhou University Model Animal Center (Yangzhou, China). Green fluorescent protein transgenic (GFP tg) mice were obtained from Prof. BJ Wu. All mice were housed under specific pathogen-free (SPF) conditions in an air-conditioned animal facility at 24°C on a 12 hours light/dark cycle. The Principles of Laboratory Animal Care (NIH publication no. 85Y23, revised 1996) were followed, and all experimental protocols were approved by the experimental animal ethics committee of Jinling Hospital affiliated to Medical School of Nanjing University (No. 20160905).

The murine pancreatic acinar 266-6 cell line was obtained from the American Type Culture Collection (ATCC, VA, USA). MaR1 was purchased from Cayman Chemical Company (MI, USA). Caerulein was obtained from AnaSpec Inc. (CA, USA). Cholecystokinin fragment 30-33 amide (CCK) and lipopolysaccharide (LPS) were purchased from Sigma-Aldrich (MO, USA); clodronate liposomes (CLs, from Vrije Universiteit Amsterdam) were purchased from Yeasen

Biotech Co., Ltd. (Shanghai, China). The lipase kits were purchased from Nanjing Jiancheng Corp. (Nanjing, China), and the amylase kits were purchased from BioSino Bio-Technology & Science Inc. (Beijing, China). Macrophage-stimulating factor (M-CSF) was purchased from MedChenExpress LLC. (Nanjing, USA). Anti-F4/80, anti-phospho-mixed lineage kinase domain like protein (p-MLKL), goat anti-rabbit, and rabbit anti-mouse secondary antibodies were purchased from Abcam (Cambridge, UK). Anti-receptor-interacting protein 3 (RIP3) antibody was purchased from Santa Cruz Biotechnology (CA, USA). All antibodies for flow cytometry were purchased from BioLegend (CA, USA). Dulbecco's modified Eagle's medium (DMEM), fetal bovine serum, penicillin, and streptomycin were obtained from Gibco (Thermo Fisher Scientific, MA, USA).

2.2. Induction of Experimental Pancreatitis. The mice were randomly assigned to five groups: control, caerulein, caerulein+0.2 ng/mice MaR1, caerulein+2 ng/mice MaR1, and caerulein+10 ng/mice MaR1. The AP model was induced by intraperitoneal (i.p.) injection of 50 μg/kg caerulein every hour for 10 hours. Normal saline (NS, 0.9% NaCl) was given instead of caerulein in the control group. MaR1 or vehicle (0.9% NaCl) was injected intraperitoneally at 0 hour after the first caerulein injection. The mice were sacrificed 12 hours after the final injection.

Pancreatic macrophage depletion was in accordance with the instructions. Briefly, the mice were intraperitoneally administered 200 μL of CLs on days 1 and 3. The control mice received the same volume of empty liposomes (phosphate-buffered saline, PBS). On the fifth day, the AP model was induced.

Chronic pancreatitis (CP) was induced by injecting of 50 μg/kg caerulein once daily for a continued cycle of 5 days on and 2 days off, for a total of 4 weeks [23]. Seven days following the start of the caerulein injection, the mice were given either NS or MaR1 (2 ng/mice, 100 μL daily for 5 days per week × 4 weeks) until sacrificed 5 weeks later.

2.3. Sample Collection and Analysis of Plasma Parameters. Blood samples were obtained from the tail veins of isoflurane-anesthetized mice 0, 6, and 12 hours after the first caerulein injection. The mice were anesthetized with sodium pentobarbital (50 mg/kg, i.p.) and sacrificed. Pancreatic tissues were taken and fixed with 4% paraformaldehyde in PBS (pH = 7.4) and embedded in paraffin.

The serum amylase and lipase activities were determined using amylase and lipase kits following the manufacturer's protocol.

2.4. Histological Examination. The paraffin sections of the pancreas and lung tissue were stained with hematoxylin and eosin (HE). Two investigators who were blinded to the experimental grouping scored the degree of pancreatic injury using light microscopy and evaluated the severity of edema, inflammation, and necrosis, as described previously [26].

2.5. Immunohistochemical Examination. The slices from paraffin-embedded pancreatic tissues were subjected to immunohistochemical (IHC) staining for RIP3, p-MLKL,

and F4/80 detection. The slides were incubated overnight at 4°C in a humid chamber with an antibody against RIP3, p-MLKL and F4/80 (1 : 200 dilution) and then incubated with goat anti-rabbit secondary antibody (1 : 500 dilution) for 60 minutes as described previously [24]. The images were acquired using a microscope (IX73, Olympus, Tokyo, Japan).

2.6. Cell Cultures and Treatment. 266-6 cells were cultured in DMEM supplemented with 10% fetal bovine serum, 100 U/mL penicillin, and 100 μg/mL streptomycin in a humidified 5% CO_2 incubator. Cholecystokinin analog CCK (8000 μM) was applied to induce AP with or without MaR1 (250 nM, 500 nM, and 1000 nM). The cells were collected after 12 hours for further investigation.

2.7. Isolation of Pancreatic Leukocytes. MaR1 or vehicle was injected to treat the AP model. After 24 hours, the mice were killed, and the pancreas was removed carefully by trimming fat and mesentery. As mentioned in the literature [27], the pancreas was minced with scissors and then washed twice with buffer A (Hank's balanced salt solution +10% fetal calf serum). The tissue was resuspended in buffer A containing 2 mg/mL collagenase type IV and incubated in a shaker at 37°C for 15 minutes. The suspension was then vortexed at low speed for 20 seconds and centrifuged, and the cell pellet was resuspended in red blood cell lysis buffer for 5 minutes. The cells were spun down, washed three times with buffer A and used for marker staining.

2.8. Isolation of Primary Pancreatic Acinar Cells (PACs). GFP tg mice emit green fluorescence spontaneously in the pancreas. PACs were isolated from GFP tg mice by collagenase digestion and then incubated in DMEM containing 10% fetal bovine serum at 37°C [28]. Bone marrow-derived macrophages (BMDMs) were coincubated with PACs, caerulein (5 μM), and MaR1 (250 nM, 500 nM, and 1000 nM) for 6-8 hours.

2.9. Isolation of BMDMs and Cell Induction. Briefly, both ends of the femur and tibia were cut and flushed with a syringe filled with complete Roswell Park Memorial Institute (RPMI) 1640 containing 10% fetal bovine serum, 100 U/mL penicillin, 100 μg/mL streptomycin, 1% N-2-hydroxyethylpi-perazine-N-2-ethane sulfonic acid (HEPES, 1 M), and 0.05% β-hydroxy-1-ethanethiol to extrude BM cells into a sterile Petri dish. After gentle resuspension and centrifugation, BM cells were cultured using 20 ng/mL M-CSF in complete RPMI. On days 2, 4, and 6, the medium was half-replaced with a fresh batch containing the CSF-conditioned medium as earlier. The cells were ready for use on day 7 [28].

BMDMs were coincubated with caerulein-stimulated acini for 6 hours. After removing acini, BMDMs were collected and stained with fluorochrome-conjugated antibody: PE/Cy7-F4/80 for flow cytometry.

2.10. Flow Cytometry. Pyridine iodide (PI, 1 μmol/L) was used to detect plasma membrane rupture characteristic of necrosis. After loading, 266-6 cells were washed and resuspended in Ca^{2+}-free buffer.

For surface staining, pancreatic leukocytes were stained with the following fluorochrome-conjugated antibodies: FITC-CD86, PE/Cy7-CD45.2, APC/Cy7-CD11b, and Percp/Cy5.5-F4/80. For intracellular tumor necrosis factor α (TNF-α) staining, the cells were cultured in DMEM complete medium and stimulated with LPS (100 ng/mL) and brefeldin A (10 μg/mL) for 4 hours at 37°C. The cells were washed and stained with surface markers. The cells were then fixed and permeabilized. PE-TNF-α and APC-CD206 (1 : 200) were used for intracellular staining. Flow cytometry data were collected on NovoCyte and analyzed using NovoExpress software (ACEA Biosciences, Inc., CA, USA).

2.11. Sirius Red and Masson Staining for Fibrosis. Paraffin sections (4 μm) were stained with Picro-Sirius red (1% Sirius red in saturated picric acid solution) for 1 hour at room temperature to analyze collagen synthesis and deposition. The sections were then washed twice with 0.5% acetic acid. The water was physically removed from the slides by vigorous shaking. After dehydration using 100% ethanol three times, the sections were cleaned with xylene and mounted in a resinous medium. Image-Pro Plus 6.1 software (Media Cybernetics, MD, USA) was used to calculate the Sirius red-positive staining proportion.

For Masson staining, pancreatic tissue slices were routinely dewaxed, hydrated, and incubated in Wiegert's solution for 5-10 minutes. They were then differentiated in acidic ethanol for 5-15 seconds, slightly washed with water, and blued in Masson bluing buffer for 3-5 minutes. After washing with water, the slices were incubated in Ponceau-Fuchsin solution for 5-10 minutes, washed with a weak acid solution for 1 minute, and washed with phosphomolybdic acid solution for 1-2 minutes. The slices were subsequently stained in aniline blue solution for 1-2 minutes. They were then washed with weak acid solution, dehydrated in absolute ethanol, made transparent with dimethylbenzene, and mounted with neutral resin.

2.12. Statistical Analysis. The unpaired-sample Student t-test was used to determine statistical significance, and a P value less than 0.05 indicated a statistically significant difference. One-way ANOVA plus Tukey post hoc test was used to determine the difference among multiple groups, and a P value less than 0.05 indicated a statistically significant difference. Values were expressed as mean ± standard error of mean (SPSS statistical software, version 22.0, IBM Analytics, NY, USA). Unless indicated, the results were from at least 3 independent experiments.

3. Results

3.1. MaR1 Ameliorated the Histopathological Alterations of the Pancreas in Mice with AP. Our group previously reported that DHA exerted a protective effect on AP. This study investigated the effect of MaR1 (metabolite of DHA) to partly explain its clinical benefit. In animal experiments, three doses of 0.2, 2, and 10 ng/mice were adopted. As expected, the caerulein group exhibited the classical edematous pancreatitis manifestations, including edema, inflammatory cell

(a)

(b)
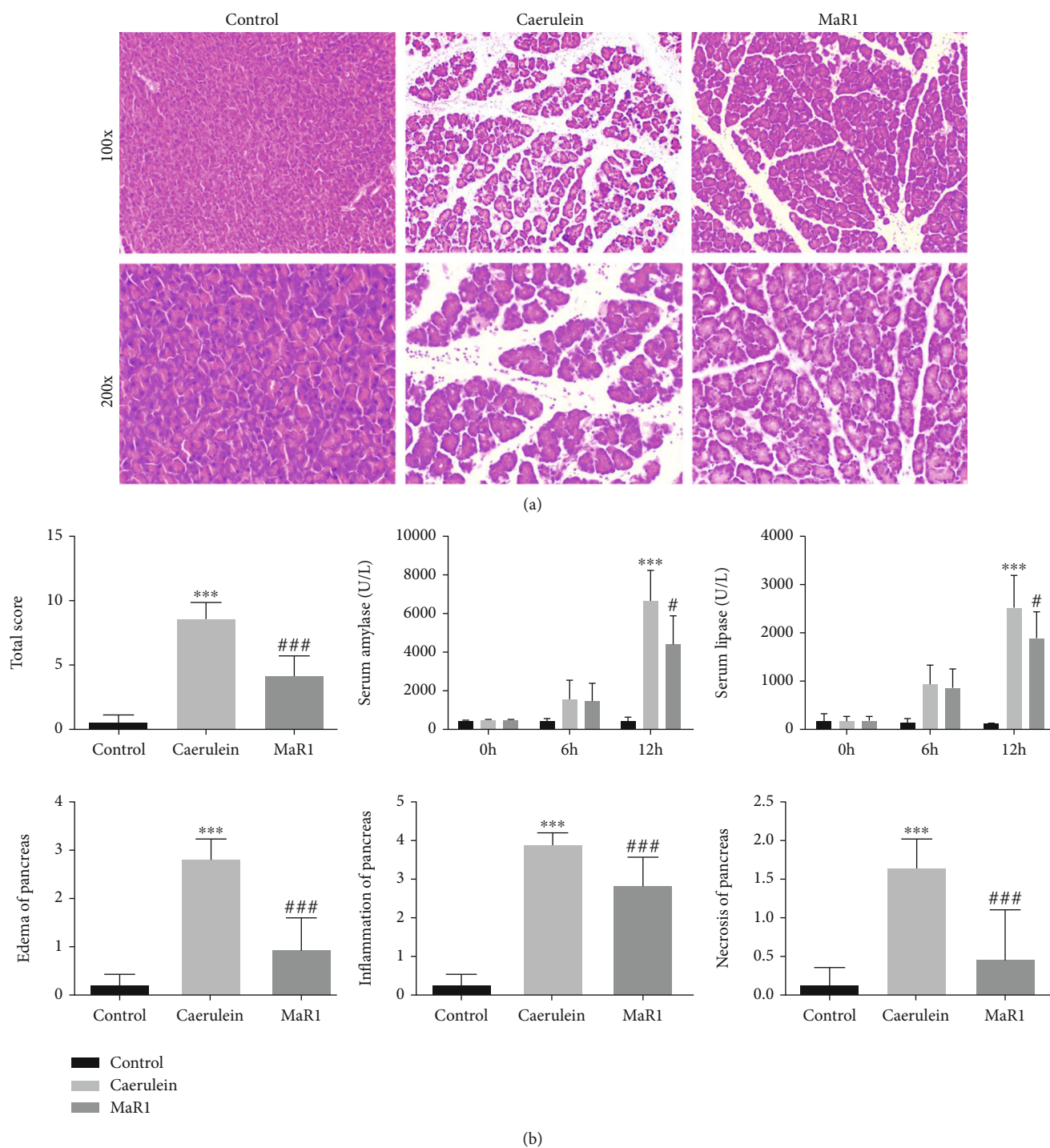
FIGURE 1: MaR1 ameliorated pancreatic tissue injury in AP mice. (a) Representative pathological changes in pancreas. HE stained sections of the pancreas in magnification 100x and 200x. (b) Histological scores of pancreatic tissues (edema, inflammation, and necrosis) and serum levels of amylase and lipase. $***P < 0.001$ vs. the control group. $^{\#}P < 0.05$, $^{\#\#}P < 0.01$, and $^{\#\#\#}P < 0.001$ vs. the caerulein group. $n \geq 6$ each group.

infiltration, and spotty acinar cell necrosis. Based on the pathological results, 2 ng/mice MaR1 was chosen in subsequent experiments to examine its obvious protective effect (Figure 1(a)). Pancreatic injury scores were assessed in parallel with pathohistological changes. In addition, MaR1-treated mice also exhibited a significant reduction of serum amylase and lipase levels (Figure 1(b)).

A few observations suggested that necroptosis mediated AP development. RIP kinases play a central role in regulating necroptosis [29]. RIP3 and MLKL are important proteins to assemble the necrosome. IHC examinations were used for detecting RIP3 and p-MLKL expressions in pancreatic tissues. As shown in Figure 2(a), the positive staining areas of RIP3 and p-MLKL showed a robust increase after PAC
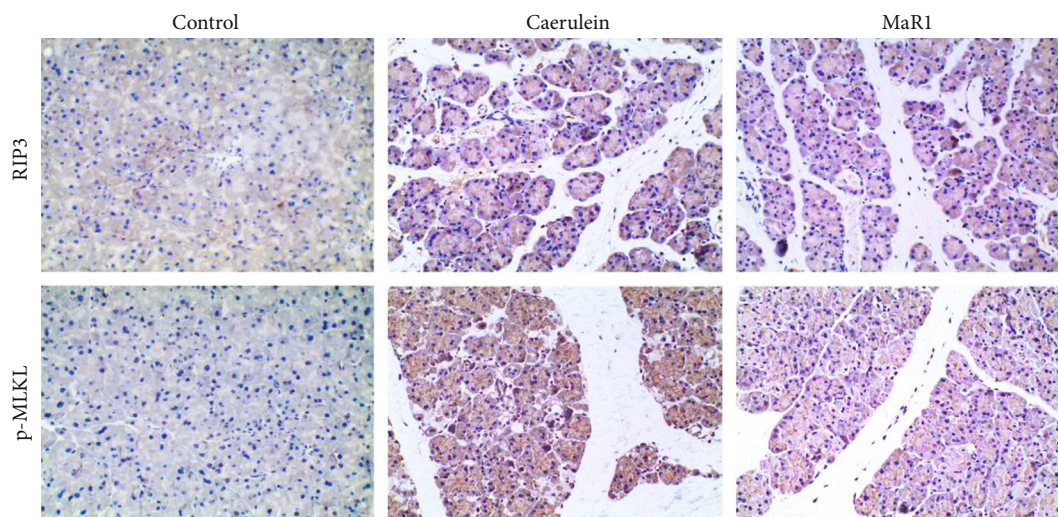
(a)
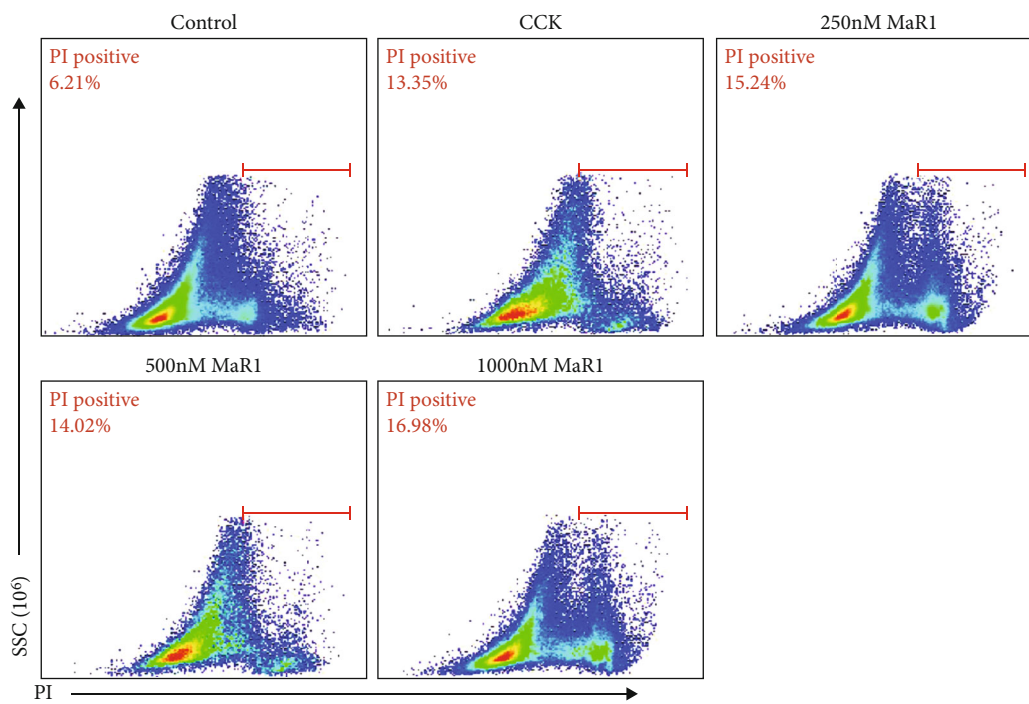
(b)
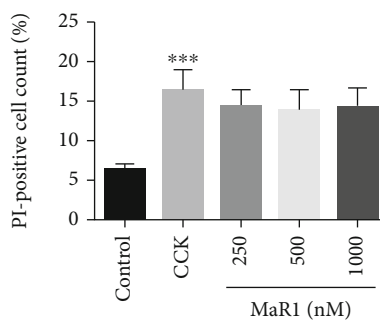
(c)

FIGURE 2: MaR1 showed protective effects independent of pancreatic acinar cells. (a) IHC examinations for RIP3 and p-MLKL of the pancreas in magnification 200x. $n \geq 6$ each group. (b, c) Flow cytometry of PI staining for 266-6 cells and relative positive cell counting was quantified. ***$P < 0.001$ vs. the control group. $n \geq 9$ each group.

(a)

(b)

(c)

(d)

(e)
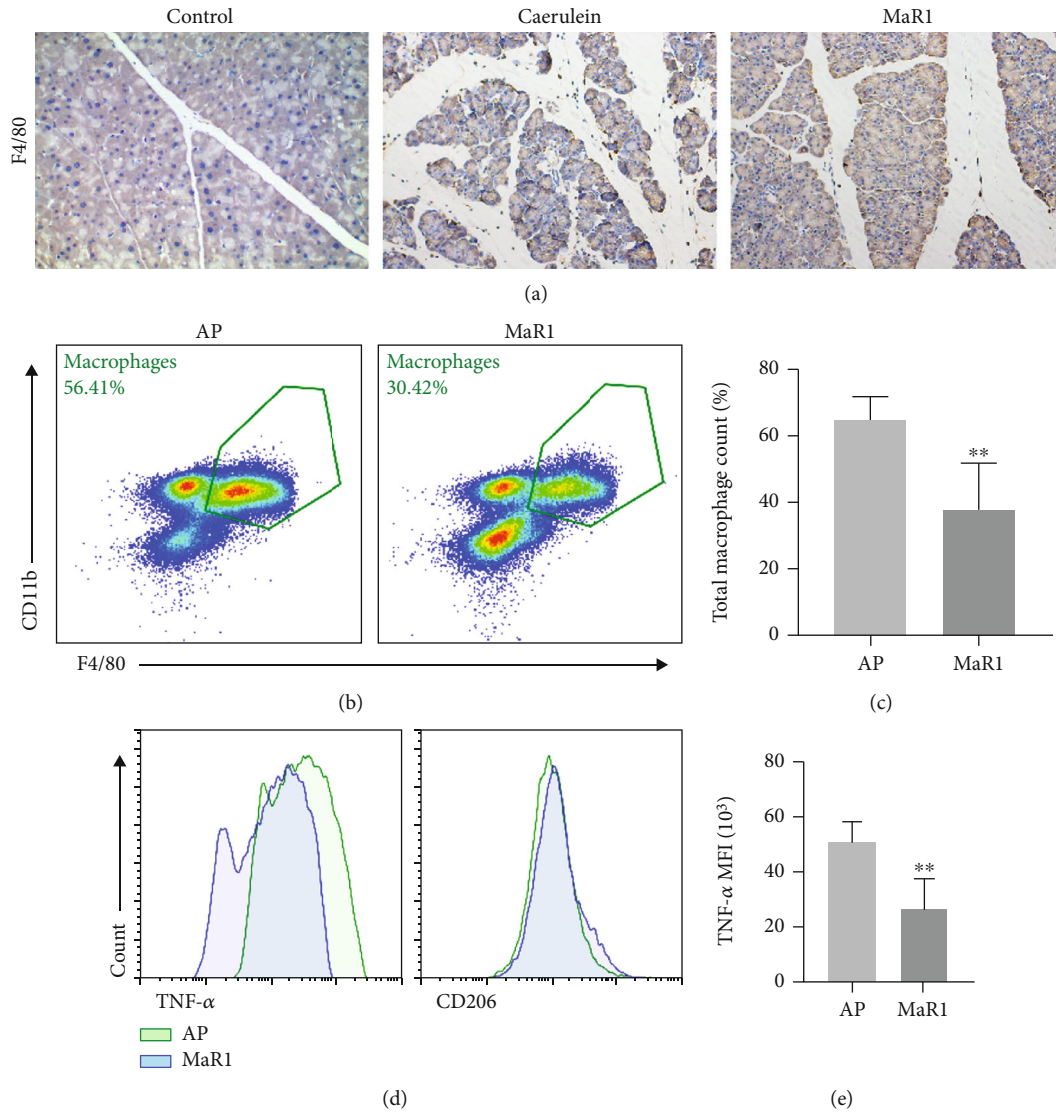
FIGURE 3: Continued.
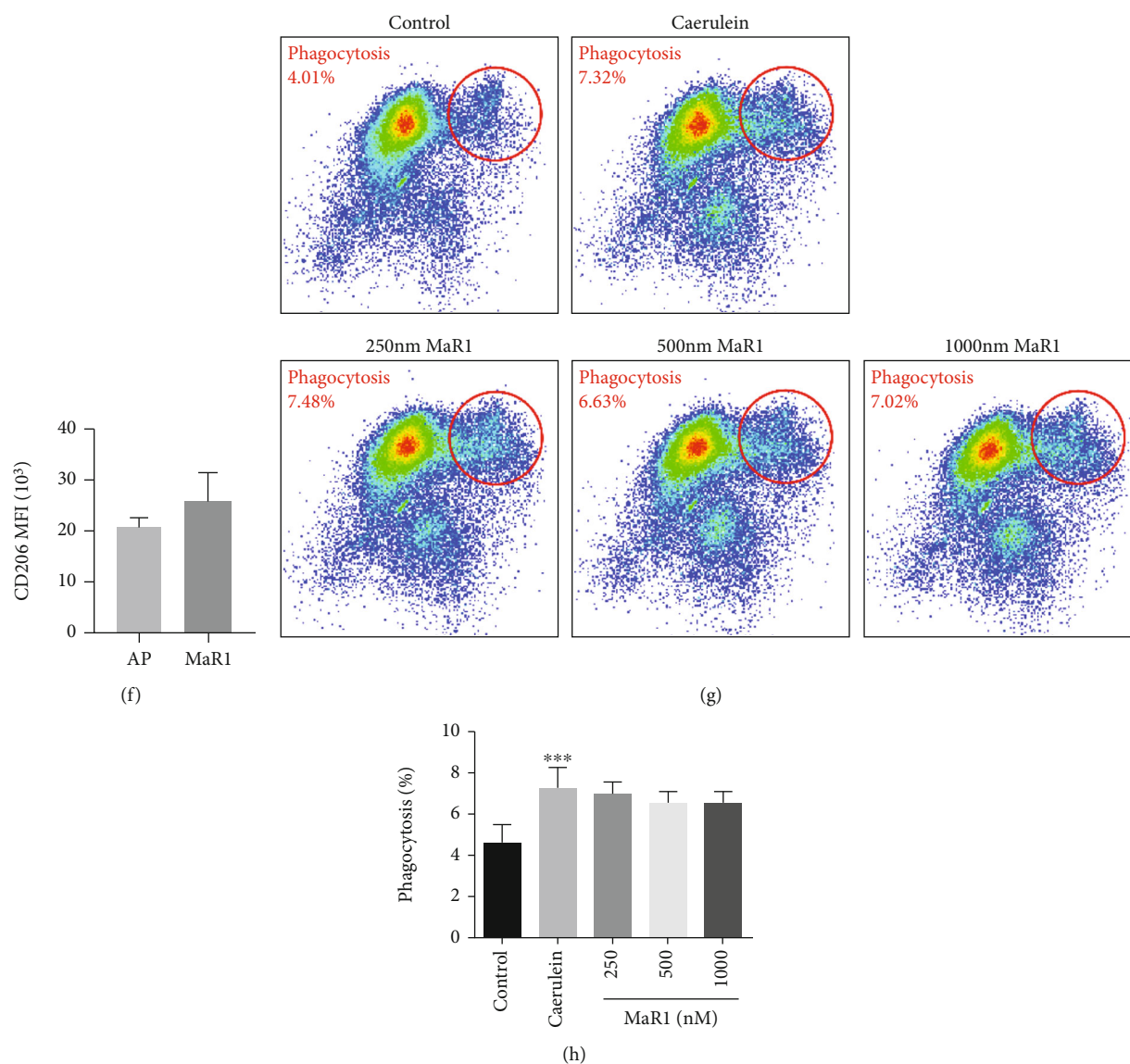
FIGURE 3: MaR1 inhibited macrophage infiltration in the pancreatic tissue. (a) IHC examinations for F4/80 of macrophages in the pancreas in magnification 200x. $n \geq 6$ each group. (b, c) Total macrophage counting in the pancreas of the AP and MaR1 groups. (d) Flow cytometry of TNFα for M1 and CD206 for M2 in the pancreas. (e) Mean fluorescence intensity of TNFα for M1 infiltration in pancreas. (f) Mean fluorescence intensity of CD206 for M2 infiltration in the pancreas. $n \geq 4$ each group. (g, h) Flow cytometry of BMDM phagocytosis of pancreatic acinar cells and related quantification. $n \geq 7$ each group. $^{**}P < 0.01$, $^{***}P < 0.001$ vs. the AP or control group.

damage. MaR1 could decrease the number of RIP3- and p-MLKL-positive cells, indicating that MaR1 mitigated the severity of PAC necroptosis in the AP model.

3.2. MaR1 Showed No Direct Effects on Pancreatic Acinar Cell Necrosis. Based on the results of *in vivo* experiments, we first considered whether MaR1 had a direct protective effect on PAC injury. The 266-6 cell line is widely used in the pancreatitis model for its exocrine function [30, 31]. Accordingly, 266-6 cells were used to explore the effect of MaR1, and CCK was used to induce an acute injury model *in vitro*. After different doses (250 nM, 500 nM, and 1000 nM) of MaR1 treatment, PI staining demonstrated that the percent of necrotic cells in the CCK group was approximately 15.24%, while the MaR1 group showed no significant differences

(Figure 2(b)). Further, the concentration gradient difference of MaR1 (50 nM, 100 nM, 250 nM, 500 nM, 750 nM, 1 μM, 5 μM, and 10 μM) was expanded, and still no sign of protection was observed (data not shown). The results confirmed that the protective effect of MaR1 on AP might not anchor in PACs.

3.3. MaR1 Inhibited the Infiltration of Macrophages in the Pancreatic Tissue. Since MaR1 was not beneficial to 266-6 cells directly, we focused on immune cells in pancreatic tissues. Macrophages play an important role in AP [32]. The IHC examination for F4/80 demonstrated that MaR1 significantly reduced macrophage infiltration in pancreatic tissues (Figure 3(a)). Primary immune cells were extracted from the pancreatic tissues of mice with AP to determine
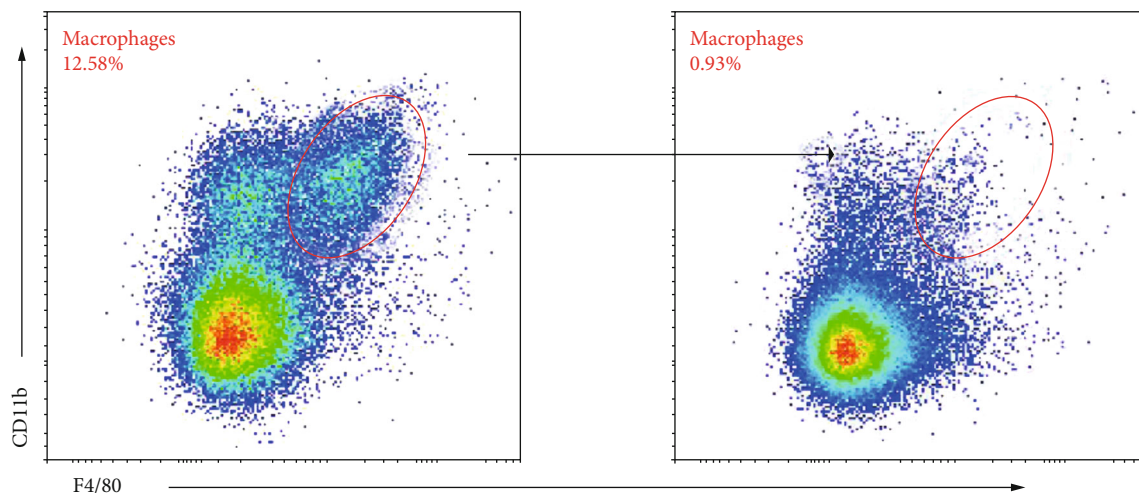
(a)
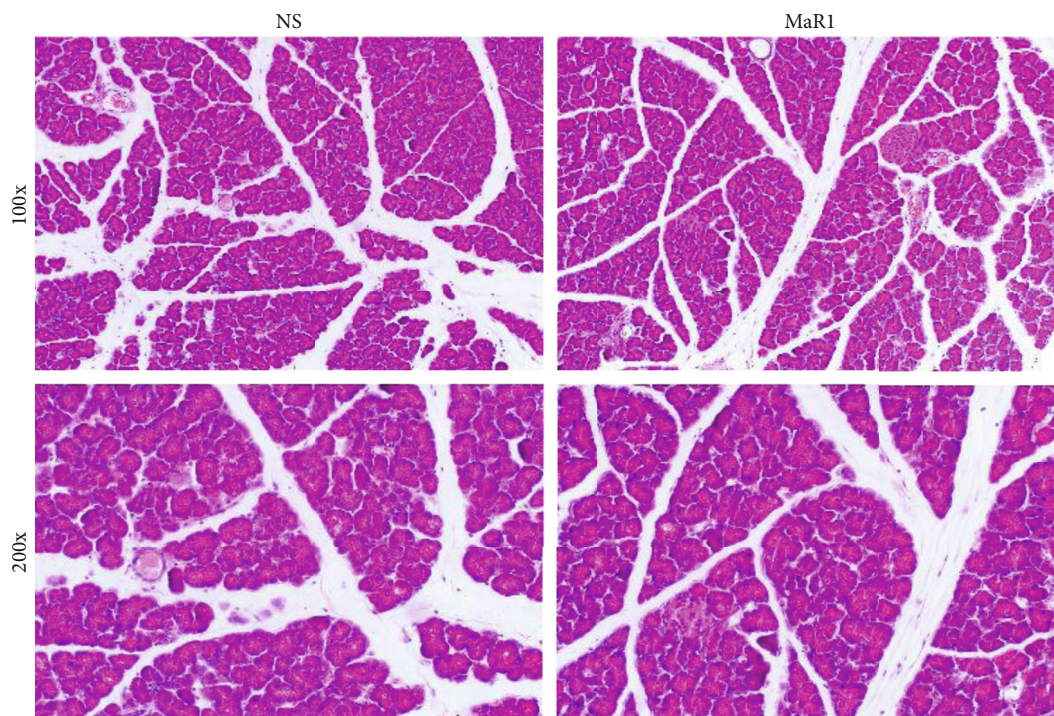
(b)

FIGURE 4: Continued.

(c)
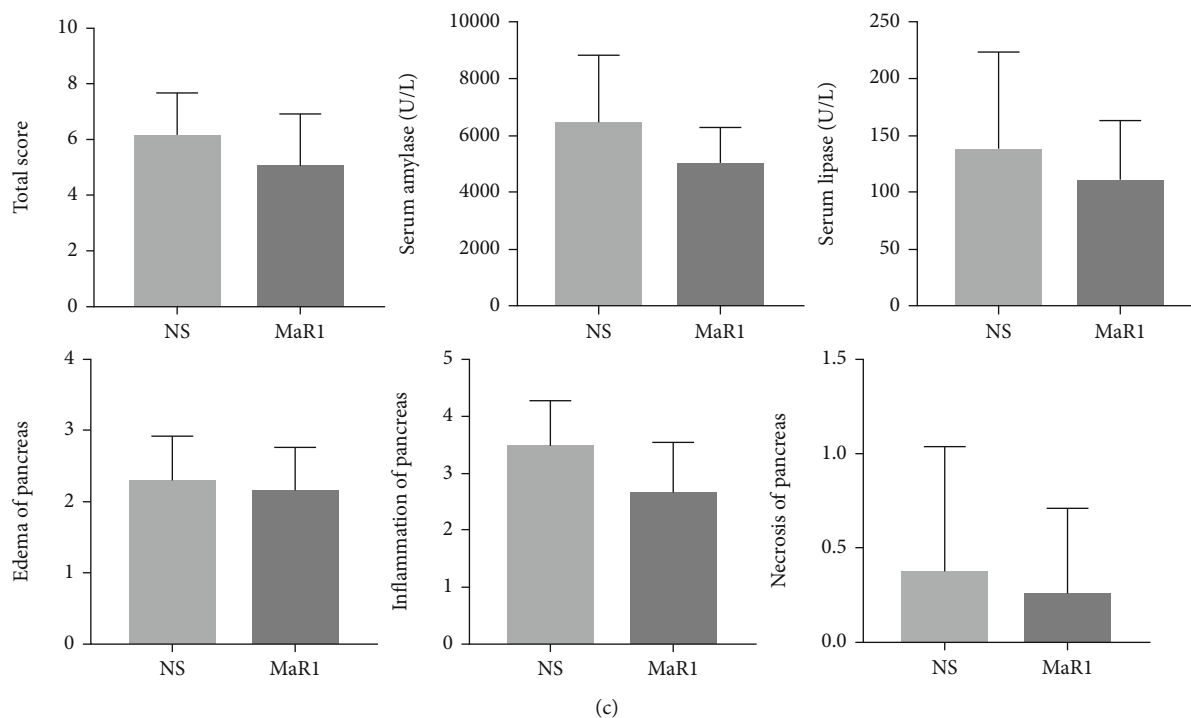
FIGURE 4: MaR1 did not further protect against AP after pancreatic macrophages clearance. (a) Flow cytometry of macrophages ratio changes in blood samples after CL injection. (b) Representative pathological changes in the pancreas after caerulein challenges. HE-stained sections of the pancreas in magnification 100x and 200x. (c) Histological scores of pancreatic tissues (edema, inflammation, and necrosis) and serum levels of amylase and lipase. $n = 7$ each group.

the polarization of macrophages. Flow cytometry was used to detect TNF-α and CD206 levels for M1- and M2-associated biomarkers, respectively. Compared to AP group, the mean fluorescence intensity (MFI) of TNF-α in the MaR1 group significantly reduced, while the MFI of CD206 increased slightly with no statistically significant difference (Figures 3(d)–3(f)). In addition, the total number of macrophages significantly reduced after MaR1 treatment, which was consistent with IHC staining results (Figures 3(b) and 3(c)).

MaR1 can enhance macrophage phagocytosis of dead cells and debris. We want to verify its effect in the AP model. PACs from GFP tg mice were extracted because their excitation by 488 nm light led to a fluorescence emission maximum around 530 nm. After coincubation with caerulein-stimulated PACs, BMDMs were collected for flow cytometry. The basic phagocytosis of PBS-stimulated PACs was around 4.01%. The caerulein group showed an obvious rise to 7.32%, while the MaR1 treatment group showed no change. MaR1 might not enhance BMDM phagocytosis of damaged PACs (Figures 3(g) and 3(h)). Collectively, these results indicated that MaR1 might protect against AP in mice by reducing macrophage infiltration, mainly proinflammatory M1 phenotype.

3.4. MaR1 Did Not Further Protect against AP after Pancreatic Macrophage Clearance.
The pancreatic macrophages were depleted using CLs before caerulein exposure. CLs could effectively clear macrophages and protect against AP in mice (Figure 4(a)). Furthermore, MaR1 could not fur-

ther alleviate the severity of experimental AP, irrespective of pathological scores or serological tests (Figures 4(b) and 4(c)). The results from both animal and cell experiments suggested that MaR1 might improve the AP severity of mice depending on pancreatic macrophages.

3.5. MaR1 Alleviated Macrophage Infiltration and Fibrosis of Pancreatic Tissues in the CP Model.
In mice, the hyperstimulation of the pancreas with caerulein led to AP. Continuous acute injury to the pancreas caused recurrent AP and finally CP, which was consistent with the pathophysiological process of human pancreatitis. The CP model was established in a repetitive manner to further examine the effect of MaR1 in vivo. The mice undergoing repetitive caerulein injection revealed macrophage infiltration, pancreatic fibrosis, and acinar cell loss. Based on previous results, 2 ng/mice MaR1 was chosen, which obviously alleviated the severity of pancreatic damage (Figure 5(a)). The Sirius red and Masson staining showed that the fibrosis in the pancreas was obviously reduced (Figure 5(c)). In addition, the MaR1 group showed less macrophage infiltration (F4/80 staining) in pancreatic tissues compared with the CP group (Figure 5(b)).

4. Discussion

Macrophages are responsible for host defense, acute inflammatory response, and its timely resolution [33]. They can be simply divided into two extreme phenotypes: classically activated macrophages (M1) and alternatively activated

(a)

(b)

(c)
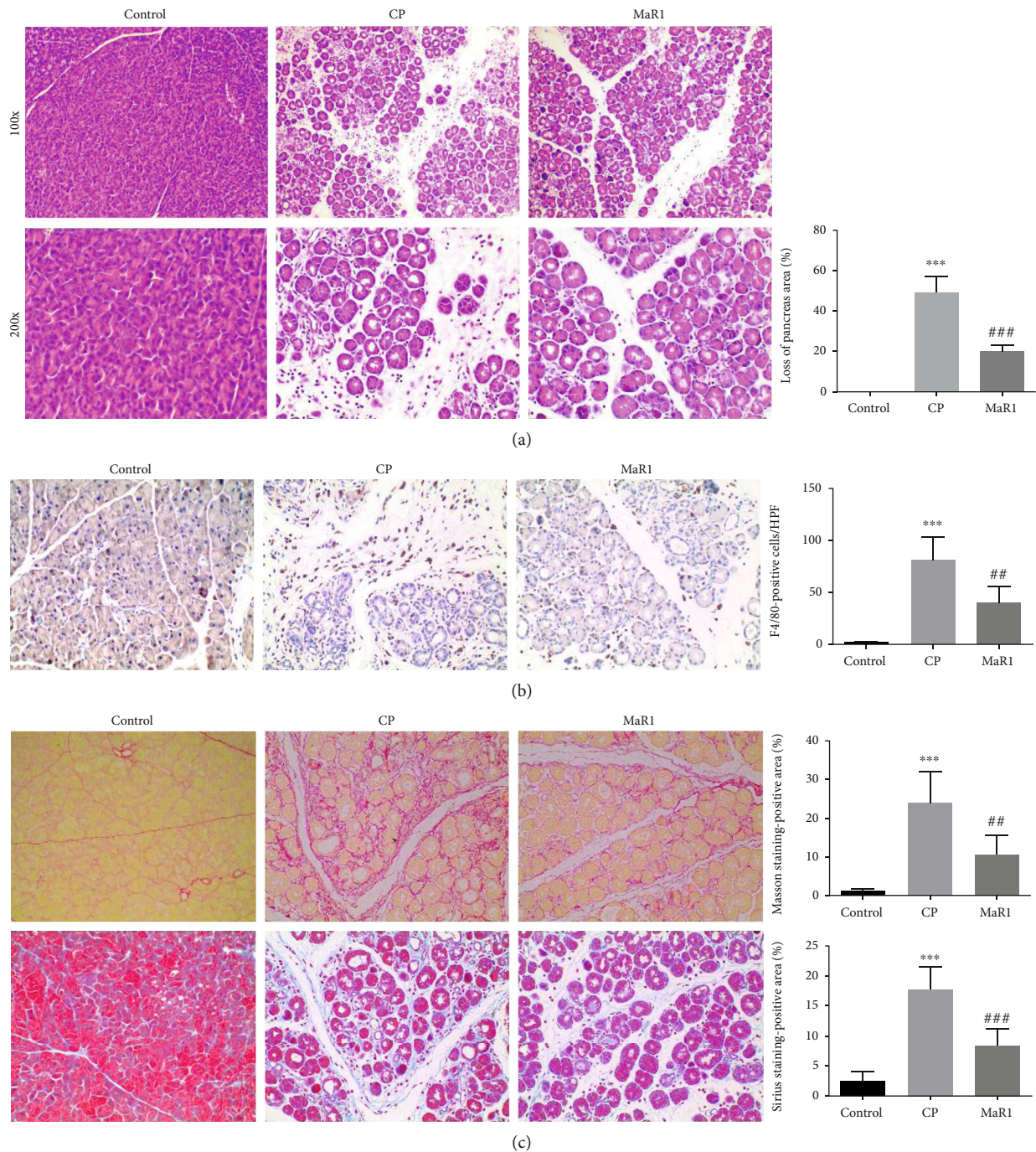
FIGURE 5: MaR1 alleviated pancreatic tissue injury and fibrosis of pancreatic tissues in CP model. (a) Representative pathological changes in the pancreas after caerulein repetitive injection. HE-stained sections of the pancreas in magnification 100x and 200x and loss of pancreas area was quantified. (b) IHC examinations and total count for F4/80 of macrophages in the pancreas in magnification 200x. (c) Masson (the upper row) and Sirius red (the lower row) staining for collagen production in the pancreas of mice. $n \geq 10$ each group. ***$P < 0.001$ vs. the control group. ##$P < 0.01$, ###$P < 0.001$ vs. the CP group.

macrophages (M2). Briefly, M1 macrophages exhibit proinflammation and immunologic defense properties, while M2 macrophages exhibit opposite properties. The switch from M1 to M2 phenotype can alleviate the severity of acute inflammation [34].

Since no specific treatment exists that targets pancreatic parenchyma cells, more researchers focus on local immune cells especially macrophages. Macrophages sense acinar cell death and activate pancreatic inflammation and determine the severity of AP [35]. Macrophages engulfing damaged

acinar cells can also be the focus of AP in conjunction with damaged acinar cells [28]. In this study, we found that MaR1 protected AP not by acting directly on PACs but through macrophages. In accordance with Wu et al., we found that macrophage quantification in the pancreatic tissue significantly increased after AP onset (1 day) [36]. After MaR1 treatment, the percentage of macrophage population declined markedly. Furthermore, the number of M1 macrophages decreased and the number of M2 macrophages slightly increased in pancreatic tissues. Macrophages may demonstrate the plasticity and pluripotency in response to local microenvironment signals in a specific time and space. M2 macrophages may be further subdivided into M2a, M2b, M2c, and M2d, of which the surface markers are very different [37]. CD206 may not be the best choice for tracking the changes of M2. Another problem is the timing of administration of MaR1 in mice. In the tibial fracture injury model, MaR1 treatment at the time of injury is ineffective in decreasing the number of proinflammatory macrophages, different from the treatment results after injury [38]. Macrophages exhibit dynamic transitions in phenotype and function as AP progresses. The number of M2 or M2-like macrophages increases after the acute inflammation stage [36]. Delayed administration for MaR1 may provide some hints about its effect on M2 macrophages. Further, like our results, some studies reported that MaR1 markedly decreased the number of proinflammatory macrophages, but not that of anti-inflammatory macrophages in inflammation models [38, 39]. In addition, MaR1 can enhance macrophage phagocytosis of neutrophils during inflammation. However, no reports mentioned the effect of MaR1 on macrophage phagocytosis of damaged acinar cells in AP. In our study, no enhancement effect of MaR1 on the phagocytosis of injured acinar cells was observed. The results indicated that MaR1 mainly regulated macrophage phenotype to mitigate inflammation. Moreover, the findings indicated that MaR1 indeed had no further protective effect on AP after macrophage clearance in the animal model. However, keeping macrophage polarization in balance is an attractive therapeutic option for AP, considering the heterogeneous function of macrophages in different stages of diseases, besides directly eliminating macrophages.

The recurrence of AP is a challenge in clinical treatment. The incidence of recurrent AP can reach 21%, and CP develops in 36% of patients [40]. Further, effective preventive and therapeutic strategies for CP treatment are still lacking. Macrophage infiltration and activation play an important role in pancreatic injury and later fibrosis. Therefore, the CP model was used in this study to explore the pharmacological action of MaR1. MaR1 obviously attenuated macrophage infiltration, fibrosis, and pancreatic damage in the CP model. These results showed that MaR1 might serve as an immune resolvent for the clinical prevention of CP.

In conclusion, our study showed that MaR1 could decrease the severity of AP via reducing macrophage infiltration, especially M1 macrophages in pancreatic tissues. This provided evidence for the protective effect of DHA against AP. Hence, MaR1 may serve as a promising clinical therapeutic drug for treating AP in the future.

Data Availability

All data included in this study are available upon request by contact with the corresponding author. Correspondence should be addressed to Weiqin Li, njzy_pancrea@163.com or Zhihui Tong, njzyantol@hotmail.com.

Conflicts of Interest

All authors of this paper have no conflict of interests to disclose.

Authors' Contributions

Guotao Lu did the conceptualization. Lin Gao did the formal analysis. Zhihui Tong and Weiqin Li did the funding acquisition and supervision. Yingying Lu did the investigation. Qingtian Zhu, Jing Xue, Xiaojie Ma, and Nan Ma did the methodology. Jingzhu Zhang and Qi Yang searched for resources. Jie Dong acquired software. Weijuan Gong provided technical guidance. All authors have read and agreed to the published version of the manuscript. Yingying Lu and Guotao Lu contributed equally to this work.

Acknowledgments

References

[1] J.-L. Frossard, M. L. Steer, and C. M. Pastor, "Acute pancreatitis," *The Lancet*, vol. 371, no. 9607, pp. 143–152, 2008.

[2] P. G. Lankisch, M. Apte, and P. A. Banks, "Acute pancreatitis," *The Lancet*, vol. 386, no. 9988, pp. 85–96, 2015.

[3] A. S. Gukovskaya, I. Gukovsky, H. Algul, and A. Habtezion, "Autophagy, inflammation, and immune dysfunction in the pathogenesis of pancreatitis," *Gastroenterology*, vol. 153, no. 5, pp. 1212–1226, 2017.

[4] A. C. Skulas-Ray, P. W. F. Wilson, W. S. Harris et al., "Omega-3 fatty acids for the management of hypertriglyceridemia: a science advisory from the american heart association," *Circulation*, vol. 140, no. 12, pp. e673–e691, 2019.

[5] A. S. Abdelhamid, T. J. Brown, J. S. Brainard et al., "Omega-3 fatty acids for the primary and secondary prevention of cardiovascular disease," *The Cochrane Database of Systematic Reviews*, vol. 7, article CD003177, 2018.

[6] N. LASZTITY, J. HAMVAS, L. BIRO et al., "Effect of enterally administered n-3 polyunsaturated fatty acids in acute pancreatitis–a prospective randomized clinical trial," *Clinical Nutrition*, vol. 24, no. 2, pp. 198–205, 2005.

[7] Q. C. Lei, X. Wang, X. Xia et al., "The role of omega-3 fatty acids in acute pancreatitis: a meta-analysis of randomized controlled trials," *Nutrients*, vol. 7, no. 4, pp. 2261–2273, 2015.

[8] X. Wang, W. Li, N. Li, and J. Li, "ω-3 fatty acids–supplemented parenteral nutrition decreases hyperinflammatory response

and attenuates systemic disease sequelae in severe acute pancreatitis: a randomized and controlled study," *Journal of Parenteral and Enteral Nutrition*, vol. 32, no. 3, pp. 236–241, 2008.

[9] X. Wang, W. Li, F. Zhang, L. Pan, N. Li, and J. Li, "Fish oil-supplemented parenteral nutrition in severe acute pancreatitis patients and effects on immune function and infectious risk: a randomized controlled trial," *Inflammation*, vol. 32, no. 5, pp. 304–309, 2009.

[10] J. N. Fullerton and D. W. Gilroy, "Resolution of inflammation: a new therapeutic frontier," *Nature Reviews. Drug Discovery*, vol. 15, no. 8, pp. 551–567, 2016.

[11] C. N. Serhan, "Pro-resolving lipid mediators are leads for resolution physiology," *Nature*, vol. 510, no. 7503, pp. 92–101, 2014.

[12] R. A. Colas, M. Shinohara, J. Dalli, N. Chiang, and C. N. Serhan, "Identification and signature profiles for pro-resolving and inflammatory lipid mediators in human tissue," *American Journal of Physiology. Cell Physiology*, vol. 307, no. 1, pp. C39–C54, 2014.

[13] J. M. Braganza, S. H. Lee, R. F. McCloy, and M. J. McMahon, "Chronic pancreatitis," *The Lancet*, vol. 377, no. 9772, pp. 1184–1197, 2011.

[14] C. N. Serhan and B. D. Levy, "Resolvins in inflammation: emergence of the pro-resolving superfamily of mediators," *The Journal of Clinical Investigation*, vol. 128, no. 7, pp. 2657–2669, 2018.

[15] C. N. Serhan, N. Chiang, J. Dalli, and B. D. Levy, "Lipid mediators in the resolution of inflammation," *Cold Spring Harbor Perspectives in Biology*, vol. 7, no. 2, article a016311, 2015.

[16] J. Dalli and C. N. Serhan, "Specific lipid mediator signatures of human phagocytes: microparticles stimulate macrophage efferocytosis and pro-resolving mediators," *Blood*, vol. 120, no. 15, pp. e60–e72, 2012.

[17] C. N. Serhan, R. Yang, K. Martinod et al., "Maresins: novel macrophage mediators with potent antiinflammatory and pro-resolving actions," *The Journal of Experimental Medicine*, vol. 206, no. 1, pp. 15–23, 2009.

[18] A. Chatterjee, A. Sharma, M. Chen, R. Toy, G. Mottola, and M. S. Conte, "The pro-resolving lipid mediator maresin 1 (MaR1) attenuates inflammatory signaling pathways in vascular smooth muscle and endothelial cells," *PLoS One*, vol. 9, no. 11, article e113480, 2014.

[19] J. Gong, H. Liu, J. Wu et al., "Maresin 1 prevents lipopolysaccharide-induced neutrophil survival and accelerates resolution of acute lung injury," *Shock*, vol. 44, no. 4, pp. 371–380, 2015.

[20] C. W. Wang, R. A. Colas, J. Dalli et al., "Maresin 1 biosynthesis and proresolving anti-infective functions with human-localized aggressive periodontitis leukocytes," *Infection and Immunity*, vol. 84, no. 3, pp. 658–665, 2016.

[21] R. Li, Z. Ma, Z. Ma et al., "Maresin 1 mitigates inflammatory response and protects mice from sepsis," *Mediators of Inflammation*, vol. 2016, Article ID 3798465, 9 pages, 2016.

[22] R. Marcon, A. F. Bento, R. C. Dutra, M. A. Bicca, D. F. P. Leite, and J. B. Calixto, "Maresin 1, a proresolving lipid mediator derived from omega-3 polyunsaturated fatty acids, exerts protective actions in murine models of colitis," *Journal of Immunology*, vol. 191, no. 8, pp. 4288–4298, 2013.

[23] Y. H. Han, K. O. Shin, J. Y. Kim et al., "A maresin 1/RORα/12-lipoxygenase autoregulatory circuit prevents inflammation and progression of nonalcoholic steatohepatitis," *The Journal of Clinical Investigation*, vol. 129, no. 4, pp. 1684–1698, 2019.

[24] C. Lv and Q. Jin, "Maresin-1 inhibits oxidative stress and inflammation and promotes apoptosis in a mouse model of caerulein-induced acute pancreatitis," *Medical science monitor: international medical journal of experimental and clinical research*, vol. 25, pp. 8181–8189, 2019.

[25] F. Munir, M. B. Jamshed, N. Shahid, S. A. Muhammad, A. Bhandari, and Q. Y. Zhang, "Protective effects of maresin 1 against inflammation in experimentally induced acute pancreatitis and related lung injury," *American Journal of Physiology. Gastrointestinal and Liver Physiology*, vol. 317, no. 3, pp. G333–G341, 2019.

[26] G. Lu, Y. Pan, A. Kayoumu et al., "Indomethacin inhabits the NLRP3 inflammasome pathway and protects severe acute pancreatitis in mice," *Biochemical and Biophysical Research Communications*, vol. 493, no. 1, pp. 827–832, 2017.

[27] J. Wu, R. Zhang, G. Hu, H. H. Zhu, W. Q. Gao, and J. Xue, "Carbon monoxide impairs CD11b(+)Ly-6C(hi) monocyte migration from the blood to inflamed pancreas via inhibition of the CCL2/CCR2 axis," *Journal of Immunology*, vol. 200, no. 6, pp. 2104–2114, 2018.

[28] M. Sendler, F. U. Weiss, J. Golchert et al., "Cathepsin B-mediated activation of trypsinogen in endocytosing macrophages increases severity of pancreatitis in mice," *Gastroenterology*, vol. 154, no. 3, pp. 704–718.e10, 2018.

[29] R. Kang, M. T. Lotze, H. J. Zeh, T. R. Billiar, and D. Tang, "Cell death and DAMPs in acute pancreatitis," *Molecular Medicine*, vol. 20, no. 1, pp. 466–477, 2014.

[30] J. T. Siveke, C. Lubeseder–Martellato, M. Lee et al., "Notch signaling is required for exocrine regeneration after acute pancreatitis," *Gastroenterology*, vol. 134, no. 2, pp. 544–555.e3, 2008.

[31] R. Talukdar, A. Sareen, H. Zhu et al., "Release of cathepsin B in cytosol causes cell death in acute pancreatitis," *Gastroenterology*, vol. 151, no. 4, pp. 747–758.e5, 2016.

[32] Y. Sakai, A. Masamune, A. Satoh, J. Nishihira, T. Yamagiwa, and T. Shimosegawa, "Macrophage migration inhibitory factor is a critical mediator of severe acute pancreatitis," *Gastroenterology*, vol. 124, no. 3, pp. 725–736, 2003.

[33] J. K. Jadapalli and G. V. Halade, "Unified nexus of macrophages and maresins in cardiac reparative mechanisms," *FASEB Journal : Official Publication of the Federation of American Societies for Experimental Biology*, vol. 32, no. 10, pp. 5227–5237, 2018.

[34] Y. Wang, Y. Xu, P. Zhang et al., "Smiglaside A ameliorates LPS-induced acute lung injury by modulating macrophage polarization via AMPK-PPARγ pathway," *Biochemical Pharmacology*, vol. 156, pp. 385–395, 2018.

[35] Q. Zhao, Y. Wei, S. J. Pandol, L. Li, and A. Habtezion, "STING signaling promotes inflammation in experimental acute pancreatitis," *Gastroenterology*, vol. 154, no. 6, pp. 1822–1835.e2, 2018.

[36] J. Wu, L. Zhang, J. Shi et al., "Macrophage phenotypic switch orchestrates the inflammation and repair/regeneration following acute pancreatitis injury," *eBioMedicine*, vol. 58, p. 102920, 2020.

[37] F. Hu, N. Lou, J. Jiao, F. Guo, H. Xiang, and D. Shang, "Macrophages in pancreatitis: mechanisms and therapeutic potential," *Biomedicine & pharmacotherapy = Biomedecine & pharmacotherapie*, vol. 131, article 110693, 2020.

[38] R. Huang, L. Vi, X. Zong, and G. S. Baht, "Maresin 1 resolves aged-associated macrophage inflammation to improve bone

regeneration," *FASEB Journal : Official Publication of the Federation of American Societies for Experimental Biology*, vol. 34, no. 10, pp. 13521–13532, 2020.

[39] I. Francos-Quijorna, E. Santos-Nogueira, K. Gronert et al., "Maresin 1 promotes inflammatory resolution, neuroprotection, and functional neurological recovery after spinal cord injury," *The Journal of Neuroscience: The Official Journal of the Society for Neuroscience*, vol. 37, no. 48, pp. 11731–11743, 2017.

[40] M. S. Petrov and D. Yadav, "Global epidemiology and holistic prevention of pancreatitis," *Nature Reviews Gastroenterology & Hepatology*, vol. 16, pp. 175–184, 2019.

Hindawi

Review Article

Exploring the Pivotal Immunomodulatory and Anti-Inflammatory Potentials of Glycyrrhizic and Glycyrrhetinic Acids

Seidu A. Richard (ORCID)

Department of Medicine, Princefield University, P. O. Box MA 128, Ho, Ghana

Correspondence should be addressed to Seidu A. Richard; gbepoo@gmail.com

Licorice extract is a Chinese herbal medication most often used as a demulcent or elixir. The extract usually consists of many components but the key ingredients are glycyrrhizic (GL) and glycyrrhetinic acid (GA). GL and GA function as potent antioxidants, anti-inflammatory, antiviral, antitumor agents, and immuneregulators. GL and GA have potent activities against hepatitis A, B, and C viruses, human immunodeficiency virus type 1, vesicular stomatitis virus, herpes simplex virus, influenza A, severe acute respiratory syndrome-related coronavirus, respiratory syncytial virus, vaccinia virus, and arboviruses. Also, GA was observed to be of therapeutic valve in human enterovirus 71, which was recognized as the utmost regular virus responsible for hand, foot, and mouth disease. The anti-inflammatory mechanism of GL and GA is realized via cytokines like interferon-γ, tumor necrotizing factor-α, interleukin- (IL-) 1β, IL-4, IL-5, IL-6, IL-8, IL-10, IL-12, and IL-17. They also modulate anti-inflammatory mechanisms like intercellular cell adhesion molecule 1 and P-selectin, enzymes like inducible nitric oxide synthase (iNOS), and transcription factors such as nuclear factor-kappa B, signal transducer and activator of transcription- (STAT-) 3, and STAT-6. Furthermore, DCs treated with GL were capable of influencing T-cell differentiation toward Th1 subset. Moreover, GA is capable of blocking prostaglandin-E2 synthesis via blockade of cyclooxygenase- (COX-) 2 resulting in concurrent augmentation nitric oxide production through the enhancement of iNOS2 mRNA secretion in Leishmania-infected macrophages. GA is capable of inhibiting toll-like receptors as well as high-mobility group box 1.

1. Introduction

Licorice extract is a Chinese herbal medication most often used as a demulcent or elixir [1]. Glycyrrhizin (GL) is one of the principally effective and efficient ingredients of licorice extract [1–3]. GL is a triterpene saponin which has aglycone component known as glycyrrhetinic acid (GA) [1]. GA is a pentacyclic triterpenoid of oleanene type with a hydroxyl group at C-3, a carboxyl moiety at C-30 as well as a ketone functional group at C-11 [2]. GL and GA have been demonstrated to possess antioxidant properties as well as robust anti-inflammatory, antiviral, antitumor, and immuneregulatory properties [4–6]. GL was capable of triggering the blockade of receptor-mediated endocytosis resulting in the inhibition of viral infiltration into the cells [5, 7].

GL triggers biological activities at the cellular level via novel gbPs, which are responsible for anti-inflammatory and antiviral effects [5, 8]. GL was capable of triggering the production of interferons (IFNs), accelerated the activities of natural killer (NK) cells as well as regulated the growth response of lymphocytes via the acceleration of interleukins- (IL-) 2 production [1, 8, 9]. Furthermore, GL has the ability to modulate the immune response at the initial stage of the disease process via the dendritic cells (DCs) [10]. GA inhibited anti-FAS antibody-triggered mouse liver injury but did not facilitate the upregulation of tumor necrotizing factor-α (TNF-α) messenger RNA (mRNA) secretion in the liver [11].

This review explores the fundamental immune and inflammatory players regulated by GL and GA. The "boolean logic" was utilized to search for the article on the subject matter. Most of the articles were indexed in PubMed with strict inclusion criteria being *in vitro* and *in vivo* up or downregulation of these immune and inflammatory biomarkers in diverse disease conditions. Inflammation, DCs, cyclooxygenase, and prostaglandins, cytokines like ILs, IFNs, TNF-α, nuclear factor-κB (NF-κB), mitogen-activated protein kinase

(MAPK), Toll-like receptors (TLRs), high-mobility group box 1 (HMGB1), and chemokines like CCL11 as known as eotaxin 1 as well as enzymes like nitric oxide were explored.

2. Uses

Glycyrrhizin (GL) obtained from the dried roots of the licorice shrub is very sweet tasting and has been utilized as flavors in diverse food products and treatment of diseases for over 4000 years [12]. Currently, GL is used to flavor consumable products like chocolate, chewing gum, some alcoholic beverages, and cigarettes [12, 13]. Carbenoxolone (GC), the derivative of glycyrrhetinic acid (3β-11-oxoolean-12-en-30-oic acid 3-hemisuccinate), was used to treat peptic ulcer disease, allergic diseases, tumors or cancers, divers' viral diseases, and premenstrual syndromes [4–6]. They possess anti-inflammatory, antioxidant, antihyperglycemic, antilipidemic, and hepatoprotective properties [4–6]. Their key therapeutic usage of GC is for the treatment of viral diseases [14]. Chronic hepatitis C is the current target for use of GC in modern medicine [12, 15].

Several *in vivo* and *in vitro* studies showed that GL and GA have potent activities against hepatitis A, B, and C viruses, human immunodeficiency virus (HIV) type 1, vesicular stomatitis virus, herpes simplex virus, influenza A, severe acute respiratory syndrome- (SARS-) related coronavirus, respiratory syncytial virus, vaccinia virus, and arboviruses [2, 7, 16–20]. Also, GA was observed to be of therapeutic valve in human enterovirus 71, which was recognized as the utmost regular virus responsible for the hand, foot, and mouth diseases [2]. GL and GA demonstrated to have antibacterial actions against gram-positive bacteria like Bacillus subtilis and Staphylococcus aureus as well as gram-negative bacteria like Escherichia coli and Pseudomonas aeruginosa [2, 21, 22]. Furthermore, GA was capable of blocking the survival of methicillin-resistant S. aureus via the attenuation of its virulence gene expression [2, 23]. Also, GA has demonstrated to have antiparasitic potentials and its efficacy as an anti-malarial as well as antileishmanial has been elaborated in experimental studies [2, 24, 25].

3. Pharmacokinetics

GA is rapidly absorbed after oral administration, and its kinetics exhibited a biphasic association with a distribution phase preceded by a slower elimination phase [12, 26]. The medication is usually in a capsule form containing 500 mg of pure GA per capsule [26]. It was established that neither absorption nor elimination of GA was dose-dependent [26]. Several studies detected GA in both rats as well as human plasma [12]. On the other hand, GL is metabolized presystemically via commercial bacteria into GA and totally absorbed into the blood stream after oral intake [12, 27].

Studies have shown that the hydrolysis of GL to GA was carried out by bacteria strains like Eubacterium sp. (strain GHL), Ruminococcus sp. (PO1–3), and Clostridium innocuum (ES2406). These commercial bacteria were isolated from human feces and demonstrated enough hydrolyzing activity for GL [12, 28, 29]. The bacteria strains capable of hydrolyzing GL into GA possess a specific β-glucuronidase, because common β-glucuronidases like Escherichia coli were unable to hydrolyze GL [12, 28]. After hydrolysis of GL into GA, intestinal bacteria convert GA partially into 3-α-18β-GA, through a metabolic intermediary 3-oxo-18β-GA [12, 27].

Also, the plasma clearance of GL after an intravenous bolus dose to rats exhibited a biphasic pattern, in which the distribution phase was preceded by a slower elimination phase [30, 31]. However, realistic plasma levels of GA were observed to be approximately 100 mg/ml after intravenous administration [30, 31]. Also, the distribution of GA to the body tissues was negligible because tissue-to-blood partition coefficients were observed to <1 for all body tissues of rats [12, 32]. Interestingly, the uptake of GL into rat hepatocytes was competitively blocked by GA (46). This means that the plasma to liver transport of GA is facilitated by the same uptake carrier [31].

Studies have demonstrated that habitual usage of GA in consumable products may lead to adverse effects [12, 33]. It was established that capacity-regulated activities facilitate the metabolism, sinusoidal, and canalicular transport of GL [12]. Furthermore, GL was hydrolyzed by glucuronidases into 18-β-GA monoglucuronide in lysozymes of both rodents and humans [12]. This process may ultimately lead to edema, hypertension, and symptoms associated with electrolyte imbalances [12, 34].

4. Inflammation

The fundamental processes involved in the eradication of threats posed to the host to organisms like bacterial and viral infections are the triggering of an acute inflammatory response [35]. Studies have shown that GL was capable of binding directly to lipoxygenase resulting in the generation of inflammatory mediators [36–38]. Also, GL selectively blocked the triggering of phosphorylation of these inflammatory mediators, which are mainly enzymes [36–38]. Specifically, GL as well as its derivatives was capable of blocking the generation of inflammatory chemokines like IL-8 and eotaxin 1, which are both powerful chemo-attractants to leukocytes during inflammation (Figure 1) [36, 39]. GL as well as its derivatives was also capable of neutralizing the secretion of these proinflammatory chemokines [36, 39].

On the other hand, GA was capable of decreasing the secretion of vascular endothelial growth factor (VEGF), inter-cellular cell adhesion molecule 1 (ICAM-1), granulocyte-macrophage colony-stimulating factor (GM-CSF), and human growth-regulated oncogene/keratinocyte chemoattractant (GRO/KC) in alcoholic hepatitis rats' models (Figure 1 and Table 1) [40]. GA was also capable of inhibiting phospholipase A2/arachidonic acid (PLA2/ARA) (Table 1) pathway metabolites, like prostaglandin-E 2 (PGE2) or prostacyclin 2, thromboxane 2 (TXA_2), and leukotriene B4 (LTB4) (Figure 1) [41, 42]. It was stipulated that the anti-inflammatory response to GL and GA was a result of direct binding the molecules to cell membrane constituents like lipocortin I (LC-1) or to enzymes such as PLA2 (Table 1), which is the prime enzyme in the arachidonic acid metabolic
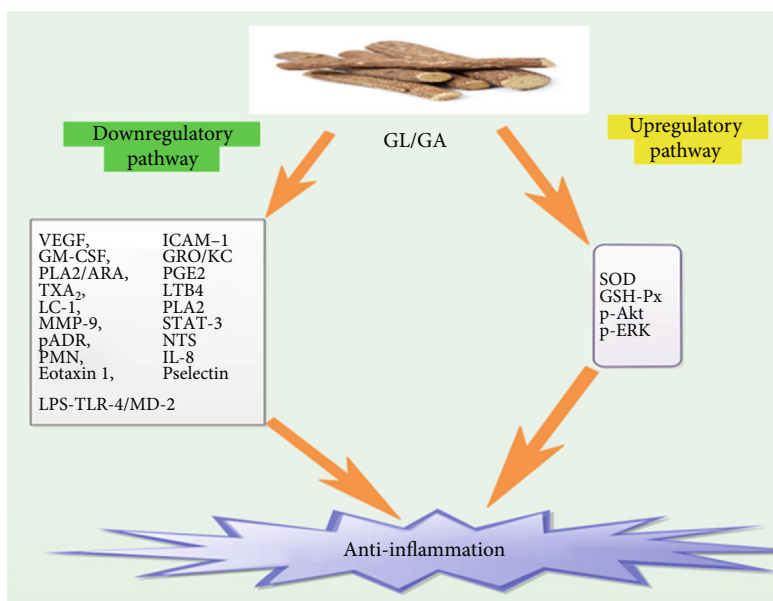
FIGURE 1: Shows a comprehensive down and upregulatory pathways via which GL and GA elicits anti-inflammation.

pathway (Figure 1) [36]. GA ominously decreased the concentration of ICAM-1 as well as matrix metalloproteinase-9 (MMP-9) (Figure 1) [41, 43]. Furthermore, it augmented the actions of Superoxide dismutase (SOD) and glutathione peroxidase (GSH-Px), as well as the secretion of p-Akt and p-ERK (Figure 1) [41, 44].

GL and GA efficiently blocked the generation of free radicals in LPS-treated Raw264.7 macrophage models [41]. They also decreased the configuration of the LPS-TLR-4/MD-2 complexes, leading to the blockade of homodimerization of TLR-4 (Figure 1) [45, 46]. Thus, GA was able to regulate the TLR-4/MD-2 complex at the receptor level, resulting in the inhibition of LPS-induced triggering of signaling cascades as well as cytokine generation [45]. This signifies that GA blocked inflammatory responses as well as regulated innate immune responses [45, 47].

Furthermore, GA inhibited the stimulation of signal transducers and activators of transcription-3 (STAT-3), decreased the upregulation of ICAM-1 as well as P-selectin secretion, decreased the configuration of poly-adenosine diphosphate-ribose (pADR) and nitrotyrosine (NTS), and decreased polymorphonuclear neutrophil infiltration (PMN) (Figure 1 and Table 1) [45–47]. Moreover, GA elicited broad anti-inflammatory actions via its interaction with the lipid bilayer resulting in the decrease of receptor-mediated signaling [45, 46]. GA was capable of blocking the lytic pathway of the complement system as well as averted tissue injury triggered by membrane attack complexes [45].

5. Dendritic Cells

Dendritic cells (DCs) are a group of bone-marrow-derived cells found in blood, tissues, and lymphoid organs [48–50]. These cells initiate and control immune responses that are affected by numerous factors like origin, phenotype, and maturation status [48–50]. Their prime function is to bridge the innate as well as adaptive immune systems [48–50]. DCs were able to accelerate allogeneic T-cell proliferation *in vitro* [4]. A study revealed that only a minute quantity of DCs was enough to trigger an allogeneic mixed lymphocyte reaction (MLR) [4, 48]. Studies have demonstrated that DCs are the most crucial antigen-presenting cells (APCs) associated with the uptake, processing, transport, and presentation of antigens to CD4$^+$ and CD8$^+$ T-cells [4, 49, 51].

Also, DC subsets are capable of triggering or inhibiting immune responses via the secretion of different costimulatory molecules and cytokines [4, 52]. DCs were able to trigger as well as target naive T-cells to differentiate into T-helper (Th)1 or T-helper (Th)2 cells [4, 53]. Thus, DCs have potential immunomodulatory therapeutic targets for some pharmacological compounds [4, 10]. Bordbar et al. demonstrated that DCs treated with GL were capable of influencing T-cell differentiation toward Th1 subset (Figure 2) (Table 1) [4]. Abe et al. also observed the upregulation of IL-10 expression by liver DCs [54]. Hua et al. established that GL was capable of augmenting IL-10 production in DC2.4 cell line (Figure 2) [55]. A current study demonstrated that GL was capable of augmenting IL-10 production along with IFN-γ in MLR [4]. On the other hand, Bhattacharjee et al. exhibited that GA was capable of blocking the expression of the Th2, IL-10, and TGF-β from the splenocytes of infected mice (Figure 2) [25].

6. Nuclear Factor-κB

The nuclear factor-κB (NF-κB) family is made up of five groups such as NF-κB1, which comprise of p50/p105 with p50 as the precursor, NF-κB2 which comprise of p52/p100 with p52 as the precursor, Rel A with p65 as the precursor, Rel B with p68 as the precursor, and c-Rel with p75 as the precursor [56, 57]. Almost all the groupings are capable of

TABLE 1: Shows the explicit effect of GL or GA on various immune/inflammatory factors.

| Immune/inflammatory factors	Type	Effect of GL/GA	Citations
Inflammation	VEGF	Inhibitory	[40]
	ICAM-1	Inhibitory	[40]
	GM-CSF	Inhibitory	[40]
	GRO/KC	Inhibitory	[40]
	PLA2/ARA	Inhibitory	[36, 41, 42]
	MMP-9	Inhibitory	[41, 43]
	STAT-3	Inhibitory	[45–47]
	STAT-6	Inhibitory	[45–47]
	pADR	Inhibitory	[45–47]
	NTS	Inhibitory	[45–47]
	PMN	Inhibitory	[45–47]
	SOD	Facilitatory	[41, 44]
	GSH-Px	Facilitatory	[41, 44]
	TGF-β	Facilitatory	[25]
Dendritic cells (DCs)	T-cell	Facilitatory	[4]
	Th1	Facilitatory	[4]
	Th2	Facilitatory	[25]
Nuclear factor-κB	—	Inhibitory	[6, 20, 62–65]
	IKK	Inhibitory	[56]
Chemokines	CXCL10	Inhibitory	[20, 30, 70, 71]
	CCL5	Inhibitory	[20, 30, 70, 71]
	CCL11	Inhibitory	[39, 76–78]
Interferons	IFN-γ	Facilitatory	[85–89]
Cyclooxygenase	COX-1	—	—
	COX-2	Inhibitory	[25, 65, 98]
Interleukins	IL-1	Inhibitory	[8, 104–106]
	IL-2	Facilitatory	[4, 9, 106]
	IL-3	Inhibitory	[8, 104–106]
	IL-4	Inhibitory	[8, 104–106]
	IL-5	Inhibitory	[8, 104–106]
	IL-6	Inhibitory	[8, 104–106]
	IL-10	Inhibitory	[8, 104–106]
	IL-12	Inhibitory	[4, 8, 104–106]
	IL-13	Inhibitory	[8, 104–106]
	IL-18	Inhibitory	[8, 104–106, 111]
Mitogen-activated protein kinase	—	Inhibitory	[6, 115, 116, 141]
	p38MAPK	Inhibitory	[6, 115, 116]
	ERK	Inhibitory	[45]
	JNK	Inhibitory	
Nitric oxide	iNOS	Inhibitory	[45]
	eNOS	—	—
	nNOS	—	—
Toll-like receptors	TLR-3	Inhibitory	[131–134]
	TLR-4	Inhibitory	[131–134, 141]
	TLR-7	Inhibitory	[131–134]
	TLR-9	Inhibitory	[131–134]
	TLR-10	Inhibitory	[131–134]
High-mobility group box 1	—	Inhibitory	[141, 142]
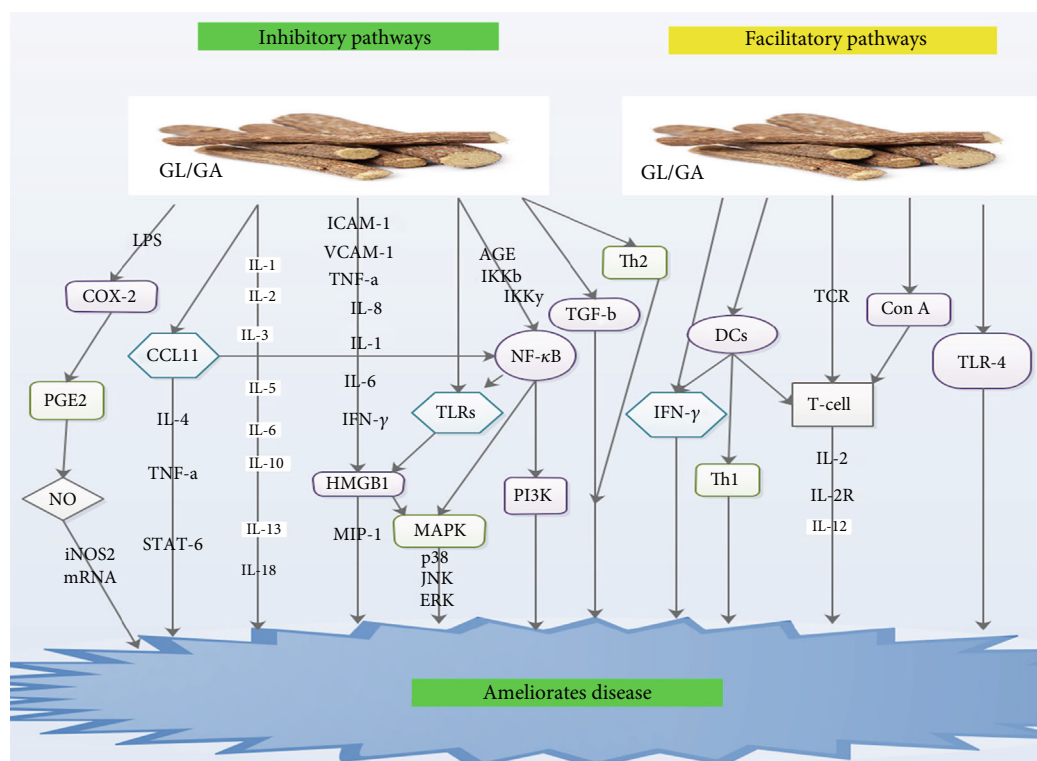
Figure 2: Shows the inhibitory and facilitatory pathways via which GL and GA ameliorate disease.

preserving homodimeric as well as heterodimeric complexes [56]. Nevertheless, the most predominant-stimulated form of NF-κB is the heterodimer p50-p65, which has the transactivity territory obligatory for gene modification [58–60]. In most cells, NF-κB exists as a latent, inactive, IκB bound complex in the cytoplasm [56]. Nevertheless, upon stimulation by extracellular stimuli, NF-κB promptly translocates to the nucleus and triggers gene release [56, 61].

IκB kinase (IKK) is a large multisubunit protein kinase active via numerous signal pathways [56]. The IKK complex when triggered results in the phosphorylation or degradation of IκBα leading to the expression of NF-κB [56]. NF-κB then translocates to the nucleus and triggers the transcription of numerous κB-dependent genes, such as iNOS as well as Th1 cytokines [56]. Thus, some pathogens are capable of blocking the action of NF-κB via the inhibition of the degradation of IκB during infection [56]. Also, in macrophages, the MAPK cascade and the NF-κB pathway are the key pathways via which modulation of inflammation as well as host defense occurs [56].

Ukil et al. demonstrated that the kinase properties of IKK were triggered in cells that were stimulated with GA via a mechanism that most probably involves upregulatory signaling pathways [56]. They however did not observe any influence of GA on IKK activity when GA was added directly to the assay mixture containing IKK immunoprecipitated from normal macrophages (Table 1) [56]. An earlier study revealed that GA influenced the inhibitory interaction between NF-κB, which is a fundamental modifier to IKKβ and IKKγ (Figure 2) [62]. Another study indicated that GA inhibited one of the essential upregulatory kinases like

NF-κB-inducing kinase, PI3K, or MAPK in the signaling pathway (Figure 2) [63].

GL was capable of treating coxsackievirus B3- (CVB3-) triggered myocarditis via the blockade of CVB3-triggered NF-κB activity via the inhibition of NF-κB inhibitor IκB (Table 1) [20, 64]. Wang and Du revealed that pretreatment with GL substantially inhibited the facilitation of NF-κB p65 protein secretion, in methotrexate-stimulated enteritis (Table 1) [6]. Cherng et al. showed that GL blocked NF-κB secretion, averted DNA damage, and accelerated DNA repair (Table 1) [65]. Feng et al. demonstrated that GA safeguards advanced glycation end-product- (AGE-) stimulated endothelial dysfunction via blockade of the receptor for AGE/NF-κB signaling pathway (Figure 2 and Table 1) [66].

7. Chemokines

Chemokines are a family of molecules associated with the trafficking of leukocytes in normal immune surveillance and recruitment of inflammatory cells in host defense [67–69]. They are made up of over 40 groups, which are classified into four classes founded on the sites of essential cysteine residues like C, CC, CXC, and CX3C [67]. GL was capable of subduing the H5N1-triggered generation of CXCL10, and CCL5 resulting in the blockade of H5N1-triggered apoptosis [20, 70]. Michaelis et al. demonstrated that 100 mg/ml of GA drastically blocked secretion of CXCL10, and CCL5 at the mRNA and the protein levels (Table 1) [30]. Augmented CXCL10 levels were observed in patients with H5N1, and the elevated levels of CXCL10 were associated with poor prognosis (Table 1) [30, 71].

CCL11 known as eotaxin 1 was primarily detected as the prime eosinophil chemoattractant in the lung lavage fluid after allergic exposure in guinea pigs [39]. Subsequently, it was cloned for further studies [39, 72, 73]. Several studies have demonstrated that numerous types of cells, such as lung or dermal fibroblasts, as well as lung or bronchial epithelial cells are capable of producing eotaxin 1 [39, 74, 75]. Studies further revealed that the production of eotaxin 1 was triggered by IL-4 and inhibited by IFN-γ [39, 74, 75]. It was also observed that eotaxin 1 facilitated the infiltration of eosinophils into allergic inflammatory sites [39, 74, 75].

Matsui et al. indicated that GL may be capable of modulating chemokine generation via the posttranscriptional level such as protein expression or mortification [39]. They demonstrated that GL derivatives had inhibitory effects on eotaxin 1 generation via TNF-α as well as IL-4 induction in lung fibroblasts (Figure 2) [39]. Studies have shown that induction of IL-4 and TNF-α in combination synergistically accelerated the generation of eotaxin 1 via the triggering of transcriptional factors like STAT-6 and NF-κB (Figure 2) [76–78]. GL and its derivatives thus blocked eotaxin 1 production at protein or mRNA secretary levels (Table 1) [39, 76].

8. Interferons

Interferons (IFNs) are a family of broad-spectrum antiviral glycoproteins expressed by cells upon attack by viruses. They are often involved in numerous immune responses as triggers, modulators, and effectors of both innate as well as adaptive immune systems during viral infections [79, 80]. They have the ability of blocking viral replication and are often the most prominent cytokines produced during viral infections [79, 80]. IFN-γ, which is expressed by lymphocytes, has been implicated in the secretion of histocompatibility antigen as well as immune modifications [6, 81]. Studies have demonstrated that IFN-γ was capable of facilitating the endotoxin-stimulated generation of NO in murine macrophages [79, 80].

Studies have shown that IFN with or without adenine arabinoside was capable of curing hepatitis B patients [1, 82, 83]. IFNs were capable of reducing the level of either DNA polymerase or hepatitis B surface antigen in hepatitis patients [1, 84]. Furthermore, GL was capable of facilitating IFN-γ production in human T-lymphocytes [85, 86]. Also, GL was capable of inducing the production of IFN in mice, which was preceded by stimulation of macrophages as well as the increase of NK activity [87, 88]. Bhattacharjee et al. demonstrated that splenic expression of IFN-γ, TNF-α, and IL-12 elevated after GA treatment. Wu et al. also demonstrated that GL drastically decreased inflammatory via IFN-γ (Figure 2) [89]. They concluded that blockade of the IFN-γ signaling pathway may be linked to anti-inflammatory effects of GL in enteritis [89].

9. Cyclooxygenase and Prostaglandins

COX-1 and COX-2 are the main cyclooxygenase (COX) isoenzymes, which catalyze the formation of prostaglandins, thromboxane, and levuloglandins [90]. Prostaglandins are autocoid facilitators that influence practically all recognized physiological as well as pathological activities via their reversible communication with G-protein attached membrane receptors [90]. Amongst the COX isoenzymes, COX-2 was more inducible with low secretory levels in most tissues under normal circumstances [6, 91]. It was established that numerous cell types such as vascular smooth muscle cells, endothelial cells, mononuclear macrophages, and fibroblasts were capable of secreting COX-2 up to about 8-10-fold the normal level when stimulated by proinflammatory cytokines [6, 92].

It was further observed that augmentation of COX-2 levels resulted in the generation as well as buildup of prostaglandin inflammatory factors, facilitating inflammatory responses as well as tissue damage [6, 91]. Studies have shown that oversecretion of COX-2 facilitated cell proliferation, blocked apoptosis, and blocked immune responses, resulting in abnormal modulation of the balance between proliferation and apoptosis [6, 91, 92]. Bhattacharjee et al. demonstrated that a robust antileishmanial protection was observed via the modulation of macrophage-secreted COX-2-determined PGE2 levels [25]. Also, Leishmania organisms were capable of using immune modulators like TGF-β, IL-4, and arachidonic acid metabolites to inhibit macrophage functions and facilitated the organism's survival within the host [93].

PGE2 biosynthesis comprises two successive enzymatic reactions [25]. The first one is a rate-limiting step involving the COX enzyme, while the second is a precise PGE synthesis step [25]. In pathophysiological processes, the inducible isoform of COX-2 was capable of modulating PGE2 production while COX-1 was principally copied [25, 94, 95]. Studies have shown that augmented level PGE2 was capable of modulating several immune responses via mechanisms involving the blockade of Th1 cytokines like IL-2, IL-12, and IFN-γ, as well as inhibition of phagocytosis and lymphocyte proliferation [25, 96, 97]. Thus, PGE2 ability to modulated immune response is champion by Th1- or Th2-associated lymphokines [25, 96].

It was established that GA was capable of blocking PGE2 synthesis via blockade of COX-2 resulting in concurrent augmentation NO production through enhancement of iNOS2 mRNA secretion in Leishmania-infected macrophages (Figure 2 and (Table 1) [25]. Wang and Du demonstrated that pretreatment with GL significantly blocked the facilitation of COX-2 activity in methotrexate-triggered enteritis [6]. Cherng et al. also demonstrated that GL was able to block COX-2 secretion, inhibited DNA damage, and promoted DNA repair (Table 1) [65]. Ni et al. observed an upsurge in COX-2 secretion in lung tissues after introducing LPS in their experiment, which was subsequently decreased in a dose-dependent manner after GL pretreatment (Figure 2 and Table 1) [98].

10. Interleukins

Interleukin belongs to a group of cytokines, which are perhaps the most essential messenger molecules generated

by leukocytes to modulate the biological activities of target cells via autocrine or paracrine means [99]. Several groupings of ILs have been identified [99]. Notable amongst them are IL-1, IL-2, IL-3, IL-5, IL-6, IL-10, IL-12, IL-13, and so many others [3, 8, 99–101]. Although most of the ILs are influenced by GL and GA, IL-12 is the most influential. IL-12 is a heterodimeric cytokine produced primarily by macrophages and monocytes [8]. Its key function is the modulation of cytokines as well as T-cell subsets [8]. A study revealed that a deficiency in endogenous IL-12 production influenced the progression of immunodeficiency in HIV-infected patients [8, 102]. Studies have proven that IL-12 salvaged numerous activities of cells infected with HIV [8, 103].

Several studies have demonstrated that IL-12 was capable of influencing T-cells and natural NK cells resulting in cell proliferation, cytolytic activities, and triggering of IFN-γ [8, 104]. Studies further revealed that the polarization of the T helper response to a Th1-dominant form via IL-12 was accelerated by IFN-γ resulting in the blockade of IL-4 production [8, 100, 101]. GA was capable of blocking IL-1β, IL-3, IL-5, IL-6, IL-10, IL-12 subtypes, IL-13 (Figure 2), eotaxin, and TNF-α expression (Table 1) [8, 104–106]. GL was also capable of accelerating the proliferation of lymphocytes and acted as a facilitator of the late signal transduction of T lymphocytes for IL-2 generation (Table 1) [4, 106].

Zhang et al. also indicated that GL facilitated TCR-mediated T-cell proliferation by selectively influencing the late signal transduction for IL-2 generation as well as IL-2R secretion [9]. They further indicated that GL exhibited two separate activities on immature thymocytes resulting in the facilitation of IL-2 generation on one hand and blocked growth response on the other [9, 107]. A hepatitis study revealed that IL-4 was capable of stimulating STAT6, which in turn stimulated eotaxin secretion as well as triggered IL-5 secretion [40, 108]. Wang and Du established that GA was capable of relieving methotrexate-stimulated upsurge of TNF-α, IL-1β, and IL-6 levels, as well as elevated IL-10 levels, in rats with enteritis (Table 1) [6]. GL was able to facilitate the IL-10 production by hepatic dendritic cells in mice with hepatitis (Table 1) [76].

Studies have proven that IL-10 is a well-known anti-inflammatory cytokine [40, 109, 110]. It was capable of modulating STAT3 in hepatocytes as well as macrophages/Kupffer cells [40, 109, 110]. A study revealed that GA was capable of accelerating LPS-triggered IL-12 generation by peritoneal macrophages (Table 1) [4, 8]. Its optimal effect on IL-12 gene secretion was linked to an upsurge in NF-κB modulation [4, 8]. Dai et al. demonstrated that GL accelerated both IL-12 mRNA buildup as well as protein expression by peritoneal macrophages in response to LPS [8]. They indicated that the priming influence of GL on IL-12 generation did not depend on IFN-γ or GM-CSF [8]. Thus, they also affirmed that the facilitation of IL-12 p40 mRNA secretion by GL may be via the modulation of NF-κB [8].

Yoshida et al. demonstrated that GL was able to block the upsurge in serum levels of IL-18 in LPS/D-galactosamine-induced liver injury (Figure 2 and Table 1) [111]. Thus, GL blocked the generation of IL-18 in this model [111]. They also observed fewer IL-18-positive infiltrating cells after the

introduction of GL [111]. Also, GL was capable of blocking the infiltration of neutrophils and macrophages in liver injury [111]. Furthermore, GL-stimulated decrease in immunoreactive IL-18 was probably due to blockade of cell infiltration in the liver [111]. GL was able to inhibit an upsurge in alanine aminotransferase activity when exogenous IL-18 was administered in mice treated with LPS/D-galactosamine [111]. Thus, GL blocked IL-18-mediated inflammatory response in the pathogenesis of liver injury [111]. Nakanishi et al. demonstrated that IL-18 was capable of triggering gene secretion as well as the synthesis of TNF-α, IL-1, FAS ligand, and many chemokines [112].

11. Mitogen-Activated Protein Kinase

Mitogen-activated protein kinase (MAPK) signal transduction pathways are linked with cell proliferation, differentiation, apoptosis, and angiogenesis [6]. Specifically, the p38 mitogen-activated protein kinase (p38MAPK) signal transduction pathway modulates stress responses, like inflammation as well as apoptosis [6, 113]. Studies have shown that LPS as well as other factors is capable of triggering the MAPK pathways resulting in the secretion of many inflammatory mediators via complex signal conduction pathways, which facilitates inflammation [6]. Furthermore, the modulation of p38MAPK was observed in various transduction pathways, which in turn stimulated many transcription factors as well as mediated a variety of biological activities [6, 114].

Wang and Du demonstrated that pretreatment with GA remarkably inhibited the facilitation of p38MAPK in methotrexate-stimulated enteritis (Table 1) [6]. They concluded that the anti-inflammatory actions of GA were probably linked to p38MAPK signaling (Figure 2) [6]. Also, studies have shown that GA lessens glycative stress in the kidneys of diabetic mice via the blockade of p-p38MAPK [115, 116]. It was further established that GA was capable of blocking the modulation of JNK, p38 protein, and ERK (Figure 2 and Table 1) in bone marrow-derived macrophages (BMMs) [45].

12. Nitric Oxide

Nitric oxide (NO) is a radical messenger molecule generated by the enzyme nitric oxide synthase (NOS) [117–119]. So far, only three isoforms of NOS have been identified. Amongst the three, only two of them, NOS in neurons (nNOS) and in the endothelial cells of blood vessels (eNOS), are intensely secreted [117–120]. These two are capable of producing only minute quantities of NO, which is sufficient to trigger cellular signaling in stress conditions.

Studies have shown that NO in an inflammatory mediator is capable of modulating innate immunity as well as pathophysiology of many infectious diseases [117, 121, 122]. The third kind of NOS is the inducible nitric oxide synthase (iNOS) [117, 119].

Studies have further proven that iNOS generates NO in hepatocytes as well as macrophages [117, 119, 121, 122]. The stimulation of iNOS is modulated via a posttranscriptional mechanism that is mediated by antisense transcripts

(asRNAs) [117, 122]. Several studies have shown that the asRNAs are transcribed from the iNOS gene and interact with iNOS mRNA to stabilize the same iNOS mRNA [122, 123]. Studies have demonstrated that the iNOS is triggered by cytokines like IFN-γ and TNF-α, which in turn produce large quantities of NO [117, 119, 121, 123]. It is well proven that NO generated by iNOS was capable of triggering an inflammatory liver damage [117, 124].

Studies have demonstrated that concanavalin A (Con A) was capable of triggering the stimulating the T-cells in mice and induced the secretion of proinflammatory cytokines associated with the progression of hepatitis (Figure 2) [119, 125]. Furthermore, GL was capable of inhibiting Con A-stimulated mouse liver damage without influencing the generation of IFN-γ and TNF-α [119, 126]. Tsuruoka et al. demonstrated that GL blockade of liver damage was via the inhibition of iNOS mRNA as well as its protein secretion (Table 1) [119]. Thus, GL inhibited iNOS mRNA and protein in Con A-stimulated hepatitis [119]. Also, GL was capable of blocking the secretion of iNOS mRNA stimulated by carbon tetrachloride in hepatic tissue (Table 1) [119, 127].

13. Toll-Like Receptors

Toll-like receptors (TLRs) are sensors for pathogen-associated molecular patterns (PAMPs) [128]. TLRs are capable of modulating several immune responses, especially during the infectious process [128]. Several studies have shown that the secretion of TLR-3, TLR-4, TLR-7, TLR-9, and TLR-10 genes from hepatic tissue was upregulated in some viral infection models [129, 130], and GA or GL is capable of inhibiting these receptors (Table 1) [131–134]. It was established that the TLR-4 pathway comprises of two dissimilar signaling pathways such as the myeloid differentiating primary response gene 88- (MyD88-) dependent as well as the MyD88-independent pathway [135, 136]. It was further revealed that stimulation of the MyD88-dependent pathway led to the generation of proinflammatory cytokines via triggering of NF-κB, while the stimulation MyD88-independent pathway led to the generation of type 1 IFNs [135, 136].

A study revealed that TLR-4 was the fundamental receptor of the innate immune signaling responses to influenza virus as well as other respiratory viruses [137]. Several studies have shown that the TLR-4 was more associated with respiratory syncytial virus and human papillomavirus infections [129, 138, 139]. Shi et al. revealed that TLR-4 gene deficiency was not associated with the downregulation of virus titer in the liver during MHV-A59 infection [129]. They observed that in MHV-A59 infection, the HMGB1-TLR-4 axis utilizes proinflammatory activities without directly influencing virus replication [129].

A study demonstrated that GA was not capable of influencing TLR-4 gene secretion during viral infection [129]. Nevertheless, the secretion of the TLR-4 gene facilitated MHV-stimulated hepatic inflammation injury as well as determined HMGB1 secretory levels in the serum (Figure 2) [129]. Several studies have proven that pretreatment with a TLR-4 inhibition agent reduced the HMGB1 levels from virus-infected cells via the TLR4-NF-κB path-

way (Figure 2) [129, 139, 140]. Studies further revealed that the inactivation of NF-κB led to a reduced expression of different proinflammatory cytokines like IL-1β, IL-6, TNF-α, and HMGB1 (Figure 2) [129, 139, 140]. GL was capable of blocking porcine epidemic diarrhea virus infection, as well as reduced proinflammatory cytokine expression via the HMGB1/TLR4-p38MAPK pathway (Figure 2 and Table 1) [141].

14. High-Mobility Group Box 1

High-mobility group box 1 (HMGB1) protein is a nuclear protein that functions as an architectural chromatin-binding factor [142, 143]. HMGB1 is the prime signal during tissue damage usually involving necrotic and apoptotic cells [142]. Furthermore, HMGB1 performs dual functions in the nucleus and the cytoplasm [142]. Also, extracellular HMGB1 facilitates both local as well as systemic responses in the organism [142]. These responses often include inflammation, modulation of innate as well as adaptive immunity [142, 143]. Several studies have demonstrated that HMGB1 is secreted by monocytes, macrophages, neutrophils, platelets, and dendritic and NK cells [142, 144].

Several studies have shown that HMGB1 induces macrophages, monocytes, and neutrophils to secrete proinflammatory cytokines like TNF-α, IL-1, IL-6, IL-8, and MIP-1 via p38- and JNK MAPK-dependent pathways (Figure 2) [145, 146]. It was established that HMGB1 was passively secreted by damage alveolar endothelial cells or macrophages during virus-mediated cytolysis [145]. Once expressed, extracellular HMGB1 was capable of mediating injurious pulmonary inflammatory response like neutrophil infiltration, derangement of epithelial barrier, lung edema, and lung injury [145, 147]. These injurious pulmonary inflammatory responses subsequently result in respiratory failure as well as death [147].

Also, human microvascular endothelial cells are capable of secreting ICAM-1, vascular adhesion molecule–1 (VCAM-1), proinflammatory cytokines like TNFα, IL-8, and chemokines in response to HMGB1 activation (Figure 2) [145, 148]. This means that HMGB1 was capable of disseminating inflammatory response in the endothelium during infection or injury [145]. Chemotactic as well as mitogenic actions of HMGB1 depends on its association with the receptor of advanced glycation end products (RAGE) [142, 149]. GL was capable of blocking the chemoattractant as well as mitogenic activities of HMGB1 (Table 1) [142].

GL was capable of binding to both HMG boxes of HMGB1 in both NMR and fluorescence studies without altering their secondary structure, which was observed as an absence of changes in CD spectra [142]. It was further established that amino acids interacting with GL clusters at the junction of both arms of the classical L-shape fold of both HMG boxes in chemical-shift perturbation experiments [142]. Furthermore, the binding sites for GL on the HMG boxes partly overlap with the DNA binding sites, shielding residues like R23, which is recognized to be crucial for DNA binding [142, 150]. Nevertheless, the RAGE-binding surface on HMGB1 was characterized with the stretch of

basic amino acids between box B and the acidic tail and did not match with the binding surfaces of GL [142, 149].

Influenza type A, B, and C viruses are responsible for influenza infection ("flu") [145]. This infection is often depicted with massive virus replication as well as excessive inflammation [145]. Studies have shown that influenza viruses are capable of infecting monocytes and macrophages resulting in the stimulation of proinflammatory cytokines like TNF-α, IL-1, IL-6, IL-8, IFN-α, and chemokines in infected areas (Figure 2) [145, 151]. Moisy et al. demonstrated that HMGB1 binds to the nucleoprotein section of influenza ribonucleoproteins (vRNPs) freely in the company of viral RNA *in vitro* and interacts with the viral nucleoprotein VCAM-1 in infected cells [152]. They revealed that HMGB1 was capable of facilitating viral growth as well as augmented the transcription or replication activity of the viral polymerase in HMGB1-depleted cells [152]. Thus, HMGB1 binding to DNA was a prerequisite for the augmentation of influenza virus replication [152]. Therefore, GA and GL may be capable of treating influenza viral infection via the HMGB1-TNF-α pathway (Figure 2). Further studies should focus on this pathway.

HMGB1 was able to trigger necrotic cell death resulting in abundant budding of West Nile (WN) progeny virus particles at higher infectious doses [145, 153]. Furthermore, HMGB1 mediated in injurious inflammatory response resulting in the pathogenesis of WN encephalitis [145, 153, 154]. Besides WN viruses, other viruses like the salmon anemia virus were capable of triggering necrotic cell death of infected cells, leading to simultaneous HMGB1 expression [145, 154]. GL and GA may be potential treatment options for WN viral via HMGB1. Further studies are warranted in this direction.

Studies have shown that an increase in proinflammatory cytokines like IL-1, IL-6, TNF-α, and IFN-γ may trigger the expression of HMGB1 from innate immune cells in SARS patients (Figure 2) [145, 155]. Thus, further studies on GL/GA-HMGB1 axis are needed to elucidate their potential role in the treatment for patients with coronavirus disease-19 in the current SARS-coronavirus pandemic. Acute viral hepatitis is caused by hepatitis A, B, C, and D viruses. Their pathogenesis is often depicted with acute necrosis of hepatocytes, inflammation, and followed by fibrosis as well as cirrhosis [145, 156]. HMGB1, passively secreted by necrotic hepatocytes, may stimulate tissue macrophages especially Kupffer cells to express proinflammatory cytokines during an acute infection [145]. Thus, HMGB1 alone or in combination with other proinflammatory cytokines may cause chronic liver damage in hepatitis patients [145]. GL and GA are potential treatment options for chronic viral hepatitis. Further studies are warranted on HMGB1 and/or GL/GA axis.

15. Conclusion

GL and GA are able to block the secretion of IL-1β, IL-3, IL-4, IL-5, IL-6, IL-10, IL-12, IL-13, eotaxin, and TNF-α expression. This means that GL and GA are capable of inhibiting cytokine storms elicited during various infectious diseases most especially viral diseases. GL and GA drastically decreased

inflammation via IFN-γ, which means that GL and GA have very crucial antiviral properties. Also, GA decreased the secretion of VEGF, MCP-1, GM-CSF, and GRO/KC in alcoholic hepatitis rats' models. GA was capable of blocking the modulation of JNK, p38 protein, and ERK in BMMs. Further studies on GL/GA-HMGB1 axis are needed to elucidate their potential role in the treatment for patients with coronavirus disease-19 in the current SARS-coronavirus pandemic.

Abbreviations

asRNAs:	Antisense transcripts
APCs:	Antigen-presenting cells
BMMs:	Bone marrow-derived macrophages
COX:	Cyclooxygenase
GC:	Carbenoxolone
CVB3:	Coxsackievirus B3
Con A:	Concanavalin A
DCs:	Dendritic cells
GM-CSF:	Granulocyte-macrophage colony-stimulating factor
GL:	Glycyrrhizin
GA:	Glycyrrhetinic acid
HMGB1:	High-mobility group box 1
GRO/KC:	Human growth-regulated oncogene/keratinocyte chemoattractant
HIV:	Human immunodeficiency virus
ICAM-1:	Intercellular cell adhesion molecule 1
IKK:	IκB kinase
IFNs:	Interferons
IL:	Interleukin
iNOS:	Inducible nitric oxide synthase
MAPK:	Mitogen-activated protein kinase
p38MAPK:	p38 mitogen-activated protein kinase
MLR:	Mixed lymphocyte reaction
mRNA:	Messenger RNA
NK:	Natural killer
NO:	Nitric oxide
NF-κB:	Nuclear factor-κB
NTS:	Nitrotyrosine
PLA2:	Phospholipase A2
pADR:	Poly-adenosine diphosphate-ribose
PMN:	Polymorphonuclear neutrophil infiltration
TNF-α:	Tumor necrotizing factor-α
PGE2:	Prostaglandin-E 2
vRNPs:	Ribonucleoproteins
TLRs:	Toll-like receptors
Th:	T-helper
SARS:	Severe acute respiratory syndrome
STAT:	Signal transducer and activator of transcription
VCAM-1:	Vascular adhesion molecule–1
VEGF:	Vascular endothelial growth factor
WN:	West Nile.

Data Availability

No data was used in this paper.

Conflicts of Interest

The authors declare that they have no conflicts of interest.

References

[1] N. Abe, T. Ebina, and N. Ishida, "Interferon induction by glycyrrhizin and glycyrrhetinic acid in mice," *Microbiology and Immunology*, vol. 26, no. 6, pp. 535–539, 1982.

[2] D. Langer, B. Czarczynska-Goslinska, and T. Goslinski, "Glycyrrhetinic acid and its derivatives in infectious diseases," *Current Issues in Pharmacy and Medical Sciences*, vol. 29, no. 3, pp. 118–123, 2016.

[3] F. Maione, P. Minosi, A. di Giannuario et al., "Long-lasting anti-inflammatory and antinociceptive effects of acute ammonium glycyrrhizinate administration: pharmacological, biochemical, and docking studies," *Molecules*, vol. 24, no. 13, p. 2453, 2019.

[4] N. Bordbar, M. H. Karimi, and Z. Amirghofran, "The effect of glycyrrhizin on maturation and T cell stimulating activity of dendritic cells," *Cellular Immunology*, vol. 280, no. 1, pp. 44–49, 2012.

[5] F. Shamsa, K. Ohtsuki, E. Hasanzadeh, and S. Rezazadeh, "The anti-inflammatory and anti-viral effects of an ethnic medicine: glycyrrhizin," *Journal of Medicinal Plants*, vol. 9, no. 33, pp. 1–28, 2010.

[6] Y. M. Wang and G. Q. Du, "Glycyrrhizic acid prevents enteritis through reduction of NF-κB p65 and p38MAPK expression in rat," *Molecular Medicine Reports*, vol. 13, no. 4, pp. 3639–3646, 2016.

[7] J.-M. Crance, F. Lévêque, E. Biziagos, H. van Cuyck-Gandré, A. Jouan, and R. Deloince, "Studies on mechanism of action of glycyrrhizin against hepatitis A virus replication in vitro," *Antiviral Research*, vol. 23, no. 1, pp. 63–76, 1994.

[8] J. H. Dai, Y. Iwatani, T. Ishida et al., "Glycyrrhizin enhances interleukin-12 production in peritoneal macrophages," *Immunology*, vol. 103, no. 2, pp. 235–243, 2001.

[9] Y. Zhang, K. Isobe, F. Nagase et al., "Glycyrrhizin as a promoter of the late signal transduction for interleukin-2 production by splenic lymphocytes," *Immunology*, vol. 79, no. 4, p. 528, 1993.

[10] X. Chen, L. Yang, O. Howard, and J. J. Oppenheim, "Dendritic cells as a pharmacological target of traditional Chinese medicine," *Cellular & Molecular Immunology*, vol. 3, no. 6, pp. 401–410, 2006.

[11] T. Okamoto, "The protective effect of glycyrrhizin on anti-Fas antibody-induced hepatitis in mice," *European Journal of Pharmacology*, vol. 387, no. 2, pp. 229–232, 2000.

[12] B. Ploeger, T. Mensinga, A. Sips, W. Seinen, J. Meulenbelt, and J. DeJongh, "The pharmacokinetics of glycyrrhizic acid evaluated by physiologically based pharmacokinetic modeling," *Drug Metabolism Reviews*, vol. 33, no. 2, pp. 125–147, 2001.

[13] G. Fenwick, J. Lutomski, and C. Nieman, "Liquorice, Glycyrrhiza glabra L. –Composition, uses and analysis," *Food Chemistry*, vol. 38, no. 2, pp. 119–143, 1990.

[14] L. J. Ming and A. C. Y. Yin, "Therapeutic effects of glycyrrhizic acid," *Natural Product Communications*, vol. 8, no. 3, article 1934578X1300800335, 2013.

[15] T. V. Rossum, Vulto, R. A. D. Man, Brouwer, and Schalm, "Glycyrrhizin as a potential treatment for chronic hepatitis C," *Alimentary Pharmacology & Therapeutics*, vol. 12, no. 3, pp. 199–205, 1998.

[16] U. A. Ashfaq, M. S. Masoud, Z. Nawaz, and S. Riazuddin, "Glycyrrhizin as antiviral agent against hepatitis C virus," *Journal of Translational Medicine*, vol. 9, no. 1, article 800, pp. 1–7, 2011.

[17] L. Baltina, R. Kondratenko, L. A. Baltina Jr., O. A. Plyasunova, A. G. Pokrovskii, and G. A. Tolstikov, "Prospects for the creation of new antiviral drugs based on glycyrrhizic acid and its derivatives (a review)," *Pharmaceutical Chemistry Journal*, vol. 43, no. 10, article 348, pp. 539–548, 2009.

[18] C. Fiore, M. Eisenhut, R. Krausse et al., "Antiviral effects of Glycyrrhiza species," *Phytotherapy Research*, vol. 22, no. 2, pp. 141–148, 2008.

[19] S. Harada, T. Maekawa, E. Haneda, Y. Morikawa, N. Nagata, and K. Ohtsuki, "Biochemical characterization of recombinant HIV-1 reverse transcriptase (rRT) as a glycyrrhizin-binding protein and the CK-II-mediated stimulation of rRT activity potently inhibited by glycyrrhetinic acid derivative," *Biological and Pharmaceutical Bulletin*, vol. 21, no. 12, pp. 1282–1285, 1998.

[20] L. Wang, R. Yang, B. Yuan, Y. Liu, and C. Liu, "The antiviral and antimicrobial activities of licorice, a widely-used Chinese herb," *Acta Pharmaceutica Sinica B*, vol. 5, no. 4, pp. 310–315, 2011.

[21] M. H. Salari, S. Eshraghi, and M. Noroozi, "Antibacterial effect of glycyrrhetinic acid on 55 hospital strains of staphylococcus aureus and 32 actinobacillus actinomycetemcomitans," *DARU Journal of Pharmaceutical Sciences*, vol. 9, no. 3-4, pp. 37–39, 2001.

[22] M. M. Nitalikar, K. C. Munde, B. V. Dhore, and S. N. Shikalgar, "Studies of antibacterial activities of Glycyrrhiza glabra root extract," *International Journal of PharmTech Research*, vol. 2, no. 1, pp. 899–901, 2010.

[23] M. Salari and Z. Kadkhoda, "In vitro antibacterial effects of glycyrrhetinic acid on periodontopathogenic and capnophilic bacteria isolated from adult periodontitis," *Clinical Microbiology and Infection*, vol. 9, no. 9, pp. 987-988, 2003.

[24] I. A. Rodrigues, A. M. Mazotto, V. Cardoso et al., "Natural products: insights into leishmaniasis inflammatory response," *Mediators of Inflammation*, vol. 2015, Article ID 835910, 12 pages, 2015.

[25] S. Bhattacharjee, A. Bhattacharjee, S. Majumder, S. B. Majumdar, and S. Majumdar, "Glycyrrhizic acid suppresses Cox-2-mediated anti-inflammatory responses during Leishmania donovani infection," *Journal of Antimicrobial Chemotherapy*, vol. 67, no. 8, pp. 1905–1914, 2012.

[26] S. Krähenbühl, F. Hasler, B. M. Frey, F. J. Frey, R. Brenneisen, and R. Krapf, "Kinetics and dynamics of orally administered 18 beta-glycyrrhetinic acid in humans," *The Journal of Clinical Endocrinology & Metabolism*, vol. 78, no. 3, pp. 581–585, 1994.

[27] T. Akao, "Localization of enzymes involved in metabolism of glycyrrhizin in contents of rat gastrointestinal tract," *Biological and Pharmaceutical Bulletin*, vol. 20, no. 2, pp. 122–126, 1997.

[28] T. Akao, T. Akao, and K. Kobashi, "Glycyrrhizin β-D-glucuronidase of Eubacterium sp. from human intestinal flora," *Chemical and Pharmaceutical Bulletin*, vol. 35, no. 2, pp. 705–710, 1987.

[29] M. Hattori, T. Sakamoto, K. Kobashi, and T. Namba, "Metabolism of glycyrrhizin by human intestinal flora," *Planta Medica*, vol. 48, no. 5, pp. 38–42, 1983.

[30] M. Michaelis, J. Geiler, P. Naczk et al., "Glycyrrhizin inhibits highly pathogenic H5N1 influenza A virus-induced pro-inflammatory cytokine and chemokine expression in human macrophages," *Medical Microbiology and Immunology*, vol. 199, no. 4, pp. 291–297, 2010.

[31] T. G. van Rossum, A. G. Vulto, W. C. Hop, and S. W. Schalm, "Pharmacokinetics of intravenous glycyrrhizin after single and multiple doses in patients with chronic hepatitis C infection," *Clinical Therapeutics*, vol. 21, no. 12, pp. 2080–2090, 1999.

[32] S. Ishida, Y. Sakiya, T. Ichikawa, and S. AwAzu, "Pharmacokinetics of glycyrrhetic acid, a major metabolite of glycyrrhizin, in rats," *Chemical and Pharmaceutical Bulletin*, vol. 37, no. 9, pp. 2509–2513, 1989.

[33] F. Størmer, R. Reistad, and J. Alexander, "Glycyrrhizic acid in liquorice—evaluation of health hazard," *Food and Chemical Toxicology*, vol. 31, no. 4, pp. 303–312, 1993.

[34] B. R. Walker and C. R. Edwards, "Licorice-induced hypertension and syndromes of apparent mineralocorticoid excess," *Endocrinology and Metabolism Clinics of North America*, vol. 23, no. 2, pp. 359–377, 1994.

[35] K. T. Feehan and D. W. Gilroy, "Is resolution the end of inflammation?," *Trends in Molecular Medicine*, vol. 25, no. 3, pp. 198–214, 2019.

[36] M. P. Manns, H. Wedemeyer, A. Singer et al., "Glycyrrhizin in patients who failed previous interferon alpha-based therapies: biochemical and histological effects after 52 weeks," *Journal of Viral Hepatitis*, vol. 19, no. 8, pp. 537–546, 2012.

[37] K. Ohtsuki, Y. Abe, Y. Shimoyama, T. Furuya, H. Munakata, and C. Takasaki, "Separation of phospholipase A2 in Habu snake venom by glycyrrhizin (GL)-affinity column chromatography and identification of a GL-sensitive enzyme," *Biological and Pharmaceutical Bulletin*, vol. 21, no. 6, pp. 574–578, 1998.

[38] Y. Shimoyama, H. Ohtaka, N. Nagata, H. Munakata, N. Hayashi, and K. Ohtsuki, "Physiological correlation between glycyrrhizin, glycyrrhizin-binding lipoxygenase and casein kinase II," *FEBS Letters*, vol. 391, no. 3, pp. 238–242, 1996.

[39] S. Matsui, H. Matsumoto, Y. Sonoda et al., "Glycyrrhizin and related compounds down-regulate production of inflammatory chemokines IL-8 and eotaxin 1 in a human lung fibroblast cell line," *International Immunopharmacology*, vol. 4, no. 13, pp. 1633–1644, 2004.

[40] X. Huo, X. Sun, Z. Cao et al., "Optimal ratio of 18α-and 18β-glycyrrhizic acid for preventing alcoholic hepatitis in rats," *Experimental and Therapeutic Medicine*, vol. 18, no. 1, pp. 172–178, 2019.

[41] R. Yang, B.-C. Yuan, Y.-S. Ma, S. Zhou, and Y. Liu, "The anti-inflammatory activity of licorice, a widely used Chinese herb," *Pharmaceutical Biology*, vol. 55, no. 1, pp. 5–18, 2017.

[42] C. Xie, X. Li, J. Wu et al., "Anti-inflammatory activity of magnesium isoglycyrrhizinate through inhibition of phospholipase A2/arachidonic acid pathway," *Inflammation*, vol. 38, no. 4, pp. 1639–1648, 2015.

[43] Z. Xiao, W. Zhang, L. Ma, and Z. Qiu, "Therapeutic effect of magnesium isoglycyrrhizinate in rats on lung injury induced by paraquat poisoning," *European Review for Medical and Pharmacological Sciences*, vol. 18, no. 3, pp. 311–320, 2014.

[44] X. Huang, J. Qin, and S. Lu, "Magnesium isoglycyrrhizinate protects hepatic L02 cells from ischemia/reperfusion induced injury," *International Journal of Clinical and Experimental Pathology*, vol. 7, no. 8, p. 4755, 2014.

[45] J. Y. Li, H. Y. Cao, P. Liu, G. H. Cheng, and M. Y. Sun, "Glycyrrhizic acid in the treatment of liver diseases: literature review," *BioMed Research International*, vol. 2014, Article ID 872139, 15 pages, 2014.

[46] B. Schröfelbauer, J. Raffetseder, M. Hauner, A. Wolkerstorfer, W. Ernst, and O. H. Szolar, "Glycyrrhizin, the main active compound in liquorice, attenuates pro-inflammatory responses by interfering with membrane-dependent receptor signalling," *Biochemical Journal*, vol. 421, no. 3, pp. 473–482, 2009.

[47] H. Honda, Y. Nagai, T. Matsunaga et al., "Glycyrrhizin and isoliquiritigenin suppress the LPS sensor toll-like receptor 4/MD-2 complex signaling in a different manner," *Journal of Leukocyte Biology*, vol. 91, no. 6, pp. 967–976, 2012.

[48] R. M. Steinman, B. Gutchinov, M. D. Witmer, and M. C. Nussenzweig, "Dendritic cells are the principal stimulators of the primary mixed leukocyte reaction in mice," *The Journal of Experimental Medicine*, vol. 157, no. 2, pp. 613–627, 1983.

[49] K. Liu and M. C. Nussenzweig, "Development and homeostasis of dendritic cells," *European Journal of Immunology*, vol. 40, no. 8, pp. 2099–2102, 2010.

[50] M. Collin and V. Bigley, "Human dendritic cell subsets: an update," *Immunology*, vol. 154, no. 1, pp. 3–20, 2018.

[51] R. Tisch, "Immunogenic versus tolerogenic dendritic cells: a matter of maturation," *International Reviews of Immunology*, vol. 29, no. 2, pp. 111–118, 2010.

[52] T. Miloud, G. J. Hämmerling, and N. Garbi, "Review of murine dendritic cells: types, location, and development," in *Dendritic Cell Protocols*, pp. 21–42, Springer, 2010.

[53] A. Azadmehr, A. A. Pourfathollah, Z. Amirghofran, Z. M. Hassan, and S. M. Moazzeni, "Enhancement of Th1 immune response by CD8α+ dendritic cells loaded with heat shock proteins enriched tumor extract in tumor-bearing mice," *Cellular Immunology*, vol. 260, no. 1, pp. 28–32, 2009.

[54] M. Abe, F. Akbar, A. Hasebe, N. Horiike, and M. Onji, "Glycyrrhizin enhances interleukin-10 production by liver dendritic cells in mice with hepatitis," *Journal of Gastroenterology*, vol. 38, no. 10, pp. 962–967, 2003.

[55] H. Hua, Z. Liang, W. Li et al., "Phenotypic and functional maturation of murine dendritic cells (DCs) induced by purified Glycyrrhizin (GL)," *International Immunopharmacology*, vol. 12, no. 3, pp. 518–525, 2012.

[56] A. Ukil, A. Biswas, T. Das, and P. K. Das, "18β-glycyrrhetinic acid triggers curative Th1 response and nitric oxide up-regulation in experimental visceral leishmaniasis associated with the activation of NF-κB," *The Journal of Immunology*, vol. 175, no. 2, pp. 1161–1169, 2005.

[57] P. Takk and G. Firestein, "NF-κB: a key role in inflammatory disease," *Journal of Clinical Investigation*, vol. 107, pp. 7–11, 2001.

[58] A. S. Baldwin Jr., "The NF-κB and IκB proteins: new discoveries and insights," *Annual review of immunology*, vol. 14, no. 1, pp. 649–681, 1996.

[59] S. S. Makarov, "NF-κB as a therapeutic target in chronic inflammation: recent advances," *Molecular medicine today*, vol. 6, no. 11, pp. 441–448, 2000.

[60] A. S. Baldwin, "Series introduction: the transcription factor NF-κB and human disease," *The Journal of clinical investigation*, vol. 107, no. 1, pp. 3–6, 2001.

[61] M. J. May and S. Ghosh, "Signal transduction through NF-κB," *Immunology Today*, vol. 19, no. 2, pp. 80–88, 1998.

[62] S. Ghosh and M. Karin, "Missing pieces in the NF-κB puzzle," *Cell*, vol. 109, no. 2, pp. S81–S96, 2002.

[63] F. Mercurio and A. M. Manning, "Multiple signals converging on NF-κB," *Current Opinion in Cell Biology*, vol. 11, no. 2, pp. 226–232, 1999.

[64] H. Zhang, Y. Song, and Z. Zhang, "Glycyrrhizin administration ameliorates coxsackievirus B3-induced myocarditis in mice," *The American journal of the medical sciences*, vol. 344, no. 3, pp. 206–210, 2012.

[65] J.-M. Cherng, K.-D. Tsai, Y.-W. Yu, and J.-C. Lin, "Molecular mechanisms underlying chemopreventive activities of glycyrrhizic acid against UVB-radiation-induced carcinogenesis in SKH-1 hairless mouse epidermis," *Radiation Research*, vol. 176, no. 2, pp. 177–186, 2011.

[66] L. Feng, M.-m. Zhu, M.-h. Zhang et al., "Protection of glycyrrhizic acid against AGEs-induced endothelial dysfunction through inhibiting RAGE/NF-κB pathway activation in human umbilical vein endothelial cells," *Journal of ethnopharmacology*, vol. 148, no. 1, pp. 27–36, 2013.

[67] J. Park, K. Choi, E. Jeong, D. Kwon, E. N. Benveniste, and C. Choi, "Reactive oxygen species mediate chloroquine-induced expression of chemokines by human astroglial cells," *Glia*, vol. 47, no. 1, pp. 9–20, 2004.

[68] W. J. Streit, J. R. Conde, and J. K. Harrison, "Chemokines and Alzheimer's disease," *Neurobiology of aging*, vol. 22, no. 6, pp. 909–913, 2001.

[69] A. Bajetto, R. Bonavia, S. Barbero, T. Florio, and G. Schettini, "Chemokines and their receptors in the central nervous system," *Frontiers in neuroendocrinology*, vol. 22, no. 3, pp. 147–184, 2001.

[70] H. Soufy, S. Yassein, A. R. Ahmed et al., "Antiviral and immune stimulant activities of glycyrrhizin against duck hepatitis virus," *African Journal of Traditional, Complementary and Alternative Medicines*, vol. 9, no. 3, pp. 389–395, 2012.

[71] M. D. de Jong, C. P. Simmons, T. T. Thanh et al., "Fatal outcome of human influenza A (H5N1) is associated with high viral load and hypercytokinemia," *Nature medicine*, vol. 12, no. 10, pp. 1203–1207, 2006.

[72] P. Jose, D. Griffiths-Johnson, P. Collins et al., "Eotaxin: a potent eosinophil chemoattractant cytokine detected in a guinea pig model of allergic airways inflammation," *The Journal of experimental medicine*, vol. 179, no. 3, pp. 881–887, 1994.

[73] M. Kitaura, T. Nakajima, T. Imai et al., "Molecular cloning of human eotaxin, an eosinophil-selective CC chemokine, and identification of a specific eosinophil eotaxin receptor, CC chemokine receptor 3," *Journal of Biological Chemistry*, vol. 271, no. 13, pp. 7725–7730, 1996.

[74] L. M. Teran, M. Mochizuki, J. Bartels et al., "Th1-and Th2-type cytokines regulate the expression and production of eotaxin and RANTES by human lung fibroblasts," *American journal of respiratory cell and molecular biology*, vol. 20, no. 4, pp. 777–786, 1999.

[75] M. Miyamasu, T. Nakajima, Y. Misaki et al., "Dermal fibroblasts represent a potent major source of human eotaxin: in vitro production and cytokine-mediated regulation," *Cytokine*, vol. 11, no. 10, pp. 751–758, 1999.

[76] S. Matsui, Y. Sonoda, T. Sekiya, E. Aizu-Yokota, and T. Kasahara, "Glycyrrhizin derivative inhibits eotaxin 1 pro-

[77] S. Matsukura, C. Stellato, J. R. Plitt et al., "Activation of eotaxin gene transcription by NF-kappa B and STAT6 in human airway epithelial cells," *The Journal of Immunology*, vol. 163, no. 12, pp. 6876–6883, 1999.

[78] J. Hoeck and M. Woisetschläger, "STAT6 mediates eotaxin-1 expression in IL-4 or TNF-α-induced fibroblasts," *The Journal of Immunology*, vol. 166, no. 7, pp. 4507–4515, 2001.

[79] L. Malmgaard, "Induction and regulation of IFNs during viral infections," *Journal of interferon & cytokine research*, vol. 24, no. 8, pp. 439–454, 2004.

[80] G. C. Sen, "Viruses and interferons," *Annual Reviews in Microbiology*, vol. 55, no. 1, pp. 255–281, 2001.

[81] C.-F. Huang, T.-C. Wu, C.-C. Wu et al., "Sublingual vaccination with sonicated Salmonella proteins and mucosal adjuvant induces mucosal and systemic immunity and protects mice from lethal enteritis," *Apmis*, vol. 119, no. 7, pp. 468–478, 2011.

[82] J. K. Dunnick and G. J. Galasso, "Update on clinical trials with exogenous interferon," *The Journal of infectious diseases*, vol. 142, no. 2, pp. 293–299, 1980.

[83] H. B. Greenberg, R. B. Pollard, L. I. Lutwick, P. B. Gregory, W. S. Robinson, and T. C. Merigan, "Effect of human leukocyte interferon on hepatitis B virus infection in patients with chronic active hepatitis," *New England Journal of Medicine*, vol. 295, no. 10, pp. 517–522, 1976.

[84] S. Matsubara, M. Suzuki, F. Suzuki, and N. Ishida, "The induction of viral inhibitor (s) in mice treated with biological and synthetic immunopotentiators," *Microbiology and immunology*, vol. 24, no. 1, pp. 87–90, 1980.

[85] Y. Kondo and F. Takano, "Nitric oxide production in mouse peritoneal macrophages enhanced with glycyrrhizin," *Biological and Pharmaceutical Bulletin*, vol. 17, no. 5, pp. 759–761, 1994.

[86] M. Shinada, M. Azuma, H. Kawai et al., "Enhancement of interferon-γ production in glycyrrhizin-treated human peripheral lymphocytes in response to concanavalin A and to surface antigen of hepatitis B virus," *Proceedings of the society for experimental biology and medicine*, vol. 181, no. 2, pp. 205–210, 1986.

[87] J. Y. Djeu, J. A. Heinbaugh, H. T. Holden, and R. B. Herberman, "Augmentation of mouse natural killer cell activity by interferon and interferon inducers," *The Journal of Immunology*, vol. 122, no. 1, pp. 175–181, 1979.

[88] R. M. Schultz, J. D. Papamatheakis, and M. A. Chirigos, "Interferon: an inducer of macrophage activation by polyanions," *Science*, vol. 197, no. 4304, pp. 674–676, 1977.

[89] Q. Wu, Y. Tang, J. Zhang, X. Hu, Q. Wang, and J. Huang, "Therapeutic effects of glycyrrhizic acid on asthma airway inflammation in mice and its mechanism," *Zhonghua yi xue za zhi*, vol. 94, no. 42, pp. 3338–3344, 2014.

[90] F. Fitzpatrick, "Cyclooxygenase enzymes: regulation and function," *Current pharmaceutical design*, vol. 10, no. 6, pp. 577–588, 2004.

[91] J. Li, G. Feng, J. Liu et al., "Renal cell carcinoma may evade the immune system by converting CD4+ Foxp3-T cells into CD4+ CD25+ Foxp3+ regulatory T cells: Role of tumor COX-2-derived PGE2," *Molecular medicine reports*, vol. 3, no. 6, pp. 959–963, 2010.

[92] L. Sun, J. Liu, D. Cui et al., "Anti-inflammatory function of Withangulatin A by targeted inhibiting COX-2 expression

via MAPK and NF-κB pathways," *Journal of cellular biochemistry*, vol. 109, no. 3, pp. 532–541, 2009.

[93] M. Olivier, D. J. Gregory, and G. Forget, "Subversion mechanisms by which Leishmania parasites can escape the host immune response: a signaling point of view," *Clinical microbiology reviews*, vol. 18, no. 2, pp. 293–305, 2005.

[94] C. E. Trebino, J. L. Stock, C. P. Gibbons et al., "Impaired inflammatory and pain responses in mice lacking an inducible prostaglandin E synthase," *Proceedings of the National Academy of Sciences*, vol. 100, no. 15, pp. 9044–9049, 2003.

[95] C. S. Williams, M. Mann, and R. N. DuBois, "The role of cyclooxygenases+ in inflammation, cancer, and development," *Oncogene*, vol. 18, no. 55, pp. 7908–7916, 1999.

[96] M. Betz and B. Fox, "Prostaglandin E2 inhibits production of Th1 lymphokines but not of Th2 lymphokines," *The Journal of Immunology*, vol. 146, no. 1, pp. 108–113, 1991.

[97] H.-G. Klingemann, M.-S. Tsoi, and R. Storb, "Inhibition of prostaglandin E2 restores defective lymphocyte proliferation and cell-mediated lympholysis in recipients after allogeneic marrow grafting," *Blood*, vol. 68, no. 1, pp. 102–107, 1986.

[98] Y.-F. Ni, J.-K. Kuai, Z.-F. Lu et al., "Glycyrrhizin treatment is associated with attenuation of lipopolysaccharide-induced acute lung injury by inhibiting cyclooxygenase-2 and inducible nitric oxide synthase expression," *Journal of Surgical Research*, vol. 165, no. 1, pp. e29–e35, 2011.

[99] W. Ouyang and A. O'Garra, "IL-10 family cytokines IL-10 and IL-22: from basic science to clinical translation," *Immunity*, vol. 50, no. 4, pp. 871–891, 2019.

[100] R. Manetti, P. Parronchi, M. G. Giudizi et al., "Natural killer cell stimulatory factor (interleukin 12 [IL-12]) induces T helper type 1 (Th1)-specific immune responses and inhibits the development of IL-4-producing Th cells," *The Journal of experimental medicine*, vol. 177, no. 4, pp. 1199–1204, 1993.

[101] G. Trinchieri, "Interleukin-12 and its role in the generation of TH1 cells," *Immunology today*, vol. 14, no. 7, pp. 335–338, 1993.

[102] J. Chehimi, S. E. Starr, I. Frank et al., "Impaired interleukin 12 production in human immunodeficiency virus-infected patients," *The Journal of experimental medicine*, vol. 179, no. 4, pp. 1361–1366, 1994.

[103] J. Chehimi, S. E. Starr, I. Frank et al., "Natural killer (NK) cell stimulatory factor increases the cytotoxic activity of NK cells from both healthy donors and human immunodeficiency virus-infected patients," *The Journal of experimental medicine*, vol. 175, no. 3, pp. 789–796, 1992.

[104] G. Trinchieri, "Interleukin-12: a cytokine produced by antigen-presenting cells with immunoregulatory functions in the generation of T-helper cells type 1 and cytotoxic lymphocytes," *Blood*, vol. 84, no. 12, pp. 4008–4027, 1994.

[105] Z. Liu, J. Y. Zhong, E. N. Gao, and H. Yang, "Effects of glycyrrhizin acid and licorice flavonoids on LPS-induced cytokines expression in macrophage," *Zhongguo Zhong Yao Za Zhi*, vol. 39, no. 19, pp. 3841–3845, 2014.

[106] T. Raphael and G. Kuttan, "Effect of naturally occurring triterpenoids glycyrrhizic acid, ursolic acid, oleanolic acid and nomilin on the immune system," *Phytomedicine*, vol. 10, no. 6-7, pp. 483–489, 2003.

[107] Y.-H. Zhang, M. Kato, K.-I. Isobe, M. Hamaguchi, T. Yokochi, and I. Nakashima, "Dissociated control by glycyrrhizin of proliferation and IL-2 production of murine thymocytes," *Cellular immunology*, vol. 162, no. 1, pp. 97–104, 1995.

[108] B. Jaruga, F. Hong, R. Sun, S. Radaeva, and B. Gao, "Crucial role of IL-4/STAT6 in T cell-mediated hepatitis: upregulating eotaxins and IL-5 and recruiting leukocytes," *The Journal of Immunology*, vol. 171, no. 6, pp. 3233–3244, 2003.

[109] A. M. Miller, N. Horiguchi, W. I. Jeong, S. Radaeva, and B. Gao, "Molecular mechanisms of alcoholic liver disease: innate immunity and cytokines," *Alcoholism: Clinical and Experimental Research*, vol. 35, no. 5, pp. 787–793, 2011.

[110] K. C. El Kasmi, A. M. Smith, L. Williams et al., "Cutting edge: a transcriptional repressor and corepressor induced by the STAT3-regulated anti-inflammatory signaling pathway," *The Journal of Immunology*, vol. 179, no. 11, pp. 7215–7219, 2007.

[111] T. Yoshida, K. Abe, T. Ikeda et al., "Inhibitory effect of glycyrrhizin on lipopolysaccharide and d-galactosamine-induced mouse liver injury," *European journal of pharmacology*, vol. 576, pp. 136–142, 2007.

[112] K. Nakanishi, T. Yoshimoto, H. Tsutsui, and H. Okamura, "Interleukin-18 regulates both Th1 and Th2 responses," *Annual review of immunology*, vol. 19, no. 1, pp. 423–474, 2001.

[113] K.-R. Park, D. Nam, H.-M. Yun et al., "β-Caryophyllene oxide inhibits growth and induces apoptosis through the suppression of PI3K/AKT/mTOR/S6K1 pathways and ROS-mediated MAPKs activation," *Cancer Letter*, vol. 312, no. 2, pp. 178–188, 2011.

[114] C.-K. Kim, Y. K. Choi, H. Lee et al., "The farnesyltransferase inhibitor LB42708 suppresses vascular endothelial growth factor-induced angiogenesis by inhibiting ras-dependent mitogen-activated protein kinase and phosphatidylinositol 3-kinase/Akt signal pathways," *Molecular pharmacology*, vol. 78, no. 1, pp. 142–150, 2010.

[115] Z.-h. Wang, C.-. H. Hsieh, W.-h. Liu, and M.-c. Yin, "Glycyrrhizic acid attenuated glycative stress in kidney of diabetic mice through enhancing glyoxalase pathway," *Molecular nutrition & food research*, vol. 58, no. 7, pp. 1426–1435, 2014.

[116] M. Wojcik, A. Zieleniak, M. Zurawska-Klis, K. Cypryk, and L. A. Wozniak, "Increased expression of immune-related genes in leukocytes of patients with diagnosed gestational diabetes mellitus (GDM)," *Experimental Biology and Medicine*, vol. 241, no. 5, pp. 457–465, 2016.

[117] R. Tanemoto, T. Okuyama, H. Matsuo, T. Okumura, Y. Ikeya, and M. Nishizawa, "The constituents of licorice (Glycyrrhiza uralensis) differentially suppress nitric oxide production in interleukin-1β-treated hepatocytes," *Biochemistry and biophysics reports*, vol. 2, pp. 153–159, 2015.

[118] A. Nakajima, Y. Yamamoto, N. Yoshinaka et al., "A new flavanone and other flavonoids from green perilla leaf extract inhibit nitric oxide production in interleukin 1β-treated hepatocytes," *Bioscience, biotechnology, and biochemistry*, vol. 79, no. 1, pp. 138–146, 2015.

[119] N. Tsuruoka, K. Abe, K. Wake et al., "Hepatic protection by glycyrrhizin and inhibition of iNOS expression in concanavalin A-induced liver injury in mice," *Inflammation Research*, vol. 58, no. 9, pp. 593–599, 2009.

[120] Y. Tanaka, M. Kaibori, H. Miki et al., "Japanese Kampo medicine, ninjinyoeito, inhibits the induction of iNOS gene expression in proinflammatory cytokine-stimulated hepatocytes," *British Journal of Pharmaceutical Research*, vol. 4, pp. 2226–2244, 2014.

[121] M. Colasanti and H. Suzuki, "The dual personality of NO," *Trends Pharmacology Science*, vol. 21, no. 7, pp. 249–252, 2000.

[122] K. Matsui, M. Nishizawa, T. Ozaki et al., "Natural antisense transcript stabilizes inducible nitric oxide synthase messenger RNA in rat hepatocytes," *Hepatology*, vol. 47, no. 2, pp. 686–697, 2007.

[123] M. Nishizawa, Y. Ikeya, T. Okumura, and T. Kimura, "Post-transcriptional inducible gene regulation by natural antisense RNA," *Frontiers in Bioscience*, vol. 20, pp. 1–36, 2015.

[124] T. Kanemaki, H. Kitade, Y. Hiramatsu, Y. Kamiyama, and T. Okumura, "Stimulation of glycogen degradation by prosta-glandin E2 in primary cultured rat hepatocytes," *Prostaglandins*, vol. 45, no. 5, pp. 459–474, 1993.

[125] B. Jaruga, F. Hong, W.-H. Kim, and B. Gao, "IFN-γ/STAT1 acts as a proinflammatory signal in T cell-mediated hepatitis via induction of multiple chemokines and adhesion mole-cules: a critical role of IRF-1," *American Journal of Physiology-Gastrointestinal and Liver Physiology*, vol. 287, no. 5, pp. G1044–G1052, 2004.

[126] T. Okamoto and T. Kanda, "Glycyrrhizin protects mice from concanavalin A-induced hepatitis without affecting cytokine expression," *International journal of molecular medicine*, vol. 4, no. 2, pp. 149–201, 1999.

[127] C.-H. Lee, S.-W. Park, Y. S. Kim et al., "Protective mechanism of glycyrrhizin on acute liver injury induced by carbon tetra-chloride in mice," *Biological and Pharmaceutical Bulletin*, vol. 30, no. 10, pp. 1898–1904, 2007.

[128] K. Takeda, T. Kaisho, and S. Akira, "Toll-like receptors," *Annual review of immunology*, vol. 21, no. 1, pp. 335–376, 2015.

[129] X. Shi, L. Yu, Y. Zhang et al., "Glycyrrhetinic acid alleviates hepatic inflammation injury in viral hepatitis disease via a HMGB1-TLR4 signaling pathway," *International immuno-pharmacology*, vol. 84, no. 106578, pp. 1–12, 2020.

[130] J. B. Williams, A. Hüppner, P. M. Mulrooney-Cousins, and T. I. Michalak, "Differential expression of woodchuck toll-like receptors 1–10 in distinct forms of infection and stages of hepatitis in experimental hepatitis B virus infection," *Fron-tiers in microbiology*, vol. 9, 2018.

[131] P. Gupta, P. K. Das, and A. Ukil, "Antileishmanial effect of 18β-glycyrrhetinic acid is mediated by toll-like receptor-dependent canonical and noncanonical p38 activation," *Anti-microbial agents and chemotherapy*, vol. 59, no. 5, pp. 2531–2539, 2015.

[132] L.-N. Peng, L. Li, Y.-F. Qiu et al., "Glycyrrhetinic acid extracted from Glycyrrhiza uralensis Fisch. induces the expression of toll-like receptor 4 in Ana-1 murine macro-phages," *Journal of Asian natural products research*, vol. 13, no. 10, pp. 942–950, 2011.

[133] C. S. Graebin, "The pharmacological activities of glycyrrhizi-nic acid ("glycyrrhizin") and glycyrrhetinic acid," *Reference Series in Phytochemistry*, pp. 245–261, 2018.

[134] W. Liu, S. Huang, Y. Li, K. Zhang, and X. Zheng, "Suppressive effect of glycyrrhizic acid against lipopolysaccharide-induced neuroinflammation and cognitive impairment in C57 mice via toll-like receptor 4 signaling pathway," *Food & nutrition research*, vol. 63, 2019.

[135] N. F. Abo El-Magd, A. El-Karef, M. M. El-Shishtawy, and L. A. Eissa, "Glycyrrhizin and Omega-3 fatty acids have hepa-toprotective roles through toll-like receptor-4," *Egyptian Journal of Basic and Applied Sciences*, vol. 6, no. 1, pp. 82–98, 2019.

[136] M. Loiarro, V. Ruggiero, and C. Sette, "Targeting TLR/IL-1R signalling in human diseases," *Mediators of inflammation*, vol. 2010, Article ID 674363, 12 pages, 2010.

[137] K. A. Shirey, W. Lai, M. C. Patel et al., "Novel strategies for targeting innate immune responses to influenza," *Mucosal immunology*, vol. 9, no. 5, pp. 1173–1182, 2016.

[138] M. G. Morale, W. da Silva Abjaude, A. M. Silva, L. L. Villa, and E. Boccardo, "HPV-transformed cells exhibit altered HMGB1-TLR4/MyD88-SARM1 signaling axis," *Scientific reports*, vol. 8, no. 1, pp. 1–11, 2018.

[139] K. Rayavara, A. Kurosky, S. J. Stafford et al., "Proinflamma-tory effects of respiratory syncytial virus–induced epithelial HMGB1 on human innate immune cell activation," *The Jour-nal of Immunology*, vol. 201, no. 9, pp. 2753–2766, 2018.

[140] G. W. Nace, H. Huang, J. R. Klune et al., "Cellular-specific role of toll-like receptor 4 in hepatic ischemia-reperfusion injury in mice," *Hepatology*, vol. 58, no. 1, pp. 374–387, 2013.

[141] R. Gao, Y. Zhang, Y. Kang et al., "Glycyrrhizin inhibits PEDV infection and proinflammatory cytokine secretion via the HMGB1/TLR4-MAPK p38 pathway," *International journal of molecular sciences*, vol. 21, no. 8, p. 2961, 2020.

[142] L. Mollica, F. De Marchis, A. Spitaleri et al., "Glycyrrhizin binds to high-mobility group box 1 protein and inhibits its cytokine activities," *Chemistry & biology*, vol. 14, no. 4, pp. 431–441, 2007.

[143] M. E. Bianchi and A. Agresti, "HMG proteins: dynamic players in gene regulation and differentiation," *Current opin-ion in genetics & development*, vol. 15, no. 5, pp. 496–506, 2005.

[144] H. Wang, O. Bloom, M. Zhang et al., "HMG-1 as a late medi-ator of endotoxin lethality in mice," *Science*, vol. 285, no. 5425, pp. 248–251, 1999.

[145] H. Wang, M. F. Ward, X.-G. Fan, A. E. Sama, and W. Li, "Potential role of high mobility group box 1 in viral infectious diseases," *Viral immunology*, vol. 19, no. 1, pp. 3–9, 2006.

[146] U. Andersson, H. Wang, K. Palmblad et al., "High mobility group 1 protein (HMG-1) stimulates proinflammatory cyto-kine synthesis in human monocytes," *Journal of Experimental Medicine*, vol. 192, no. 4, pp. 565–570, 2000.

[147] G. Chen, D.-z. Chen, J. Li et al., "Pathogenic role of HMGB1 in SARS?," *Medical hypotheses*, vol. 63, no. 4, pp. 691–695, 2004.

[148] C. Fiuza, M. Bustin, S. Talwar et al., "Inflammation-promot-ing activity of HMGB1 on human microvascular endothelial cells," *Blood, The Journal of the American Society of Hematol-ogy*, vol. 101, no. 7, pp. 2652–2660, 2003.

[149] R. Palumbo, M. Sampaolesi, F. De Marchis et al., "Extracellu-lar HMGB1, a signal of tissue damage, induces mesoangio-blast migration and proliferation," *The Journal of cell biology*, vol. 164, no. 3, pp. 441–449, 2004.

[150] U.-M. Ohndorf, M. A. Rould, Q. He, C. O. Pabo, and S. J. Lip-pard, "Basis for recognition of cisplatin-modified DNA by high-mobility-group proteins," *Nature*, vol. 399, no. 6737, pp. 708–712, 1999.

[151] I. Julkunen, T. Sareneva, J. Pirhonen, T. Ronni, K. Melén, and S. Matikainen, "Molecular pathogenesis of influenza A virus infection and virus-induced regulation of cytokine gene expression," *Cytokine Growth Factor Rev*, vol. 12, no. 2-3, pp. 171–180, 2001.

[152] D. Moisy, S. V. Avilov, Y. Jacob et al., "HMGB1 protein binds to influenza virus nucleoprotein and promotes viral replication," *Journal of virology*, vol. 86, no. 17, pp. 9122–9133, 2012.

[153] J. Chu and M. Ng, "The mechanism of cell death during West Nile virus infection is dependent on initial infectious dose," *Journal of General Virology*, vol. 84, no. 12, pp. 3305–3314, 2003.

[154] T. Joseph, A. Cepica, L. Brown, B. O. Ikede, and F. S. Kibenge, "Mechanism of cell death during infectious salmon anemia virus infection is cell type-specific," *Journal of General Virology*, vol. 85, no. 10, pp. 3027–3036, 2004.

[155] J. F. Bermejo and M. A. Muñoz-Fernandez, "Severe acute respiratory syndrome, a pathological immune response to the new coronavirus—implications for understanding of pathogenesis, therapy, design of vaccines, and epidemiology," *Viral immunology*, vol. 17, no. 4, pp. 535–544, 2004.

[156] H. Popper, "Clinical pathologic correlation in viral hepatitis. The effect of the virus on the liver," *The American journal of pathology*, vol. 81, no. 3, p. 609, 1975.